Characterizing astrocytic heterogeneity in the brain of healthy individuals and depressed suicides

Liam O'Leary

Integrated Program in Neuroscience (IPN)

McGill University, Montreal

A thesis submitted to McGill University in partial fulfilment of the requirements of the degree of Doctor of Philosophy

Initial Thesis Submission: December 2020

Final Submission: March 2021

ABSTRACT

Background: Several postmortem studies have revealed that brain regions from individuals with major depressive disorder (MDD) have lower glial densities, and a lower expression of the astrocytic marker glial fibrillary acidic protein (GFAP), than matched controls. However, no study has assessed whether MDD is associated with lower regional astrocyte densities or altered morphologies in different brain regions using more than one astrocyte markers, so the extent of these differences throughout the brain remains unclear. This thesis aimed to characterize the regional heterogeneity of astrocyte density and morphology in brain samples of healthy and depressed individuals, using an unexplored astrocyte marker, vimentin (VIM), to clarify the extent of changes to astrocyte anatomy in MDD.

Methods: In the prefrontal cortex, thalamus and caudate nucleus of middle-aged depressed suicides and matched psychiatrically healthy controls, we assessed the following: stereological densities of VIM-IR or GFAP-IR astrocytes; the morphology of VIM-IR astrocytes; the vascular density of CD31-IR blood vessels. Vascular density was assessed via % coverage analysis, all other measurements used workflows within Neurolucida or Stereoinvestigator softwares (MBF Bioscience, United States). We also compared VIM-IR astrocyte morphology in homologous brain regions of healthy adult mice.

Results: In the healthy human brain, VIM-IR astrocytes often have lower regional densities than GFAP-IR astrocytes, and are 2–3 times larger in size than in the mouse brain. Remarkably, VIM-IR astrocytes are absent from the mediodorsal thalamus. Both VIM-IR and GFAP-IR astrocyte densities inversely correlated with vascular densities in healthy brain regions. In depressed suicides, reduced densities of either VIM-IR or GFAP-IR astrocytes were observed in all regions, relative to healthy controls. Other features displayed less widespread and strong differences in depressed suicides — the prefrontal cortex white matter exhibited increased vascularization and astrocytes with fewer processes.

Conclusions: Astrocyte density is regionally heterogeneous and more widely and strongly affected in the brains of depressed suicides than astrocyte morphology or vascular density. This strengthens support for extensive astrocyte pathology in MDD, and that abnormal astrocyte densities are a more widespread anatomical hallmark of MDD than GFAP dysfunction.

RESUMÉ

Contexte: Plusieurs études post-mortem ont révélé que le cerveau des personnes atteintes de dépression majeure (DM) ont une densité gliale plus faible et une expression réduite de la protéine acide fibrillaire gliale (GFAP), un marqueur astrocytaire. Cependant, aucune étude n'a évalué si la DM est associée à des changements dans les densités ou les morphologies d'astrocytes au sein de différentes régions cérébrales et en utilisant d'autres marqueurs que la GFAP. Cette thèse visait à caractériser l'hétérogénéité régionale de la densité et de la morphologie des astrocytes au sein d'échantillons cérébraux d'individus sains et dépressifs, en utilisant un marqueur astrocytaire sous-utilisé, la vimentine (VIM) afin d'explorer l'étendue des changements astrocytaires survenant dans le DM.

Méthodes: Dans le cortex préfrontal, le thalamus et le noyau caudé de dépressifs suicidés adultes et de témoins psychiatriques sains, nous avons évalué les éléments suivants : les densités stéréologiques des astrocytes VIM-IR ou GFAP-IR; la morphologie des astrocytes VIM-IR; et la densité des vaisseaux sanguins CD31-IR. La densité vasculaire a été évaluée par l'analyse de la couverture en %, alors que toutes les autres mesures ont utilisé les flux de travail des logiciels Neurolucida ou Stereoinvestigator (MBF Bioscience, États-Unis). Nous avons également comparé la morphologie des astrocytes VIM-IR dans les régions homologues du cerveau de souris adultes.

Résultats: Dans le cerveau humain sain, les astrocytes VIM-IR ont souvent des densités régionales plus faibles que les astrocytes GFAP-IR, mais de 2 à 3 fois plus importantes que dans le cerveau de la souris. Fait remarquable, les astrocytes VIM-IR sont absents du thalamus médiodorsal. Les densités d'astrocytes VIM-IR et GFAP-IR sont inversement corrélées aux densités vasculaires des régions cérébrales saines. Dans les cas de dépressifs suicidés, des densités réduites d'astrocytes VIM-IR ou GFAP-IR ont été observées dans toutes les régions par comparaison aux témoins sains. D'autres caractéristiques ont montré des différences moins étendues et moins importantes chez les dépressifs suicidés : la substance blanche du cortex préfrontal présentait une vascularisation accrue et des astrocytes déployaient moins de prolongements.

Conclusions: La densité astrocytaire dans le cerveau humain est régionalement hétérogène et beaucoup plus largement et fortement affectée dans le cerveau des dépressifs suicidés que la morphologie astrocytaire ou la densité vasculaire. Ces observations impliquent davantage les

astrocytes dans la DM et indiquant que la réduction du nombre d'astrocyte survient dans plusieurs régions cérébrales et que ce phénomène peut s'observer à l'aide d'autres marqueurs que la GFAP.

FRONTISPIECE

Starlight Gone (2019) by Liam O'Leary & Elizabeth Parent — an artwork on astrocytes in depression, exhibited April 12th–27th at Concordia Faculty of Fine Arts Black Box via the Convergence Initiative.

DEDICATION

Nowadays not even a suicide kills himself in desperation. Before taking the step he deliberates so long and so carefully that he literally chokes with thought. It is even questionable whether he ought to be called a suicide, since it is really thought which takes his life. He does not die with deliberation, but from deliberation.
—Søren Kierkegaard, The Present Age (1846), p.1.

There is but one truly serious philosophical problem, and that is suicide. Judging whether life is or is not worth living amounts to answering the fundamental question of philosophy. All the rest—whether or not the world has three dimensions, whether the mind has nine or twelve categories—comes afterwards.
—Albert Camus, The Myth of Sisyphus (1942), p.1.

But even if each and every case of suicide had not been undertaken out of a feeling of meaninglessness, it may well be that an individual's impulse to take his life would have been overcome had he been aware of some meaning of purpose worth living for.
—Viktor E. Frankl, Man's Search For Meaning (1946), pp.141–142.

Even the starry patterns can deceive us.
And yet we may be happy, if only for a while,
Putting our faith in a figure. It is enough.
—Rainer Maria Rilke, Sonnets to Orpheus (1923), 1 II

We are all in the gutter, but some of us are looking at the stars.
—Oscar Wilde, Lady Windermere's Fan (1892), pp.47

Twinkle, twinkle, little star,
How I wonder what you are!
Up above the world so high,
Like a diamond in the sky.

When the blazing sun is gone,
When he nothing shines upon,
Then you show your little light,
Twinkle, twinkle, all the night.

Then the trav'ller in the dark,
Thanks you for your tiny spark,
He could not see which way to go,
If you did not twinkle so.

In the dark blue sky you keep,
And often thro' my curtains peep,
For you never shut your eye,
Till the sun is in the sky.

'Tis your bright and tiny spark,
Lights the trav'ller in the dark :
Tho' I know not what you are,
Twinkle, twinkle, little star.
—Jane Taylor, The Star (1806)

When they saw the star, they rejoiced exceedingly with great joy.
—Matthew 2:10 KJV

ACKNOWLEDGEMENTS

I thank the IPN for accepting my application, and Edward Ruthazer and Carl Ernst for providing effective support at rotation meetings in my first year. I thank Maia Kokoeva and Edith Hamel for providing engaging and fascinating rotation projects, which reassured me that I, personally, was unsuited for rodent work.

I have sincerely felt very fortunate throughout my PhD to study the human brain with many incredible people. This project would not have been possible without support from the McGill Group for Suicide Studies (MGSS). Above all, I thank my supervisor, Naguib Mechawar, for welcoming me into a work environment where I could succeed and grow. By encouraging open inquiry with close guidance, you allowed me to make truly unexpected discoveries. I am very appreciative of the experimental contributions of Maria Antonietta Davoli (M.A.), Arnaud Tanti, Claudia Belliveau and Christopher Ma which facilitated my experimental progress. I thank Keith Murai and Todd Farmer for preparing and providing excellent samples in a collaboration that critically confirmed my early results. I thank Gustavo Turecki for comments in MGSS meetings which have been pivotal to the design and interpretation of my experiments. I appreciate the rare fortune to work closely with the technical expertise of Maâmar Bouchouka, Josée Prud'homme and Dominique Mirault, who provided precise and timely dissections of postmortem brain samples. I appreciate the technical support and microscopy guidance of Étienne Labrie-Dion, M.A. and Melina Jaramillo Garcia.

I thank Naguib, Carl and Cristian Zaelzer for motivating and providing opportunities for my science design and art, which has greatly facilitated my professional abilities inside, outside and beyond of the lab. Including all those previously mentioned, I would like to additionally thank Volodymyr Yerko, Elena Leonova-Yerko, Jennie Yang, Gang Chen, Scott Bell, Malvin Jefri, Nuwan Hettige, Daniel Almeida, Léa Perret and Katherine Vaillancourt for making my time pleasant here. It would be amiss not to expressively thank M.A. for the personal support she provides to graduate students in the MGSS, which goes above and beyond her exceptional ability to train new students in lab procedures with a friendly and patient grace — we value you, greatly. I would like to thank God for granting me the patience, peace and resilience to persevere with the many experimental hurdles and difficulties I encountered getting here. Finally, I would like to thank my family for supporting me in every way imaginable. No amount of willpower would have got me here without you.

AUTHOR CONTRIBUTIONS

Chapter 1: Introduction

Literature review and writing: Liam O'Leary

Supervision: Naguib Mechawar

Chapter 2: Characterization of vimentin-immunoreactive astrocytes in the human brain

Project idea, experimental design and manuscript preparation: Liam O'Leary and Naguib Mechawar

Experimental work: Liam O'Leary, Claudia Belliveau, Arnaud Tanti, Maria Antonietta Davoli, Jie Christopher Ma, William Todd Farmer

Data Analysis: Liam O'Leary

Interpretation: All authors

Supervision: Naguib Mechawar

Chapter 3: Widespread decrease of cerebral vimentin-immunoreactive astrocytes in depressed suicides

Project idea, experimental design and manuscript preparation: Liam O'Leary and Naguib Mechawar

Experimental work: Liam O'Leary, Claudia Belliveau, Arnaud Tanti, Maria Antonietta Davoli, Jie Christopher Ma

Data Analysis: Liam O'Leary

Interpretation: All authors

Supervision: Naguib Mechawar

Chapter 4: Implication of cerebral astrocytes in major depression: a review of fine neuroanatomical evidence in humans

Literature review and writing: Liam O'Leary

Supervision: Naguib Mechawar

Chapter 5: Conclusions & Future Directions

Writing: Liam O'Leary

Supervision: Naguib Mechawar

ORIGINAL CONTRIBUTIONS TO KNOWLEDGE

During Easter of 2016 I began my third IPN rotation in the Mechawar lab, and this thesis presents the experimental work gathered in the subsequent four years. This has resulted in two research papers and one review paper. The unified goal of these publications was to quantitatively characterize the regional heterogeneity of astrocyte density and morphology in brains of healthy and depressed adults. The original contributions to knowledge are as follows:

1. Establishing vimentin as an astrocyte marker

O'Leary, L. A., *et al.* (2020). Characterization of vimentin-immunoreactive astrocytes in the human brain. *Frontiers in Neuroanatomy*, *14*, 31. https://doi.org/10.3389/fnana.2020.00031

- First demonstration that VIM is a reliable astrocyte marker in postmortem brain samples, due to its expression in GFAP-IR and Aldh1L1-IR astrocytes.
- First distributional profile of VIM-IR astrocytes in the healthy adult human brain, revealing they are often absent in the mediodorsal thalamus.
- First demonstration that VIM label all known morphological subtypes of GFAP-IR astrocyte.
- First observation that VIM is biased toward labelling twin cells, and additionally labels blood vessels and long bundles of fibres with no clear origin or target.
- First stereological counts of VIM-IR astrocytes, and first cross-regional stereological counts of GFAP-IR astrocytes.
- First assessment of astrocyte morphology in human subcortical regions.
- First precise, cross-regional demonstration of a 2-3 fold scaling of astrocyte morphology between mouse and human brain.
- First comparison of vascular density between mouse and human brain.
- First report of an inverse correlation of astrocyte density to vascular density in human brain.

2. Characterizing astrocyte heterogeneity in the human brain

O'Leary, L. A., Belliveau, C., Davoli, M. A., Ma, J. C., Tanti, A., Turecki, G., & Mechawar, N. (2021). Widespread decrease of cerebral vimentin-immunoreactive astrocytes in depressed suicides. *Frontiers in Psychiatry*, 12. https://doi.org/10.3389/fpsyt.2021.640963

- First cross-regional demonstration of reduced GFAP-IR astrocyte densities in depressed suicides.
- First demonstration of reduced VIM-IR astrocyte densities in depressed suicides.
- First study of VIM-IR astrocyte morphometry, and first study of subcortical astrocyte morphometry, in depressed suicides.
- First comparison of CD31-IR vascular density in depressed suicides.

3. The regional heterogeneity of astrocytes in the human brain

O'Leary, L. A., & Mechawar, N. (2021). Implication of cerebral astrocytes in major depression: a review of fine neuroanatomical evidence in humans. *Glia*, in press.

- First *in-silico* model based on quantitative cellular neuroanatomy in the human brain (stereology and 3D morphology) used to deduce a meaningful theory of human brain anatomy. By creating a 3D reconstruction that combines my VIM-IR astrocyte morphology measurements with previously reported stereology data, I propose that non-overlapping domains cannot theoretically be a feature of most human cortical astrocytes due to a lack of physical space.

TABLE OF CONTENTS

CHAPTER I

Introduction

1. Glia

Brain cells, or neural cells, are those considered to be responsible for brain activity. Many non-neuroscientists do not realize that not all neural cells are neurons — neurons constitute only half of the neural cells in the brain of humans and other primates (Herculano-Houzel *et al*., 2009). The non-neuronal neural cells of the brain are classified as glia, and glia mostly consists of three cell types: oligodendrocytes, astrocytes and microglia. Glia were initially defined as neural cells that cannot fire action potentials but instead provide passive structural support to neurons (reviewed in Allen & Barres, 2009). These initial criteria were later contested by experimental evidence: some glia conduct action potentials, not all glial cells develop from neural ectoderm, some glia can independently regulate global brain functions, and glial cell types interact with each other (Káradóttir *et al*., 2008; Ginhoux *et al*., 2010; Domingues *et al*., 2016; Brancaccio *et al*., 2019). Moreover, all three main types of glia directly modulate neuronal signalling, which indicates they are active players in neural signalling rather than passive structural support cells for neurons (Parpura *et al*., 1994; Coull *et al*., 2005; Káradóttir *et al*., 2005). There is also debate about whether glia is a useful classification, as these three main glial cell types have vast differences in their general function, and their gene expression profiles are equally distinct from each other as they are from neurons (Cahoy *et al*., 2008). Collectively, these findings have been acknowledged by the scientific community with consistent etymological updates in the literature in the last two decades: neuroglia ("nerve glue") became glia ("glue"), astroglia ("star glue") became astrocyte ("star cell"), oligodendroglia ("glue with few branches") became oligodendrocyte ("cell with few branches"). The growing popularity of these newer terms reflect a growing interest to better characterize the structural and functional properties of specific glial cell types in the brain. This thesis contributes to the fundamental description of astrocytes in the human brain in health and illness.

2. Astrocytes: Functional Definitions

Current evidence indicates astrocytes constitute approximately 20% of glial cells, and 10% of all neural cells, of the human brain (Pelvig *et al*., 2008). Astrocytes can be anatomically visualized using a variety of histological techniques and markers, each of which provides insight into their versatile functions in the brain.

Astrocytes were first identified after the introduction of the Golgi stain, which revealed their distinctive stellate or spider-like morphology — a large spherical cell soma from which many processes extend outwards with radial symmetry (Andriezen, 1893; von Lenhossek, 1895; Eurich, 1897). This radial distribution of astrocyte processes facilitates their contact with local vasculature via vascular endfeet, which can sometimes cover the entire surface area of blood vessels (Mathiisen *et al*., 2010). This organization facilitates one important role of astrocytes, which is to recruit blood flow to regions of neuronal activity through vascular endfeet (Takano *et al*., 2006; Attwell *et al*., 2010). In response to an external sensory stimulus or experimentally induced change in cerebral blood pressure, astrocytes release intracellularly calcium waves and simultaneously alter local rate of blood flow (Takano *et al*., 2006; Wang *et al*., 2006; Kuga *et al*., 2011). An additional function of astrocytes involving vascular endfeet is the removal of metabolites, like amyloid beta, from the interstitial fluid through water transport at astrocyte vascular endfeet through aquaporin-4 water channels, especially during sleep, using a system known as the glymphatic system (Xie *et al*., 2013; Iliff *et al*., 2013). Both vascular endfeet responses are coordinated at the macroscale of entire brain regions due to the propagation of these calcium waves through an extensive network of gap junction coupling between neighbouring astrocytes, known as the astrocyte syncytium (Kuffler, 1967; Sasaki *et* al., 2011; Kiyoshi *et al*., 2018). This network organization also facilitates an astrocyte function not involving vascular endfeet, which is the regulation of potassium homeostasis for energetically efficient neuronal firing. Syncytial coupling makes astrocytes isopotential and thereby minimally depolarized, enabling a high driving force for potassium uptake by active neurons (Ma *et al*., 2016). This has meaningful effects at the level of brain activity, because disrupting either the rate of potassium uptake by astrocytes or syncytial coupling between astrocytes can alter the firing rate profile of neighboring neurons to an extent that induces behavioural changes (Morquette *et al*., 2015; Condamine *et al*., 2018; Cui *et al*., 2018). The preferential coupling of astrocytes within functional boundaries — for example thalamic barreloids, cortical barreloids or olfactory glomeruli — allows the syncytium to modulate specific neuronal circuits or signal

specific pathological insults (Houades *et al*., 2008; Kuchibhotla *et al*., 2009; Roux *et al*., 2011; Claus *et al*., 2018). Collectively, these studies show astrocyte networks actively regulate brain activity by controlling the rate of vascular, glymphatic and neuronal activity.

Astrocytes can also be distinguished due to the large presence of glycogen granules in their cytoplasm, which is the primary reserve of glycogen in the adult brain (Maxwell & Kruger, 1965; Vaughn & Grieshaber, 1972). This relates to a primary role of astrocytes as a metabolic supply for neurons, leading to the concept that neurons are the 'oxidative cells', whereas astrocytes are the 'glycolytic cells' of the brain. In the astrocyte-neuron lactate shuttle hypothesis, astrocytes supply neurons with neurotransmitter metabolites (glutamine) and energy supply (lactate) when glutamate is released at a synapse, by the reuptake glutamate through excitatory amino acid transporter (EAAT) 1 and EAAT2 through a mechanism coupled to the glycolysis of glycogen stores or glucose absorbed from vessels (Pellerin & Magistretti, 1994; Mächler *et al*., 2016). Lactate production is stimulated in aglycaemic conditions, and lactate can account as an energy substrate for approximately only 30% of cerebral energy expenditure in humans (van Hall *et al*., 2009; Choi *et al*., 2012). Metabolic supply from astrocytes to neurons appears necessary for healthy brain activity, as reducing lactate production by inhibiting astrocytic glycogenolysis impairs memory formation in rats in chickens (Gibbs *et al*., 2006; Newman *et al*., 2011; Suzuki *et al*., 2011). These findings indicate that glycogen storage and catabolism is an essential specialization of astrocytes, as lactate derived by astrocytes from glucose metabolism alone is insufficient for healthy neuronal function. These functions directly involve proteins which serve as astrocyte markers, including EAAT1, EAAT2 and glutamine synthetase (GS), as well as astrocyte markers that are indirectly involved, such as aldehyde dehydrogenase 1 family member 1 (Aldh1L1) which removes formate in the process of converting folic acid into glutamate (Champion *et al*., 1994).

Astrocytes can also be distinguished by the complex folding of the plasma membrane at the ultrastructural level, and by using haematoxylin and eosin staining due to the strong acidophilia of the cytoplasm (Luse, 1956). In glioma large 60-angstrom thick fibrils that are extremely acidophilic appear, which were later found to be most characteristic of Alexander Disease which results from a mutation in glial fibrillary acidic protein (GFAP), a highly acidic protein specifically expressed in astrocytes in the adult brain (Alexander, 1949; Brenner *et al*., 2001). This is related to reactive astrogliosis, wherein 'reactive astrocytes' migrate to site of a pathological insult and become hypertrophic by upregulating type III intermediate filament proteins including GFAP, vimentin (VIM) and nestin (Sofroniew & Vinters, 2010). This can

lead to the formation of the glial scar, which is a tight formation of astrocytes that secrete inhibitory molecules to prevent neuronal regeneration, which is thought to be one of the primary barriers to effective recovery from lesions to the central nervous system (CNS) (McKeon *et al*., 1991). However, it is now known that not all reactive astrocytes have harmful effects, as although A1 astrocytes which upregulate classical complement cascade genes for neurotoxic effects, A2 astrocytes upregulate neurotrophic factors that are protective (Zamanian *et al*., 2012; Liddelow *et al*., 2017). Blocking A1 astrocytes appears to be effective at treating the loss of neurons in models of CNS injury, which indicates reactive astrogliosis plays a key role in how the brain responds to injury (Yun *et al*., 2018; Guttenplan *et al*., 2020). However, the mechanism and role of glial scar formation remains unclear. Glial scar formation is impaired in $GFAP^{-/-}/VIM^{-/-}$ mice, but not $GFAP^{-/-}$ or $VIM^{-/-}$ mice, indicating these two intermediate filaments can functionally compensate for each other (Pekny *et al*., 1999). This view is also supported by their reciprocal expression profile GFAP and VIM during development, in which VIM is predominantly expressed in radial glia until they begin to differentiate into astrocytes, at which point GFAP becomes predominantly expressed (Dahl *et al*., 1981). Generally, $GFAP^{-/-}/VIM^{-/-}$ mice display a slower healing of the CNS and altered astrocyte responses to neurotoxic damage, however, they also show generally better neuronal regeneration (Menet *et al*., 2003; Wilhelmsson *et al*., 2004; Kamphius *et al*., 2015). Mice deficient in GFAP lack astrocytes with intermediate filaments, yet surprisingly $GFAP^{-/-}$ mice still survive and reproduce normally, and $VIM^{-/-}$ mice are healthy except for a few specific changes in their response to pathology, and otherwise benign factors like body fat accumulation (Pekny *et al*., 1995; dos Santos *et al*., 2015; Wilhelmsson *et al*., 2019). It may be that intermediate filaments accelerate reactive astrogliosis, but are otherwise not essential to survival, as the speed of vesicle trafficking is significantly reduced in astrocytes deficient in VIM and GFAP, or nestin, in response to inflammation (Potokar *et al*., 2010; Vardjan *et al*., 2012; Pekny *et al*., 2020). Nevertheless, GFAP and VIM expression serves as a useful marker of reactive astrogliosis when investigating astrocytes in pathological conditions. Surprisingly, VIM has been relatively rarely studied as an astrocyte marker, and a better understanding of its role will reveal insights into the role of astrocytes in cerebral pathologies.

3. Astrocytes: Regional Heterogeneity

The contribution of astrocytes to region-specific brain functions is supported by their developmental trajectory in developing mouse brain and their regional heterogeneity in the adult mouse brain. Interactions between neurons and astrocytes during the development of the central nervous system suggest that the heterogeneous regional distributions of astrocytes are genetically patterned from early life. Cortical columns of the mouse neocortex contain neurons and astrocytes that share a common precursor — radial glial cells projecting from the ventricular to the pial surface that acts as a scaffold for differentiating cells to migrate along within the column (Noctor *et al*., 2001; Noctor *et al*., 2004; Magavi *et al*., 2012; Gao *et al*., 2014). The differentiation, astrocyte subtype, position and regional gene expression profile of spinal cord astrocytes is genetically patterned prenatally during neurulation by the position of neural progenitor cells, and disrupting this patterning impairs the postnatal development of motor circuits (Pringle *et al*., 2003; Muroyama *et al*., 2005; Hochstim *et al*., 2008; Tsai *et al*., 2012; Molofsky *et al*., 2014). In the postnatal mouse cerebellum, astrocytes and GABAergic interneurons of the white matter emerge from the same neural progenitor cells, and purkinje neuron signaling to neighboring astrocytes can induce switches between the specialized astrocytic types found in the cerebellum (Parmigiani *et al*., 2015; Farmer *et al*., 2016). Together these studies show that the differentiation of neurons and astrocytes is closely associated in all three major subdivisions of the central nervous system, and that astrocytes appear to be positioned with respect to surrounding neuronal circuits.

In the mammalian brain, astrocytes are arranged in a non-overlapping organization known as domains, such that their morphologies rarely overlap in space, maximizing the spatial efficiency of their contacts with surrounding cells (Bushong *et al*., 2002). However, the density of astrocytes in the adult mouse brain varies dramatically between regions, indicating their involvement is varies dependent on brain functions (Emsley & Macklis, 2006). The involvement of astrocytes in synaptogenesis also varies regionally in the mouse brain, as the expression of SPARC varies along the dorsoventral axis of the mouse brain, such that mouse astrocyte:neuron cocultures must be both from cortical or subcortical regions for functional synapses to form (Morel *et al*., 2017). Heterogeneity in astrocyte function exists even within cortical areas, as astrocyte subtypes in the mouse cortex can be distinguished both by their transcriptomic profile and their location within cortical layers (Batiuk *et al*., 2020; Bayraktar *et al*., 2020). These transcriptomic profiles also exhibit a region-dependent aging response,

which can determine whether they exhibit a neuroinflammatory phenotype (Boisvert *et al*., 2018; Clarke *et al*., 2018).

In the adult brain, astrocytes can modulate region-specific neuronal circuits to affect behavioural outputs. In many brain regions astrocytes are arranged such that they preferentially interact with specific neuronal populations, as they can differentially modulate motor pathways in the basal ganglia and cortical interneuron subpopulations in the visual cortex and hippocampus (Perea *et al.*, 2014; Martin *et al*., 2015; Tan *et al*., 2017). Many region-specific brain functions can be impaired by genetically ablating astrocytes in the given region, including long-term memory formation in the hippocampus, attentional control in the striatum, glucose-sensing by the hypothalamus, and reward signaling in the nucleus accumbens (Suzuki *et al.*, 2011; García-Cáceres *et al.,* 2016; Nagai *et al*., 2019; Corkrum *et al*., 2020). Astrocyte activity is also capable of compensating for neuronal activity, as the pacemaker function of the suprachiasmatic nucleus can be initiated and sustained solely by either astrocytic *or* neuronal clock gene expression, albeit with different period length (Brancaccio *et al*., 2019). The exact mechanism by which astrocytes modulate specific neuronal circuits is normally suggested to relate to gliotransmission, the ability of astrocytes to participate in synaptic signalling ATP, d-serine or glutamate to neurons (Covelo & Araque, 2018). However, there is an ongoing debate as to whether gliotransmission occurs at meaningful levels *in vivo* and is not based on non-physiological methods (Fiacco & McCarthy, 2018; Savtchouk & Volterra, 2018).

4. Human studies

While these findings demonstrate regional specificity of astrocytic signalling and connectivity in the brain, they were derived almost exclusively from animal models. Human astrocytes are far more diverse and complex in structure than those found in rodents (Oberheim et al., 2009), such that regional specificities may be even more pronounced in the human brain. A regional characterisation of human astrocytes could provide important knowledge for the entire neuroscience field, shedding further light on the organization and evolution of human brain circuitries.

i. Morphology

Astrocytes may distinguish human brain function from other mammals. First, from mouse to man cortical astrocytes have increased in size more than cortical neurons, which may reflect a relative increase in functional priority (Oberheim *et al*., 2006). Second, human protoplasmic astrocytes are similarly arranged in domains, however human astrocytes appear more functionally efficient as they fire calcium waves at a rate four times faster than those of mouse astrocytes (Oberheim *et al*., 2009). Presently, human astrocytic subtypes are qualitatively identified by their morphology and cortical location. Interlaminar and varicose projection astrocytes may mediate higher-order cognitive processes as both have exceptionally long processes, and lower-order primates lack only varicose projection astrocytes (Sosunov *et al*., 2014). Third, human astrocytes appear to have functional differences. For example, protoplasmic astrocytes of the human anterior cingulate cortex (ACC) display thorny spine-like protrusions that are not found in rodents (Torres-Platas *et al*., 2011; Sosunov *et al*., 2014). Such features may explain why human protoplasmic astrocytes grafts can improve learning in adult chimeric mice and propagate intracellular calcium signals threefold faster than mouse protoplasmic astrocytes in the same regions (Han *et al*., 2013).

ii. Gene expression

Although astrocytic subtypes are currently classified by qualitative morphology, they may also differ in their function. Functional subtypes of astrocytes can be identified by gene expression comparisons from single-cell RNA sequencing data—the transcriptome—of cells isolated from tissue using methods such as fluorescent-activated cell sorting (FACS) or laser capture microdissection (LCM). These methods have identified glial subtypes based on differential gene expression profiles for oligodendrocytes, microglia and astrocytes in the mouse brain (Grabert *et al*., 2015; Marques *et al*., 2016; Batiuk *et al*., 2020; Bayraktar *et al*., 2020). However, astrocytes in the human brain express genes not found in astrocytes of the mouse brain, which raises doubt about whether regional heterogeneity of astrocyte gene expression in the mouse brain is accurately representative of astrocytes in the human brain (Zhang *et al*., 2016). This is suggested by recent studies using unsupervised clustering of differential gene expression in postmortem human brain tissue, which revealed only two major clusters for astrocytes, which seems less heterogeneous than that for neurons, microglia and

oligodendrocytes based on current findings (Masuda *et al*., 2019; Nagy *et al*., 2020). For now, this suggests that the regional heterogeneity of astrocytes in the human brain may be better represented by features other than differential regional expression, such as regional densities.

iii. Density

The distribution of astrocyte morphological or functional subtypes may also be informative to the cellular organisation of brain circuits. While the human brain has an average glia/neuron ratio of approximately 1:1, regions with lower neuronal density have higher glia/neuron ratios (Herculano-Houzel *et al*., 2008; Herculano-Houzel, 2014). In the cerebral lobes of healthy human adults, the density of astrocytes identified using morphological criteria (soma shape and size) does not appear to significantly vary with sex or age, and densities are relatively similar except in the occipital lobe (Pelvig *et al*., 2008; Fabricius *et al*., 2013; Kaalund *et al*., 2019). This non-uniform distribution of astrocytes may be more prominent in subcortical regions, based on previous work by the Mechawar lab showing regional differences in the mRNA and protein expression of GFAP in postmortem brain regions from healthy adults (Torres-Platas *et al*., 2016). Briefly, the caudate nucleus and mediodorsal thalamus had significantly greater GFAP mRNA levels than cerebellar, motor and visual cortex, and GFAP-immunoreactive (GFAP-IR) astrocytes in the caudate and thalamus were qualitatively distinct in their morphology and distribution. This was the first study suggesting region-specific differences in human astrocyte populations of the healthy human brain. However, the relationship between elevated GFAP expression and astrocyte distribution in human subcortical regions remains unclear.

5. Astrocytes in depression and suicide

i. Clinical definitions

Given astrocytes have many roles in the human brain, it is unsurprising that they have been implicated by postmortem studies in many neurological and psychiatric conditions (Pekny *et al*., 2016; Kim *et al*., 2018). Our interest in studying astrocytes partly stems with the consistent and extensive literature of postmortem investigations on major depressive disorder (MDD)

(Rajkowska *et al*., 2013). More than 250 million individuals are diagnosed globally with MDD, and the incidence rate has been increasing from 1990 to 2017 (Liu *et al*., 2020). An individual can be diagnosed with MDD when for a two week period they consistently experience either depressed mood or anhedonia, along with four of the following secondary symptoms: appetite or weight changes, sleep difficulties, psychomotor agitation, physical fatigue, attentional difficulties, feelings of guilt or worthlessness, or suicidal ideation. Interestingly, severe depression rating scores are more commonly include non-somatic symptoms, namely depressed mood, anhedonia, feelings of worthlessness and suicidal ideation (Tolentino & Schmidt, 2018). Approximately 15% of individuals with a lifetime diagnosis of MDD attempt suicide, this is more likely in those with severe depression scores (Chen & Dilsaver, 1996). As both MDD and suicide show increased prevalence in twin studies, suggesting MDD cases which eventually leads to suicide may partly involve heritable factors (Lester, 1986; McGuffin *et al*., 1996). However, suicide is also associated with polygenic risk scores for other psychiatric conditions, including bipolar disorder and schizophrenia (Mullins *et al*., 2019). Suicide accounts for over 800,000 deaths worldwide each year, and although the total number has increased from 1990 to 2016, the age standardized mortality rate during this period has in fact decreased similarly to the general global decrease in mortality (Naghavi, 2019). Despite this, suicide is the leading cause of death among young adults, and decreased suicide rates have in some cases led to increased male:female ratio of suicide (WHO, 2014; Østergaard, 2018). Moreover, the suicide rates of certain countries are veering further away from their 2030 sustainable development goals, which motivates a greater effort to understand and prevent suicide (Dandona et al., 2018).

ii. Animal studies

Although many neurological and psychiatric conditions have genetic models based on mutations identified in human patients, MDD has no single risk allele and no reliable genetic rodent model. Mice susceptible to chronic social defeat stress have been shown to have an electrophysiological signature in MDD-associated networks that is distinct from those involved with MDD pathology and treatment, suggesting that stress networks and MDD networks are functionally associated but structurally distinct in the rodent brain (Hultman *et al*., 2018). Rodent models of stress also induce changes in DNA methylation of neurons and glia, suggesting depression might result from epigenetic mechanisms which modify the transcription

of important proteins (Bagot *et al*., 2014; Lorsch *et al*., 2019). Given the heterogeneity of MDD and its differences to stress, animal models of MDD focus on replicating a specific symptom of MDD, such that no single model alone can clearly identify an MDD phenotype (Nestler & Hyman, 2010). Popular models involve a physical or social stressor mimicking a life event that would predispose a human to MDD, and include maternal separation, learned helplessness, repeated restraint stress, chronic unpredictable stress, social isolation and chronic social defeat stress (Ménard *et al*., 2016). Many models have focused on modelling anhedonia, as it is a symptom of severe forms of MDD, which has led to many investigations of dopaminergic reward systems in rodent stress models. Astrocytes may play important roles in rodent stress models, given recent reports implicating astrocytes in associated behavioural responses including fear, memory formation, drug-induced reward and movement (Martín *et al*., 2015; Martin-Fernandez *et al*., 2017; Yu *et al*., 2018; Corkrum *et al*., 2019; Gomez *et al*., 2019; Corkrum *et al*., 2020; Mazaré *et al*., 2020; Kol *et al*., 2020; Cavaccini *et al*., 2020).

For many rodent models of depression, tonic inhibition of dopaminergic neurons in the ventral tegmental area (VTA) mediates a susceptibility phenotype, whereas phasic activation of these neurons mediates a resilient phenotype (Tye *et al*., 2013). An increased proportion of phasic firing by dopaminergic neurons in the VTA that then project to the nucleus accumbens (NAc) is associated with susceptibility to social defeat stress and inducing phasic firing optogenetically can convert resilient mice into susceptible mice (Chaudhury *et al*., 2013). Synaptic potentiation of excitatory synapses onto lateral habenula (LH) neurons that then project to the VTA has been implicated in two learned helplessness models, indicating overactivity of the LH may mediate animal models of depression (Li *et al*., 2011). This contributes to the idea the LH as the 'anti-reward centre', its activity is normally time-locked to the absence of an expected reward (Stamatakis *et al*., 2012). The increased proportion of bursting neurons in the LH in congenital learned helplessness of rats has been strongly associated with an upregulation of an astrocyte potassium channel ($K_{ir}4.1$) at membranes apposing neuronal cell bodies, depleting local extracellular potassium levels which in turn alters neuronal firing profiles (Li *et al*., 2013; Cui *et al*., 2018). As $K_{ir}4.1$ upregulation in astrocytes prevents the voltage-dependent block of NMDA receptors, the antidepressant effect of ketamine has been partly explained by pharmacologically inhibiting overactive NMDA receptors in the LH, which otherwise lead to inhibition of glutamatergic input to reward centres (Yang *et al*., 2018). However, it is important to note that ketamine mediates antidepressant effects in rodent models not associated with NMDA receptor inhibition, but rather, AMPA

receptor upregulation, which indicates ketamine does not have a simple unidirectional antidepressant effect on glutamatergic signalling (Autry *et al*., 2011; Zanos *et al*., 2016). Nevertheless, this evidence implicates astrocyte dysfunction in MDD and is presently the strongest argument to date for the antidepressant actions of ketamine, which is perhaps the most suitable pharmacological candidate for responding to suicidal crisis due to its uniquely rapid ability to potently reduce suicidal ideation (Wilkinson *et al*., 2017).

Inhibiting hippocampal neurogenesis slows the glucocorticoid and behavioural recovery of mice to many depression models, suggesting that hippocampal neurogenesis moderates the ability of the HPA axis to accelerate recovery to stressor (Snyder *et al*., 2011). Astrocytes may partly mediate this effect as they integrate newborn hippocampal neurons into glutamatergic circuits and have impaired glutamate transport in the hippocampus in rodent models of depression (Sultan *et al*., 2015; Nasca *et al*., 2017). Impaired glutamatergic output from the hippocampus to reward circuitry is implicated in rodent models of depression, as reactivating positive memories in male mice by photostimulating the same glutamatergic hippocampal circuits to the NAc that were previously active during exposure to a female mouse induces resilience to stress in swim tests (Ramirez *et al*., 2015).

The role of astrocytes in the inflammation and neurodegeneration theory of depression has been less extensively studied in rodent models. It is difficult to dissociate whether astrocyte differences in inflammatory responses to stress reflect only differences to the physical stressor rather than differences in affective response to the experience of stress (Sántha *et al*., 2016). However, genetically and pharmacologically impairing inflammatory signalling by astrocytes can mediate depressive-like behaviours, indicating they are sufficient and associated with depressive-like behaviours (Leng *et al*., 2018; Xiong *et al*., 2019).

Collectively, the above rodent studies provide the strongest available support for roles of astrocytes in depression. However, they are not the primary support for postmortem studies for the roles of astrocytes in depression. This is because postmortem research cannot rely on *in vivo* manipulations, but instead makes *in situ* comparisons of the distribution, density and morphology of cells, or of mRNA, protein and methylation levels. Regarding astrocytes in depression, postmortem studies are most related to animal studies which have consistently shown a downregulation of GFAP protein, or a lower density of GFAP-IR astrocytes, in MDD-associated brain regions. For instance, when astrocyte densities were assessed in the Wistar Kyoto rat breed which has a depressive phenotype, mood-associated regions were found to

have lower GFAP-IR astrocyte densities although S100B-IR astrocyte and NeuN-IR neuron densities were unchanged (Gosselin *et al*., 2009). Another study also found a decrease in GFAP-IR, but not S100B-IR, astrocytes in chronically stressed Sprague-Dawley rats, along with a significantly decreased length and spatial distribution of GFAP-IR astrocyte morphology (Tynan *et al*., 2013). Similarly, chronic stress can decrease the morphological volume and number of GFAP-IR astrocytes in the hippocampus of C57BL/6J mice and has been linked to a downregulation of circular RNAs which also occurs in the blood of human patients (Zhao *et al*., 2018; Zhang *et al*., 2020). As this circular RNA has been linked to decreasing the demethylation of other genes in astrocytes, this implicates depression may involve epigenetic changes in astrocytes leading to abnormally smaller morphologies and lower numbers in the hippocampus. However, the density of astrocytes varies across many regions in rodent models of depression, as early life deprivation to Fischer rats induces greater reductions of GFAP-IR astrocyte density than total cell density in many regions, including the hippocampus, cingulate cortex, prefrontal cortex and basolateral amygdala, suggesting depression-like phenotypes preferentially affect GFAP-IR astrocyte densities (Leventopoulos *et al*., 2007). Chronic unpredictable stress in Sprague-Dawley rats induces a decrease in acetate metabolism and GFAP expression, and its correction by riluzole is correlated with upregulation EAAT2 (Banasr *et al*., 2010). This finding particularly suggests that increasing the activity of remaining GFAP-IR astrocytes can normalize astrocyte pathology in depression, which may in part associated with insufficient glutamate reuptake. Surprisingly, even alternative non-prescribed treatments for depression such as electroacupuncture, xiaoyaosan and the alkaloid hallucinogens have also been shown to reverse both depression phenotypes and hippocampal decreases in GFAP mRNA and protein in chronically stressed rodents (Liu *et al*., 2011; Liu *et al*., 2017; Ding *et al*., 2017). Together these findings have been used to support the findings that MDD-associated astrocyte changes are specific to GFAP-IR astrocytes, and may involve downregulated GFAP expression, impaired glutamate reuptake or morphological atrophy. As toxic lesions of astrocytes in the rat medial prefrontal cortex lead to deficits in attention and memory, but also the progressive loss of neurons, if depression induces losses of GFAP-IR astrocytes it might precede neuronal dysfunction or atrophy (Lima *et al*., 2014).

iii. Human studies

Human postmortem studies have shown a general loss of function of astrocytes in mood-associated brain regions of depressed individuals. First, there are decreased mRNA and protein levels of GFAP in mood-associated brain regions in individuals with MDD, relative to matched controls (Torres-Platas *et al*., 2016). Second, there is a decreased number of overall glia, and of GFAP-IR astrocytes, observed in postmortem samples from individuals with MDD, relative to matched controls (Gittins & Harrison, 2011; Rajkowska *et al*., 2018). Third, there is a downregulation of functional proteins mediating astrocyte functions, including glutamate transporters and gap junction proteins (Powers *et al*., 2019; Tanti *et al*., 2019). In contrast to this generally decreased function of astrocytes in depressed suicides, an abnormal hypertrophy of fibrous astrocyte processes has been observed in the anterior cingulate cortex of depressed suicides, relative to matched controls (Torres-Platas *et al*., 2011).

Together these postmortem findings suggest that astrocytes are less effective in their general functions in depression and may in response take on pathological phenotypes as suggested by their morphology. However, a critical question and motivating factor for this research project is determining whether the general decrease in GFAP levels and GFAP-IR astrocytes corresponds either to a decreased number of astrocytes, or instead to a general downregulation of astrocyte markers. As almost all postmortem astrocyte studies have focused on GFAP-IR astrocytes, it is difficult to determine whether other astrocyte populations are affected, and as a result, whether depression is only specifically affecting reactive astrogliosis. It is also unclear whether changes in astrocyte density accompany changes in other factors, such as astrocyte morphology or vascular density, as most studies only compare one cell type at a time, making it difficult to determine which pathological features are most prominent in depression. Both a decreased number of astrocytes, or a decreased expression of astrocyte functional proteins, would lead to reduced neurotransmitter clearance which may be involved with the monoaminergic hypothesis and glutamate hypothesis of depression. By distinguishing between reduced number or reduced activity of astrocytes, it will provide a better understanding of the aetiopathology of depression and will also narrow the potential treatment strategies for strengthening astrocyte activity in depressed individuals.

6. Rationale & Objectives

This project was undertaken to answer fundamental questions underlying the association of astrocytes with depression and suicide. No study had assessed the regional variations of astrocyte density and morphology in human brain samples from healthy or depressed individuals, or assessed this using multiple astrocyte markers, so it was difficult to acknowledge how strong and widespread astrocyte differences could be in individuals with MDD. Moreover, no study had assessed whether vascular densities were associated with the regional heterogeneity of astrocyte densities throughout the brains of healthy or depressed individuals, so it was difficult to acknowledge whether the anatomical distribution of astrocytes is more evidently affected by depression than the vasculature they interact with, and to rule out the possibility that astrocyte abnormalities are not the result of changes in their signalling partners.

Our global working hypothesis was that, in mood-associated brain regions, depressed suicides would have reduced regional astrocyte densities and abnormal astrocyte morphology relative to matched healthy controls. This hypothesis is supported by previous findings from our group (Torres-Platas *et al*., 2011; Torres-Platas *et al*., 2016). We decided on using VIM as an additional, secondary marker to GFAP in all experiments in the present project, due to its lack of characterization in postmortem human brain and because it has a clear functional relationship with GFAP. We also recognized its clarity at high magnifications of immunohistochemical staining uniquely facilitated fine morphometric tracing of astrocyte-specific labelling in postmortem samples, which prioritized its use over other alternative astrocyte markers to GFAP. By using two astrocyte markers in the same samples, this ensured that observations were not limited to the expression of the chosen protein, allowing for a more representative and reliable view of astrocytes in the human brain, and to help determine whether depression-related effects were not limited to GFAP expression.

The overarching goal of this thesis was to characterize the regional heterogeneity of the density and morphology of astrocytes in postmortem adult brain samples from depressed suicides and matched controls. The strength of our approach was the unparalleled use of multiple analyses within the same postmortem samples.

With this in mind, the following specific objectives were experimentally pursued:

1) *To characterize the regional density, morphology and distribution of VIM-IR and GFAP-IR in mood-associated brain regions of the healthy adult brain.*

2) *To quantitatively compare the density of VIM-IR and GFAP-IR astrocytes, and the morphology of VIM-IR astrocytes, between depressed suicides and matched controls in mood-associated brain regions.*

3) *To quantitatively compare the density of CD31-IR blood vessels between depressed suicides and matched controls in mood-associated brain regions.*

CHAPTER II

Characterization of vimentin-immunoreactive astrocytes in the human brain

Preface

I first arrived in the Mechawar lab in Easter of 2016 as part of my third rotation, shortly after the publication of a paper by the McGill Group for Suicide showing that the mRNA and protein levels of an astrocyte marker — glial fibrillary acidic protein (GFAP) — were downregulated in subcortical brain regions from depressed suicides (Torres-Platas *et al*., 2016). While qualitatively it appeared that GFAP mRNA levels correlated with the relative abundance of astrocytes immunoreactive (-IR) for GFAP in healthy controls, it remained unclear whether these regional protein and mRNA decreases in depressed suicides were accompanied by a reduced density of GFAP-IR astrocytes. No papers had characterized the properties of GFAP-IR astrocytes in human subcortical regions, nor were there any alternative astrocyte markers that worked as effectively as GFAP for immunohistochemistry in postmortem brain tissue using our experimental setup. Vimentin (VIM) was chosen as a marker for testing, as it shared similar localization and function to GFAP, and no detailed characterization of VIM-IR astrocytes had been performed in postmortem samples from healthy adult individuals. As VIM is more strongly expressed in astrocytes of the developing brain, we were surprised to see that with DAB immunolabelling for VIM in adult postmortem brain samples revealed a very clear view of intricate astrocyte morphology, and also revealed many blood vessels.

Given these preliminary observations, my PhD project in the Mechawar lab in the fall of 2016 began with the following objective:

> *To characterize the regional density, morphology and distribution of VIM-IR and GFAP-IR in mood-associated brain regions of the healthy adult brain.*

The rationale of this first study was to demonstrate VIM as an effective marker for studying astrocytes in postmortem brain samples from healthy adult individuals, and to fundamentally characterize astrocytes in brain regions that have been previously reported to have astrocyte abnormalities in depression. We observed VIM-IR and GFAP-IR astrocytes differed in their regional densities, and that the fine morphometry of protoplasmic VIM-IR astrocytes in the human brain was 2-to-3-fold larger than in the mouse brain. We also found that both VIM-IR

and GFAP-IR astrocyte densities inversely correlated with vascular densities, indicating for the first time that regional heterogeneity in astrocyte densities may be related to the vascular organization of the brain.

Characterization of vimentin-immunoreactive astrocytes in the human brain

Liam Anuj O'Leary[1,2], Maria Antonietta Davoli[1], Claudia Belliveau[1,2], Arnaud Tanti[1], Jie Christopher Ma[1], William Todd Farmer[3], Gustavo Turecki[1,2,4], Keith Kazuo Murai[3], Naguib Mechawar[1,2,4*]

[1]McGill Group for Suicide Studies, Douglas Mental Health University Institute, Verdun, QC, Canada

[2]Integrated Program in Neuroscience, McGill University, Montreal, Canada

[3]Centre for Research in Neuroscience, Brain Repair and Integrative Neuroscience Program, Department of Neurology and Neurosurgery, The Research Institute of McGill University Health Centre, Montreal General Hospital, Montreal, QC, Canada

[4]Department of Psychiatry, McGill University, Montreal, QC, Canada

* Correspondence:
Naguib Mechawar, PhD
naguib.mechawar@mcgill.ca

Keywords: human, mouse, astrocyte, vimentin, GFAP, stereology, morphology (Min.5-Max. 8)

References: 59

Words: 7688

Figures: 9

Tables: 2

Abstract

Astrocytes are commonly identified by their expression of the intermediate filament protein glial fibrillary acidic protein (GFAP). GFAP-immunoreactive (GFAP-IR) astrocytes exhibit regional heterogeneity in density and morphology in the mouse brain as well as morphological

diversity in the human cortex. However, regional variations in astrocyte distribution and morphology remain to be assessed comprehensively. This was the overarching objective of this postmortem study, which mainly exploited the immunolabeling of vimentin (VIM), an intermediate filament protein expressed by astrocytes and endothelial cells which presents the advantage of more extensively labelling cell structures. We compared the densities of VIM-immunoreactive (VIM-IR) and GFAP-IR astrocytes in various brain regions (prefrontal and primary visual cortex, caudate nucleus, mediodorsal thalamus) from male individuals having died suddenly in the absence of neurological or psychiatric conditions. The morphometric properties of VIM-IR in these brain regions were also assessed. We found that VIM-IR astrocytes generally express the canonical astrocytic markers Aldh1L1 and GFAP but that VIM-IR astrocytes are less abundant than GFAP-IR astrocytes in all human brain regions, particularly in the thalamus, where VIM-IR cells were nearly absent. About 20% of all VIM-IR astrocytes presented a twin cell morphology, a phenomenon rarely observed for GFAP-IR astrocytes. Furthermore VIM-IR astrocytes in the striatum were often seen to extend numerous parallel processes which seemed to give rise to large VIM-IR fiber bundles projecting over long distances. Moreover, morphometric analyses revealed that VIM-IR astrocytes were more complex than their mouse counterparts in functionally homologous brain regions, as has been previously reported for GFAP-IR astrocytes. Lastly, the density of GFAP-IR astrocytes in grey and white matter were inversely correlated with vascular density, but for VIM-IR astrocytes this was only the case in grey matter, suggesting that gliovascular interactions may especially influence the regional heterogeneity of GFAP-IR astrocytes. Taken together, these findings reveal special features displayed uniquely by human VIM-IR astrocytes and illustrate that astrocytes display important region- and marker-specific differences in the healthy human brain.

Introduction

Astrocytes constitute approximately 20% of glial cells in the human neocortex, although they vary considerably in abundance throughout this region (Pakkenberg *et al.*, 2003; Pelvig *et al*., 2008; von Bartheld *et al*., 2016). Astrocytes have many functions that regulate the central nervous system (CNS), including coupling neuronal activity to blood flow, providing metabolic support and neurotransmitters to neurons, reuptaking neurotransmitters from the

synaptic cleft, and controlling the proliferation and repair of neurons (Takano *et al*., 2006; Choi *et al*., 2012; Covelo & Araque, 2017; Garcia *et al*., 2004; McKeon *et al*., 1994; Pellerin & Magistretti, 1994). Despite their ubiquity and importance, the distributional and morphological features of astrocytes in the human brain have not been extensively characterized, particularly in non-cortical regions. Elegant work by the Nedergaard group has highlighted that human cortical astrocytes display larger cell bodies and more numerous and extensively branched processes than their rodent counterparts (Oberheim *et al*., 2009). These investigators also described astrocyte subtypes in human cortical gray matter (interlaminar and varicose projection) that are absent in rodents (Oberheim *et al*., 2009). More recently, Sosunov and colleagues described a similar diversity of astrocytes in the human hippocampus (Sosunov *et al.*, 2014). Little information has been published on non-cortical astrocytes however, and a systematic comparison of astrocyte densities and morphological properties across human brain regions has yet to be published. Such work has been done for mouse astrocytes, which exhibit substantial regional heterogeneity in their density and morphology (Emsley & Macklis, 2006; Eilam *et al*., 2016), and their functional interactions with neurons (Morel *et al*., 2017). Moreover, regional differences in the distribution and function of astrocytes in the mouse brain are developmentally patterned and actively maintained by their neighboring neurons (Magavi *et al*., 2012; Gao *et al*., 2014; Farmer *et al*., 2016). The regional patterning of astrocytes likely coordinates their functional roles in neuronal circuits, given that mouse astrocytes can selectively contact specific subtypes of neurons and mediate region-specific functions (Suzuki *et al*., 2011; Perea *et al*., 2014; Martín *et al*., 2015; Garcia-Caceres *et al*., 2016).

The cytoskeleton of astrocytes is characteristically defined by the relatively high expression of three components: actin, glial fibrillary acidic protein (GFAP), and vimentin (VIM) (Chui *et al*., 1981). Both VIM and GFAP share functional properties, as they are type III intermediate filaments predominantly found in astrocytes and upregulated in cells undergoing reactive astrogliosis (Pixley & De Vellis, 1984). Moreover, mouse astrocytes that lack both VIM and GFAP have impaired glial scar formation and decelerated immune response at the level of vesicle trafficking, indicating that VIM and GFAP regulate how astrocytes responses to inflammation and can functionally compensate for each other (Wilhelmsson *et al.*, 2004; Potokar *et al*., 2010; Vardjan *et al*., 2012). However, VIM appears to have more regulatory roles for astrocyte structure, as the translation of two other intermediate filaments common to astrocytes — nestin and synemin — require VIM, but not GFAP (Pekny *et al*., 1999; Jing *et al*., 2007). Moreover, there is a reciprocal relationship between the relative expression of VIM

and GFAP with age, such that prior to cortical myelination, developing astrocytes have high VIM and low GFAP expression, whereas in adulthood, mature astrocytes have low VIM and high GFAP expression (Dahl, 1981). This may be why most morphological descriptions of mature astrocytes, in both model species and humans, have been largely based on the analysis of cells immunoreactive (-IR) for GFAP, but not VIM. As in the mouse brain, there may be substantial regional heterogeneity of GFAP-IR astrocytes in the human brain, given that there are significant inter-regional differences in GFAP mRNA and protein expression which appear qualitatively related to the distribution of human GFAP-IR astrocytes (Torres-Platas *et al*., 2016). In contrast to GFAP-IR astrocytes, little is known of the general properties or regional heterogeneity of VIM-IR astrocytes in adult CNS tissues, even though they were observed in postmortem human brain tissue nearly three decades ago (Yamada *et al.*, 1992).

Based on our preliminary observations in adult human cerebral cortex that VIM clearly labels astrocytic cell bodies and their processes (unpublished data), and that VIM-IR and GFAP-IR astrocytes are both abundant, we pursued a more systematic analysis of VIM-IR astrocytes in different regions of the human brain. Here, we report the first quantitative regional data on human VIM-IR astrocytes. More specifically, we determined the densities and morphometric properties of VIM-IR astrocytes in four regions of the adult human brain: prefrontal cortex, primary visual cortex, caudate nucleus and dorsomedial thalamus. We selected the same cortical and subcortical regions we previously used in regional comparisons of astrocytic markers (Torres-Platas et al., 2016; Nagy et al., 2017). The visual cortex was of particular interest as it presents interlaminar astrocytes, a primate-specific subtype of astrocyte (Oberheim et al., 2009). In addition to co-immunolabeling experiments to determine the overlap of VIM-IR astrocytes with two other canonical astrocyte markers — GFAP and Aldh1L1 — we generated similar data for mouse VIM-IR astrocytes which allowed for cross-species comparisons. Finally, we assessed whether the regional heterogeneity in vascular density was associated with that of astrocyte density and morphometry. This study is the first to characterize VIM-IR astrocytes in adult human and mouse brains and to quantify the extent of regional heterogeneity for astrocytes across regions, markers and species.

Materials and Methods

Brain samples

This study was approved by the Douglas Hospital Research Ethics Board. Brains were donated to the Douglas-Bell Canada Brain Bank by familial consent through the Quebec Coroner's Office, which ascertained the cause of death. Brain samples from 10 Caucasian male individuals having died suddenly without any known inflammatory, psychiatric or neurological disorder were analyzed (**Table 1**). Four brain regions were dissected from freshly received specimens of mediodorsal thalamus, dorsal caudate nucleus (precommissural level), and two cortical areas: prefrontal cortex (Brodmann area (BA) 8/9) and primary visual cortex (BA17).

Brain samples were also used from five adult male C57BL/6 mice (Charles-River Canada) which served as controls in a previous study (sub-chronic subcutaneous saline administration; Mahar *et al.*, 2011) approved by McGill University's Animal Care Committee (MACC approval ID: 5473). Four mouse brain regions were studied: the mediodorsal thalamus, the caudate-putamen (CPu, precomissural level), the frontal association cortex (FrA) and primary visual cortex (V1). Human BA8/9 and BA17 were seen as homologous to FrA and V1, respectively.

Furthermore, we examined three brains from adult *Aldh1L1*-Cre/ERT2; *Rosa26-TdTomato* transgenic mice (Montreal General Hospital Animal Use Protocol ID: 6005) generated by crossing Aldh1L1-Cre/ERT2 mice (JAX stock no. 031008) with Ai9 Rosa26-TdTomato reporter line mice (JAX stock no. 007909) (Madisen *et al.*, 2010; Srinivasan *et al.*, 2016). This Cre reporter strain enables highly specific targeting of TdTomato fluorescence in astrocytes in adult mouse CNS with a stronger signal and less background than antibody staining, and reveals over 90% of astrocytes immunolabelled with the astrocyte marker S100B (Winchenbach et al., 2016). All mice were group-housed on a 12:12 light:dark cycle with *ad libitum* access to food and water and sacrificed at two months of age (see below) following the policies and guidelines of the Canadian Council on Animal Care.

Tissue Processing

For 8 of the 10 human subjects, fresh 1cm^3 blocks of cerebral tissue were fixed overnight in 10% neutral buffered formalin, suspended in 30% sucrose solution until equilibrium was reached, flash frozen in -35°C isopentane, and cut on a sliding microtome into 50 µm-thick serial sections that were stored at -20°C in a cryoprotectant solution until they were processed for immunohistochemistry (IHC). For the remaining 2 subjects, samples were processed in the same way except that they were cut on a cryostat into 10 µm-thick serial sections until they were processed for double-labeling immunofluorescence (IF) and fluorescent *in situ* hybridization (FISH).

As described previously (Mahar *et al*., 2011), mice were anaesthetized using a mixture of ketamine (50 mg/kg, Vetrepharm, Canada), xylazine (5 mg/kg, Novopharm, Canada) and acepromazine (0.5 mg/kg, Ayerst, Canada), then perfused intracardially with ice-cold phosphate-buffered saline (PBS) followed by 4% formaldehyde in 0.1 M phosphate buffer. Brains were rapidly removed, fixed and suspended in sucrose as above before being cut coronally into 40 µm-thick serial sections on a cryostat and stored in cryoprotectant at -20°C until they were processed for IHC and IF.

Immunolabeling

All IHC and IF procedures were conducted at room temperature with three 5 min washes in phosphate-buffered saline (PBS) after each step except for after the pre-incubation blocking step. For IHC, sections were incubated for 20 min in 3% H_2O_2 to quench endogenous peroxidase activity, blocked for 1 hour in PBS containing 0.2% Triton-X (PBS-Tx-100) and 10% normal serum from the secondary antibody host species, and incubated overnight in PBS-Tx-100 containing 2% normal serum and primary antibody (**Table 2**). On the following day, sections were incubated in biotinylated secondary antibodies (Jackson; 1:500) for 1 hour, and then in avidin-biotin-peroxidase complex (Vector) for 30 min. Immunostaining was revealed by a 3 min incubation with a 3-3'-diaminobenzidine (DAB) peroxidase substrate kit (Vector Laboratories, SK-4100). Sections were mounted onto glass slides, dried overnight, dehydrated in a graded ethanol series, cleared in xylene, and coverslipped with Permount medium (Fisher Scientific). For double-labeling IF experiments, sections were incubated with both rabbit anti-VIM and chicken anti-GFAP primary antibodies to be bound respectively to secondary Alexa

Fluor 488- and Cy5-conjugated antibodies (Thermo Fisher). Sections were mounted onto glass slides and coverslipped in DAPI mounting medium (Vector).

For the IF experiment using transgenic mice, we assessed VIM-immunofluorescent cells in the mouse CPu, as in our sections it was the largest mouse brain region that was homologous to one of the human brain regions in this study. To assess whether VIM was commonly found in mouse GFAP-IR astrocytes and the extent to which it was expressed in all astrocytes in a given brain region, we made use of an available mouse genetic line for the astrocyte marker Aldh1L1. Of all known astrocyte markers to date, Aldh1L1 is the best for representing the majority of astrocytes, as it is expressed in the largest number of astrocytes. Transgenic animals were needed to assess the proportion of all astrocytes (as best revealed by Aldh1L1) that express VIM, because Aldh1L1 immunostaining is particularly challenging in mouse brain tissue (unpublished observations). Transgenic fluorescent reporter proteins also reveal the entire cell morphology, enabling us to qualitatively compare the extent of morphology revealed by VIM immunolabelling. Moreover, the increased strength and specificity of fluorescent reporter proteins over immunolabelling approaches facilitated a more precise localization between astrocytes expressing both VIM and Aldh1L1 proteins.

Fluorescent *in situ* hybridization (FISH)

To clearly confirm that human VIM-IR cells are astrocytes, we labeled Aldh1L1 expression, as it is the most widely and homogeneously expressed astrocytic marker (Cahoy *et al*., 2008). An RNAScope Multiplex Fluorescent v2 kit (Advanced Cell Diagnostics, Newark, CA, USA) with ALDH1L1 (catalogue no. 438881) and GFAP (catalogue no. 311801-C2) mRNA probes was used in combination with IF to label VIM (using the same protocol for VIM IF as in double-labeling experiments). Fresh-frozen sections (10 μm-thick) of prefrontal cortex were mounted onto charged glass slides, and stored at -80°C until the FISH assay was performed according to the manufacturer's instructions. Following the FISH protocol, a standard IF protocol was performed on slides, which involved an overnight incubation in primary antibody solution and an hour-long incubation in secondary antibody solution on the following day prior to coverslipping with mounting medium containing DAPI.

Double-labeling analysis

To assess the cellular co-localization of VIM protein with canonical astrocyte markers, images were acquired at 40X using a FV1200 laser scanning confocal microscope equipped with a motorized stage (Olympus, Japan). Sections from the caudate nucleus and prefrontal cortex were used, and as they were thin (10 µm thick), single acquisitions were performed instead of z-stacks to increase the efficiency of sampling. Cells were identified as GFAP+, VIM+ or GFAP+/VIM+. Data was expressed as the mean proportion of GFAP+ cells that were also VIM+ (GFAP+/VIM+), and the mean proportion of VIM+ cells that were also GFAP+ (VIM+/GFAP+). The same method was used for comparing VIM and Aldh1L1 co-localization. Per subject and region, GFAP protein co-localization was assessed in at least 85 VIM-IR cells, GFAP RNA co-localization was assessed in at least 70 VIM-IR cells, and Aldh1L1 RNA co-localization was assessed in at least 100 VIM-IR cells. For mouse co-localization analysis, a similar approach was used on all VIM-IR cells imaged within the CPu of one hemisphere in all three transgenic mice.

Stereological cell counting

VIM-IR and GFAP-IR astrocytes were counted using DAB immunolabelling visualized with brightfield microscopy on a workstation connected to a BX51 microscope equipped with a motorized stage and CX9000 camera (Olympus, Japan). An unbiased stereological approach was performed using StereoInvestigator software (MBF Bioscience, USA) and average regional astrocyte densities were calculated by dividing the total regional population estimate (obtained with the Optical Fractionator probe) by the total regional volume (obtained with the Cavalieri probe). For each subject and region counted, we selected four equally spaced sections from a series consisting of every twelfth section of the region of interest. We chose four sections as, across all subjects and regions, this was the largest stereological series available, and the largest number of sections that could fit on a single slide (preventing potential differences in mounted thickness between slides for the same subject and region). A contour was drawn around the perimeter of each section avoiding sectioning and staining artefacts. The Optical Fractionator Probe facilitates unbiased counting by randomly assigning counting frames at either a consistent number of sites or that cover a consistent area of the section contour. For this study, we chose to sample a consistent percentage area, to ensure the same

proportion was sampled for each slide despite considerable differences in section area between subjects and regions. Stereological counting rules were applied to the cell body of strongly stained cells with astrocytic morphology. A pilot study was performed on to identify the largest dissector height (18 µm with 1 µm guard zones) and smallest contour sampling size (5%) with which the probe could then provide total regional population estimates with an accurate Gundersen coefficient of error (CE, m=1) < 0.10. This pilot study was repeated for all objective magnifications at which astrocytes could be reliably distinguished with both markers — X40, X60 and x100. As all magnifications produced similar results, X40 magnification was chosen to increase the speed of counting. After all regional cell number estimates were acquired, the Cavalieri Estimator probe was used on the same contours used for cell counting (100µm grid spacing). These parameters for regional density estimates were sufficient to account for the heterogeneous distribution of astrocytes within each region, as there was very little difference between estimates achieved using the same parameters within the same contours in the pilot study.

Morphometric features

With the same slides and workstation used for stereological analysis, the fine morphometry of representative VIM-IR astrocytes was manually traced live using a computer-based tracing system with a 100X oil immersion objective and Neurolucida software (MBF Bioscience, USA). We employed manual 3D tracing as we have previously shown this method to be effective at revealing intricate differences in the fine morphology of human astrocytes (Torres-Platas *et al*., 2011). Briefly, the entire slide was scanned at 10X objective magnification and the location of representative cells for tracing was digitally recorded with respect to a reference point. Representative cells were identified and had to be: (1) unobstructed by neighboring cells; (2) similarly sized to neighboring cells; (3) equally stained across cellular compartments; (4) contained within the thickness of the section; (5) in contact with VIM-IR blood vessels via clear endfeet contacts. After switching to the 100X oil immersion objective, the locations were revisited in chronological order, and the first four cells that continued to fulfil the criteria for representative cells at 100X magnification were traced. A biased sampling method for selecting representative cells was needed due to the low number of cells traced, and to avoid inconsistencies in the quality of VIM-IR immunostaining evident only at high magnification that prevent precise reconstructions. The cell body was reconstructed by drawing a single ring

around the perimeter while maintaining focus in the z-axis. Processes were then selected for tracing in a clockwise manner; the length and width of each process was traced outwards from the cell body towards its terminals in XYZ coordinates, including each branch point (node). For human astrocyte morphometry, cortical grey and white matter were analyzed separately, resulting in four cells being reconstructed in six areas of five subjects (**Table 1**), for a total of 120 VIM-IR cells. For mouse astrocyte morphometry, four cells were analyzed in three areas of five animals, for a total of 60 mouse VIM-IR cells. A branched Structure Analysis (BSA) was performed on all reconstructed cells using Neurolucida to compare essential structural features of astrocyte morphology. These include the mean number of primary processes (process number), the mean number of process branch points (node number) and the mean number of process end points (terminal number), and the size and area of processes and cell bodies.

Vascular density

As the processes of VIM-IR astrocytes clearly contacted VIM-IR blood vessels that qualitatively varied in density across regions, the vascular density was quantified to assess whether it correlated with the density or morphometry of VIM-IR astrocytes. For reliable estimates of vascular density, we immunolabelled a receptor called cluster of differentiation 31 (CD31), also known as platelet endothelial cell adhesion molecule (PECAM-1), that is abundantly expressed in vascular endothelium (Ogunshola *et al*., 2000). Sections were prepared as for stereology and morphology and to estimate the vascularization of each region, CD31- and VIM-IR blood vessels were imaged in a random systematic manner using the SRS Image Series workflow in StereoInvestigator software (MBF Bioscience, USA). All images were taken at low (10X objective) magnification, and 5% of the area of each section immunolabeled for stereology was imaged. The area occupied by blood vessels was determined by manually drawing the contours of blood vessels using the ROI manager of the ImageJ software in five images per region per subject. In each case, these were the first five images found to contain no observable artefacts or background staining. A similar method was used for CD31-IR blood vessels in the mouse brain, except fewer than 5 images were required to cover 5% of the area of the sections.

Statistical analysis

All statistical analyses were performed using Prism v. 6.04 (GraphPad Software, San Diego, CA, USA). Data were assessed for a normal distribution using the D'Agostino & Pearson omnibus normality test. For non-parametric data which compared two groups or regions, two-tailed Mann-Whitney U tests were performed. For parametric data which compared more than two groups or regions, group differences were detected using a Matched One-Way ANOVA with multiple comparisons corrected for by the Bonferroni post hoc test. Non-parametric data sets obtained using the same samples had within-group differences detected using a standard Friedman Test with multiple comparisons corrected for by Dunn's post hoc test. All measurements are expressed as mean +/- SEM, and adjusted P-values are reported with a significance threshold of 0.05.

Results

Vimentin immunoreactivity in the human brain: general observations

As illustrated in **Fig. 1**, VIM immunoreactivity was observed to strongly label blood vessels in all human brain regions examined; a pattern consistent with the reported expression of VIM as the principal intermediate filament of endothelial cells (Gabbani *et al*., 1981). In addition to vascular immunolabelling, VIM-IR cells with all the morphological attributes of astrocytes — including making contact with a nearby VIM-IR blood vessel (**Fig. 1A**) — were also reliably observed in all regions, with variable densities. For both cortical areas examined, VIM-IR astrocytes were consistently more abundant in grey matter than in white matter. Most protoplasmic astrocytes were localized in deeper grey matter layers and were noticeably aligned above the grey/white matter boundary. We observed more protoplasmic astrocytes in prefrontal (**Fig. 1B**) than in visual cortex (**Fig. 1C**), mostly due to an increased thickness and continuity of this lower-layer band. In the caudate nucleus, VIM-IR astrocytes were densely distributed mainly around large VIM-IR blood vessels. While these astrocytes had a protoplasmic-like morphology, they often had many processes that closely overlapped those of neighboring astrocytes in the z-axis, and so were not clearly organized in domains as in the cortex for GFAP-IR astrocytes (**Fig. 1D**). Certain sections of mediodorsal thalamus were completely devoid of VIM-IR astrocytes despite the presence of blood vessels strongly

immunostained for VIM (**Fig. 1E**). When present, thalamic VIM-IR astrocytes had a fibrous-like morphology but appeared notably smaller than cortical VIM-IR protoplasmic and fibrous astrocytes. In addition to strongly labelling astrocytes and endothelial cells, VIM-IHC faintly labelled small ramified microglia in cortical white matter, as has been previously reported in postmortem human brain tissue (Yamada *et al*., 1992). Such VIM-IR microglia were never observed in cortical grey matter nor in subcortical regions, and were not taken into consideration in our cell density and morphometric analyses.

Vimentin is mostly co-expressed with other astrocytic markers

To further confirm the phenotype of VIM-IR cells as astrocytes, we used FISH and IF in the prefrontal cortex and caudate nucleus to localize the cellular expression of VIM with two commonly used astrocyte markers, Aldh1L1 and GFAP (**Fig. 2**). By combining FISH for both Aldh1L1 and GFAP mRNA probes and immunofluorescence for VIM protein, Aldh1L1 and GFAP mRNA expression was observed within the DAPI-stained nucleus of VIM-IR cells in the prefrontal cortex (**Fig. 2A**). In both regions, more than 80% of VIM-IR astrocytes were positive for Aldh1L1 mRNA, and more than 70% of cells expressing Aldh1L1 mRNA were immunofluorescent for VIM (**Fig. 2B**). Similar findings were made for GFAP mRNA, as 90% of VIM-IR astrocytes co-expressed GFAP mRNA, and more than 60% of astrocytes expressing GFAP mRNA also displayed VIM immunoreactivity (**Fig. 2C**). Co-immunofluorescence was then used to further examine the extent to which VIM protein and GFAP protein are localized to the same cellular population, and in both regions more than 90% of VIM-IR astrocytes were also GFAP-IR, and more than 70% of GFAP-IR astrocytes were VIM-IR as well (**Fig. 2D**). In the mouse CPu, we found more than 80% of VIM-immunofluorescent astrocytes were labeled by Cre-driven reporter protein expression for Aldh1L1, whereas only more than 40% of these transgenically labelled cells were also VIM-immunofluorescent (**Fig. 2E**). In these Aldh1L1-TdTom astrocytes, VIM immunofluorescence labelled thick processes but not the fine perisynaptic astrocytic processes extended by these cells (**Fig. 2F**). Collectively, these observations confirm that most, but not all, VIM-IR astrocytes express the canonical astrocytic markers GFAP and Aldh1L1.Vimentin immunoreactivity labels previously described morphological subtypes of astrocytes.

VIM immunoreactivity revealed all four known morphological subtypes of human cortical astrocytes previously described with GFAP IHC (Oberheim *et al.,* 2009) (**Fig. 3**). In layer I, astrocytes with a unipolar morphology extending long, direct and unbranching processes into layer III were observed, displaying the characteristic features of interlaminar astrocytes (**Fig. 3A**). Although VIM-IR interlaminar astrocytes were clearly visible in primary visual cortex, they were not clearly identifiable in prefrontal cortex — all other morphological subtypes were found in both prefrontal and visual cortex. In the remaining layers (II–VI) of neocortical grey matter, VIM-IR astrocytes displayed the stellate morphology conferred by extensively branched bushy processes that is characteristic of protoplasmic astrocytes (**Fig. 3B**). VIM-IR protoplasmic astrocytes were sparsely distributed and, in areas of high local density, occupied non-overlapping domains. In deep cortical grey matter (layers V-VI) VIM-IR varicose projection astrocytes extending exceptionally long processes bearing regularly spaced varicosities were observed (**Fig. 3C**). These processes more often radiated toward upper layers than toward white matter. Few varicose projection astrocytes were seen however, particularly in the visual cortex. In cortical white matter, we observed astrocytes with straight, finely tortuous and rarely branching processes, as is characteristic of fibrous astrocytes (**Fig. 3D**).

Vimentin Immunoreactivity: Regional Astrocytic Features

Some unique regional features were observed for human VIM-IR astrocytes that have not previously been reported following labelling with other astrocyte markers (**Fig. 4**). A high proportion (approximately 20%) of neocortical protoplasmic or striatal protoplasmic-like VIM-IR astrocytes exhibited a twin cell morphology, consisting of two abutting cell bodies apparently formed from astrocyte cell division (**Fig. 4A**); a phenomenon rarely observed for GFAP-IR astrocytes (not shown). Furthermore, long varicose bundles of VIM-IR processes with no identifiable cellular origin were also observed in the caudate nucleus (**Fig. 4B**). These fasciculi appeared to form networks as they seemed connected to each other and received projections from nearby astrocytes (**Fig. 4B–C**). They appeared similar in density to the processes of some VIM-IR astrocytes, which can project many unbranching, parallel processes toward VIM-IR blood vessels (**Fig. 4C**).

Regional densities of vimentin- and GFAP-immunoreactive astrocytes

As the distribution and features of VIM-IR astrocytes varied across regions, a stereological approach was used to quantify regional differences in astrocyte densities (**Fig. 5**). Strongly significant differences in the regional densities of VIM-IR astrocytes were found (**Fig. 5A**). In cortical grey matter, about five times more VIM-IR astrocytes were observed in the prefrontal cortex than in the primary visual cortex (586 ± 132 cells/mm^3 vs. 108 ± 32 cells/mm^3). These differences were even larger in cortical white matter, where fifteen times more VIM-IR astrocytes were observed in the prefrontal cortex than in the primary visual cortex (252 ± 85 cells/mm^3 vs. 14 ± 4 cells/mm^3). The caudate nucleus was significantly more densely populated with VIM-IR astrocytes than all other regions studied (1753 ± 339 cells/mm^3), with nearly three times more VIM-IR astrocytes than in prefrontal cortex grey matter. Caudate astrocytes were often localized in the vicinity of larger blood vessels. VIM-IR astrocytes were rarely observed in the mediodorsal thalamus (1 ± 1 cell/mm^3), with many immunostained sections containing no VIM-IR astrocytes at all.

For comparison, the density of GFAP-IR astrocytes was assessed in the same subjects and found to be more similar across regions than for VIM-IR astrocytes (**Fig. 5B**). In cortical grey matter, more GFAP-IR astrocytes were found in the visual cortex than in the prefrontal cortex (1256 ± 129 cells/mm^3 vs. 1059 ± 133 cells/mm^3). The opposite pattern was found in cortical white matter, where more GFAP-IR astrocytes were found in the prefrontal cortex than in the visual cortex (2011 ± 222 cells/mm^3 vs. 1686 ± 153 cells/mm^3). The density of GFAP-IR astrocytes in either the caudate nucleus (2771 ± 551 cells/mm^3) or the thalamus (2555 ± 448 cells/mm^3) was significantly greater in the gray matter, but not the white matter, of both cortical regions. As there were more GFAP-IR than VIM-IR astrocytes in all regions, this suggests that VIM reveals a relatively small subset of astrocytes.

Morphometric properties of vimentin-immunoreactive astrocytes

The morphology of VIM-IR astrocytes varied significantly across regions for all branched structured analysis (BSA) features (Fig. 6). The process number of VIM-IR astrocytes in visual cortex white matter (28 ± 3 processes) was significantly lower than that in prefrontal cortex white matter (39 ± 2 processes) and visual cortex grey matter (38 ± 2 processes), but no significant differences were found between neocortical grey matter regions or between subcortical regions (Fig. 6B). The strongest regional difference for VIM-IR astrocytes was in

the number of nodes, which constitute branch points in astrocyte processes (Fig. 6C). There was twice as many nodes for VIM-IR astrocytes in the gray matter than in the white matter compartment of prefrontal cortex (70 ± 7 vs. 28 ± 3 nodes) and visual cortex (69 ± 7 vs. 24 ± 4 nodes), and thrice as many nodes for VIM-IR astrocytes in the caudate nucleus than in the mediodorsal thalamus (65 ± 9 vs. 22 ± 3 nodes). No significant differences in VIM-IR node number were found between neocortical grey or white matter compartments. The VIM-IR terminal number had the same pattern of significant differences as for VIM-IR node number (Fig. 6D), except that the terminal number in the caudate nucleus (101 ± 9 terminals) did not significantly differ from those found in prefrontal cortex or visual cortex white matter (69 ± 4 and 66 ± 6 terminals, respectively). The total process length of VIM-IR astrocytes was significantly greater only in visual cortex grey matter relative to the mediodorsal thalamus (2820.0 ± 189.2 vs. 1860.0 ± 122.6 μm), confirming qualitative observations of smaller VIM-IR astrocytes in the mediodorsal thalamus (**Fig. 6E**). As for VIM-IR process number, VIM-IR mean process length significantly differed only between visual cortex white matter (55.4 ± 4.1 μm) and the two highest regional values (**Fig. 6F**), in this instance being those for the caudate nucleus and visual cortex grey matter (89.3 ± 9.6 vs. 78.8 ± 7.6 μm, respectively). A similar finding was made for the total process surface area of VIM-IR astrocytes (**Fig. 6G**), which was significantly larger in the caudate nucleus (2321.0 ± 251.9 μm^2) and prefrontal cortex grey matter (2238.0 ± 183.8 μm^2) than in the mediodorsal thalamus (1423.0 ± 137.1 μm^2). The soma area of VIM-IR astrocytes was typically smaller in cortical white matter (**Fig. 6H**), as there was a significant difference in VIM-IR soma area between visual cortex grey and white matter (82.85 ± 8.2 vs. 53.2 ± 7.0 μm^2), and between the caudate nucleus (89.1 ± 6.9 μm^2) and either prefrontal or visual white matter (62.0 ± 6.8 μm^2 and 53.2 ± 7.0 μm^2, respectively). These observations generally show that cortical VIM-IR astrocytes have a more complex morphology in grey matter than in white matter.

Comparison of human and mouse vimentin-immunoreactive astrocytes

Given the regional heterogeneity of human VIM-IR astrocytes, we then assessed whether morphological differences exist in three equivalent regions of the adult mouse brain. We did not assess the mouse mediodorsal thalamus due to its relatively small size and as it mostly lacked VIM-IR astrocytes similarly to what we observed in the human thalamus. Surprisingly,

no regional differences were seen in the BSA measurements for VIM-IR astrocytes across these three mouse brain regions (**Fig. 7**).

To quantify species differences in VIM-IR astrocyte morphometry, comparisons were made within these regions between BSA values for human and mouse VIM-IR astrocytes (**Fig. 8**). This revealed human VIM-IR morphometry to be significantly more complex than mouse VIM-IR morphometry for all cases, except for process number in the striatum. The process number for human VIM-IR astrocytes was only 12% higher in the striatum (29 ± 2 vs. 26 ± 2 processes) but was 64% higher in the prefrontal cortex (36 ± 2 vs. 22 ± 2 processes) and 65% higher in the visual cortex (38 ± 2 vs. 23 ± 2 processes) **(Fig. 8B).** The node number was 2.6-fold higher in the striatum (64.8 ± 8.6 vs. 24.5 ± 2.0 nodes), 2.9-fold higher in the prefrontal cortex (69.9 ± 6.7 vs. 24.1 ± 2.6 nodes), and 2.7-fold higher in the visual cortex (69.2 ± 7.5 vs. 25.2 ± 1.5 nodes) for human VIM-IR astrocytes relative to those in mouse (**Fig. 8C**). The terminal number was almost 2-fold higher in the striatum (100.9 ± 9.0 vs. 51.9 ± 3.0 terminals), and 2.3-fold higher in both the prefrontal cortex (111.8 ± 7.8 vs. 47.8 ± 3.4 terminals) and visual cortex (113.8 ± 8.1 vs. 50 ± 2.8 terminals) for human VIM-IR astrocytes relative to those in mouse (**Fig. 8D**). The total process length was 2.6-fold higher in the striatum (2396.4 ± 157.5 vs. 911.0 ± 47.8 μm), 2.9-fold higher in the prefrontal cortex (2642.1 ± 903.3 vs. 903.3 ± 69.4 μm), and 3.2-fold higher in the visual cortex (2819.7 ± 189.2 vs. 886.0 ± 61.1 μm) for human VIM-IR astrocytes relative to those in mouse (**Fig. 8E**). The mean process length was 2.4-fold higher in the striatum (89.3 ± 9.6 vs. 36.6 ± 1.6 μm), 1.8-fold higher in the prefrontal cortex (75.5 ± 4.6 vs. 40.9 ± 2.5 μm), and 1.9-fold higher in the visual cortex (78.8 ± 7.6 vs. 39.9 ± 2.2 μm) for human VIM-IR astrocytes relative to those in mouse (**Fig. 8F**). The process surface area was 3.5-fold higher in the striatum (2321.1 ± 251.9 vs. 648.0 ± 39.4 μm^2), 3.3-fold higher in the prefrontal cortex (2237.7 ± 183.8 vs. 672.0 ± 60.1 μm^2), and 3.5-fold higher in the visual cortex (2106.5 ± 128.4 vs. 601.3 ± 43.0 μm^2) for human VIM-IR astrocytes relative to those in mouse (**Fig. 8G**). The soma area was 2.3-fold higher in the striatum (89.1 ± 6.9 vs. 39.3 ± 2.6 μm^2), 2-fold higher in the prefrontal cortex (84.5 ± 8.6 vs. 42.9 ± 4.2 μm^2), and 2.4-fold higher in the visual cortex (82.9 ± 8.2 vs. 37.2 ± 2.4 μm^2) for human VIM-IR astrocytes relative to those in mouse (**Fig. 8H**). Together these morphometric comparisons reveal that human VIM-IR astrocytes are 2–3 fold greater in size than mouse VIM-IR astrocytes.

Regional vascular density correlates with GFAP-IR and VIM-IR astrocyte density

Given the abundance of VIM-IR astrocytes in close proximity to blood vessels in the caudate nucleus, we investigated a potential vascular basis for the regional heterogeneity of astrocytes by comparing the regional vascularization by CD31-immnoreactive (CD31-IR) or VIM-IR blood vessels in the same regions and subjects (**Fig. 9)**. In the same human and mouse subjects, significant regional differences were found for the area occupied by CD31-immunoreactive (CD31-IR) or VIM-IR blood vessels in human brain, but not for CD31-IR blood vessels in the mouse brain (**Fig. 9A–C**). A significant negative correlation between regional CD31-IR vascularization and VIM-IR astrocyte density was found only when regions with a low VIM-IR astrocyte density (thalamus and cortical white matter) were excluded from the analysis (**Fig. 9D)**. A similar correlation was found between CD31-IR vascularization and GFAP-IR astrocyte density, however this pattern occurred across all regions, indicating that highly vascularized human brain regions are generally less densely populated with VIM-IR or GFAP-IR astrocytes (**Fig. 9D**).

Discussion

To our knowledge, the present study is the first to anatomically assess the regional heterogeneity in density and morphology of astrocytes in the healthy human brain, to directly relate astrocytic and vascular densities, and to comprehensively compare human and mouse astrocytes. This study also provides the first quantitative description of VIM-IR astrocytes. Taken together, our results provide general patterns for astrocyte density, astrocyte morphology and vascular density across cortical and subcortical regions of the human brain.

Vimentin reliably labels a subset of astrocytes in adult brain

As an astrocyte marker, VIM gives unprecedented access for visualizing the morphology of individual astrocytes, as it strongly reveals the fine morphology of a small, sparsely distributed population of astrocytes and its association with neighboring blood vessels. We also found

VIM to be effective as a vascular marker, as it revealed a similar density of blood vessels as the conventional vascular marker CD31 in adult human brain, and both markers indicated that there is a significantly greater vascular density in cortical regions than in subcortical regions. VIM immunolabelling also revealed new subcortical structures. The presence of large, faintly labelled bundles of thin VIM-IR filaments of no clear cellular origin indicates either that VIM-IR astrocyte processes span long distances that often extend outside of the z-plane of a 50 µm-thick section, or that a vast network of VIM-IR fibers exist in the human brain. In addition, the common observation of VIM-IR twin cell morphology in the cortex and caudate nucleus suggests that VIM may have different roles than GFAP for cell division and differentiation in the adult human brain.

We found that most, but not all, VIM-IR cells co-express the commonly used astrocyte markers GFAP and Aldh1L1. We did not expect all VIM-IR cells to express GFAP, as not all mouse and human cortical astrocytes express GFAP (Sofroniew & Vinters, 2010; Sosunov *et al*., 2014), and the relatively frequent presence of twin cells in VIM IHC suggests that VIM may also label differentiating cells in the adult brain which are not mature GFAP-IR astrocytes. As in previous descriptions of GFAP-IR astrocytes, VIM labelling was localized to the soma and thick primary processes but not found in fine perisynaptic astrocytic processes (PAPs) lining the domains of protoplasmic astrocytes only visible with diolistic or transgenic labelling methods (Oberheim *et al*., 2009). Although Aldh1L1 is often reported to label all astrocytes, we found that only 85% of VIM-IR astrocytes also expressed Aldh1L1 in the mouse CPu. However, this particular transgenic Cre reporter line has previously been reported to show similar overlap (85–92% depending on the region chosen) with astrocytes immunolabelled with S100B, indicating that Aldh1L1 may not reveal the entire astrocyte population (Winchenbach *et al*., 2016). Nevertheless, the common coexpression of other astrocyte markers in VIM-IR cells indicates that VIM reliably labels astrocytes in adult human and mouse brains.

Most previous postmortem studies and animal studies have used GFAP as an astrocyte marker to implicate an abnormal distribution, density or morphology of astrocytes in psychiatric and neurological conditions (Brenner *et al.,* 2001; Kim *et al.,* 2018; Liddelow & Sofroniew, 2019). Of note, the regional expression of GFAP and the regional density of GFAP-IR astrocytes is consistently reduced in mood-associated brain regions in cases of major depressive disorder (MDD) and suicide (Torres-Platas *et al.*, 2016; Nagy *et al.*, 2017; Rajkowska *et al*., 2018). It would be interesting to examine whether the density of VIM-IR astrocytes is also reduced in samples from depressed patients. To date, however, more studies have associated VIM-IR

astrocytes with neurological conditions. The first postmortem study of VIM-IR astrocytes qualitatively reported that they were hypertrophic in postmortem brain tissue from individuals with Pick's Disease, multiple sclerosis (MS), amyotrophic lateral sclerosis (ALS), and Alzheimer's Disease, and that VIM-IR astrocytes were almost exclusively associated with plaques labelled with β-amyloid protein (Yamada *et al*., 1992). Similarly, another postmortem study reported a reduced density of human VIM-IR astrocytes in the entorhinal cortex of individuals with Disease (Arnold *et al*., 1996). The only other postmortem immunohistochemical studies of human VIM-IR astrocytes have confirmed their presence in the brainstem, where, unlike GFAP-IR astrocytes, they have a reduced density in sudden unexpected death in epilepsy (Rusu *et al*., 2013; Patodia *et al*., 2019). Rodent studies have implicated that VIM protein can be released in astrocytic exosomes, and extracellular VIM protein promotes axonal regrowth in models of spinal cord injury (Shigyo & Tohda, 2016; Adolf *et al*., 2018). Together, these studies indicate the potential clinical importance of characterizing VIM-IR astrocytes in the healthy human brain.

Regional heterogeneity of VIM-IR astrocyte density and morphology

Using an unbiased stereological approach, we found consistently fewer VIM-IR astrocytes than GFAP-IR astrocytes in all studied regions. These results alone indicate that VIM protein cannot be detectably expressed in all GFAP-IR astrocytes, as was also suggested using by FISH and coimmunofluorescence. We also show for the first time that VIM-IR and GFAP-IR astrocytes in subcortical regions can outnumber those in neocortical grey and white matter regions. This corresponds well with previous comparisons of regional GFAP mRNA levels and qualitative IHC observations (Torres-Platas *et al*., 2016), and may indicate that the human neocortex exhibits relatively limited regional heterogeneity of astrocyte density. Due to their particularly low number, pathological changes may be more readily observable for VIM-IR astrocytes than GFAP-IR astrocytes, and postmortem studies have already identified differences in the number and morphology of VIM-IR astrocytes in neurological conditions (Yamada *et al*., 1992; Arnold *et al*., 1996; Patodia *et al*., 2019). We found variety in subcortical astrocyte morphology, as VIM-IR caudate nucleus astrocytes had a protoplasmic-like morphology, whereas thalamic astrocytes had a fibrous-like morphology. A major finding, contrasting heavily with the very high density of GFAP-IR astrocytes in this region, was the almost complete absence of VIM-IR astrocytes in the human mediodorsal thalamus. This finding indicates that while many

astrocytes co-express VIM and GFAP, GFAP can be expressed without VIM in at least one brain region. We also observed very few VIM-IR astrocytes in the mouse mediodorsal thalamus (not shown). This was unexpected given that the human mediodorsal thalamus has higher regional GFAP protein levels than many cortical regions (Torres-Platas *et al*., 2016). The lack of thalamic VIM-IR cells may indicate a regional difference in astrocyte division or differentiation, as early investigations indicated that immature astrocytes primarily express VIM until the time of cortical myelination, when they mature by switching to primarily expressing GFAP (Dahl, 1981; Pixley & DeVellis, 1984). The absence of thalamic VIM-IR cells also indicates that thalamic astrocytes have a particular cytoskeletal organization, as mouse astrocytes require VIM, but not GFAP, to synthesize other astrocyte-enriched type III intermediate filaments (Pekny *et al*., 1999; Jing *et al*., 2007). Finally, the absence of VIM might affect the functional efficiency of mediodorsal thalamic astrocytes, as intermediate filaments increase the rate of chemokine-induced vesicular trafficking of astrocytes *in vitro* (Vardjan *et al*., 2012). These findings may not generalize to other thalamic nuclei, as there are large differences in GFAP-IR astrocyte density across thalamic nuclei in mouse (Emsley & Macklis, 2006). Nevertheless, a recent study has shown that astrocyte activity coordinated with local neurons in the mediodorsal thalamus is involved in initiating cortical blood-oxygen-level-dependent responses (Wang *et al*., 2018). On this basis we tentatively speculate that, as for neurons, astrocytes may have different functional roles in the thalamus than in the striatum or neocortex.

All measured morphometric features of VIM-IR astrocytes varied significantly across regions, which further supports region-specific functions for VIM-IR astrocytes. For instance, we qualitatively and quantitatively observed astrocytes in the caudate nucleus to have a protoplasmic-like morphology, whereas those in the mediodorsal thalamus to have a fibrous-like morphology. To our knowledge this is one of the first quantitative indications of morphological diversity for non-cortical astrocytes in the human brain. Additionally, while human protoplasmic and fibrous cortical astrocytes are usually defined qualitatively by their location and morphology, previous studies have not clearly provided a quantitative basis for the fundamental morphological distinction (Oberheim *et al*., 2009; Torres-Platas *et al*., 2011). Here, our results indicate that VIM-IR protoplasmic and fibrous astrocytes in the human cortex are most reliably distinguished by terminal number and branching than by the number, length or surface area of processes. This quantitative distinction should inform future studies on

cortical human astrocytes, especially in experiments where astrocytes are not clearly situated in grey or white matter.

To complement our morphological findings, we compared the complexity and diversity of VIM-IR protoplasmic astrocytes in equivalent grey matter regions of the human and mouse brain. As expected, based on previous reports for GFAP-IR astrocytes (Oberheim *et al*., 2006; Oberheim *et al*., 2009), VIM-IR astrocyte morphology was considerably more complex in human than in mouse for all features and regions studied, except for process number in the caudate nucleus. The latter does not signify an important region-specific species difference, as the morphometric species differences for striatal VIM-IR astrocytes were similar to those for cortical VIM-IR astrocytes for all other features. Interestingly, no regional differences were found for mouse VIM-IR astrocyte morphometry, suggesting that VIM-IR astrocytes are more regionally diverse in the human brain.

VIM-IR and GFAP-IR astrocyte density inversely correlates with vascular density

We extended our species comparisons to regional vascularization and found that human brain regions were 2– to 5–fold more vascularized than equivalent mouse brain regions. Both VIM and CD31 showed significant differences between human subcortical regions and cortical regions, by contrast, CD31 showed no significant differences between mouse brain regions. While the vascular density of these human brain regions has not, to our knowledge, been reported before, our measurements for mouse brain vascular density are similar to previous estimates using more precise methods (Chugh *et al*., 2009).

Given our observation of regional heterogeneity of VIM-IR astrocyte morphometry and vascularization in the human brain, but not in mouse brain, we then assessed whether these were quantitatively related. While no correlation was found for any human VIM-IR astrocyte morphometric features and vascularization (not shown), we found that VIM-IR astrocyte density inversely correlated with regional vascular density in cortical grey matter and the caudate nucleus (but not in the thalamus or cortical white matter). By comparison, GFAP-IR astrocyte density inversely correlated with vascular density for all studied regions, suggesting that gliovascular interactions play a more consistent role distributing GFAP-IR astrocytes than VIM-IR astrocytes throughout the human brain. Gliovascular interactions may be relatively

robust for GFAP-IR astrocytes, given that depressed individuals have altered vascular coverage for astrocytes labeled by aquaporin-4, but not for those labeled by GFAP (Rajkowska et al., 2013). A more precise analysis of vascular contacts of VIM-IR and GFAP-IR astrocytes across regions may reveal whether this inverse correlation between astrocyte and vascular density is mediated by regional alterations in gliovascular interactions, perhaps in the number or volume of vascular endfeet contacts per astrocyte.

Limitations and Future Directions

To our knowledge this is the most systematic morphological and stereological investigation of astrocytes in the human brain to date. However, this study presents two main limitations: its relatively limited sample size, which underpowered some statistical comparisons, and the fact that only samples from males were analyzed. Although a total of 180 VIM-IR astrocytes were manually traced in this study, this meant only four representative cells per region per subject, which constitutes a limitation in the statistical power of morphometric comparisons made in this study. Despite this, we are confident that the strong effect sizes observed reflect important regional and cross-species trends in astrocyte morphometry. While sex differences have been reported for astrocyte density and morphology in the mouse amygdala (Johnson *et al*., 2008), and for transcriptional changes in prefrontal cortex astrocytes in depressed patients and stressed mice (Labonté *et al*., 2017), sex differences have yet to be reported for astrocytes in the healthy adult brain. Including different age groups would also have helped elucidate the effect age has on VIM-IR and GFAP-IR astrocytes in healthy human brain, given that cerebral GFAP is known to increase with age in mice and humans (Boisvert *et al.*, 2018; Wruck & Adjaye, 2020). We were unable to assess these differences mostly because of the limited availability of matched female samples, but also because of the small sample size suitable for an extensive cross-regional comparison which would have been difficult to achieve robust comparisons. Future studies should examine potential sex differences and further explore the functional consequences associated with regional differences in astrocytic densities and morphologies. Such knowledge, together with the data presented in this study, will be useful for studies examining astrocytes in cerebral pathologies.

References

1. Adolf, A., Rohrbeck, A., Münster-Wandowski, A., Johansson, M., Kuhn, H.-G., Kopp, M. A., et al. (2019) Release of astroglial vimentin by extracellular vesicles: Modulation of binding and internalization of C3 transferase in astrocytes and neurons. Glia 67, 703–717. doi:10.1002/glia.23566

2. Arnold, S. E., Franz, B. R., Trojanowski, J. Q., Moberg, P. J., & Gur, R. E. (1996) Glial fibrillary acidic protein-immunoreactive astrocytosis in elderly patients with schizophrenia and dementia. Acta Neuropathol 91, 269–277. doi:10.1007/s004010050425

3. Bartheld, C. S. von, Bahney, J. & Herculano-Houzel, S. (2016) The search for true numbers of neurons and glial cells in the human brain: A review of 150 years of cell counting. Journal of Comparative Neurology 524, 3865–3895

4. Boisvert, M. M., Erikson, G. A., Shokhirev, M. N., & Allen, N. J. (2018). The Aging Astrocyte Transcriptome from Multiple Regions of the Mouse Brain. Cell Reports 22, 269–285. doi:10.1016/j.celrep.2017.12.039

5. Brenner, M., Johnson, A. B., Boespflug-Tanguy, O., Rodriguez, D., Goldman, J. E., & Messing, A. (2001) Mutations in GFAP, encoding glial fibrillary acidic protein, are associated with Alexander disease. Nature Genetics 27, 117–120. doi:10.1038/83679

6. Cahoy, J. D. et al. (2008) A Transcriptome Database for Astrocytes, Neurons, and Oligodendrocytes: A New Resource for Understanding Brain Development and Function. J. Neurosci. 28, 264–278

7. Chiu, F.-C., Norton, W. T. & Fields, K. L. (1981) The Cytoskeleton of Primary Astrocytes in Culture Contains Actin, Glial Fibrillary Acidic Protein, and the Fibroblast-Type Filament Protein, Vimentin. Journal of Neurochemistry 37, 147–155

8. Choi, H. B. et al. (2012) Metabolic Communication between Astrocytes and Neurons via Bicarbonate-Responsive Soluble Adenylyl Cyclase. Neuron 75, 1094–1104

9. Christopherson, K. S. et al. (2005) Thrombospondins Are Astrocyte-Secreted Proteins that Promote CNS Synaptogenesis. Cell 120, 421–433

10. Chugh, B. P. et al. (2009) Measurement of cerebral blood volume in mouse brain regions using micro-computed tomography. NeuroImage 47, 1312–1318

11. Covelo, A. & Araque, A. (2018) Neuronal activity determines distinct gliotransmitter release from a single astrocyte. eLife 7, e32237

12. Dahl, D (1981) The vimentin-GFA protein transition in rat neuroglia cytoskeleton occurs at the time of myelination. Journal of Neuroscience Research 6, 741–748

13. Eilam, R., Aharoni, R., Arnon, R. & Malach, R. (2016) Astrocyte morphology is confined by cortical functional boundaries in mammals ranging from mice to human. eLife 5, e15915

14. Emsley, J. G. & Macklis, J. D. (2006) Astroglial heterogeneity closely reflects the neuronal-defined anatomy of the adult murine CNS. Neuron Glia Biology 2, 175–186

15. Farmer, W. T. et al. (2016) Neurons diversify astrocytes in the adult brain through sonic hedgehog signaling. Science 351, 849–854

16. Gabbiani, G. et al. (2014) Vascular smooth muscle cells differ from other smooth muscle cells: predominance of vimentin filaments and a specific alpha-type actin. PNAS 78, 298–302 (1981).

17. Gao, P. et al. (2014) Deterministic Progenitor Behavior and Unitary Production of Neurons in the Neocortex. Cell 159, 775–788

18. Garcia, A. D. R., Doan, N. B., Imura, T., Bush, T. G., & Sofroniew, M. V. (2004). GFAP-expressing progenitors are the principal source of constitutive neurogenesis in adult mouse forebrain. Nature Neuroscience 7, 1233–1241, doi:10.1038/nn1340

19. García-Cáceres, C. et al. (2016) Astrocytic Insulin Signaling Couples Brain Glucose Uptake with Nutrient Availability. Cell 166, 867–880

20. Jing, R. et al. (2007) Synemin is expressed in reactive astrocytes in neurotrauma and interacts differentially with vimentin and GFAP intermediate filament networks. Journal of Cell Science 120, 1267–1277

21. Johnson, R. T., Breedlove, S. M. & Jordan, C. L. (2008) Sex differences and laterality in astrocyte number and complexity in the adult rat medial amygdala. Journal of Comparative Neurology 511, 599–609

22. Kim, R., Healey, K. L., Sepulveda-Orengo, M. T., & Reissner, K. J. (2018) Astroglial correlates of neuropsychiatric disease: From astrocytopathy to astrogliosis. Progress in Neuro-Psychopharmacology and Biological Psychiatry 87, 126–146. doi:10.1016/j.pnpbp.2017.10.002

23. Labonté, B. et al. (2017) Sex-Specific Transcriptional Signatures in Human Depression. Nat Med 23, 1102–1111

24. Liddelow, S. A., & Sofroniew, M. V. (2019) Astrocytes usurp neurons as a disease focus. Nature Neuroscience 22, 512–513. doi:10.1038/s41593-019-0367-6

25. Madisen, L., Zwingman, T. A., Sunkin, S. M., Oh, S. W., Zariwala, H. A., Gu, H., et al. (2010) A robust and high-throughput Cre reporting and characterization system for the whole mouse brain. Nature Neuroscience 13, 133–140. doi:10.1038/nn.2467

26. Magavi, S., Friedmann, D., Banks, G., Stolfi, A. & Lois, C. (2012) Coincident Generation of Pyramidal Neurons and Protoplasmic Astrocytes in Neocortical Columns. J. Neurosci. 32, 4762–4772

27. Mahar, I., et al. (2011) Subchronic Peripheral Neuregulin-1 Increases Ventral Hippocampal Neurogenesis and Induces Antidepressant-Like Effects. PLOS ONE 6, e26610

28. Martín, R., Bajo-Grañeras, R., Moratalla, R., Perea, G. & Araque, A. (2015) Circuit-specific signaling in astrocyte-neuron networks in basal ganglia pathways. Science 349, 730–734

29. McKeon, R. J., Schreiber, R. C., Rudge, J. S., & Silver, J. (1991) Reduction of neurite outgrowth in a model of glial scarring following CNS injury is correlated with the expression of inhibitory molecules on reactive astrocytes. J. Neurosci. 11, 3398–3411. doi:10.1523/JNEUROSCI.11-11-03398.1991

30. Morel, L., Chiang, M. S. R., Higashimori, H., Shoneye, T., Iyer, L. K., Yelick, J., et al. (2017) Molecular and Functional Properties of Regional Astrocytes in the Adult Brain. J. Neurosci. 37, 8706–8717. doi:10.1523/JNEUROSCI.3956-16.2017

31. Nagy, C., Torres-Platas, S. G., Mechawar, N., & Turecki, G. (2017) Repression of Astrocytic Connexins in Cortical and Subcortical Brain Regions and Prefrontal Enrichment of H3K9me3 in Depression and Suicide. Int J Neuropsychopharmacol 20, 50–57. doi:10.1093/ijnp/pyw071.

32. Oberheim, N. A. et al. (2009) Uniquely hominid features of adult human astrocytes. J. Neurosci. 29, 3276–3287

33. Oberheim, N. A., Wang, X., Goldman, S. & Nedergaard, M. (2006) Astrocytic complexity distinguishes the human brain. Trends in Neurosciences 29, 547–553

34. Ogunshola, O. O., Stewart, W. B., Mihalcik, V., Solli, T., Madri, J. A., and Ment, L. R. (2000) Neuronal VEGF expression correlates with angiogenesis in postnatal developing rat brain. Developmental Brain Research 119, 139–153. doi:10.1016/S0165-3806(99)00125-X

35. Pakkenberg, B. et al. (2003) Aging and the human neocortex. Experimental Gerontology 38, 95–99

36. Patodia, S., Paradiso, B., Ellis, M., Somani, A., Sisodiya, S. M., Devinsky, O., et al. (2019) Characterisation of medullary astrocytic populations in respiratory nuclei and alterations in sudden unexpected death in epilepsy. Epilepsy Research 157, 106213. doi:10.1016/j.eplepsyres.2019.106213

37. Pekny, M., et al. (1999) Abnormal reaction to central nervous system injury in mice lacking glial fibrillary acidic protein and vimentin. The Journal of Cell Biology 145, 503–514

38. Pellerin, L., & Magistretti, P. J. (1994) Glutamate uptake into astrocytes stimulates aerobic glycolysis: a mechanism coupling neuronal activity to glucose utilization. PNAS 91, 10625–10629

39. Pelvig, D. P., Pakkenberg, H., Stark, A. K. & Pakkenberg, B. (2008) Neocortical glial cell numbers in human brains. Neurobiology of Aging 29, 1754–1762

40. Perea, G., Yang, A., Boyden, E. S. & Sur, M. (2014) Optogenetic astrocyte activation modulates response selectivity of visual cortex neurons in vivo. Nature Communications 5, 3262

41. Pixley, S. K. R. & de Vellis, J. (1984) Transition between immature radial glia and mature astrocytes studied with a monoclonal antibody to vimentin. Developmental Brain Research 15, 201–209

42. Potokar, M. et al. (2010) Intermediate filaments attenuate stimulation-dependent mobility of endosomes/lysosomes in astrocytes. Glia 58, 1208–1219

43. Rajkowska, G., Hughes, J., Stockmeier, C. A., Javier Miguel-Hidalgo, J. & Maciag, D. (2013) Coverage of blood vessels by astrocytic endfeet is reduced in major depressive disorder. Biological Psychiatry 73, 613–621

44. Rajkowska, G., Legutko, B., Moulana, M., Syed, M., Romero, D. G., Stockmeier, C. A., et al. (2018) Astrocyte pathology in the ventral prefrontal white matter in depression. Journal of Psychiatric Research 102, 150–158. doi:10.1016/j.jpsychires.2018.04.005.

45. Rusu, M. C., Dermengiu, D., Loreto, C., Motoc, A. G. M., & Pop, E. (2013) Astrocitary niches in human adult medulla oblongata. Acta Histochemica 115, 296–300. doi:10.1016/j.acthis.2012.07.004

46. Shigyo, M., & Tohda, C. (2016) Extracellular vimentin is a novel axonal growth facilitator for functional recovery in spinal cord-injured mice. Scientific Reports 6, 1–9. doi:10.1038/srep28293.

47. Sofroniew, M. V. & Vinters, H. V. (2010) Astrocytes: biology and pathology. Acta Neuropathol 119, 7–35

48. Sosunov, A. A. et al. (2014) Phenotypic heterogeneity and plasticity of isocortical and hippocampal astrocytes in the human brain. J. Neurosci. 34, 2285–2298

49. Srinivasan, R., Lu, T.-Y., Chai, H., Xu, J., Huang, B. S., Golshani, P., et al. (2016). New Transgenic Mouse Lines for Selectively Targeting Astrocytes and Studying Calcium Signals in Astrocyte Processes In Situ and In Vivo. Neuron 92, 1181–1195. doi:10.1016/j.neuron.2016.11.030.

50. Suzuki, A. et al. (2011) Astrocyte-Neuron Lactate Transport Is Required for Long-Term Memory Formation. Cell 144, 810–823

51. Takano, T. et al. (2006) Astrocyte-mediated control of cerebral blood flow. Nature Neuroscience 9, 260–267

52. Torres-Platas, S. G. et al. (2011) Astrocytic hypertrophy in anterior cingulate white matter of depressed suicides. Neuropsychopharmacology 36, 2650–2658

53. Torres-Platas, S. G., Nagy, C., Wakid, M., Turecki, G. & Mechawar, N. (2016) Glial fibrillary acidic protein is differentially expressed across cortical and subcortical regions in healthy brains and downregulated in the thalamus and caudate nucleus of depressed suicides. Molecular Psychiatry 21, 509–515

54. Vardjan, N. et al. (2012) IFN-γ-induced increase in the mobility of MHC class II compartments in astrocytes depends on intermediate filaments. Journal of Neuroinflammation 9, 144

55. Wang, M., He, Y., Sejnowski, T. J. & Yu, X. (2018) Brain-state dependent astrocytic Ca2+ signals are coupled to both positive and negative BOLD-fMRI signals. PNAS 115, E1647–E1656

56. Wilhelmsson, U. et al. (2004) Absence of glial fibrillary acidic protein and vimentin prevents hypertrophy of astrocytic processes and improves post-traumatic regeneration. J. Neurosci. 24, 5016–5021

57. Winchenbach, J., Düking, T., Berghoff, S. A., Stumpf, S. K., Hülsmann, S., Nave, K.-A., et al. (2016) Inducible targeting of CNS astrocytes in Aldh1l1-CreERT2 BAC transgenic mice. F1000Res 5. doi:10.12688/f1000research.10509.1.

58. Wruck, W., & Adjaye, J. (2020) Meta-analysis of human prefrontal cortex reveals activation of GFAP and decline of synaptic transmission in the aging brain. Acta Neuropathologica Communications 8, 26. doi:10.1186/s40478-020-00907-8.

59. Yamada, T., Kawamata, T., Walker, D. G. & McGeer, P. L. (1992) Vimentin immunoreactivity in normal and pathological human brain tissue. Acta Neuropathol 84, 157–162

Acknowledgments

The present study used the services of the Douglas-Bell Canada Brain Bank and of the Molecular and Cellular Microscopy Platform at the Douglas Hospital Research Centre. The authors are grateful to Maâmar Bouchouka, Josée Prud'homme, Dominique Mirault and Melina Jaramillo Garcia for their kind assistance.

Author Contributions

LAO and NM conceived the project, designed the experiments and prepared the manuscript. LAO, CB, AT and MAD performed immunolabelling experiments. LAO and JCM carried out the stereological cell counts. LAO performed the morphometric and statistical analyses. WTF and KKM contributed to the mouse experiments, including providing transgenic mouse brains. All authors contributed to the interpretation of the results in addition to participating in the finalization of the manuscript.

Conflict of Interest

The authors declare that the research was conducted in the absence of any commercial or financial relationships that could be construed as a potential conflict of interest.

Contribution to the Field Statement

Astrocytes are glial cells that critically support neuronal activity. Astrocytes have not yet been compared between human brain regions before, although it is known that they vary significantly in number, size and function across different mouse brain regions. Moreover, many studies have used the expression of glial fibrillary acidic protein (GFAP) to label

astrocytes, which has been criticized for not revealing much of the entire volume and population of astrocytes. In this study, we performed the first inter-regional comparison of the number and size of astrocytes in the human brain, using both GFAP and a previously understudied astrocyte marker, vimentin. This is the first extensive anatomical characterization of astrocytes labelled with vimentin in the healthy human and mouse brain, which we show to have strikingly different properties from astrocytes labelled with GFAP. These observations provide fundamental insights into human astrocyte morphology, suggesting that astrocytes can vary in function across brain regions, can be distributed in relation to vasculature and form subsets that vary in density and morphology between brain regions, and also differ between species. Taken together, our findings further illustrate the diversity and complexity of astrocytes in the human brain and help us better understand their roles in healthy brain function.

Funding

This study was funded by an NSERC Discovery grant to NM. The Molecular and Cellular Microscopy Platform and the Douglas-Bell Canada Brain Bank (DBCBB) are partly funded by a Healthy Brains for Healthy Lives (CFREF) Platform Grant to GT and NM. The DBCBB is also funded by the Réseau Québécois sur le suicide, le troubles de l'humeur et les troubles associés (FRQS).

Tables & Figures

Table 1: Subject Information

	Subject Information
Age	57.0 ± 6.9
Sex	10M
Tissue pH	6.3 ± 0.1
Postmortem interval (hours)	54.8 ± 9.2
Cause of death	6 natural, 4 accidental

Table 2: Antibodies Used

Primary Antibody	**Species**	**Clone**	**Dilution**	**Source**
Vimentin	Rabbit	ab92547	1:500 (IHC-DAB) 1:250 (IF)	Abcam
GFAP	Chicken	ab4674	1:1000 (IHC-DAB) 1:1000 (IF)	Abcam
CD31	Mouse	JC70	1:250	Santa Cruz

Figure 1

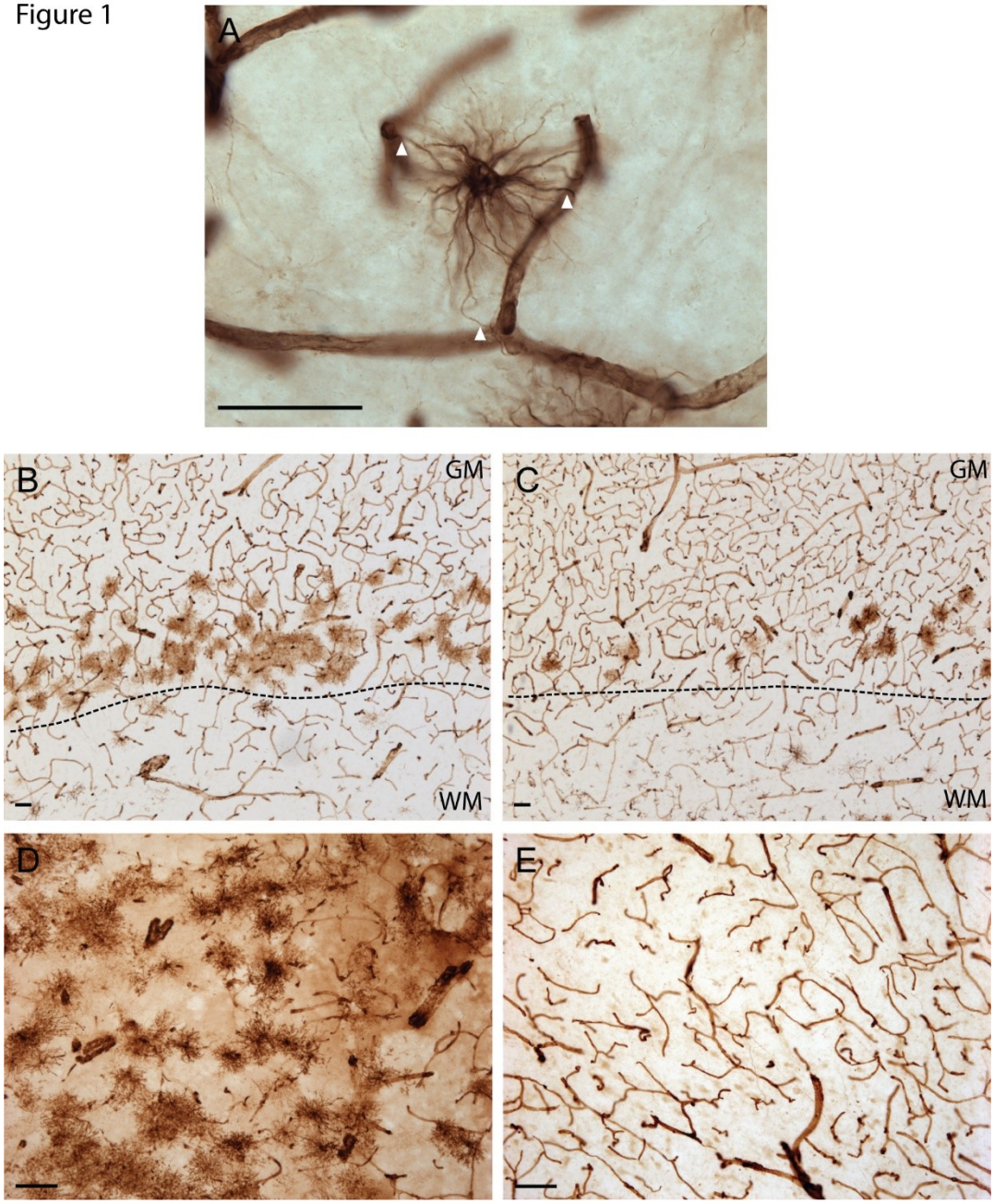

Figure 1 | Vimentin immunohistochemistry strongly labels blood vessels and astrocytes in healthy adult human brain. (A) Example of a VIM-IR astrocyte in the caudate nucleus juxtaposed to and contacting (arrowheads) VIM-IR blood vessels. **(B)** VIM-IR astrocytes in the prefrontal cortex grey matter outnumbered those in white matter and are clustered along the grey/white matter boundary (dashed line). **(C)** Although distributed in a similar pattern along the grey/white matter boundary (dashed line), fewer VIM-IR astrocytes were observed in the primary visual cortex compared to the prefrontal cortex. **(D)** VIM-IR astrocytes were most abundant in the caudate nucleus. **(E)** VIM-IR astrocytes were almost completely absent from the mediodorsal thalamus. Scale bars = 50µm.

Figure 2

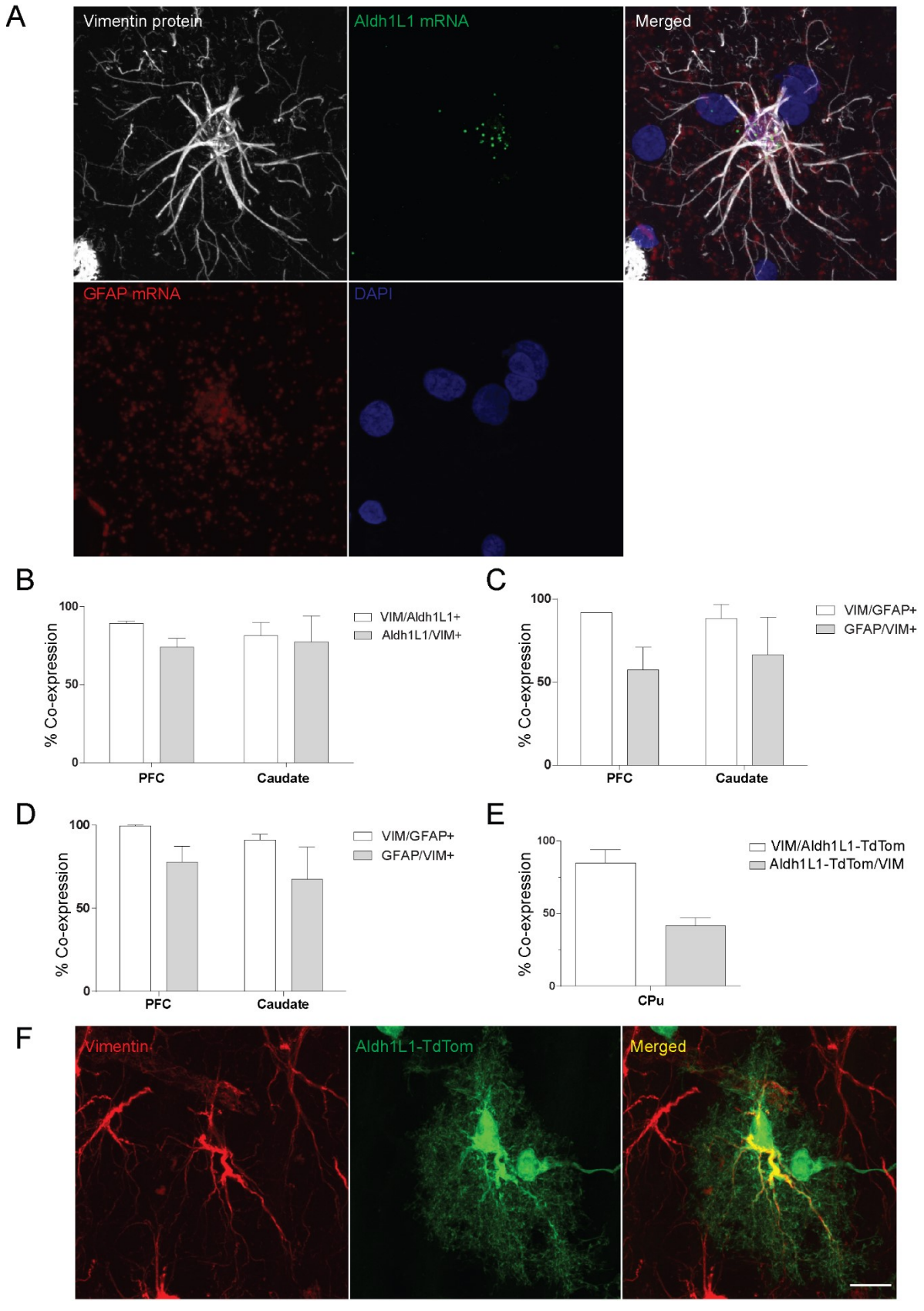
A
Vimentin protein
Aldh1L1 mRNA
Merged
GFAP mRNA
DAPI
B
% Co-expression
100
50
0
PFC
Caudate
VIM/Aldh1L1+
Aldh1L1/VIM+
C
% Co-expression
100
50
0
PFC
Caudate
VIM/GFAP+
GFAP/VIM+
D
% Co-expression
100
50
0
PFC
Caudate
VIM/GFAP+
GFAP/VIM+
E
% Co-expression
100
50
0
CPu
VIM/Aldh1L1-TdTom
Aldh1L1-TdTom/VIM
F
Vimentin
Aldh1L1-TdTom
Merged

Figure 2 | VIM-IR cells express other astrocytic markers in adult human and mouse brain. (A) Representative example in the human prefrontal cortex of a VIM-IR astrocyte revealed using immunofluorescence (white), containing Aldh1L1 mRNA (green) and GFAP mRNA (red), revealed using fluorescent *in situ* hybridization (FISH), within the nucleus (DAPI-stained, blue). **(B)** By combining FISH with immunofluorescence, Aldh1L1 mRNA was observed in the majority of DAPI-stained nuclei of VIM-IR astrocytes in the PFC and the caudate nucleus (n=2). **(C)** By combining FISH with immunofluorescence, GFAP mRNA was observed in the majority of DAPI-stained nuclei of VIM-IR astrocytes in the PFC and the caudate nucleus (n=2). **(D)** Using coimmunofluorescence, the majority of astrocytes in the PFC and the caudate nucleus coexpressed VIM protein and GFAP protein (n=2). **(E)** In transgenic adult mice, the fluorescence of cre reporter proteins in astrocytes expressing Aldh1L1 was observed in many VIM-IR astrocytes in the caudate-putamen (CPu) (n=3). **(F)** VIM protein expression (red) was located within thick processes of transgenically Aldh1L1-labelled (green) astrocytes in the mouse CPu. Scale bars = 25μm.

Figure 3

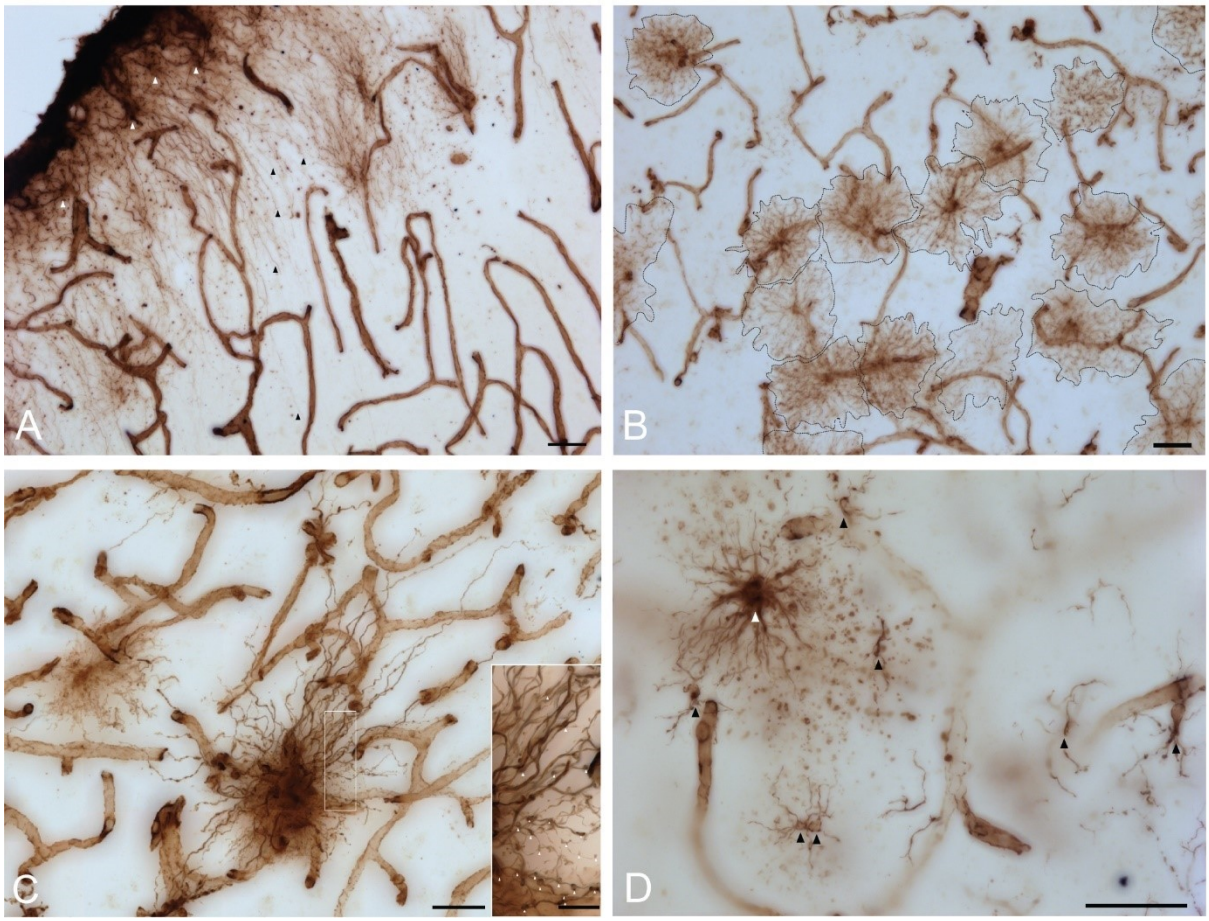

Figure 3 | VIM immunohistochemistry labels astrocytic subtypes previously described for GFAP-IR astrocytes in human neocortex. (A) Fine unbranched fibers (black arrowheads) emerging from darkly labelled VIM-IR interlaminar astrocytes (white arrowheads) and projecting to layer III. (B) VIM-IR astrocytes in the prefrontal cortex grey matter have a non-overlapping domain organization. (C) An example of a VIM-IR astrocyte in deep cortical grey matter (prefrontal cortex) with the attributes of a varicose projection astrocyte. The inset shows a magnified view of regularly spaced varicosities (arrows) on VIM-IR varicose projection astrocyte processes. (D) In cortical white matter and thalamus, VIM-IR astrocytes (white arrowhead) extended rather straight and mostly unbranched processes, as is typical for GFAP-IR fibrous astrocytes. VIM-IR microglia (black arrowheads) were also observed in cortical white matter. In general, these cells were weekly stained and easily distinguishable from VIM-IR astrocytes. Scale bars = 50μm.

Figure 4

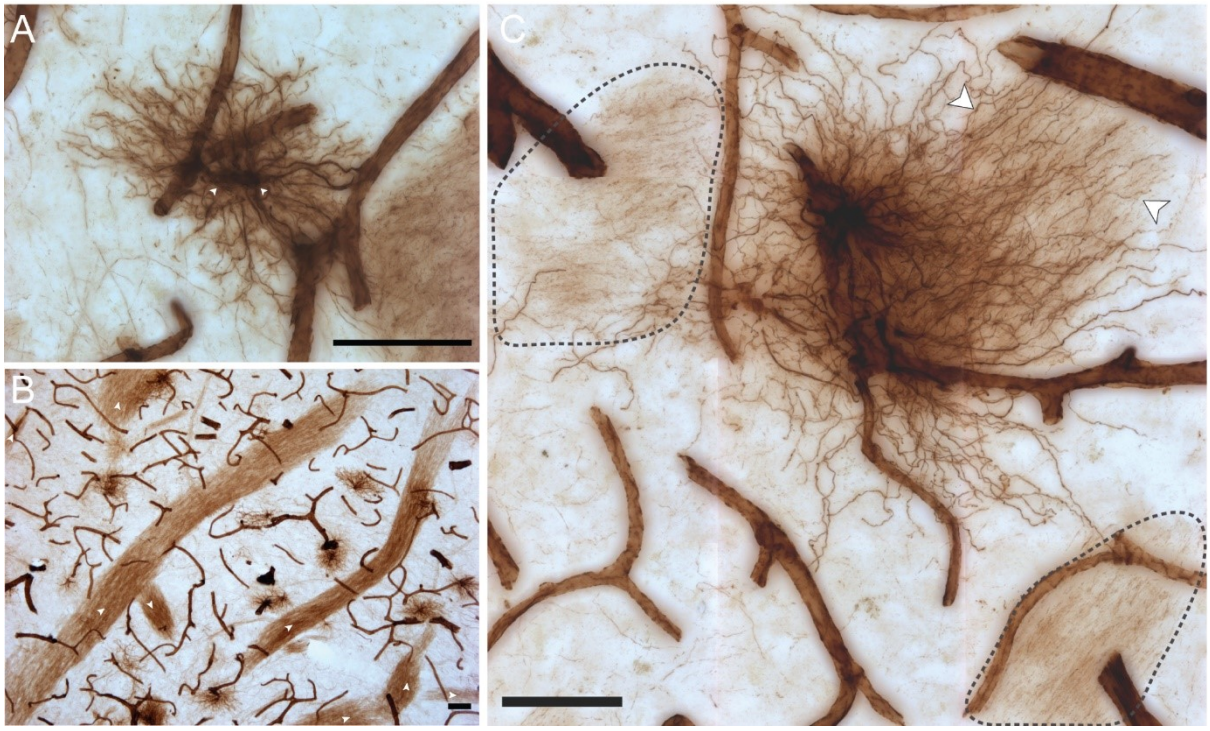

Figure 4 | VIM-IR astrocytes display diverse morphological features. (A) Two adjacent VIM-IR astrocyte cell somas (arrowheads) displaying a twin cell morphology were commonly observed in all human brain regions examined. **(B)** In the caudate nucleus, we observed long bundles of parallel VIM-IR fibers (arrowheads) of no immediately discernable cell origin or target, but which often received contacts from neighboring VIM-IR astrocytes. **(C)** Some VIM-IR astrocytes extended parallel projections (arrowheads) which may be the origin of the fiber bundles illustrated in **(C)** and which appear (black outline) from outside of the z-plane of the section, suggesting that VIM-IR astrocytes contact distal targets. Scale bars = 50µm.

Figure 5

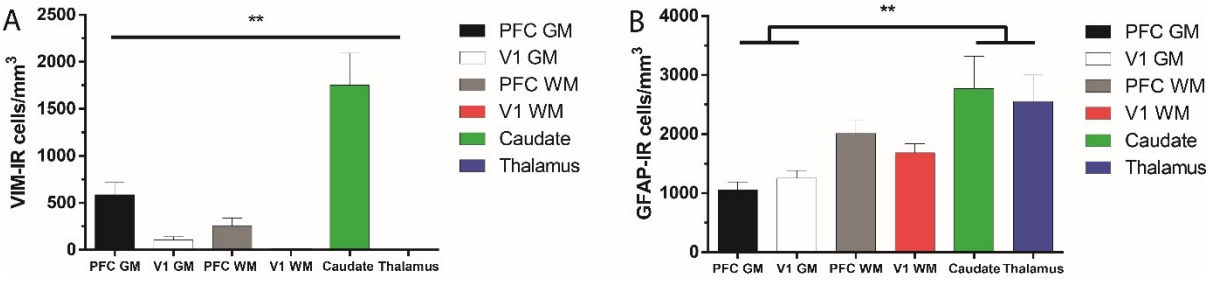

Figure 5 | Regional stereological estimates of VIM-IR and GFAP-IR astrocyte density in the adult human brain. (A) There were significantly more VIM-IR astrocytes in the caudate nucleus than in all other brain regions examined, including the thalamus where VIM-IR astrocytes were mostly absent. **(B)** All human brain regions included in this study were more densely populated by GFAP-IR astrocytes than by VIM-IR astrocytes. There were also significantly more GFAP-IR astrocytes in either subcortical region than in neocortical areas. ** $p \leq 0.01$ ($n = 8$; Matched One-Way ANOVA).

Figure 6

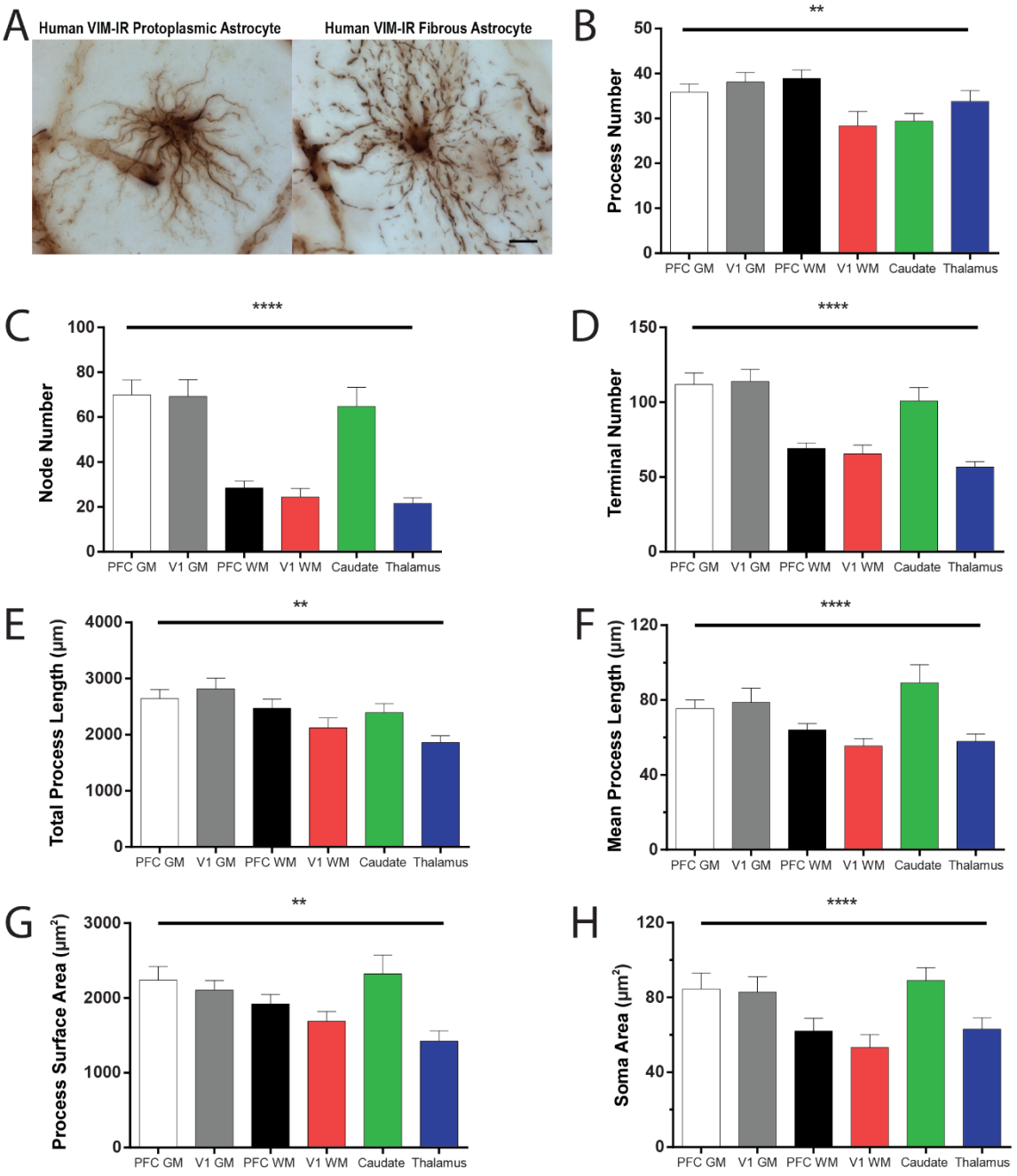

Figure 6 | Regional heterogeneity in human VIM-IR astrocyte morphometry. (A) Representative VIM-IR astrocytes from prefrontal cortex grey matter (left) and white matter (right). **(B–H)** Branched Structure Analysis (BSA) of VIM-IR astrocytes revealed morphometric differences across markers and regions. BSA measurements for VIM-IR astrocytes were generally similar for cortical grey matter and caudate nucleus, and for cortical white matter and mediodorsal thalamus. Scale bars = 50µm. ** $p \leq 0.01$, **** $p \leq 0.0001$ (n = 5; Friedman Test).

Figure 7

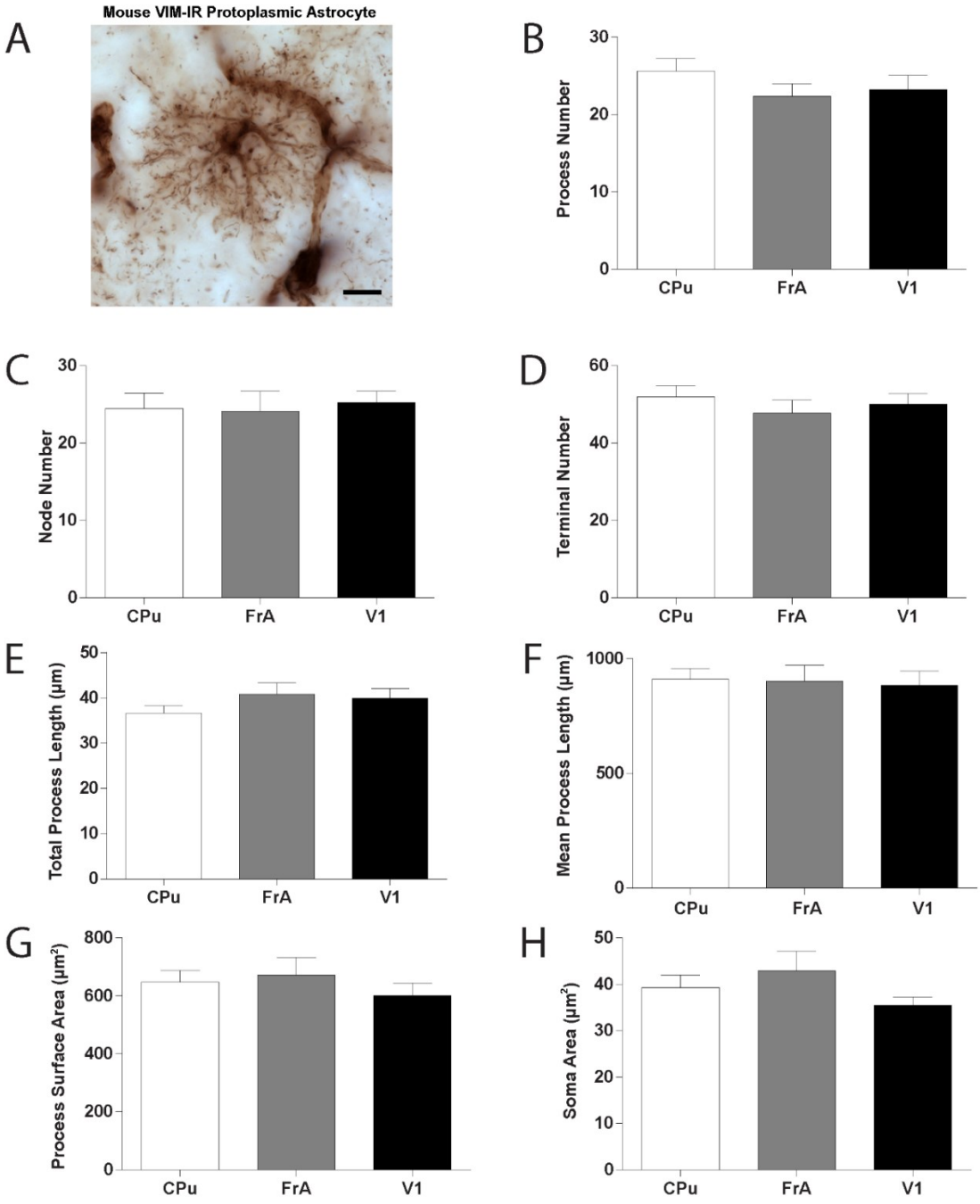

Figure 7 | Lack of regional heterogeneity in mouse VIM-IR astrocyte morphometry. (A) Representative VIM-IR astrocyte from the mouse frontal association cortex grey matter. **(B-H)** In the mouse brain, comparing VIM-IR astrocytes between regions revealed no significant difference ($p > 0.05$) for any of the BSA. Scale bars = 10µm (n = 5; Friedman Test).

Figure 8

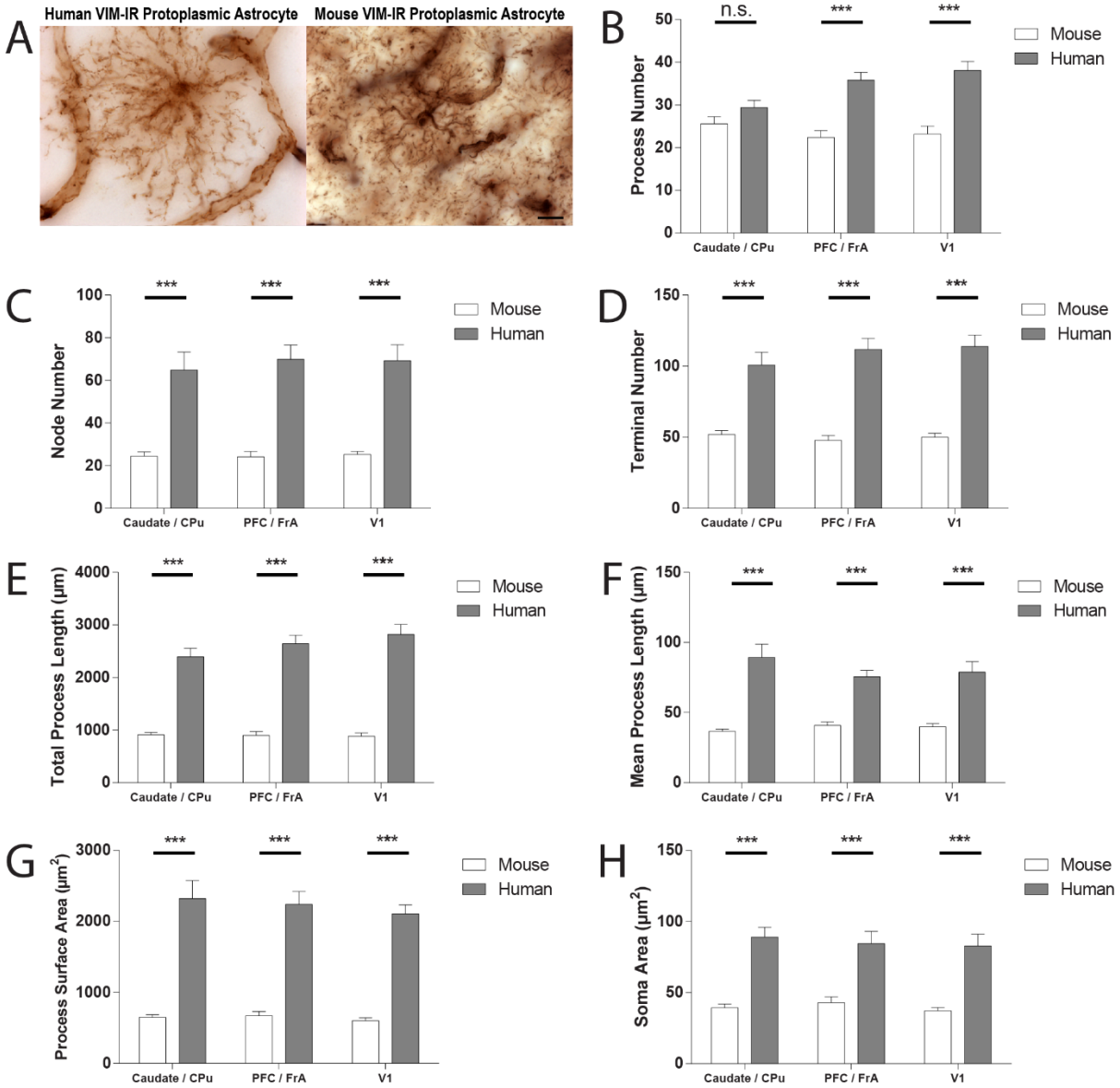

Figure 8 | VIM-IR astrocyte morphometry reveals considerably more complex cerebral astrocytes in humans than in mouse. (A) Representative VIM-IR astrocytes from the human (left) and the mouse (right) primary visual cortex. (B-H) Human VIM-IR astrocytes were distinguishable from mouse VIM-IR astrocytes for all regions and BSA measures, except for process number in the caudate nucleus. Scale bars = 10µm. n.s. $p > 0.05$, *** $p \leq 0.001$ (n = 5; Mann-Whitney U test)

Figure 9

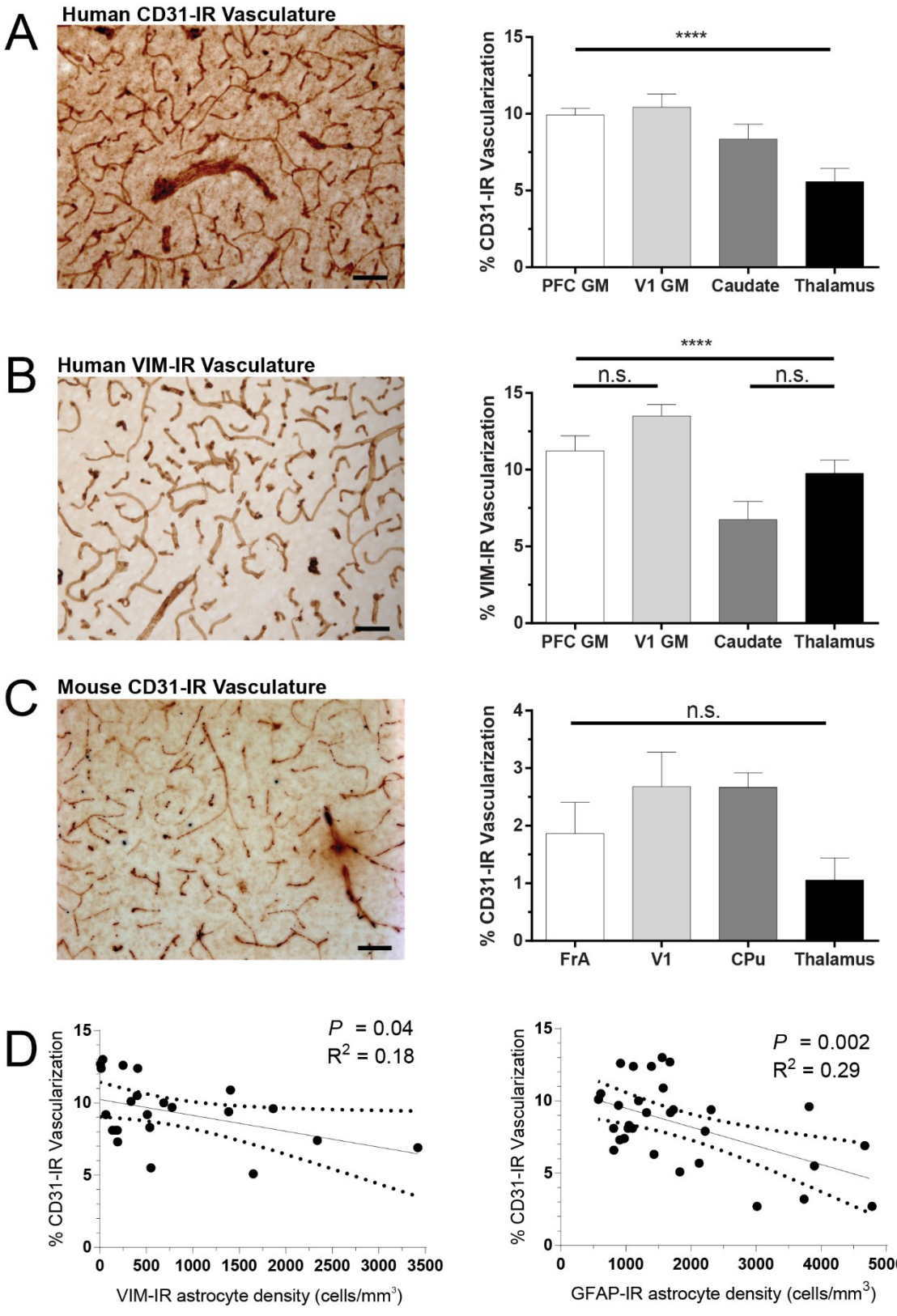
A
Human CD31-IR Vasculature
% CD31-IR Vascularization
****
PFC GM
V1 GM
Caudate
Thalamus
B
Human VIM-IR Vasculature
% VIM-IR Vascularization
****
n.s.
n.s.
PFC GM
V1 GM
Caudate
Thalamus
C
Mouse CD31-IR Vasculature
% CD31-IR Vascularization
n.s.
FrA
V1
CPu
Thalamus
D
% CD31-IR Vascularization
P = 0.04
R2 = 0.18
VIM-IR astrocyte density (cells/mm3)
% CD31-IR Vascularization
P = 0.002
R2 = 0.29
GFAP-IR astrocyte density (cells/mm3)

Figure 9 | Regional differences in vascularization correlate with regional differences in astrocyte density. (A, B) The area occupied by CD31-IR and VIM-IR blood vessels was significantly greater in cortical than in subcortical regions. **(C)** There were no significant differences in the area occupied by CD31-IR blood vessels between mouse brain regions, but this coverage was substantially lower that that measured in human samples **(A, B)**. **(D)** Human VIM-IR and GFAP-IR astrocyte density negatively correlated with CD31-IR vascularization across regions. One value from the caudate nucleus was excluded as an outlier for both regressions, and both the thalamus and cortical white matter values were excluded from the VIM-IR density regression as VIM-IR cells were mostly absent from these regions. Scale bars = 50µm. n.s. $p > 0.05$, **** $p \leq 0.0001$ (Human: n=8; Mouse: n=5; Matched One-Way ANOVAs).

CHAPTER III

Widespread decrease of cerebral vimentin-immunoreactive astrocytes in depressed suicides

Preface

Previous postmortem studies have found decreased densities of astrocytes immunoreactive (-IR) for glial fibrillary acidic protein (GFAP) in mood-associated brain regions from individuals with major depressive disorder (MDD). However, few studies use more than one region and immunohistochemical marker, making it difficult to determine the extent of these changes for the entire astrocyte population, or for other cellular populations, or how widespread they are throughout the brain. Our first study of vimentin (VIM) showed that GFAP-IR and VIM-IR astrocyte densities are regionally heterogeneous in the healthy brain (Chapter II), which suggests that VIM-IR and GFAP-IR astrocyte densities may be differently affected in MDD. Moreover, it is unclear whether regions with lower GFAP-IR astrocyte densities in MDD also contain morphometry differences, as these have been previously observed by our group (Torres-Platas *et al*., 2011).

To improve our understanding of astrocyte abnormalities in MDD, we performed a study with the objectives:

1) *To quantitatively compare the density of VIM-IR and GFAP-IR astrocytes, and the morphology of VIM-IR astrocytes, between depressed suicides and matched controls in mood-associated brain regions.*

2) *To quantitatively compare the density of CD31-IR blood vessels between depressed suicides and matched controls in mood-associated brain regions.*

The rationale of this study was to provide a wider context to the consistent finding of lower GFAP-IR astrocyte densities in MDD, to provide new avenues for investigation. This is the first study implicating a psychopathological role for VIM-IR astrocytes. Though we found widespread reductions in VIM-IR and GFAP-IR astrocyte densities, only VIM-IR astrocytes were affected in cortical white matter, which advises the use of multiple astrocyte markers in future investigations of MDD. As changes in vascular density were more varied than those in astrocyte morphology, this highlights the potential for gliovascular impairments in MDD.

Widespread decrease of cerebral vimentin-immunoreactive astrocytes in depressed suicides

Liam Anuj O'Leary[1,2], Claudia Belliveau[1,2], Maria Antonietta Davoli[1], Jie Christopher Ma[1], Arnaud Tanti[1], Gustavo Turecki[1-3], Naguib Mechawar[1-3]*

[1]McGill Group for Suicide Studies, Douglas Mental Health University Institute, 6875 Boulevard LaSalle, Verdun, QC, Canada, H4H 1R3

[2]Integrated Program in Neuroscience, McGill University, 3801 University Street, Montreal, Canada, H3A 2B4

[3]Department of Psychiatry, McGill University, 1033 Avenue des Pins, Montreal, QC, Canada, H3A 1A1

*Corresponding Author:

Naguib Mechawar, PhD
naguib.mechawar@mcgill.ca

Keywords: human, post-mortem, depression, suicide, astrocyte, vimentin, GFAP (Min.5-Max. 8)

References: 52

Words: 5035

Figures: 5

Tables: 2

Abstract

Postmortem investigations have implicated cerebral astrocytes immunoreactive (-IR) for glial fibrillary acidic protein (GFAP) in the etiopathology of depression and suicide. However, it remains unclear whether astrocytic subpopulations IR for other astrocytic markers are similarly affected. Astrocytes IR to vimentin (VIM) display different regional densities than GFAP-IR astrocytes in the healthy brain, and so may be differently altered in depression and suicide. To

investigate this, we compared the densities of GFAP-IR astrocytes and VIM-IR astrocytes in postmortem brain samples from depressed suicides and matched non-psychiatric controls in three brain regions (dorsomedial prefrontal cortex, dorsal caudate nucleus and mediodorsal thalamus). A quantitative comparison of the fine morphology of VIM-IR astrocytes was also performed in the same regions and subjects. Finally, given the close association between astrocytes and blood vessels, we also assessed densities of CD31-IR blood vessels. Like for GFAP-IR astrocytes, VIM-IR astrocyte densities were found to be globally reduced in depressed suicide relative to controls. By contrast, CD31-IR blood vessel density and VIM-IR astrocyte morphometric features in these regions were similar between groups, except in prefrontal white matter, in which vascularization was increased and astrocytes displayed fewer primary processes. By revealing a widespread reduction of cerebral VIM-IR astrocytes in cases vs. controls, these findings further implicate astrocytic dysfunctions in depression and suicide.

Introduction

Astrocytes were first identified as a glial cell type in the human brain more than a hundred years ago, and until a few decades ago were mostly seen to have a passive role of providing nutritional support for neurons (Andriezen, 1893). Animal studies have since revealed that astrocytes can strongly modulate most facets of neuronal activity, including neuronal firing, neurotransmitter synthesis, neurotransmitter reuptake, and synaptic transmission (Norenberg & Martinez-Hernandez, 1979; Rothstein *et al*., 1996; Duan *et al*., 1999; Cui *et al*., 2018; Covelo & Araque, 2018). Astrocytes might especially influence neuronal activity in the human brain, as they are almost threefold larger in volume and fourfold faster at signaling in the human cortex than in the mouse cortex (Oberheim *et al*., 2009; O'Leary *et al*., 2020).

The first postmortem investigations of major depressive disorder (MDD) reported reduced glial (but not neuronal) densities in the ventral anterior cingulate cortex (Öngür et al., 1998), the orbitofrontal cortex (Rajkowska et al., 1999), and the amygdala (Bowley et al., 2002). These findings were later attributed to a reduced number of cerebral astrocytes, particularly those immunoreactive (-IR) for the astrocyte-specific marker glial fibrillary acidic protein (GFAP). Postmortem brain samples from depressed individuals have fewer GFAP-IR astrocytes (Miguel-Hidalgo et al., 2000; Webster et al., 2001; Si et al., 2004; Altshuler et al., 2010; Cobb et al., 2016; Rajkowska et al., 2018), and lower levels of GFAP mRNA and protein (Chandley

et al., 2013; Fatemi et al., 2004; Torres-Platas et al., 2016). Of all psychiatric conditions, GFAP is most implicated in MDD (Kim et al., 2018). However, GFAP labels only a minority of astrocytes, and so may misrepresent astrocytic phenotypes in MDD (Sofroniew & Vinters, 2010). For instance, the hippocampal CA1 region has lower densities of S100B-IR, but not GFAP-IR, astrocytes in MDD (Gos et al., 2013). Conversely, the amygdala has lower densities of GFAP-IR, but not S100B-IR, astrocytes in MDD (Altshuler et al., 2010; Hamidi et al., 2004). Hence, GFAP expression might not capture the widespread phenotype of astrocyte dysfunction in postmortem studies of MDD, including morphometric differences in cortical fibrous astrocytes (Torres-Platas et al., 2011), reduced vascular coverage (Rajkowska et al., 2013), differential methylation patterns for genes enriched in astrocytes (Nagy et al., 2015), and abnormally low expression levels of astrocytic glutamate transporters (Chandley et al., 2013; Nagy et al., 2015; Zhao et al., 2016), and gap junction proteins (Ernst et al., 2011; Miguel-Hidalgo et al., 2014; Tanti et al., 2019).

Like GFAP, vimentin (VIM) is a type III intermediate filament that is strongly expressed in cerebral astrocytes, however, it is also expressed in vascular endothelial cells. The study of VIM-IR astrocytes has been relative rare, especially given the functional relationship between VIM and GFAP proteins. For instance, VIM has a reciprocal expression profile with GFAP during development, can functionally compensate for the transgenic loss of GFAP expression, and is peculiarly absent in Rosenthal fibres — a defining pathological feature of Alexander disease, a genetic condition associated with GFAP mutations (Dahl, 1981; Tomokane *et al*., 1991; Wilhelmsson *et al*., 2004). A previous postmortem study has found qualitative differences in VIM-IR astrocytes in neurological conditions (Yamada et al., 1992). In a recent postmortem study, we characterized VIM immunoreactivity in different cortical and subcortical brain regions using samples from healthy individuals having died suddenly, and found that VIM-IR astrocytes had different densities from GFAP-IR astrocytes, but that both GFAP-IR and VIM-IR astrocyte density inversely correlated with CD31-IR vascular density (O'Leary *et al*., 2020). We were then interested in how these findings might relate to depression.

Here, we compare the densities of GFAP-IR astrocytes, VIM-IR astrocytes and CD31-IR blood vessels in three brain regions from depressed suicides and matched non-psychiatric controls. In addition, we assessed VIM-IR astrocyte morphometry in MDD in the same sections. In depressed suicides, we found a general and consistent reduction in the density of GFAP-IR and VIM-IR astrocytes, as well as a significant increase in CD31-IR vascularization in the

prefrontal cortex white matter. However, observed almost unaltered VIM-IR astrocyte morphometry in depressed suicides relative to controls. These findings indicate that in the brains of depressed individuals, regional variations in astrocyte densities are much stronger and widespread than changes in astrocyte morphometry.

Materials and Methods

Subjects and Tissue Processing

This study was approved by the Douglas Hospital Research Ethics Board. Brain samples were analyzed from adult Caucasian male depressed suicides (n=10) and non-psychiatric controls (n=10). Subject information is available in **Table 1**. All depressed suicides died during a major depressive episode. All controls died suddenly without any known inflammatory, psychiatric or neurological disorder. Brain donation and psychiatric diagnosis were as described previously (Torres-Platas et al., 2011). Prior to tissue selection, optimal subject groups were matched for three covariates, which were assessed using paired t-tests: age ($p = 0.75$), tissue pH ($p = 0.40$), and postmortem interval (PMI; $p = 0.38$). For all 20 subjects, three brain regions were dissected from thick frozen sections: the dorsomedial prefrontal cortex (Brodmann Area (BA) 8/9), the dorsal caudate nucleus (precommissural) and the mediodorsal thalamus. These brain regions were selected as our recent study characterized GFAP-IR and VIM-IR astrocytes in healthy adults in these regions, and previous work from our group and collaborators suggested gene expression differences in astrocytes of these regions in depression (Nagy et al., 2015; Torres-Platas et al., 2016; O'Leary et al., 2020). We studied the PFC gray matter (PFC GM) and white matter (PFC WM) independently. Fresh-frozen $1cm^3$ tissue blocks from each region were fixed overnight in 10% formalin, suspended in 30% sucrose solution until equilibrium was reached, flash-frozen in -35°C isopentane, and cut on a sliding microtome into 50 µm-thick serial sections that were stored at -20°C in a cryoprotectant solution until processing for immunohistochemistry (IHC). Immunolabeling involved independently using each antibody listed in **Table 2** within a conventional DAB IHC protocol and a separate stereological series of sections, as described previously (O'Leary et al., 2020).

Stereology and Morphology

Stereological cell counting and live tracing was performed as described previously (O'Leary et al., 2020), while additionally blinded to subject identities. Reliable stereological estimates, with a Gunderson coefficient of error (CE, m=1) < 0.10, were obtained by sampling the following percentage areas from section contours: 5% for GFAP in all regions; and 10% for VIM in the PFC GM and the caudate nucleus, 25% in the PFC WM, and 100% in the mediodorsal thalamus. A total of 320 VIM-IR astrocytes were reconstructed, four from the PFC GM, the PFC WM, the thalamus and the caudate nucleus of each subject.

Vascular Density

To estimate vascular density for its comparison with stereological cell densities, 15 brightfield images of CD31-IR vasculature were taken across four sections of a stereological series of sections for each region at low (10X objective) magnification. Using ImageJ software (NIH, USA), each image was converted into an 8-bit format and then manually thresholded to remove most background staining before the percentage area was measured. To reduce noise from background staining and artefacts, only ten values closest to the original mean value were used to calculate the mean % CD31-IR density for each region and subject.

Morphometric features

With the same slides and workstation used for stereological analysis, the morphometry of VIM-IR astrocytes were manually traced live using a 100X oil immersion objective and a computer-based tracing system (Neurolucida Explorer, MBF Bioscience). Immunostained cells were randomly selected, but had to display the following features in ordered to be selected for reconstruction: (1) unobstructed by neighboring cells; (2) of representative size and shape; (3) of equal staining across cellular compartments; (4) contained within the thickness of the section; (5) forming clear endfeet contacts with a VIM-IR blood vessel. A total of 320 VIM-IR cells were traced in this study, as four cells per region were reconstructed and analyzed for all three regions of all 20 subjects (where cortical grey and white matter were considered as independent compartments). Analyses were performed on all reconstructed cells with

Neurolucida Explorer (MBF Bioscience) by an experimenter blinded to the group identity of each sample. Branched Structure Analysis (BSA) was used to compare seven structural features of astrocytes: process number, node number, terminal number, mean process length, total process length, mean process area, and soma area.

3D Reconstructions

All 3D reconstructions were created in Blender (Amsterdam, the Netherlands), which is a free, open-source 3D software suite. For the morphological reconstructions featured in Figure 3A, Neurolucida .DAT files were converted online into .SWC files for two morphological tracings of VIM-IR astrocytes in the prefrontal cortex white matter, which had process numbers representative of controls and depressed suicides in this region. These were then imported into Blender with the assistance of the Neuromorphovis plugin, and BSA features were manually colored and annotated for demonstration purposes (Abdellah *et al*., 2018). For the 'stereological cube' models featured in Figure 6, a randomly distributed particle system of 25mm^3 spheres within the volume of 1m^3 cube was used to visualize regional densities of 25µm^3 diameter cell bodies counted within the regional brain volume of 1mm^3. Sphere volume was kept constant across markers and regions to facilitate cell density comparisons.

Statistical analysis

All measurements are expressed as mean ± standard error of the mean (SEM), graphs display corrected p values on data after outlier removal, and $p < 0.05$ was considered significant in all statistical tests. Preliminary statistical analyses were performed using Prism v. 6.04 (GraphPad Software, San Diego, CA, USA). Data were assessed for a normal distribution using the Kolmogorov–Smirnov test. Statistical outliers were identified using a ROUT outlier test with Q = 1%, which is a conventionally used method for identifying outliers (Motulsky & Brown, 2006). We decided to remove outliers rather than perform non-parametric tests as very few outliers were present in this study and it facilitated more meaningful comparisons by allowing the same statistical tests to be used for all related data sets. Three data points were identified as outliers in this study, one for VIM-IR astrocyte density in PFC GM of a depressed suicide, and two for GFAP-IR astrocyte density in the thalamus of depressed suicides. In these two

instances we provide in-text the p value before outlier removal, as assessed by the Mann-Whitney test — outliers were removed to normalize both data sets, so they met parametric test assumptions. All other instances of uncorrected and corrected group differences were assessed for each region using unpaired t-tests using SPSS version 21 software (IBM Corporation), correction was made for three covariates — age, pH and PMI — to correct for any potential effects they may have had on density or morphometry measurements.

Results

GFAP-IR astrocyte densities are generally reduced in depressed suicides

Using a stereological approach to assess the regional densities of astrocytes in an unbiased fashion, GFAP-IR astrocytes were found to be lower in all regions for depressed suicides relative to controls (**Fig. 1A**). Prefrontal cortex grey matter had half as many GFAP-IR astrocytes in depressed suicides than in controls (444 ± 73 cells/mm^3 vs. 1035 ± 232 cells/mm^3; p [uncorrected] = 0.03, p [corrected] = 0.04). Prefrontal cortex white mater had almost half as many GFAP-IR astrocytes in depressed suicides than in controls, although this difference was not statistically significant (1353 ± 373 cells/mm^3 vs. 2668 ± 510 cells/mm^3; p [uncorrected] = 0.05, p [corrected] = 0.07). The mediodorsal thalamus had the greatest difference between groups, with depressed suicides displaying 5-fold fewer GFAP-IR astrocytes than depressed suicides (1049 ± 400 cells/mm^3 vs. 5902 ± 1348 cells/mm^3; p [uncorrected] = 0.003), but this became 12-fold after removing one statistical outlier that prevented parametric testing (491 ± 101 cells/mm^3 vs. 5902 ± 1348 cells/mm^3; p [uncorrected] = 0.003, p [corrected] = 0.005). Similarly, the caudate nucleus also had 5-fold fewer GFAP-IR astrocytes in depressed suicides than in controls (204 ± 87 cells/mm^3 vs. 1142 ± 356 cells/mm^3; p [uncorrected] = 0.02, p [corrected] = 0.03).

Vimentin-IR astrocyte densities are generally reduced in depressed suicides

As the regional densities of GFAP-IR and VIM-IR were recently reported to differ in postmortem samples from healthy human brains (O'Leary *et al*., 2020), we next assessed whether VIM-IR astrocytes would also display altered regional densities in depressed suicides (**Fig. 2A**). Prefrontal cortex grey matter had 6-fold fewer VIM-IR astrocytes in depressed suicides than in controls (137 ± 100 vs. 886 ± 316 cells/mm^3; p [uncorrected] = 0.08), and this difference became over 20-fold and statistically significant after removing one statistical outlier (38 ± 15 vs. 886 ± 316 cells/mm^3; p [uncorrected] = 0.02, p [corrected] = 0.03). Prefrontal cortex white matter had 20-fold fewer VIM-IR astrocytes in depressed suicides than in controls (14 ± 5 vs. 278 ± 98 cells/mm^3; p [uncorrected] = 0.002, p [corrected] = 0.001). There were slightly fewer VIM-IR astrocytes in the mediodorsal thalamus of controls relative to depressed suicides, but this was not statistically significant due to there being very few cells in both groups (1.2 ± 0.2 vs. 2.1 ± 0.5 cells/mm^3; p [uncorrected] = 0.12, p [corrected] = 0.05). The caudate nucleus had 10-fold fewer VIM-IR astrocytes in depressed suicides than in controls (104 ± 38 vs. 1179 ± 355 cells/mm^3; p [uncorrected] = 0.01, p [corrected] = 0.01).

Vimentin-immunoreactive astrocytes: mostly unchanged morphology in depressed suicides

Process structure

The morphology of VIM-IR astrocytes mostly did not differ significantly between depressed suicides and controls (**Fig. 3;** see parameters assessed in **3A**). The only statistically significant group difference for process number was in the prefrontal cortex white matter (**Fig. 3B**); relative to controls, astrocytes from depressed suicides had on average two more processes in prefrontal cortex grey matter (30 ± 1 vs. 28 ± 2 processes; p [uncorrected] = 0.60, p [corrected] = 0.83), six fewer processes in prefrontal white matter (29 ± 2 vs. 35 ± 1 processes; p [uncorrected] = 0.008, p [corrected] = 0.02), three fewer processes in the thalamus (18 ± 1 vs. 21 ± 1 processes; p [uncorrected] = 0.07, p [corrected] = 0.06), and the same number of processes in the caudate nucleus (27 ± 1 vs. 27 ± 1 processes; p [uncorrected] = 0.63, p [corrected] = 0.77). Astrocyte node number did not significantly differ between groups for any region (**Fig. 3C**); relative to controls, astrocytes from depressed suicides had on average three fewer nodes in prefrontal cortex grey matter (30 ± 3 vs. 33 ± 2 nodes; p [uncorrected] = 0.47, p [corrected] = 0.26), two fewer nodes in prefrontal white matter (20 ± 2 vs. 22 ± 2 nodes; p

[uncorrected] = 0.50, p [corrected] = 0.59), the same number of nodes in the thalamus (14 ± 1 vs. 14 ± 2 nodes; p [uncorrected] = 0.85, p [corrected] = 0.95), and one less node in the caudate nucleus (32 ± 3 vs. 33 ± 3 nodes; p [uncorrected] = 0.82, p [corrected] = 0.91). Similarly, terminal number was not significantly affected in depressed suicides (**Fig. 3D**); relative to controls, astrocytes from depressed suicides had on average two fewer terminals in prefrontal cortex grey matter (60 ± 4 vs. 62 ± 4 terminals; p [uncorrected] = 0.70, p [corrected] = 0.43), eight fewer terminals in prefrontal white matter (49 ± 2 vs. 57 ± 3 terminals; p [uncorrected] = 0.05, p [corrected] = 0.08), two fewer terminals in the thalamus (33 ± 2 vs. 35 ± 2 terminals; p [uncorrected] = 0.39, p [corrected] = 0.33), and the same number of terminals in the caudate nucleus (61 ± 3 vs. 61 ± 3 terminals; p [uncorrected] = 0.94, p [corrected] = 0.87).

Process length

Astrocyte total process length did not significantly differ between groups in any region (**Fig. 3E**); relative to controls, the mean total process length for astrocytes from depressed suicides was consistently lower in the prefrontal cortex grey matter (1800 ± 108 vs. 1911 ± 108 μm; p [uncorrected] = 0.47, p [corrected] = 0.29), the prefrontal white matter (1750 ± 98 vs. 1968 ± 133 μm; p [uncorrected] = 0.21, p [corrected] = 0.29), the thalamus (1100 ± 121 vs. 1192 ± 92 μm; p [uncorrected] = 0.55, p [corrected] = 0.46), and the caudate nucleus (1798 ± 91 vs. 1882 ± 126 μm; p [uncorrected] = 0.59, p [corrected] = 0.79). Across all regions astrocyte mean process length did not significantly or consistently differ between groups (**Fig. 3F**); relative to healthy controls, astrocyte processes from depressed suicides were shorter in prefrontal cortex grey matter (62 ± 3 vs. 68 ± 2 μm; p [uncorrected] = 0.14, p [corrected] = 0.14), longer in prefrontal white matter (62 ± 1 vs. 57 ± 2 μm; p [uncorrected] = 0.06, p [corrected] = 0.08), longer in the thalamus (62 ± 5 vs. 58 ± 4 μm; p [uncorrected] = 0.56, p [corrected] = 0.73) and shorter in the caudate nucleus (67 ± 4 vs. 71 ± 4 μm; p [uncorrected] = 0.39, p [corrected] = 0.53).

Cell size

The surface area of astrocyte processes did not significantly differ between groups for any region (**Fig. 3G**); relative to controls, the surface area of astrocyte processes from depressed suicides was smaller in the prefrontal cortex grey matter (1377 ± 79 vs. 1401 ± 112 μm^2; p

[uncorrected] = 0.86, p [corrected] = 0.80), the prefrontal white matter (1381 ± 119 vs. 1625 ± 119 μm^2; p [uncorrected] = 0.16, p [corrected] = 0.20), the thalamus (907 ± 133 vs. 1019 ± 98 μm^2; p = [uncorrected] 0.50, p [corrected] = 0.47), and the caudate nucleus (1519 ± 81 vs. 1657 ± 128 μm^2; p [uncorrected] = 0.38, p [corrected] = 0.53). As for total process length, the volume occupied by astrocyte processes did not significantly differ between group in any region (**Fig. 3H**), but relative to healthy controls, the mean volume of astrocyte processes from depressed suicides was consistently smaller in the prefrontal cortex grey matter (87 ± 8 vs. 108 ± 9 μm^3; p [uncorrected] = 0.25, p [corrected] = 0.24), the prefrontal white matter (102 ± 12 vs. 132 ± 14 μm^3; p [uncorrected] = 0.30, p [corrected] = 0.16), the thalamus (63 ± 10 vs. 89 ± 12 μm^3; p [uncorrected] = 0.31, p [corrected] = 0.30), and the caudate nucleus (121 ± 8 vs. 140 ± 14 μm^3; p [uncorrected] = 0.32, p [corrected] = 0.25). The soma area of astrocytes did not significantly differ between groups for any region (**Fig. 3I**); relative to healthy controls, the soma area of astrocytes from depressed suicides was smaller in the prefrontal cortex grey matter (69 ± 5 vs. 70 ± 5 μm^2; p [uncorrected] = 0.92, p [corrected] = 0.76), smaller in the prefrontal white matter (29 ± 1 vs. 32 ± 2 μm^2; p [uncorrected] = 0.07, p [corrected] = 0.06), larger in the thalamus (68 ± 7 vs. 56 ± 4 μm^2; p [uncorrected] = 0.19, p [corrected] = 0.24), and smaller in the caudate nucleus (60 ± 3 vs. 62 ± 5 μm^2; p [uncorrected] = 0.60, p [corrected] = 0.50).

CD31-immunoreactive vascular density is increased in the prefrontal cortex white matter of depressed suicides

There was no general trend for group differences in vascular density (Fig. 4A). In prefrontal cortex grey matter, it was found to be comparable between depressed suicides and controls (6.9% ± 0.6 vs. 7.4% ± 0.5% coverage; p [uncorrected] = 0.55, p [corrected] = 0.76). Similar results were found in the mediodorsal thalamus and caudate nucleus, in which vascular densities were also comparable between depressed suicides and controls (thalamus: 7.2% ± 0.4% vs. 7.5% ± 0.4% coverage; p [uncorrected] = 0.58, p [corrected] = 0.96; caudate: 8.1% ± 0.3% vs. 7.7% ± 0.5% coverage; p [uncorrected] = 0.46, p [corrected] = 0.28). Only in prefrontal cortex white matter was there a significant group difference in vascular density, with greater vascularization in depressed suicides than in controls (3.4% ± 1.2% vs. 2.6% ± 0.2% coverage; p [uncorrected] = 0.003, p [corrected] = 0.002).

Discussion

To our knowledge, this is the first study investigating VIM-IR astrocytes in MDD and suicide, and the first cross-regional study of astrocyte density or morphology in MDD. This is one of few postmortem studies comparing the same samples with more than one astrocytic marker. The main results (1) further support previous reports of greater differences in GFAP expression in subcortical regions than in cortical regions of depressed suicides (Torres-Platas et al., 2016); (2) show that VIM-IR astrocyte densities are even more robustly decreased (without morphological changes) in cortical regions; (3) reveal altered CD31-IR vascular density in the PFC WM of depressed suicides. Presenting our data as densities using a stereological approach avoided the potential bias in counting from cortical volumes altered by depression or other factors. As depression generally decreases cortical volumes (Grieve et al., 2013), a non-stereological approach would likely give rise to increased or unchanged cortical astrocyte densities in case samples. However, previous stereological postmortem studies have reported decreased glial densities in the prefrontal cortex in depression (Rajkowska et al., 1999; Cotter et al., 2002), where we now report a decreased density of VIM-IR astrocytes.

Astrocyte densities

In this study, we revealed lower GFAP-IR and VIM-IR astrocyte densities in both cortical and subcortical brain samples from well-characterized depressed suicides compared to matched controls **(Fig. 5).** For GFAP-IR astrocytes, this decrease was statistically significant in all regions except for the prefrontal cortex white matter ($p = 0.053$). This reveals a widespread alteration in GFAP-IR astrocytes throughout a number of cerebral networks in depressed individuals. The density of VIM-IR astrocytes was also assessed in the same subjects and regions. As our previous study showed that VIM mostly labels a subset of GFAP-IR astrocytes (O'Leary *et al*., 2020), this approach helped clarify whether reduced GFAP-IR astrocyte densities in depressed suicides reflects a reduction in astrocyte density as opposed to a reduction of GFAP immunoreactivity. In depressed suicides, the density of VIM-IR astrocytes was strongly and significantly lower in the prefrontal cortex and caudate nucleus, but not in the mediodorsal thalamus, in which exceedingly rare VIM-IR astrocytes are observed in controls. The lower densities of both GFAP-IR and VIM-IR astrocytes favors a hypothesis of a reduced number of astrocytes over a reduced reactive profile of astrocytes in depressed suicides.

The brain regions examined in this study are closely associated in a prominent frontal-subcortical circuit implicated in executive function — neurons project from the caudate nucleus to the mediodorsal thalamus and then to the dorsomedial prefrontal cortex gray matter (Bonelli & Cummings, 2007). This executive circuit has been found to be dysregulated in depression, with patients displaying a relatively lower resting state connectivity between the prefrontal cortex and either the striatum or the thalamus are more likely to have a positive treatment response to repetitive transcranial magnetic stimulation of the prefrontal cortex (Salomons *et al*., 2014). The connectivity of the prefrontal cortex seems essential to the neuroanatomy of depression — no single brain region consistently associates with MDD when lesioned, however, brain regions with relatively high resting state connectivity to the dorsomedial prefrontal cortex are consistently associated with MDD following lesions (Padmanabhan *et al*., 2019). In the context of our results, astrocyte dysfunction may directly regulate resting state functional connectivity to the prefrontal cortex, as astrocytes mediate vasodilation responsible for changes in regional cerebral blood flow. If our results do represent a reduction in numbers of astrocytes, this may represent a compensatory mechanism by which the brain is indirectly reducing functional connectivity by impairing the efficiency of gliovascular coupling in a circuit that becomes hyperconnected in depression.

A reduction in GFAP-IR astrocyte density in multiple brain regions from depressed suicides supports a strong consensus in the literature for decreased regional GFAP protein levels in postmortem studies and animal models of depression (Kim et al., 2018). Our findings also support postmortem studies on depression which have found semi-qualitative decreases in the number of GFAP-IR astrocytes in other brain regions, such as the hippocampus (Müller et al., 2001). We observed greater differences in GFAP-IR astrocyte densities in subcortical regions than in cortical regions, which is in agreement with a previous report of GFAP protein levels being even more downregulated in the mediodorsal thalamus and caudate nucleus than in cortical regions of depressed suicides relative to controls (Torres-Platas *et al*., 2016). This previous study also found the mediodorsal thalamus and caudate nucleus have greater regional GFAP expression levels than many cortical regions in healthy adults, and so our findings indicate that brain regions that normally have a high GFAP expression in healthy adults may have particularly strong depression-related changes in GFAP-IR astrocyte densities. The association between regional GFAP expression and GFAP-IR astrocyte density is supported by a previous study that correlated low regional GFAP protein levels with low GFAP-IR area fraction in the dorsomedial prefrontal cortex gray matter of depressed suicides (Si *et al*., 2004),

which may well resemble a reduction in cell density given our findings. Although we found no significant difference in GFAP-IR astrocyte density in dorsomedial prefrontal cortex white matter, a previous study reported a significantly lower density of GFAP-IR astrocytes in the ventromedial prefrontal cortex white matter of depressed suicides — a difference that was 5-fold greater than was observed for dorsomedial prefrontal cortex white matter in the present study (Rajkowska *et al*., 2018). This suggests that prefrontal cortex white matter may have a particularly strong subregional heterogeneity for depression-related changes in GFAP-IR astrocyte density.

While VIM-IR astrocytes clearly represent a minority of the total astrocyte population in healthy controls (O'Leary et al., 2020), VIM is a valuable marker as it is strongly immunoreactive in both cell body and processes. The group differences in astrocyte density in the prefrontal cortex grey matter and caudate nucleus were twice as great for VIM-IR astrocytes than for GFAP-IR astrocytes, indicating astrocytes strongly expressing VIM may be especially affected in depressed suicides. The lack of a significant decrease of VIM-IR astrocyte density in the mediodorsal thalamus was unsurprising, given that many sections from the thalamus of control subjects in this and our previous study contained no VIM-IR astrocytes at all (O'Leary *et al*., 2020). While the density of VIM-IR astrocytes is extremely low in our analyses of the mediodorsal thalamus, VIM-IR astrocytes have previously been reported to be almost absent in postmortem hippocampal samples (Arnold et al., 1996). This paucity of VIM-IR astrocytes in certain brain regions is further suggested by the substantial differences in astrocyte density in different nuclei of the thalamus in mouse brain (Emsley & Macklis, 2006). However, we suspect this indicates an unrecognized functional role of thalamic astrocytes that does not require VIM expression. As VIM expression affects the speed of vesicular transport and the expression of other astrocytic intermediate filaments, this low VIM expression may reflect both structural and functional differences for thalamic astrocytes that otherwise express GFAP (Jing et al., 2007; Vardjan et al., 2012). Following from this, the widespread loss of VIM-IR astrocytes in MDD suggests the loss vesicular trafficking and cell division properties more commonly seen in non-VIM-IR astrocytes.

To date, only one other postmortem study has assessed VIM in the context of depression and found no significant decrease of VIM mRNA levels in MDD in the anterior cingulate cortex of depressed individuals who died by natural causes (not by suicide) (Qi *et al*., 2019). Although this may reflect an effect unique to the anterior cingulate cortex, this does not reliably imply no change of VIM-IR astrocyte density in the ACC, given that the most VIM expression in the

brain is found in vascular endothelial cells (Nagy *et al*., 2020; O'Leary et al., 2020). As for astrocytes labelled with glutamine synthetase, there is a reduced number of VIM-IR astrocytes in postmortem brain samples from individuals with MDD, but due to its expression in other cell types, this effect is not detected at the regional level of protein or mRNA (Bernstein *et al*., 2015). The reduction of VIM-IR astrocyte density in depressed suicides suggests that reduced GFAP levels do not correspond specifically to GFAP dysfunction, but rather a widespread loss or dysfunction of astrocytes. A pan-astrocytic marker like Aldh1L1 will be needed to infer whether only reactive astrocytes expressing VIM and GFAP are affected in depression; however, this seems unlikely, as genes specific to both non-reactive and reactive astrocytes are downregulated in many brain regions in depressed suicides (Nagy *et al*., 2015; Nagy *et al*., 2017; Zhao *et al*., 2016) and depressed non-suicides (Zhao *et al*., 2018). We do not exclude the possibility that astrocyte density differences may differ in postmortem samples from depressed non-suicides. However, investigations having compared regional astrocyte densities between depressed individuals having died by suicide or non-suicidal causes found no significant difference between groups (Cobb et al., 2016; Zhao et al., 2019). As our depressed suicide cohort died by hanging, one might expect vascular changes from asphyxia may have systematically altered gliovascular interactions in a way that might not be observed for other methods of suicide.

Vascular densities

In a previous study, our group showed that regional astrocyte density inversely correlates with regional vascular density in postmortem brain samples from controls (O'Leary *et al.,* 2020). In the present study, brain regions from depressed suicides had significantly lower astrocyte density than controls, and so we anticipated that they may also have a correspondingly greater vascular density. Depressed suicides had a significantly different (higher) vascular density than controls only in prefrontal cortex white matter— no other significant differences or general trends were observed for regional vascular density. This finding suggest that gliovascular interactions in cortical white matter may be preferentially affected by depression, as also suggested by a previous report of reduced coverage of blood vessels by astrocytic endfeet in prefrontal cortex grey matter, but not white matter (Rajkowska *et al*., 2013). It is also likely that vascular density does not reflect the full extent of vascular changes in depressed individuals, such as the known reduction in claudin-5 protein levels in postmortem vascular

endothelial cells of the nucleus accumbens in depressed suicides, which in animal models has been associated with an abnormally increased permeability of the blood brain barrier (Menard *et al*., 2017; Dudek *et al*., 2020). Future studies on gliovascular interactions in depression may need to resolve this with finer precision with a non-stereological method, given the absence of a clear region-wide relationship between astrocyte and vascular density in depression.

Limitations and Future Directions

The two main limitations of this study were its relatively small sample size and lack of samples from females. Female samples were not included due to the low availability of such samples from depressed suicides which could be effectively matched for factors that are known to greatly affect astrocyte regional densities and gene expression in postmortem samples, including age and postmortem interval (Miguel-Hidalgo *et al*., 2000; Nagy *et al*., 2015). Furthermore, some important questions remain that could not be assessed with the current sample, including whether the number, duration and severity of depressive episodes may have an incidence on VIM-IR or GFAP-IR astrocyte densities. In conclusion, different brain regions in depressed suicides exhibit robust reductions in VIM-IR astrocyte densities that are even greater than those for GFAP-IR astrocytes. Our data also more generally revealed a consistent cross-regional trend for reduced astrocyte densities in depressed suicides, and a unique change in vascular density in the prefrontal cortex white matter. With the minor exception of fibrous astrocytes in the prefrontal cortex, there were no clear changes in the morphology of VIM-IR astrocytes that we could most clearly and precisely observe, indicating that depression has a larger and more widespread effect on astrocyte density than on astrocyte morphology in mood-associated brain regions. In the future, single cell sequencing approaches will be informative for establishing whether the function of these smaller populations of cells in depressed suicides are altered in depressed suicides.

References

1. Abdellah, M., Hernando, J., Eilemann, S., Lapere, S., Antille, N., Markram, H., et al. (2018). NeuroMorphoVis: a collaborative framework for analysis and visualization of

neuronal morphology skeletons reconstructed from microscopy stacks. Bioinformatics 34, i574–i582. doi:10.1093/bioinformatics/bty231.

2. Andriezen, W. L. (1893). The Neuroglia Elements in the Human Brain. Br Med J 2, 227–230.

3. Altshuler, L. L., Abulseoud, O. A., Foland-Ross, L., Bartzokis, G., Chang, S., Mintz, J., et al. (2010). Amygdala astrocyte reduction in subjects with major depressive disorder but not bipolar disorder. Bipolar Disorders 12, 541–549. doi:10.1111/j.1399-5618.2010.00838.x.

4. Bernstein, H.-G., Meyer-Lotz, G., Dobrowolny, H., Bannier, J., Steiner, J., Walter, M., et al. (2015). Reduced density of glutamine synthetase immunoreactive astrocytes in different cortical areas in major depression but not in bipolar I disorder. Front. Cell. Neurosci. 9. doi:10.3389/fncel.2015.00273.

5. Bonelli, R. M., and Cummings, J. L. (2007). Frontal-subcortical circuitry and behavior. Dialogues Clin Neurosci 9, 141–151.

6. Bowley, M. P., Drevets, W. C., Öngür, D., and Price, J. L. (2002). Low glial numbers in the amygdala in major depressive disorder. Biological Psychiatry 52, 404–412. doi:10.1016/S0006-3223(02)01404-X.

7. Chandley, M. J., Szebeni, K., Szebeni, A., Crawford, J., Stockmeier, C. A., Turecki, G., et al. (2013). Gene expression deficits in pontine locus coeruleus astrocytes in men with major depressive disorder. J Psychiatry Neurosci 38, 276–284. doi:10.1503/jpn.120110.

8. Cobb, J. A., O'Neill, K., Milner, J., Mahajan, G. J., Lawrence, T. J., May, W. L., et al. (2016). Density of GFAP-immunoreactive astrocytes is decreased in left hippocampi in major depressive disorder. Neuroscience 316, 209–220. doi:10.1016/j.neuroscience.2015.12.044.

9. Cotter, D., Mackay, D., Chana, G., Beasley, C., Landau, S., & Everall, I. P. (2002) Reduced neuronal size and glial cell density in area 9 of the dorsolateral prefrontal cortex in subjects with major depressive disorder. Cerebral Cortex, 12(4), 386–394. https://doi.org/10.1093/cercor/12.4.386

10. Covelo, A., and Araque, A. (2018). Neuronal activity determines distinct gliotransmitter release from a single astrocyte. eLife 7, e32237. doi:10.7554/eLife.32237.

11. Cui, Y., Yang, Y., Ni, Z., Dong, Y., Cai, G., Foncelle, A., et al. (2018). Astroglial Kir4.1 in the lateral habenula drives neuronal bursts in depression. Nature 554, 323–327. doi:10.1038/nature25752.

12. Dahl, D. (1981). The vimentin-GFA protein transition in rat neuroglia cytoskeleton occurs at the time of myelination. Journal of Neuroscience Research 6, 741–748. doi:10.1002/jnr.490060608.

13. Duan, S., Anderson, C. M., Stein, B. A., and Swanson, R. A. (1999). Glutamate Induces Rapid Upregulation of Astrocyte Glutamate Transport and Cell-Surface Expression of GLAST. J. Neurosci. 19, 10193–10200. doi:10.1523/JNEUROSCI.19-23-10193.1999.

14. Dudek, K. A., Dion-Albert, L., Lebel, M., LeClair, K., Labrecque, S., Tuck, E., et al. (2020). Molecular adaptations of the blood–brain barrier promote stress resilience vs. depression. PNAS 117, 3326–3336. doi:10.1073/pnas.1914655117.

15. Emsley, J. G., and Macklis, J. D. (2006). Astroglial heterogeneity closely reflects the neuronal-defined anatomy of the adult murine CNS. Neuron Glia Biol 2, 175–186. doi:10.1017/S1740925X06000202.

16. Ernst, C., Nagy, C., Kim, S., Yang, J. P., Deng, X., Hellstrom, I. C., et al. (2011). Dysfunction of Astrocyte Connexins 30 and 43 in Dorsal Lateral Prefrontal Cortex of Suicide Completers. Biological Psychiatry 70, 312–319. doi:10.1016/j.biopsych.2011.03.038.

17. Fatemi, S. H., Laurence, J. A., Araghi-Niknam, M., Stary, J. M., Schulz, S. C., Lee, S., et al. (2004). Glial fibrillary acidic protein is reduced in cerebellum of subjects with major depression, but not schizophrenia. Schizophrenia Research 69, 317–323. doi:10.1016/j.schres.2003.08.014.

18. Gos, T., Schroeter, M. L., Lessel, W., Bernstein, H.-G., Dobrowolny, H., Schiltz, K., et al. (2013). S100B-immunopositive astrocytes and oligodendrocytes in the

hippocampus are differentially afflicted in unipolar and bipolar depression: A postmortem study. Journal of Psychiatric Research 47, 1694–1699. doi:10.1016/j.jpsychires.2013.07.005.

19. Grieve, S. M., Korgaonkar, M. S., Koslow, S. H., Gordon, E., Williams, L. M. (2013) Widespread reductions in gray matter volume in depression. NeuroImage: Clinical, 3, 332–339. doi.org/10.1016/j.nicl.2013.08.016

20. Hamidi, M., Drevets, W. C., and Price, J. L. (2004). Glial reduction in amygdala in major depressive disorder is due to oligodendrocytes. Biological Psychiatry 55, 563–569. doi:10.1016/j.biopsych.2003.11.006.

21. Kim, R., Healey, K. L., Sepulveda-Orengo, M. T., and Reissner, K. J. (2018). Astroglial correlates of neuropsychiatric disease: From astrocytopathy to astrogliosis. Progress in Neuro-Psychopharmacology and Biological Psychiatry 87, 126–146. doi:10.1016/j.pnpbp.2017.10.002.

22. Menard, C., Pfau, M. L., Hodes, G. E., Kana, V., Wang, V. X., Bouchard, S., et al. (2017). Social stress induces neurovascular pathology promoting depression. Nature Neuroscience 20, 1752–1760. doi:10.1038/s41593-017-0010-3.

23. Miguel-Hidalgo, J. J., Baucom, C., Dilley, G., Overholser, J. C., Meltzer, H. Y., Stockmeier, C. A., et al. (2000). Glial fibrillary acidic protein immunoreactivity in the prefrontal cortex distinguishes younger from older adults in major depressive disorder. Biological Psychiatry 48, 861–873. doi:10.1016/S0006-3223(00)00999-9.

24. Miguel-Hidalgo, J. J., Waltzer, R., Whittom, A. A., Austin, M. C., Rajkowska, G., and Stockmeier, C. A. (2010). Glial and glutamatergic markers in depression, alcoholism, and their comorbidity. Journal of Affective Disorders 127, 230–240. doi:10.1016/j.jad.2010.06.003.

25. Miguel-Hidalgo, J. J., Wilson, B. A., Hussain, S., Meshram, A., Rajkowska, G., and Stockmeier, C. A. (2014). Reduced connexin 43 immunolabeling in the orbitofrontal cortex in alcohol dependence and depression. Journal of Psychiatric Research 55, 101–109. doi:10.1016/j.jpsychires.2014.04.007.

26. Motulsky, H. J., and Brown, R. E. (2006). Detecting outliers when fitting data with nonlinear regression – a new method based on robust nonlinear regression and the false discovery rate. BMC Bioinformatics 7, 123. doi:10.1186/1471-2105-7-123.

27. Nagy, C., Suderman, M., Yang, J., Szyf, M., Mechawar, N., Ernst, C., et al. (2015). Astrocytic abnormalities and global DNA methylation patterns in depression and suicide. Molecular Psychiatry 20, 320–328. doi:10.1038/mp.2014.21.

28. Nagy, C., Torres-Platas, S. G., Mechawar, N., and Turecki, G. (2017). Repression of Astrocytic Connexins in Cortical and Subcortical Brain Regions and Prefrontal Enrichment of H3K9me3 in Depression and Suicide. Int J Neuropsychopharmacol 20, 50–57. doi:10.1093/ijnp/pyw071.

29. Nagy, C., Maitra, M., Tanti, A., Suderman, M., Théroux, J.-F., Davoli, M. A., et al. (2020). Single-nucleus transcriptomics of the prefrontal cortex in major depressive disorder implicates oligodendrocyte precursor cells and excitatory neurons. Nature Neuroscience 23, 771–781. doi:10.1038/s41593-020-0621-y.

30. Norenberg, M. D., and Martinez-Hernandez, A. (1979). Fine structural localization of glutamine synthetase in astrocytes of rat brain. Brain Research 161, 303–310. doi:10.1016/0006-8993(79)90071-4.

31. Oberheim, N. A., Takano, T., Han, X., He, W., Lin, J. H. C., Wang, F., et al. (2009). Uniquely Hominid Features of Adult Human Astrocytes. J. Neurosci. 29, 3276–3287. doi:10.1523/JNEUROSCI.4707-08.2009.

32. O'Leary, L. A., Davoli, M. A., Belliveau, C., Tanti, A., Ma, C., Farmer, W. T., et al. (2020). Characterization of vimentin-immunoreactive astrocytes in the human brain. Front. Neuroanat. 14. doi:10.3389/fnana.2020.00031.

33. Öngür, D., Drevets, W. C., and Price, J. L. (1998). Glial reduction in the subgenual prefrontal cortex in mood disorders. PNAS 95, 13290–13295. doi:10.1073/pnas.95.22.13290.

34. Padmanabhan, J. L., Cooke, D., Joutsa, J., Siddiqi, S. H., Ferguson, M., Darby, R. R., et al. (2019). A Human Depression Circuit Derived From Focal Brain Lesions. Biological Psychiatry 86, 749–758. doi:10.1016/j.biopsych.2019.07.023.

35. Powers, B., Kleinman, J. E., Hyde, T. M., Ajilore, O., Leow, A., and Sodhi, M. S. (2019). Differential expression of glutamate transporters and monoaminergic genes in major depression and suicide. bioRxiv, 596403. doi:10.1101/596403.

36. Qi, X.-R., Kamphuis, W., and Shan, L. (2019). Astrocyte Changes in the Prefrontal Cortex From Aged Non-suicidal Depressed Patients. Front. Cell. Neurosci. 13. doi:10.3389/fncel.2019.00503.

37. Rajkowska, G., Miguel-Hidalgo, J. J., Wei, J., Dilley, G., Pittman, S. D., Meltzer, H. Y., et al. (1999). Morphometric evidence for neuronal and glial prefrontal cell pathology in major depression∗∗See accompanying Editorial, in this issue. Biological Psychiatry 45, 1085–1098. doi:10.1016/S0006-3223(99)00041-4.

38. Rajkowska, G., Hughes, J., Stockmeier, C. A., Javier Miguel-Hidalgo, J., and Maciag, D. (2013). Coverage of Blood Vessels by Astrocytic Endfeet Is Reduced in Major Depressive Disorder. Biological Psychiatry 73, 613–621. doi:10.1016/j.biopsych.2012.09.024.

39. Rajkowska, G., Legutko, B., Moulana, M., Syed, M., Romero, D. G., Stockmeier, C. A., et al. (2018). Astrocyte pathology in the ventral prefrontal white matter in depression. Journal of Psychiatric Research 102, 150–158. doi:10.1016/j.jpsychires.2018.04.005.

40. Rothstein, J. D., Dykes-Hoberg, M., Pardo, C. A., Bristol, L. A., Jin, L., Kuncl, R. W., et al. (1996). Knockout of Glutamate Transporters Reveals a Major Role for Astroglial Transport in Excitotoxicity and Clearance of Glutamate. Neuron 16, 675–686. doi:10.1016/S0896-6273(00)80086-0.

41. Salomons, T. V., Dunlop, K., Kennedy, S. H., Flint, A., Geraci, J., Giacobbe, P., et al. (2014). Resting-State Cortico-Thalamic-Striatal Connectivity Predicts Response to Dorsomedial Prefrontal rTMS in Major Depressive Disorder. Neuropsychopharmacology 39, 488–498. doi:10.1038/npp.2013.222.

42. Si, X., Miguel-Hidalgo, J. J., O'Dwyer, G., Stockmeier, C. A., and Rajkowska, G. (2004). Age-Dependent Reductions in the Level of Glial Fibrillary Acidic Protein in

the Prefrontal Cortex in Major Depression. Neuropsychopharmacology 29, 2088–2096. doi:10.1038/sj.npp.1300525.

43. Sofroniew, M. V., and Vinters, H. V. (2010). Astrocytes: biology and pathology. Acta Neuropathol 119, 7–35. doi:10.1007/s00401-009-0619-8.

44. Tanti, A., Lutz, P.-E., Kim, J., O'Leary, L., Théroux, J.-F., Turecki, G., et al. (2019). Evidence of decreased gap junction coupling between astrocytes and oligodendrocytes in the anterior cingulate cortex of depressed suicides. Neuropsychopharmacology 44, 2099–2111. doi:10.1038/s41386-019-0471-z.

45. Tomokane, N., Iwaki, T., Tateishi, J., Iwaki, A., and Goldman, J. E. (1991). Rosenthal fibers share epitopes with alpha B-crystallin, glial fibrillary acidic protein, and ubiquitin, but not with vimentin. Immunoelectron microscopy with colloidal gold. Am J Pathol 138, 875–885.

46. Torres-Platas, S. G., Hercher, C., Davoli, M. A., Maussion, G., Labonté, B., Turecki, G., et al. (2011). Astrocytic Hypertrophy in Anterior Cingulate White Matter of Depressed Suicides. Neuropsychopharmacology 36, 2650–2658. doi:10.1038/npp.2011.154.

47. Torres-Platas, S. G., Nagy, C., Wakid, M., Turecki, G., and Mechawar, N. (2016). Glial fibrillary acidic protein is differentially expressed across cortical and subcortical regions in healthy brains and downregulated in the thalamus and caudate nucleus of depressed suicides. Molecular Psychiatry 21, 509–515. doi:10.1038/mp.2015.65.

48. Webster, M. J., Knable, M. B., Johnston-Wilson, N., Nagata, K., Inagaki, M., and Yolken, R. H. (2001). Immunohistochemical Localization of Phosphorylated Glial Fibrillary Acidic Protein in the Prefrontal Cortex and Hippocampus from Patients with Schizophrenia, Bipolar Disorder, and Depression. Brain, Behavior, and Immunity 15, 388–400. doi:10.1006/brbi.2001.0646.

49. Wilhelmsson, U., Li, L., Pekna, M., Berthold, C.-H., Blom, S., Eliasson, C., et al. (2004). Absence of Glial Fibrillary Acidic Protein and Vimentin Prevents Hypertrophy of Astrocytic Processes and Improves Post-Traumatic Regeneration. J. Neurosci. 24, 5016–5021. doi:10.1523/JNEUROSCI.0820-04.2004.

50. Yamada, T., Kawamata, T., Walker, D. G., & McGeer, P. L. (1992). Vimentin immunoreactivity in normal and pathological human brain tissue. Acta Neuropathologica, 84(2), 157–162. https://doi.org/10.1007/BF00311389

51. Zhao, J., Verwer, R. W. H., van Wamelen, D. J., Qi, X.-R., Gao, S.-F., Lucassen, P. J., et al. (2016). Prefrontal changes in the glutamate-glutamine cycle and neuronal/glial glutamate transporters in depression with and without suicide. Journal of Psychiatric Research 82, 8–15. doi:10.1016/j.jpsychires.2016.06.017.

52. Zhao, J., Verwer, R. W. H., Gao, S.-F., Qi, X.-R., Lucassen, P. J., Kessels, H. W., et al. (2018). Prefrontal alterations in GABAergic and glutamatergic gene expression in relation to depression and suicide. Journal of Psychiatric Research 102, 261–274. doi:10.1016/j.jpsychires.2018.04.020.

Acknowledgments

The present study used the services of the Douglas-Bell Canada Brain Bank and of the Molecular and Cellular Microscopy Platform at the Douglas Hospital Research Centre. The authors are grateful to Maâmar Bouchouka, Josée Prud'homme, Dominique Mirault and Melina Jaramillo Garcia for their kind assistance.

Author Contributions

LAO and NM conceived the project, designed the experiments and drafted the manuscript. CB, MAD and LAO conducted tissue processing, and LAO conducted the IHC experiments. LAO and JCM performed the cell counting experiments. LAO performed vascular density and astrocyte morphometry experiments and analyzed all the data. All authors contributed to the interpretation of the results in addition to participating in the finalization of the manuscript.

Conflict of Interest

The authors declare that the research was conducted in the absence of any commercial or financial relationships that could be construed as a potential conflict of interest.

Contribution to the Field Statement

Astrocytes are a glial cell type in the brain that are less abundant in the brains of depressed individuals. It is unclear exactly which astrocyte populations or brain regions are most affected in depression, because most previous studies have studied only one astrocyte population in one brain region in the same individuals. It is also unclear whether the reduced number of astrocytes during depression is accompanied with changes to their physical structure or to the blood vessels they normally contact. This study is also the first anatomical comparison of astrocytes labelled by the protein vimentin in postmortem brain tissue from depressed individuals. We performed the first cross-regional assessment of astrocyte density and morphometry using two distinct astrocytic markers, as well as of vascular density in postmortem brain samples from depressed individuals and matched controls. We found a significant and widespread reduction in astrocyte densities (but no significant change in cell morphology) in depressed suicides relative to controls. Blood vessel density was only different (increased) in prefrontal cortex white matter of depressed suicides. This study reveals a widespread alteration of cerebral astrocytes in depression and suicide.

Funding

This study was funded by an NSERC Discovery grant and a CIHR Project grant to NM. The Molecular and Cellular Microscopy Platform and the Douglas-Bell Canada Brain Bank (DBCBB) are partly funded by a Healthy Brains for Healthy Lives (CFREF) Platform Grant to GT and NM. The DBCBB is also funded by the Réseau Québécois sur le suicide, le troubles de l'humeur et les troubles associés (FRQS).

Tables & Figures

Table 1: Subject Information

	Controls (n = 10)	**Depressed Suicides (n = 10)**
	Mean ± SEM	**Mean ± SEM**
Age	40.6 ± 5.0	38.5 ± 4.2
Sex	10M	10M
Tissue pH	6.5 ± 0.0	6.6 ± 0.0
PMI (h)	15.3 ± 2.8	21.8 ± 5.9
Cause of death	8 cardiovascular, 2 accidental falls	10 Hanging
Depression Status	0	10
Toxicology Report		
Alcohol	1	3
Cocaine	0	2
Antidepressants	0	1 (desvenlafaxine)

Table 2: Antibodies: specifications

Primary Antibody	*Species*	*Clone*	*Dilution*	*Source*
Vimentin	Rabbit	ab92547	1:500	Abcam
GFAP	Chicken	ab4674	1:1000	Abcam
CD31	Mouse	JC70	1:250	Santa Cruz

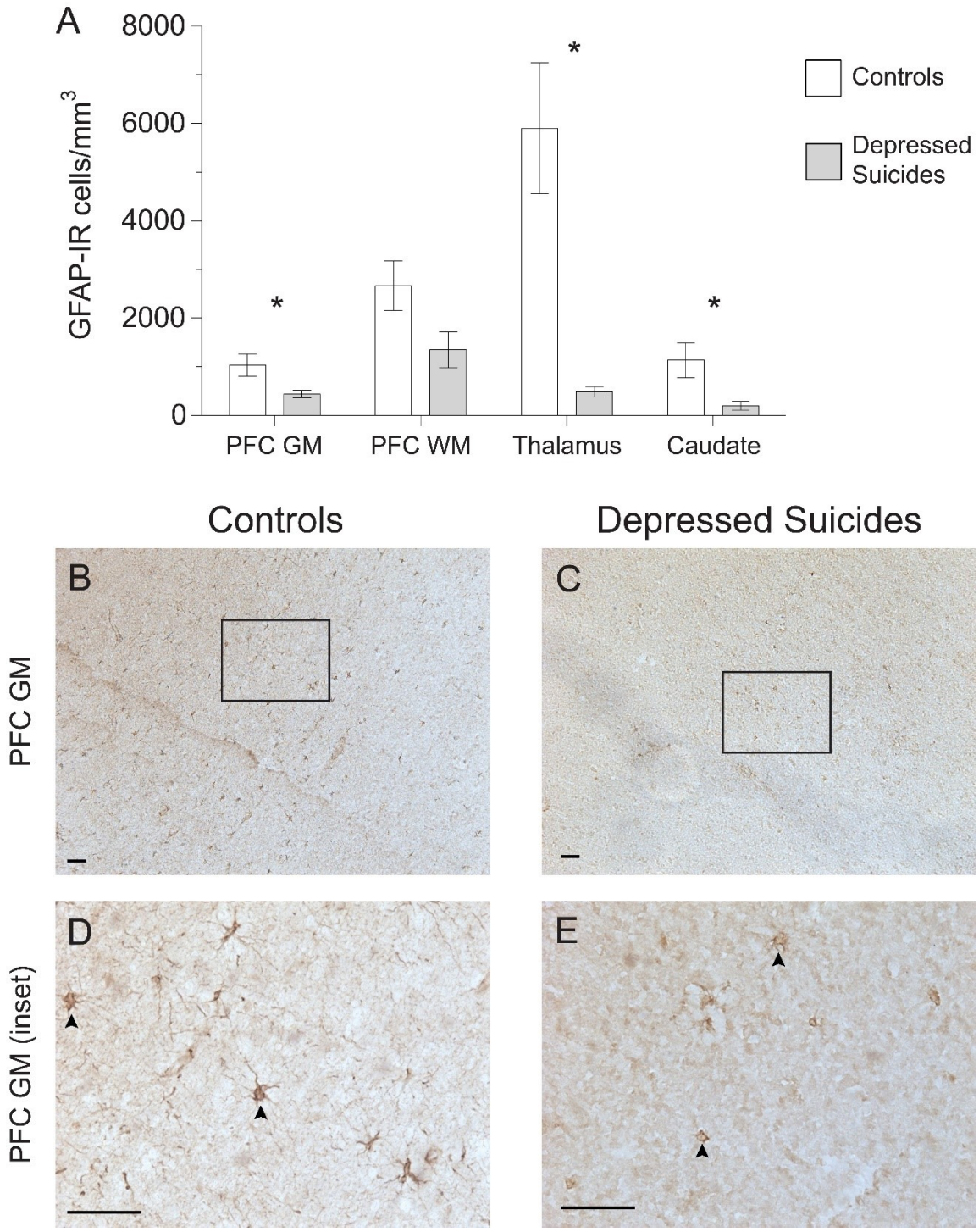

Figure 1 | Lower densities of GFAP-IR cerebral astrocytes in depressed suicides relative to controls. (A) Representative micrographs illustrating GFAP-IR astrocytes in the prefrontal cortex gray matter (PFC GM). Scale bars = 50μm. **(B)** Depressed suicides had significantly lower densities of GFAP-IR astrocytes than controls in all regions examined except in the prefrontal cortex white matter (PFC WM), in which the difference was nearly significant. * $p \leq 0.05$; $n = 10$; unpaired t-tests corrected for age, pH and postmortem interval.

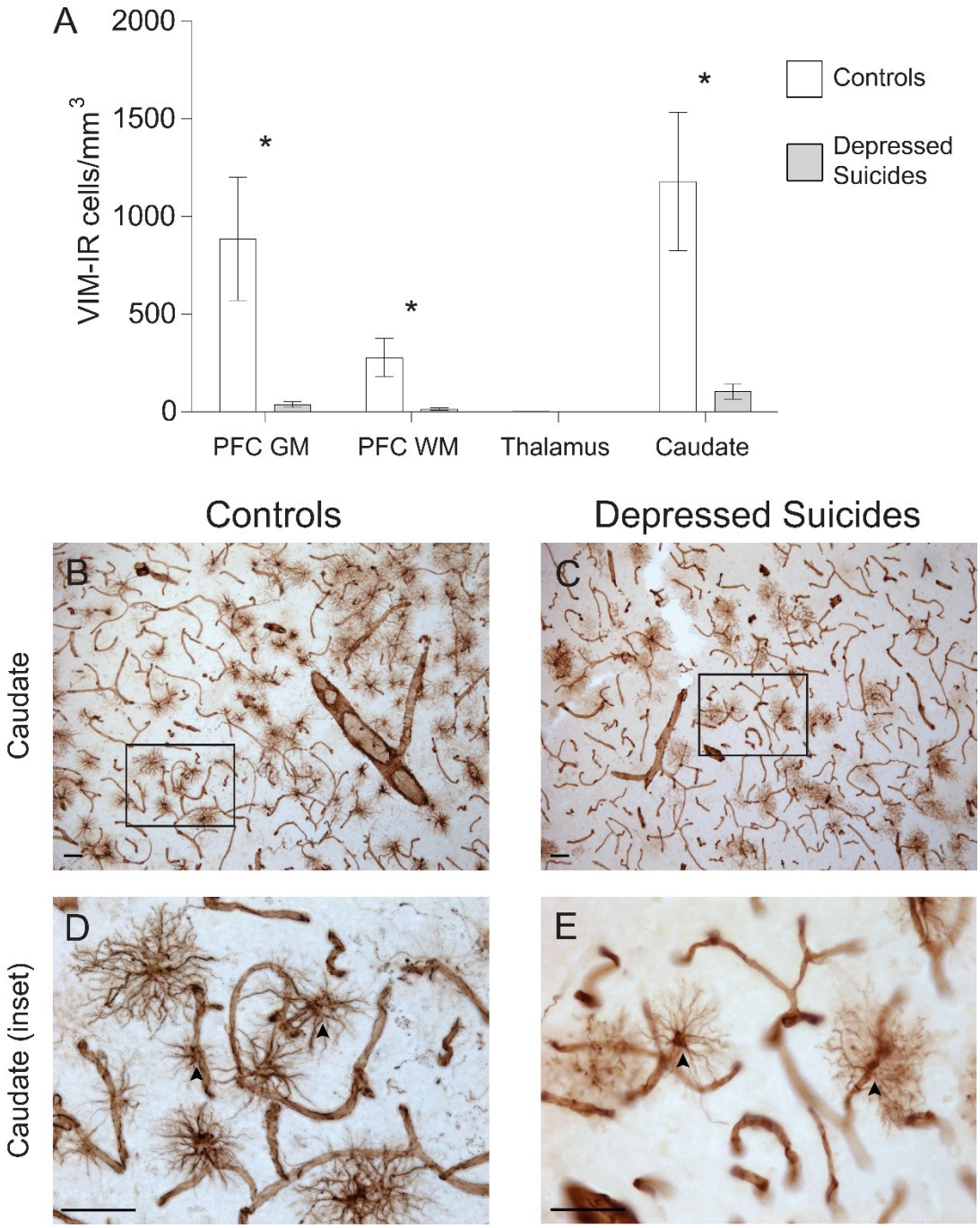

Figure 2 | Lower densities of VIM-IR cerebral astrocytes in depressed suicides relative to controls. (A) Representative micrographs illustrating VIM-IR astrocytes in the caudate nucleus. Scale bars = 50µm. **(B)** Depressed suicides had significantly lower densities of GFAP-IR astrocytes than controls in the caudate nucleus, the prefrontal cortex gray matter (PFC GM) and the prefrontal cortex white matter (PFC WM). No group difference was observed in the mediodorsal thalamus, which presented exceedingly few VIM-IR astrocytes in both groups. * $p \leq 0.05$; n = 10; unpaired t-tests corrected for age, pH and postmortem interval.

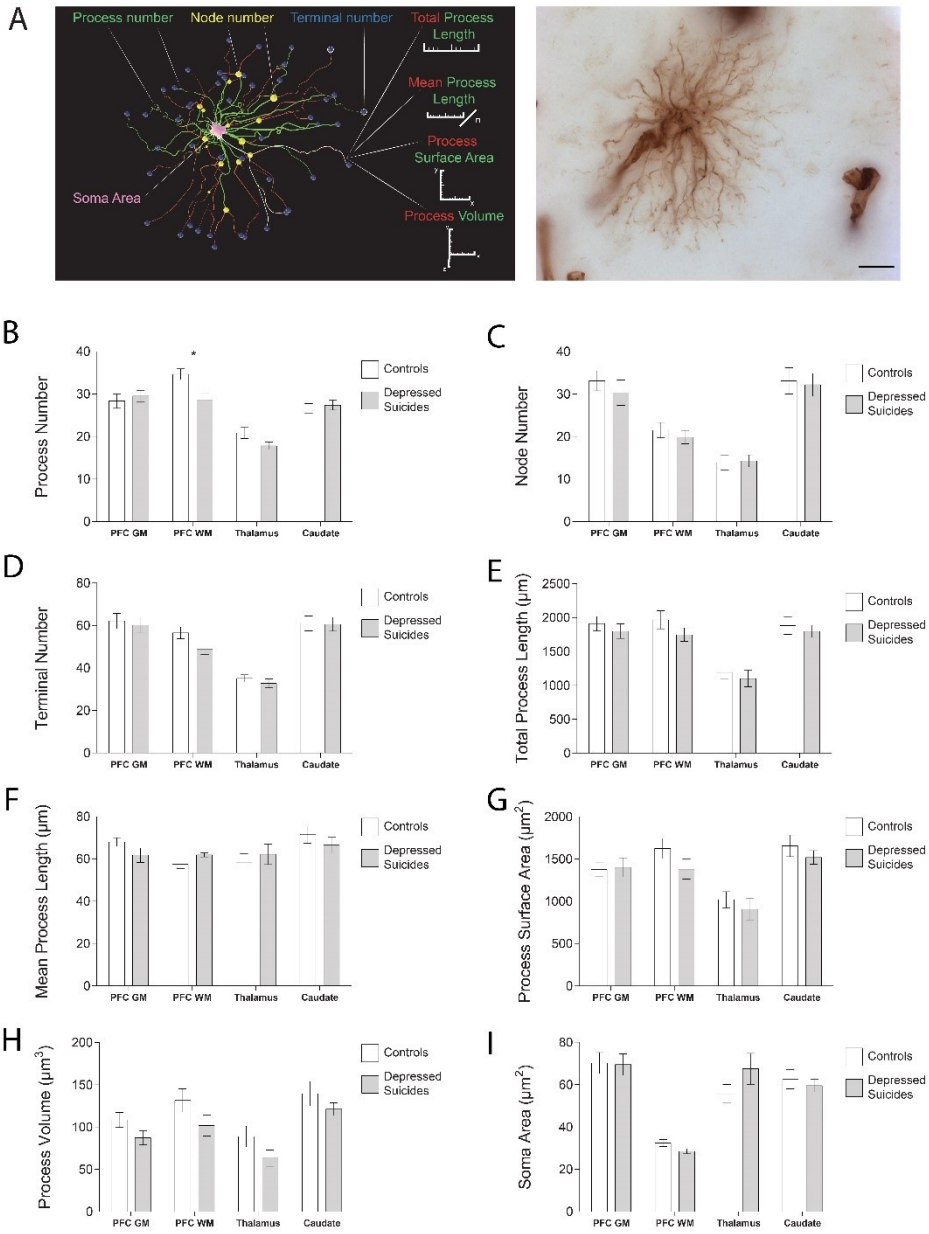

Figure 3 | VIM-IR astrocyte morphology is generally similar in depressed suicides vs controls. (**A)** 3D reconstruction of a VIM-IR astrocyte from the prefrontal cortex white matter (PFC WM) representative of those from depressed suicides (left). The soma (pink) that extends primary processes (green) which can branch at nodes (yellow) into secondary processes (red) that eventually end as terminals (blue). Branched Structure Analysis (BSA) measurements have been annotated (left), and a minimum intensity projection of a representative VIM-IR astrocyte from the caudate nucleus of a depressed suicide is illustrated (right). **(B–H)** The BSA revealed a lower (primary) process number for VIM-IR astrocytes in the PFC WM of depressed suicides relative to controls. There were no group differences for any BSA measurements of VIM-IR astrocytes in the prefrontal cortex gray matter (PFC GM), thalamus or caudate nucleus. *$p \leq 0.05$; $n = 10$; unpaired t-tests corrected for age, pH and postmortem interval.

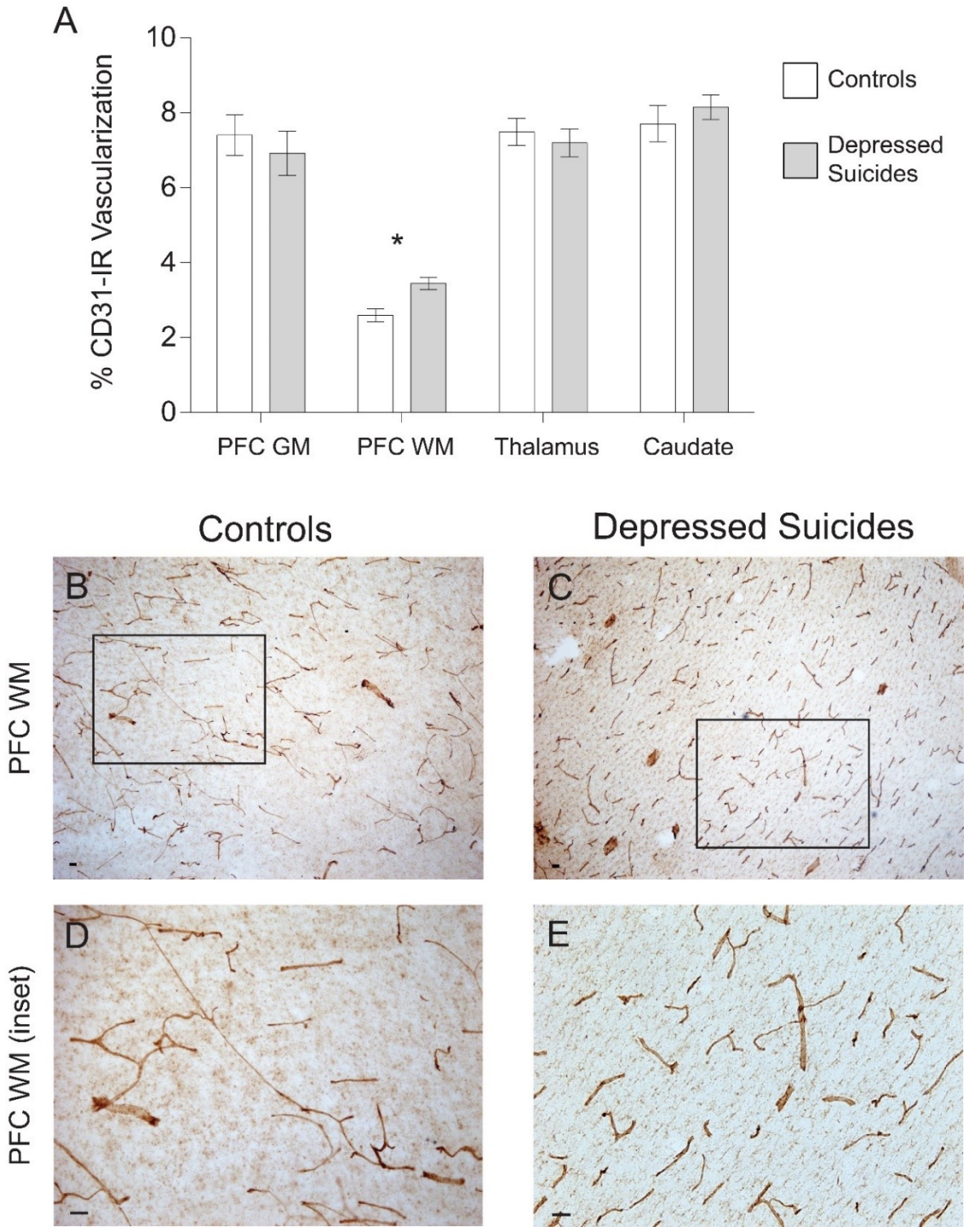

Figure 4 | Increased CD31-IR vascular density in cortical white matter from depressed suicides relative to controls. (A) Representative micrographs showing that CD31-IR vascular density in the prefrontal cortex white matter (PFC WM). Scale bars = 50µm. **(B)** Depressed suicides had a significantly higher vascular density than controls in the mediodorsal thalamus. No group differences were observed in the prefrontal cortex gray matter (PFC GM), the caudate nucleus or the mediodorsal thalamus. * $p \leq 0.05$; n = 10; unpaired t-tests corrected for age, pH and postmortem interval.

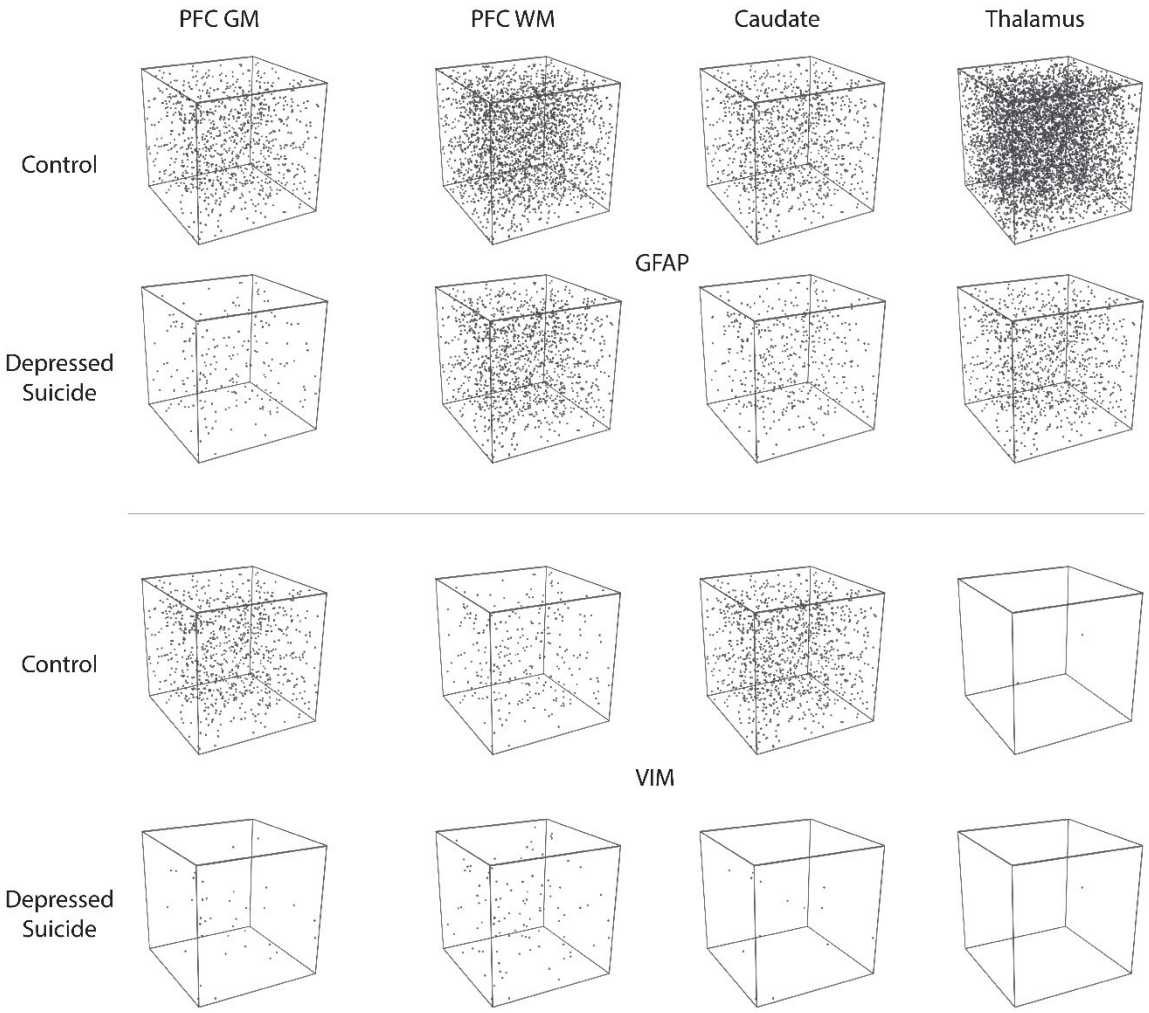

Figure 5 | Visual representation of astrocyte densities in depressed suicides. Each cube represents 1mm^3 of cerebral tissue in which are distributed the stereological estimates of cell densities reported in Figures 1 and 2 (cell body diameter = 25µm). These illustrations demonstrate that astrocyte density is greatly and widely affected in depressed suicides relative to controls.

CHAPTER IV

Regional heterogeneity of astrocyte density and morphology in the human brain

Preface

Chapters II and III of this dissertation establish vimentin (VIM) as an astrocyte marker in the human brain that, relative to glial fibrillary acidic protein (GFAP), reveals unparalleled access to astrocyte morphometry for immunohistochemical protocols, and unique features of astrocytes both in the brains of healthy controls and depressed suicides. This review was written with the following goal:

To integrate our findings into what is known for astrocyte density and morphology from postmortem studies, and into emerging models of MDD from clinical literature and animal studies.

As glial hypotheses of neurological and psychiatric conditions are relatively new to the neuroscience community, the rationale for this chapter was to emphasize the potential of VIM as an astrocyte marker and contextualize changes in astrocyte densities in MDD to a wider audience.

This chapter provides the first comprehensive comparison of astrocyte stereological and morphometric data from postmortem studies. It highlights stereology studies using Giemsa staining which are rarely discussed within the astrocyte field, but that together reveal that astrocyte densities in the healthy human brain are consistently greater in subcortical regions than in cortical regions. This review provided the first categorization of subcortical astrocyte morphometry based on studies featured in the second and third chapters of this dissertation. Combining stereological and morphometric data prompted a model that visually demonstrates that domains must be a feature mostly limited to GFAP-IR astrocytes. We provide interpretations that explain how reduced astrocyte densities can be compatible with different lines of evidence for astrocytes in MDD, including increased levels of astrocyte markers in the cerebrospinal fluid serum of depressed individuals, and a rodent model of depression involving increased expression of a potassium channel in astrocytes. Together, this comprehensively shows the regional heterogeneity of astrocytes in the adult human brain in healthy and depressed individuals.

Implication of cerebral astrocytes in major depression: a review of fine neuroanatomical evidence in humans

Liam Anuj O'Leary[1,2], Naguib Mechawar[1,2,3*]

[1] McGill Group for Suicide Studies, Douglas Mental Health University Institute, Verdun, QC, Canada

[2]Integrated Program in Neuroscience, McGill University, Montreal, Canada

[3]Department of Psychiatry, McGill University, Montreal, QC, Canada

*** Correspondence:**
Naguib Mechawar, PhD
naguib.mechawar@mcgill.ca

Keywords: human, postmortem, astrocyte, stereology, morphology (Max. 5)

Reference Count: 173

Word Count: 7188

Figure Count: 6

Table Count: 4

Abstract

Postmortem investigations have implicated astrocytes in many neurological and psychiatric conditions. Brain regions from individuals with major depressive disorder (MDD) have lower expression levels of astrocyte markers and lower densities of astrocytes labelled for these markers, suggesting a loss of astrocytes in this mental illness. This paper reviews the general properties of human astrocytes, the methods to study them, and the postmortem evidence for astrocyte pathology in MDD. When comparing astrocyte density and morphometry studies, astrocytes are more abundant and smaller in human subcortical than cortical brain regions, and immunohistochemical labelling for the astrocyte markers glial fibrillary acidic protein (GFAP) and vimentin (VIM) reveals fewer than 15% of all astrocytes that are present in cortical and

subcortical regions, as revealed using other staining techniques. By combining astrocyte densities and morphometry, a model was made to illustrate that domain organization is mostly limited to GFAP-IR astrocytes. Using these markers and others, alterations of astrocyte densities appear more widespread than those for astrocyte morphologies throughout the brain of individuals having died with MDD. This review indicates how reduced astrocyte densities could relate to the association of depressive episodes in MDD with elevated S100 beta (S100B) cerebrospinal fluid serum levels. Finally, a potassium imbalance theory is proposed that integrates the reduced astrocyte densities generated from postmortem studies with a hypothesis for the antidepressant effects of ketamine generated from rodent studies.

Introduction

In recent years, emerging evidence has further positioned astrocytes as a major player in brain activity. A simplified view of the role of astrocytes in the brain is that they critically maintain healthy neuronal function in five essential ways (**Figure 1**). First, astrocytes regulate neuronal metabolism through coordination with pericytes to monitor cerebral blood pressure and blood flow in response to local neuronal activity, while also providing lactate as an energy substrate to active neurons, and clearing metabolic byproducts from the brain (Pellerin & Magistretti, 1994; Takano *et al*., 2006; Choi *et al*., 2012; Iliff *et al*., 2012; Hall *et al*., 2014; Marina *et al*., 2020). Second, astrocytes regulate synaptic function and plasticity via bidirectional signaling with neurons in accordance with the 'tripartite synapse' model, primarily by removing and converting excess glutamate, potassium ion buffering, and releasing gliotransmitters at synapses (Tanaka *et al*., 1997; Pascual *et al.,* 2005; Wallraff *et al.*, 2006; Perea *et al*., 2009; Fujita *et al*., 2014; Arizono *et al*., 2020). Third, astrocytes and microglia participate in activity-dependent synaptic remodelling during early brain development, known as pruning, to refine mature neural circuits in the adult brain (Chung *et al*., 2013; Chung *et al*., 2016; Koeppen *et al*., 2018). Fourth, astrocytes have a critical role in antioxidant defense for brain neurons through activation of the Nrf2 pathway, which leads to the upregulation of many antioxidant compounds, notably glutathione, which act against neurotoxic reactive oxygen species such as nitric oxide (Chen *et al.*, 2001; Bell *et al*., 2011; Correa *et al*., 2011). Fifth, through a process known as reactive astrogliosis, astrocytes responding to pathological lesions undergo characteristic changes in gene expression to adopt distinct molecular states, and this remodeling

can potentially affect many general properties of astrocytes, including astrocyte morphology, proliferation and cellular signaling (McKeon *et al*., 1991; Bardehle *et al*., 2013; Barres & Liddelow, 2017; Escartin *et al*., 2021). This final feature of astrocytes, reactive astrogliosis, is commonly seen in many cerebral pathologies, and has prompted investigations into how astrocytes contribute to the mechanisms of brain disorders (Dossi *et al*., 2018).

The broad functional range of astrocytes indicates that they are particularly dynamic cells, continually adjusting brain physiology to meet the demands of neuronal activity (Poskanzer & Molofsky, 2018). Many papers have shown astrocytes can functionally adapt to stressors and antidepressant responses in animal models of depression (Murphy-Royal *et al*., 2019). However, most foundational studies of astrocytes have been conducted in rodent cortex, where astrocytes have a less diverse and complex morphology than in humans (Andriezen, 1893; Oberheim *et al*., 2009; O'Leary *et al*., 2020). Moreover, most rodent studies have used only one astrocyte marker — glial fibrillary acidic protein (GFAP) — which preferentially labels a small subpopulation of astrocytes with roles in pathology. Because astrocytic dysfunctions have been consistently implicated in major depressive disorder (MDD) this review provides an overview of postmortem studies of astrocytes, with special attention to studies comparing astrocyte densities in the healthy human brain and in the brain of individuals affected by MDD.

Methods for visualizing human astrocytes

Histology

Glia were first defined by Rudolph Virchow in 1858, and astrocytes were first defined in the human brain 40 years later using the Golgi stain (Golgi, 1873; Andriezen, 1893; von Lenhossek, 1895; Kettenman & Verkhratsky, 2008). Golgi staining reveals the entire coarse morphology of astrocytes, but stains at random, and so cannot reveal astrocyte densities in the human brain. Golgi studies identified interlaminar astrocytes, a cortical astrocyte subtype with a unique morphology and molecular profile in the human and non-human primate cortex (Colombo *et al*., 2004; Falcone *et al*., 2020). Golgi studies also led to the hypothesis that human astrocyte morphology has physiological relevance, as astrocyte volume was found — much like the conductive properties of neuronal axons — to adhere to a length constant, that may maintain their potassium buffering and metabolic capacity with respect to cell size (Siegel *et*

al., 1991; Reichenbach *et al*., 1992). Spine-like structures have been uniquely observed on Golgi-stained astrocytes in the human cortex, which may suggest human cortical astrocyte may have uniquely human functions (Torres-Platas *et al*., 2011; Sosunov *et al*., 2013). Golgi studies have shown that radial glia differentiate into astrocytes during neocortical development in a manner ordered by region and astrocyte subtype (Choi & Lapham, 1978; Choi & Lapham, 1980; Marín-Padilla, 1995).

Astrocyte morphology was later observed with histological stains, which increased interest for studying these cells in humans. For instance, surgical cannulae inserted into the neocortex led to gliosis — a dense formation of astrocytes lining the perimeter of the lesion — which can be visualized with silver carbonate staining (Penfield & Buckley, 1928). Similarly, haemotoxylin and eosin staining reveals strongly acidophilic astrocyte processes in the gliosis surrounding glioma and other conditions in cerebral autopsies, and this was later associated with an acidity change from GFAP upregulation in reactive astrocytes (Luse *et al*., 1956; Grcevic & Yates, 1957). Many histological stains for astrocytes in postmortem samples, such as Holzer's stain, are now rarely used in research because they work by relatively unknown mechanisms (Stevens *et al*., 1992). One exception is the Giemsa stain, which non-selectively stains the nucleus and cytoplasm of all cells, and is used in the only known method to determine regional densities of all astrocytes within postmortem brain tissue sections, based on the characteristic size and shape of the cytoplasm and nuclei in astrocytes (Pelvig *et al*., 2008). However, as cell type identification with Giemsa staining relies wholly on morphological assessment, it has a greater potential for variations in interobserver reliability for stereological studies than alternative methods, making it most suitable for observing astrocytes in large areas of interest.

Immunohistochemistry

Since the discovery of GFAP in the 1970s, most postmortem astrocyte studies have used immunohistochemistry (IHC), as this method selectively labels immunoreactive (-IR) astrocytes, and in tissue preparations that are compatible with more conventional anatomical methods. Antibodies to astrocyte markers of interest can be revealed using chromogenic methods, such as 3'-diaminobenzidine (DAB) labelling visualized using brightfield microscopy, or using fluorescent methods, where secondary antibodies conjugated to fluorophores allow for the visualization of multiple targets using fluorescence microscopy.

There are many astrocyte markers that have been used to visualize astrocytes in adult postmortem brain tissue: GFAP, vimentin (VIM), Aldh1L1, S100 Beta (S100B), glutamine synthetase (GS), cluster of differentiation 44 (CD44), aquaporin-4 (AQP4) and Sox9 **(Table 1)**. There are additional markers which label astrocyte components: the glutamate transporter proteins excitatory amino acid transporter 1 (EAAT1) and 2 (EAAT2); the gap junction proteins connexin 30 (Cx30) and 43 (Cx43). The choice of IHC marker for postmortem studies of astrocytes should depend on the region and type of analysis, as no known IHC marker reveals the entire population ('pan-astrocytic') of astrocytes **(Table 1)**. This is why Giemsa staining studies reveal consistently higher regional astrocyte densities than those attained using a single IHC marker.

Diolistic Labeling

An important ultrastructural feature of astrocyte morphology are perisynaptic astrocyte processes (PAPs), which are finger-like projections from the larger processes of astrocytes, at which proteins are locally translated and secreted to the synapse to modulate neuronal signalling (Mazaré *et al*., 2020). The only postmortem method with the resolution to reveal PAPs is diolistic labelling, when combined with super-resolution microscopy techniques like stimulated emission depletion (STED) microscopy. For this reason, diolistic labelling is the only method that completely reveals the ultrafine morphology of astrocytes in postmortem tissue, however, it labels only a few cells seemingly at random much like Golgi staining and so is not suitable for assessing astrocyte densities (Oberheim *et al*., 2009). Diolistic labelling has also been prominently used to demonstrate that there are four morphological subtypes of GFAP-IR astrocyte in the human cortex, and that GFAP-IR astrocytes in the human neocortex are arranged in domains (Oberheim *et al*., 2009).

Methodological Considerations

Alterations in brain cell number are a diagnostic feature of most cerebral pathologies. When the acidophilic property of astrocytes and basophilic property of oligodendrocytes were first described, it was observed that oligodendrocytes generally outnumber astrocytes in the human brain (Luse *et al*., 1956). In the last two decades, new methods to precisely quantify the number

of cells in the human brain have been established (Herculano-Houzel *et al*., 2005; Pelvig *et al*., 2008). For instance, using the isotropic fractionator method with NeuN IHC staining has revealed there is a 1:1 ratio of NeuN-positive neurons to NeuN-negative glia throughout the entire human brain (Herculano-Houzel *et al*., 2009; von Bartheld *et al*., 2016). This method has not yet been used to count astrocytes, but has recently shown that microglia comprise approximately 7% of non-neuronal human brain cells (Dos Santos *et al*., 2020). A stereological study of Giemsa staining throughout the human brain also similarly found microglia comprised approximately 6-7% of glial cells, with astrocytes amounting to 17-20% of glial cells (Pelvig *et al*., 2008). Together, this indicates good consistency between these two counting methods, and after factoring in neurons, they show that approximately 8.5-10% of all brain cells are astrocytes. Despite this consensus, many highly-cited papers still begin with an unevidenced claim that grossly exaggerates the number of astrocytes in the brain, and contrasts with all existing evidence, indicating cell counting studies are widely unknown to the astrocyte research community (Sofroniew & Vinters, 2010; von Bartheld *et al*., 2016; Liddelow & Barres, 2017). We advocate the strength of reporting unbiased regional astrocyte densities (total astrocyte count divided by total regional volume) instead of total astrocyte counts, as they facilitate comparisons between studies, regions and species by correcting for interindividual differences in regional volumes. Reporting regional densities also prevents additional confusion, such as whether to double the total count for bilateral structures, and how to justify doing this for regions with known bilateral symmetry of function, such as the hippocampus (Iglói *et al*., 2010).

We demonstrate the strength of reporting cell densities in this review, by presenting a map of astrocyte densities throughout the healthy human brain (**Figure 2**). This map clearly shows that in the healthy human brain, astrocytes are consistently more abundant in subcortical than cortical regions, and that immunofluorescence labellings for markers like GFAP and VIM reveal a minority of the total number of astrocytes revealed using Giemsa staining (**Table 2)**. We propose discrepancies between regional astrocyte densities acquired using Giemsa staining or IHC staining is primarily due to IHC markers labelling only a subpopulation of astrocytes.

Cortical astrocytes

Total counts of astrocytes in the healthy neocortex were first reported in a postmortem study of Alzheimer's Disease, which found no change in the total number of astrocytes stained in any lobe, or in the neocortex considered as a whole (Pelvig *et al*., 2003). A similar lack of change in Giemsa-stained astrocytes in cortex of any cerebral lobe, or in the neocortex considered as a whole, from individuals with untreated acquired immunodeficiency syndrome (AIDS), here also despite a reduced number of neurons and oligodendrocytes in the same samples (Kaalund *et al*., 2020). Moreover, in Multiple System Atrophy (MSA), regional astrocyte and neuronal numbers are not correlated, even though they are significantly decreased in the frontal, parietal and temporal lobes, but not in the occipital lobe (Salvesen *et al*., 2017). These studies suggest that in pathology, altered neuronal densities are not consistently linked to altered neocortical astrocyte densities. The latter two studies provide the only data for total astrocyte counts in the neocortex of specific cerebral lobes, which are particularly variable in the occipital lobe **(Table 2)**.

Total cortical astrocyte densities, as assessed using Giemsa staining, also do not appear strongly related to demographic variables including age and sex. One study revealed neocortical samples from male adults have 1.6-fold more astrocytes than those from female adults, however, there were no significant age or sex differences in astrocyte number after correcting for brain volume (Pelvig *et al*., 2008). Furthermore, age does not affect the number of astrocytes stained with haemoxylin and eosin in the elderly, which is surprising given the general upregulation of cerebral GFAP levels with age that might conceivably increase the detectability of astrocytes using acidophilic histological stains (Fabricius *et al*., 2013; Wruck & Adjaye, 2020). This indicates that demographic factors do not strongly affect astrocyte densities in healthy human neocortex. However, it is unclear what accounts for the differences between studies for astrocyte density estimates in healthy human neocortex, which can be more than double for haemoxylin and eosin staining (11,779–26,804 astrocytes/mm^3), but more modestly variable in Giemsa staining (11,545–15,472 astrocytes/mm^3) (Pelvig *et al*., 2003; Pelvig *et al*., 2008; Fabricius *et al*., 2013).

Subcortex

Certain medical conditions alter the total number of astrocytes in structures of the basal ganglia. In MSA, an increased number of astrocytes was observed in the striatum and globus pallidus, but not in the subthalamic nucleus (Salvesen *et al*., 2015). This study also provided the only stereological count of astrocytes in a midbrain region, the red nucleus, which had an average regional astrocyte density that was similar to those in the globus pallidus, but far lower than those in the striatum or the thalamus. A similar observation was made for schizophrenia, where the total number of astrocytes was affected in some, but not all, basal ganglia regions — the mediodorsal thalamus and nucleus accumbens exhibited fewer astrocytes, whereas the basolateral amygdala and ventral pallidum were unchanged (Pakkenberg *et al*., 1990). Subcortical astrocytes are relatively abundant in the healthy adult brain, with both the mediodorsal thalamus and basal ganglia having higher astrocyte densities than any previous estimate for the neocortex as a whole (Karlsen & Pakkenberg, 2011; Karlsen *et al*., 2014). In Down Syndrome, total astrocyte counts were found to be lower in the anterior principal nuclei of the thalamus, but unchanged in either the mediodorsal thalamus or basal ganglia, despite significantly reduced numbers of neurons and oligodendrocytes being observed in these regions, respectively (Karlsen & Pakkenberg, 2011; Karlsen *et al*., 2014; Perry *et al*., 2019). Together these findings show that pathological changes to subcortical astrocyte densities can be specific to subregions, and do not always accompany density changes in neighboring cell types.

Subpopulation Densities

As GFAP-IR astrocytes are strongly implicated in astrocyte pathology, many studies have assessed these immunolabelled cells in disease. However, relatively few studies have stereologically quantified the number of GFAP-IR astrocytes, opting instead for semi-quantitative methods including area fraction or regional GFAP expression. Here we review only postmortem studies with unbiased stereological counts of astrocytes labelled by IHC, with most of these studies being investigations of major depressive disorder (MDD). In most reports, GFAP-IR astrocyte densities are less than half of Giemsa-stained astrocyte densities **(Figure 3)**, indicating that GFAP detection by immunohistological methods reveals only a fraction of the total astrocytes present in healthy regions of the adult human brain.

One fundamental postmortem observation of GFAP-IR astrocytes is that GFAP-IR protoplasmic astrocytes are mainly observed in deeper cortical layers (layer V vs. layer III-IV), suggesting that, like neurons, the distribution of astrocytes greatly varies between cortical layers (Miguel-Hidalgo *et al*., 2000). Further postmortem evidence using more precise and varied techniques is needed to address the heterogeneity of astrocyte densities across cortical regions and layers that has recently been observed at the molecular level by rodent studies (Batiuk *et al.,* 2020; Bayraktar *et al*., 2020).

Another feature of GFAP-IR astrocytes is that in human neocortex, GFAP-IR densities might positively correlate with age, although the evidence is conflicting. Stereological studies of astrocytes labelled by GFAP or haematoxylin & eosin indicate that age does not strongly correlate with astrocyte densities, as astrocyte densities are not significantly greater in older age groups (Miguel-Hidalgo *et al*., 2000; Fabricus *et al*., 2013). This contrasts with a meta-analysis showing GFAP expression increases with age in the human prefrontal cortex, and with a previous study showing GFAP-IR astrocyte densities increase with age in the mouse brain (Mouton *et al*., 2002; Wruck & Adjaye, 2020). This conflicting evidence makes it difficult to determine whether ageing increases the density of GFAP-IR astrocytes in the adult neocortex. We suggest that standardizing common age groups and a cutoff for 'elderly' in postmortem studies would increase the reliability of comparing postmortem studies investigating age effects. A review of postmortem Golgi studies comparing glial cell densities in MDD found that glial differences are less pronounced in younger (45-60 years old) than in older (75+ years old) adults with MDD, and from this, we would recommend future postmortem studies exploring this topic to break down age groups in a similar fashion (Khundakar & Thomas, 2009). Further investigation in this area will help address the related question of whether the molecular profile of astrocytes in older organisms relates to reactive astrogliosis in response to pathology, or from cellular senescence due to physiological ageing (Escartin *et al*., 2021).

Postmortem studies have generally reported that healthy individuals have more GFAP-IR astrocytes in cortical white matter than in cortical grey matter, and vice-versa for VIM-IR astrocytes in the same subject and regions (McNeal *et al.*, 2016; O'Leary *et al*., 2020; O'Leary *et al*., 2021). Remarkably, VIM-IR astrocytes are almost absent in the mediodorsal thalamus, a region where GFAP-IR astrocytes are especially abundant in samples from the same subjects (O'Leary *et al*., 2020; O'Leary *et al*., 2021).

VIM and GFAP are often coexpressed in reactive astrocytes, yet VIM-IR and GFAP-IR astrocytes have heterogeneous densities in health and illness. While GFAP-IR astrocyte densities are generally reduced in depressed individuals, in the prefrontal cortex these changes vary for morphological subtype (Rajkowska *et al*., 2018). For instance, in the ventromedial prefrontal cortex white matter, densities of GFAP-IR fibrous astrocytes are more affected in depressed individuals than those for GFAP-IR smooth astrocytes, which the authors first defined morphologically as white matter astrocytes with especially small cell bodies and very few, thin and truncated processes (Rajkowska *et al*., 2018). Moreover, in the dorsolateral prefrontal cortex, densities of GFAP-IR protoplasmic astrocytes are more affected than for GFAP-IR fibrous astrocytes in depressed suicides (O'Leary *et al*., 2021). Moreover, in the same region of healthy control subjects, there are proportionally greater differences between studies for GFAP-IR densities than Giemsa-stained densities, suggesting that neocortical GFAP-IR astrocyte densities may be more heterogeneous than total neocortical astrocyte densities in healthy individuals. Only one postmortem IHC study of astrocytes has performed 2D stereological counts and has observed an increase in Aldh1L1-IR astrocyte density in the temporopolar area in Alzheimer's Disease (Serrano-Pozo *et al*., 2013). Interestingly, GFAP-IR and GS-IR astrocyte numbers were also observed to differentially vary in Alzheimer's Disease in this study, showing how astrocyte subpopulations can be differentially affected in illness. While Aldh1L1 appears to be the best marker for representing total astrocyte densities, it fails to reveal the majority of astrocytes via immunohistochemistry with postmortem samples, as the reported density was far lower than those for Giemsa staining in cortical lobes (Cahoy *et al*., 2008; Serrano-Pozo *et al*., 2013; Kaalund *et al*., 2020).

Astrocyte Morphology

To our knowledge, there are only five studies which have traced and provided quantitative data on the fine morphology of astrocytes in the adult human brain, three of which are from our group (**Table 3**). The benefit of using VIM instead of GFAP for stereological postmortem studies is that, unlike GFAP, it is also suitable for fine morphological assessments of astrocyte processes using the same sections. In our experience, VIM DAB immunolabelling has strikingly low background relative to other astrocyte markers in the same postmortem samples,

which may be due to many factors, including the specificity and affinity of the primary antibodies tested, or VIM expression levels being slightly more consistent and specific to astrocytes than GFAP as indicated by previous cell sequencing studies (Zhang *et al*., 2016; O'Leary *et al*., 2020). Some studies have discouraged the use of GFAP to study astrocyte morphology, when it was discovered that GFAP immunoreactivity reveals only 15% of the volume of rat astrocytes in CA1 region of the hippocampus, based on subsequent dye injection (Bushong *et al*., 2002). However, GFAP strongly labels astrocyte somas, and GFAP-IR soma volume has been used to morphologically distinguish astrocytes in ventral prefrontal white matter from fibrous astrocytes (255 ± 34 μm^3) and smooth astrocytes (44 ± 2 μm^3) (Rajkowska *et al*., 2018). Using a two-dimensional assessment, we found both GFAP-IR and VIM-IR fibrous astrocyte soma sizes in the dorsolateral prefrontal cortex are similar to these findings in ventral prefrontal cortex (O'Leary *et al*., 2020; O'Leary *et al*., 2021). Another study used fresh resected cortical tissue, leading to brilliant visualization of astrocytes using a combination of GFAP immunostaining and diolistic labelling, and found human protoplasmic astrocytes have 38±5 processes and a mean process length of 98±5μm (Oberheim *et al*., 2009). These figures are similar to those reported for protoplasmic VIM-IR astrocytes in the prefrontal cortex (36±2 processes, mean process length of 76±5 μm) and primary visual cortex (38±2 processes, mean process length 79±8 μm) (O'Leary *et al*., 2020). Moreover, both studies found a 2-to-3-fold increase in the size of human cortical astrocytes compared to mouse cortical astrocytes, indicating that DAB immunolabelling for VIM is as accurate for revealing coarse astrocyte morphology than diolistic labeling. Moreover, our fine morphometric comparison using a branched structure analysis (BSA) showed that node number, terminal number, process length and soma area were all approximately 2-to-3-fold larger in 3 homologous regions of the human brain than in the mouse brain, which indicates that evolution has increased the *scale* of astrocyte morphometry from the mouse to the human brain (O'Leary *et al*., 2020). By aggregating morphology data for VIM-IR astrocytes **(Table 4)**, general trends can be observed that quantitatively support the qualitative classification of protoplasmic and fibrous astrocytes in healthy human neocortex **(Figure 4)**. Using this approach we also propose that although subcortical astrocytes appear generally smaller than cortical astrocytes in the human brain due to their smaller process number and total process length, striatal and thalamic astrocytes have characteristic morphological profiles that are protoplasmic-like and fibrous-like, respectively **(Figure 4)**.

A previous study from our group found Golgi-stained astrocytes in healthy individuals have a larger soma and simpler branch complexity (process numbers, nodes, and terminals) than VIM-IR astrocytes, however, fibrous astrocytes had a comparable total process length (Torres-Platas *et al*., 2011; O'Leary *et al*., 2021). We suspect the discrepancies in soma diameter and branch complexity for Golgi-stained astrocytes relative to other studies is due to distortion from overimpregnation, and that process length differences may be a regional feature seen in proisocortex but not isocortex.

Distribution — are domains a universal feature of astrocytes?

Dye labelling studies revealed that GFAP-IR and S100B-IR rat hippocampal astrocytes are distributed evenly and occupy 'domains' — neighboring astrocytes interdigitate extensively but only right on the periphery (5%) of the territorial boundary occupied by the volume of each cell (Bushong *et al*., 2002; Ogata & Kosaka, 2002). The even distribution of GFAP-IR astrocyte 'domains' is a common feature in the brains of many organisms, including humans, and appears to be established during developmental pruning in a process termed 'contact spacing' or 'tiling' (Distler *et al*., 1991; Bushong *et al*., 2004; Oberheim *et al*., 2009).

The developmental origin and regional heterogeneity of astrocyte tiling in the human brain is unclear, and some lines of evidence suggest our current perspective of tiling is incomplete. First, human GFAP-IR astrocytes transplanted into the chimeric mouse cortex retain their size and penetrate many native mouse GFAP-IR astrocyte domains, which suggests either that domains are established by intrinsic factors (during development) or by non-homologous extrinsic factors (species-specific signaling) (Han *et al*., 2013). Second, specific species and types of reactive astrogliosis can cause overlap between domains to increase to up to 50% of shared volume between astrocytes (Oberheim *et al*., 2008; López-Hidalgo *et al*., 2016). Third, some long processes of GFAP-IR and CD44-IR astrocytes clearly traverse domains of neighboring astrocytes in heathy neocortex (Oberheim *et al.*, 2009; Sosunov *et al*., 2013). These three limitations also lead to a bigger question: does tiling occur for all astrocytes? This possibility is never addressed in experiments using dye-filling of GFAP-IR and S100B-IR astrocytes, despite a consensus that GFAP immunolabels a small subpopulation of astrocytes.

A related issue is whether astrocyte markers reliably reveal distinct populations of astrocytes, or instead reveal astrocytes incidentally undergoing a dynamic change in gene expression.

Here we propose that tiling (or 'contact spacing') is a feature of GFAP-IR astrocytes in the healthy human brain, based on a virtual simulation integrating previously reported morphometry and stereology data (**Figure 5**). This model combines cortical VIM-IR astrocyte morphometry with regional densities of Giemsa-stained astrocytes to reveal that tiling would be spatially impossible for the vast majority of astrocytes in cortical regions, as neighboring astrocyte domains would frequently and extensively overlap due to a lack of physical space. By contrast, ours and other reports of GFAP-IR astrocyte density allow for the extent of overlap expected for tiling, based on a previous study of astrocyte domains in human tissue (Oberheim *et al*., 2009; O'Leary *et al*., 2020; O'Leary *et al*., 2021). This model indicates that if tiling is indeed a common feature of astrocyte organization in the human brain, it could not feature for an astrocyte population much larger than the GFAP-IR astrocytes already known to display it, as shown in studies of both human and rodent brain (Bushong *et al*., 2002; Bushong *et al*., 2004; Oberheim *et al*., 2009). The structural consequence of tiling as an arrangement is the optimal spatial efficiency for the span of GFAP-IR astrocyte processes. The functional implications of this might be that GFAP-IR astrocytes are specialized for macro-level communication within the astrocyte syncytium because fewer astrocytes are needed to propagate signals for long distances with energetically efficient trajectories. An example of macro-level communication would be 'glissandi', a type of astrocytic calcium wave that is particularly fast (60μm/s) and propagates from an astrocyte to its neighbors for long distances through the mouse hippocampus and neocortex (Kuga *et al*., 2011). While astrocytes that do not display tiling or detectable GFAP immunoreactivity also communicate through gap junctions, their densities and lack of tiling make them better situated than GFAP-IR astrocytes for local signaling in the astrocyte syncytium. From these observations, we propose the tiling and density of GFAP-IR astrocytes suggests they may have specialized communication roles within the astrocyte syncytium of the human brain. From this perspective, reactive astrogliosis can then be seen as a remodeling of the astrocyte syncytium to better respond to pathology.

Astrocytic alterations in illness

Many studies have provided roles for astrocytes in neurological and psychiatric conditions (Verkhratsky *et al*., 2013; Pekny *et al*., 2016). Some of the earliest postmortem reports of well-studied neurological conditions observed unique features of astrocytes at pathological lesions, including Alzheimer's Disease (Itagaki *et al*., 1989), amyotrophic lateral sclerosis (Kato *et al*., 1997), Huntington's disease (Vonsattel *et al*., 1985), Parkinson's disease (Mirza *et al*., 1999) and multiple sclerosis (Van Der Voorn *et al*., 1999). Furthermore, despite the absence of characteristic cerebral lesions in psychiatric conditions, many postmortem studies have found that they are associated with differences in regional astrocyte densities including MDD (Rajkowska *et al*., 2000), bipolar disorder (Webster *et al*., 2005), alcohol use disorder (Korbo *et al*., 1999), and schizophrenia (Williams *et al*., 2013; Hercher *et al*., 2014).

The rest of this review will focus on postmortem studies investigating astrocytes in MDD, which is one of the most active areas of postmortem research involving astrocytes. Postmortem studies have consistently provided anatomical and molecular evidence suggesting a loss-of-function of astrocytes in MDD, especially relative to the more varied results for other psychiatric conditions like schizophrenia (Kim *et al*., 2018). Here we present an interpretation of the evidence in favor of loss of number rather than a generalized downregulation of astrocyte markers in MDD.

Astrocyte loss in MDD

Many postmortem studies using cresyl violet staining have indicated that depressed individuals have reduced densities of glia overall — when all glial cell types are counted together — in mood-associated brain regions (Öngür *et al*., 1998; Rajkowska *et al*., 1999; Cotter *et al*., 2001; Cotter *et al*., 2002; Bowley *et al*., 2002; Gittins & Harrison, 2011), however, some studies have found no differences in this regard (Cotter *et al*., 2004; Bezchlibnyk *et al*., 2007; Hercher *et al.,* 2009; Khundakar *et al*., 2009; Khundakar *et al*., 2011a; Khundakar *et al*., 2011b; Khundakar *et al*., 2011c; Smiley *et al*., 2016). We suspect reports of no difference may be due to lack of detectability of the relatively small effect size of changes in astrocyte density on glial density, as the best available stereological studies indicate that the glial cell fraction of the adult human brain is composed of 75% oligodendrocytes, 7% microglia and 18% astrocytes (Pelvig

et al., 2008; Dos Santos *et al*., 2020). This interpretation is also supported by the absence of reports of increased glial density in MDD. By contrast, total neuronal densities are not affected in individuals that died with MDD, however occasionally reductions are seen only in small subpopulations of some regions (Rajkowska *et al*., 2007; Maciag *et al*., 2010).

Three lines of evidence suggest reduced astrocyte densities in depression are associated with deficits in the number or function of astrocytes. First, multiple research groups have observed reduced astrocyte densities in multiple brain regions of individuals with MDD (Hamidi *et al*., 2004; Altshuler *et al*., 2010; Gos *et al.*, 2013; Bernstein *et al.*, 2015; Cobb *et al*., 2016; Rajkowska *et al*., 2018; O'Leary *et al*., 2021). Second, there is also a decrease in the area fraction of immunostaining for astrocyte markers — which is an indirect measure for a reduced number of astrocytes — in individuals with MDD (Miguel-Hidalgo *et al*., 2000; Webster *et al*., 2001; Si *et al*., 2004; Miguel-Hidalgo *et al*., 2014). Third, depressed individuals have a reduced regional expression of GFAP mRNA and protein (Fatemi *et al*., 2004; Chandley *et al*., 2013; Torres-Platas *et al*., 2016). This evidence may rather indicate a downregulation of GFAP rather than a loss of astrocytes, as rodent models of MDD have found no changes to total astrocyte densities as assessed using transgenic approaches with Aldh1L1 as a marker (Tynan *et al*., 2013; Simard *et al*., 2018). However, as GFAP-IR astrocytes strongly express GFAP, and GFAP upregulation is commonly seen in reactive astrogliosis, this should at least suggest the frequency or intensity of reactive astrogliosis is reduced in MDD.

The consistently reduced regional expression of GFAP and density of GFAP-IR astrocytes in MDD has led to the hypothesis that MDD involves impaired reactive astrogliosis — that reactive astrocytes fail to upregulate GFAP to normal levels — or astrocytopathy — that astrocytes that detectably express GFAP by IHC are being lost (Kim *et al*., 2018). As Golgi and cresyl violet studies also found reduced glial densities overall in MDD, this favours the interpretation that astrocytes are being lost in MDD, however clearly there is a need for direct evidence of elevated cell death markers in astrocytes in MDD subjects to resolve whether MDD is associated with a pathological loss of astrocytes (Öngür *et al*., 1998; Rajkowska *et al*., 1999).

Other lines of evidence show a generalized loss of function of astrocytes which is also more readily explained by astrocyte loss than by a programmed state of reactive astrogliosis specific to MDD. In MDD, postmortem data suggest that astrocytes have reduced communication with other cell types. For instance, there is a reduced expression of glutamate transporters in depressed individuals, indicating a reduced capacity for astrocytes to uptake glutamate released

by neurons into the synapse during MDD (Choudary *et al*., 2005; Miguel-Hidalgo et al., 2010; Bernard *et al*., 2011; Chandley *et al*., 2013; Medina et al., 2016; Zhao et al., 2016; Powers et al., 2019). There is also a decrease in neurotrophic factors released by astrocytes both in the locus coeruleus of MDD patients and rats exposed to chronic social defeat, indicating astrocyte-neuron signaling is impaired outside of the tripartite synapse in MDD (Ordway *et al*., 2012). Astrocytes also have impaired interactions with cell types other than neurons, as they have fewer vascular contacts and form fewer gap junctions composed of connexin 30 with oligodendrocytes (Ernst *et al*., 2011; Rajkowska *et al*., 2013; Miguel-Hidalgo *et al*., 2014; Tanti *et al*., 2019). However, VIM-IR astrocytes have a mostly unaltered morphological profile in MDD patients, and this is surprising given that connexin 30 is known to regulate astrocyte morphology (Pannasch et al., 2014; O'Leary et al., 2021). While altered astrocyte morphology has been previously reported for Golgi staining in anterior cingulate cortical white matter of depressed suicides, this has not been observed for VIM-IR astrocytes in four other areas of the brain which showed lower VIM-IR astrocyte densities in depressed suicides (Torres-Platas *et al.,* 2011; O'Leary *et al*., 2021). As morphological changes are not widely apparent brain regions which have reduced astrocyte densities and a lower expression of functional markers in MDD, it tentatively appears that astrocyte loss is a more reasonable interpretation for the decreased expression of astrocyte markers in MDD, rather than a state of reactive astrogliosis where most astrocyte genes with important functions are downregulated (Nagy *et al*., 2015; Torres-Platas *et al*., 2016; O'Leary *et al*., 2021). The latter interpretation would contrast with currently known states of reactive astrogliosis characterized by an upregulation of VIM and GFAP and the potential for morphological changes and increased astrocyte signaling to other cell types (Escartin *et al*., 2021). Nevertheless, there are, however, interesting exceptions where astrocyte protein levels are higher in MDD or animal models of MDD, two of which (S100B and $K_{ir}4.1$) we discuss in the following sections.

Astrocyte loss in MDD: relation to biomarkers

Although no biomarker of astrocyte pathology in MDD has been established, studies have indicated the potential for astrocytes in the brain to release factors which could be used as biomarkers of mood disorders. A hypothesis-free comparison found CSF serum proteins were differentially regulated between depressed and psychiatrically healthy individuals, including a downregulation of two astrocytic proteins — CD44 and aldolase C (ALDOC) (Kumanishi *et*

al., 1985; Ditzen *et al*., 2011; Sosunov *et al*., 2014). Later animal studies have shown that ALDOC synthesized by brain astrocytes is found in both CSF serum and extracellular vesicles in peripheral blood, and in both cases is significantly reduced by immobilization stress paradigms (Ampuero *et al*., 2015; Gómez-Molina *et al*., 2019). Given the strong, widespread reduction of immunoreactive astrocyte densities throughout the brain in MDD, this highlights the potential for reduced serum levels of astrocyte-derived proteins to serve as biomarkers of MDD. As ALDOC is a glycolytic enzyme, one might expect ALDOC downregulation in MDD at least partly corresponds to the downregulation of astrocytic glutamate transporters which is also seen in MDD, as by the lactate-shuttle hypothesis, astrocytes increase glycolysis to produce lactate when glutamate is taken up from the synapse (Pellering & Magistretti, 1994; Zhao *et al*., 2016).

By contrast, some astrocytic proteins are elevated in CSF serum during MDD. The widespread reduction of astrocyte densities in MDD may underlie the characteristic changes of S100B levels in cerebrospinal fluid serum (CSF), which is emerging as a diagnostic biomarker during depressive episodes in MDD (Güleş *et al*., 2020). In the human brain, S100B expression is mostly found in astrocytes rather than oligodendrocytes of neocortical grey matter, but the converse is true in white matter regions, where over 70% of S100B-IR cells are oligodendrocytes (Steiner *et al*., 2007). In astrocytes, S100B acts as a neurotrophic factor that is released extracellularly to stimulate local astrocyte proliferation, whereas in oligodendrocytes, S100B expression within oligodendrocyte precursor cells (OPC) promotes their maturation into oligodendrocytes (Selinfreund *et al*., 1991; Deloulme *et al*., 2004). As both reduced astrocyte densities and decreased OPC:oligodendrocyte ratios are seen in postmortem studies of MDD (Tanti *et al*., 2018; O'Leary *et al*., 2021), elevated S100B CSF serum levels in MDD could be a diagnostic marker for excess S100B signaling contributing to glial pathology in MDD.

Elevated S100B CSF serum levels have been consistently correlated with MDD as a state marker in unmedicated patients, and some studies have shown they correlate with symptom severity and their normalization is predictive of successful treatment response (Ambrée *et al*., 2016; Fang *et al*., 2016; Gulen *et al*., 2016; Güleş *et al*., 2020). Much like astrocyte loss in mood disorders, elevated S100B CSF serum levels are more consistently and strongly associated with MDD than bipolar disorder or schizophrenia (Shroeter & Steiner, 2009; Kim *et al.*, 2018). However, elevated S100B CSF serum levels are not specific to mood disorders and act as a pathological indicator of many neurological conditions, including traumatic brain

injury, amyotrophic lateral sclerosis, malignant melanoma and subarachnoid haemorrhage (Djukanovic *et al*., 2000; Moritz *et al*., 2010; Süssmuth *et al*., 2010; Egea-Guerrero *et al*., 2011). Mean S100B CSF serum levels are approximately in the range of 50-70ng/L for healthy adults, 70-150ng/L for unmedicated adults with schizophrenia or MDD, and 150-400ng/L for adults with neurological conditions, including traumatic brain injury and Creutzfeldt-Jakob disease (Otto *et al*., 1998; Rainey *et al*., 2009; Shroeter *et al*., 2008; Shroeter *et al*., 2009; Streitburger *et al*., 2012). By comparison, only one study has assessed the CSF serum levels of GFAP in depressed elderly cohort and found no association with MDD symptoms (Gudmundsson *et al*., 2010).

These ranges appear to distinguish psychiatric and neurological conditions, especially on the basis of a mathematical model which proposes that S100B CSF serum levels exceeding 340ng/L indicate blood-brain barrier failure (Marchi *et al*., 2004). Together these observations indicate elevated S100B CSF serum levels in neurological conditions are more likely to be associated with damage to the blood-brain barrier than those for psychiatric conditions (Streitburger *et al*., 2012). Nevertheless, more subtle alterations in blood-brain barrier integrity could contribute to elevated S100B CSF serum levels, as they have been identified in animal models and postmortem studies of MDD (Menard *et al*., 2017; Dudek *et al*., 2020).

Although a direct link between elevated S100B CSF serum levels and astrocyte loss in MDD has not yet been established, indirect evidence is available. First, oligodendrocytes do not appear related to S100B CSF serum levels in MDD, as densities of S100B-IR astrocytes, but not S100B-IR oligodendrocytes, are reduced in postmortem hippocampal samples from patients with MDD (Gos *et al*., 2013). Second, astrocytes can be related to pathological S100B CSF serum levels, as the elevation of CSF serum levels of both S100B and GFAP after traumatic brain injury are highly predictive of mortality, however this approach has not yet been performed for MDD (Pelinka *et al*., 2004; Vos *et al*., 2010). Third, in animal models of depression, fluoxetine normalizes astrocyte density and S100B CSF serum levels, and increases S100B expression in the hippocampus (Akhisaroglu *et al*., 2003; Czéh *et al*., 2006; Baudry *et al*., 2010). Fourth, astrocyte loss and elevated S100B CSF serum levels are both greater in older subjects with MDD (Miguel-Hidalgo *et al*., 2000; Shroeter *et al*., 2011). By comparison to other mood disorders, elevated S100B CSF serum levels in schizophrenia do not clearly implicate astrocytes, as they do not correlate with those for GFAP, vary between sexes and ethnicity, and correlate with abnormal white matter integrity where S100B-IR

oligodendrocytes are more abundant (Steiner *et al*., 2006; Gos *et al*., 2013; O'Connell *et al*., 2013; Milleit *et al*., 2016; Gannon *et al*., 2020).

Astrocyte loss in MDD: a potassium imbalance theory

A relatively new line of rodent studies has implicated a pathological upregulation of an inwardly rectifying potassium channel in MDD (Hu *et al*., 2020). Here, we propose a 'potassium imbalance theory' for MDD which contextualizes how this excessive influx of potassium into astrocytes may be indirectly associated with the loss of astrocytes in MDD in humans.

The potassium imbalance theory of MDD is based on a ketamine-reversible rodent model of depression involving aberrant neuronal activity in the lateral habenula driven by astrocytes overexpressing the inwardly rectifying potassium channel, $K_{ir}4.1$ (Yang *et al*., 2018; Cui *et al*., 2018). Here, depression results from unbalanced glutamatergic and GABAergic signaling onto postsynaptic terminals in the lateral habenula, as increasing glutamate reuptake by astrocytes or increasing GABA signaling reverses depressive behavior (Shabel *et al*., 2014; Kang *et al*., 2018). Ketamine also reverses this phenotype by blocking NMDA receptors on postsynaptic terminals in the lateral habenula, that become disinhibited by an increase in resting membrane potential in the postsynaptic terminal **(Figure 6)**. Ketamine also directly alters astrocyte membrane composition and the mobility of vesicles containing $K_{ir}4.1$ (Lasič *et al*., 2019; Stenovec *et al*., 2020). As lateral habenula activity is associated with disappointment, the resultant neuronal burst firing triggered by pathological upregulation of $K_{ir}4.1$ may implicate astrocytes with MDD symptoms related to disappointment, including anhedonia and feelings of worthlessness. While potassium channels have not yet been directly studied in human astrocytes in MDD, the regional expression $K_{ir}4.1$ is increased in parietal cortex samples from individuals with MDD, indicating the potential for this mechanism in postmortem samples (Xiong *et al*., 2019).

Together these findings suggest a potential link for potassium imbalance theory in MDD with the already established glutamate theory of depression (**Figure 6**). Chronic stress, known to precipitate depression, upregulates $K_{ir}4.1$ expression in astrocytes and MDD results from these changes to neuronal firing in mood-associated brain regions. Astrocytes are then lost, which destabilizes glutamate homeostasis by reducing both glutamate reuptake and synthesis by

astrocytes. This reduction in astrocyte densities is also associated with a decreased expression of connexin 30, a gap junction protein that normally mediates oligodendrocyte-astrocyte communication, astrocytic glutamate reuptake, and sustains neuronal bursting (Ernst *et al*., 2011; Pannasch et al*.,* 2014; Tanti *et al*., 2019). From this perspective, in the lateral habenula, a therapeutic approach that directly corrects for astrocyte potassium homeostasis or potentiates astrocytic glutamate reuptake might be effective strategies for treating MDD symptoms **(Figure 6)**. Given the widespread reduction of astrocyte densities in the human brain of individuals with MDD, and the lack of a reliable lesion study for MDD, it remains to be seen whether potassium imbalance and excessive synaptic glutamate occurs in other brain regions during MDD. Moreover, a close postmortem examination of the density of astrocytes and astrocytic $K_{ir}4.1$ expression in the lateral habenula is needed to determine whether there is a link between these two astrocytic features of MDD in in the human brain.

Future directions

Future studies which address whether the total population of astrocytes are affected in postmortem samples from clinical cohorts will be insightful to the effect size of astrocyte abnormalities in both neurological and psychiatric conditions. Further investigating the cell signalling factors which determine the proliferation of astrocytes in adult organisms will be beneficial for identifying targets that correct for the widespread reduction of cerebral astrocytes in depression. The use of *in vitro* cultures from patient-derived stem cells would provide a method of assessing the effect of potential antidepressants on astrocyte density, and the glutamate and potassium homeostasis of astrocyte populations. It remains unknown whether optogenetic silencing of astrocyte populations in mood-associated brain regions could mimic or exacerbate depressive-like states in rodents. Furthermore, the potential for astrocyte dysfunction in MDD requires further exploration by postmortem studies which can directly compare the localization of functional proteins on astrocytes. Finally, translational studies which combine biomarker measurements of S100B in blood and CSF serum with cellular approaches, including patient-derived human induced pluripotent stem cells and postmortem stereological assessments, will be needed to confirm whether astrocyte loss is predictive of MDD or if it is a consequence of this psychopathology.

References

1. Akhisaroglu, M., Manev, R., Akhisaroglu, E., Uz, T., & Manev, H. (2003). Both aging and chronic fluoxetine increase S100B content in the mouse hippocampus. Neuroreport, 14(11), 1471–1473. https://doi.org/10.1097/00001756-200308060-00013

2. Altshuler, L. L., Abulseoud, O. A., Foland-Ross, L., Bartzokis, G., Chang, S., Mintz, J., Hellemann, G., & Vinters, H. V. (2010). Amygdala astrocyte reduction in subjects with major depressive disorder but not bipolar disorder. Bipolar Disorders, 12(5), 541–549. https://doi.org/10.1111/j.1399-5618.2010.00838.x

3. Ambrée, O., Bergink, V., Grosse, L., Alferink, J., Drexhage, H. A., Rothermundt, M., Arolt, V., & Birkenhäger, T. K. (2016). S100b serum levels predict treatment response in patients with melancholic depression. International Journal of Neuropsychopharmacology, 19(3). https://doi.org/10.1093/ijnp/pyv103

4. Andriezen, W. L. (1893). The neuroglia elements in the human brain. British Medical Journal, 2(1700), 227–230.

5. Arizono, M., Inavalli, V. V. G. K., Panatier, A., Pfeiffer, T., Angibaud, J., Levet, F., Ter Veer, M. J. T., Stobart, J., Bellocchio, L., Mikoshiba, K., Marsicano, G., Weber, B., Oliet, S. H. R., & Nägerl, U. V. (2020). Structural basis of astrocytic Ca 2+ signals at tripartite synapses. Nature Communications, 11(1), 1–15. https://doi.org/10.1038/s41467-020-15648-4

6. Bardehle, S., Krüger, M., Buggenthin, F., Schwausch, J., Ninkovic, J., Clevers, H., Snippert, H. J., Theis, F. J., Meyer-Luehmann, M., Bechmann, I., Dimou, L., & Götz, M. (2013). Live imaging of astrocyte responses to acute injury reveals selective juxtavascular proliferation. Nature Neuroscience, 16(5), 580–586. https://doi.org/10.1038/nn.3371

7. Bartheld, C. S. von, Bahney, J., & Herculano-Houzel, S. (2016). The search for true numbers of neurons and glial cells in the human brain: A review of 150 years of cell counting. Journal of Comparative Neurology, 524(18), 3865–3895. https://doi.org/10.1002/cne.24040

8. Batiuk, M. Y., Martirosyan, A., Wahis, J., de Vin, F., Marneffe, C., Kusserow, C., Koeppen, J., Viana, J. F., Oliveira, J. F., Voet, T., Ponting, C. P., Belgard, T. G., & Holt, M. G. (2020). Identification of region-specific astrocyte subtypes at single cell resolution. Nature Communications, 11(1), 1220. https://doi.org/10.1038/s41467-019-14198-8

9. Baudry, A., Mouillet-Richard, S., Schneider, B., Launay, J.-M., & Kellermann, O. (2010). Mir-16 targets the serotonin transporter: A new facet for adaptive responses to antidepressants. Science, 329(5998), 1537–1541

10. Bayraktar, O. A., Bartels, T., Holmqvist, S., Kleshchevnikov, V., Martirosyan, A., Polioudakis, D., Ben Haim, L., Young, A. M. H., Batiuk, M. Y., Prakash, K., Brown, A., Roberts, K., Paredes, M. F., Kawaguchi, R., Stockley, J. H., Sabeur, K., Chang, S. M., Huang, E., Hutchinson, P., … Rowitch, D. H. (2020). Astrocyte layers in the mammalian cerebral cortex revealed by a single-cell in situ transcriptomic map. Nature Neuroscience, 23(4), 500–509. https://doi.org/10.1038/s41593-020-0602-1

11. Bell, K. F., Al-Mubarak, B., Fowler, J. H., Baxter, P. S., Gupta, K., Tsujita, T., Chowdhry, S., Patani, R., Chandran, S., Horsburgh, K., Hayes, J. D., & Hardingham, G. E. (2011). Mild oxidative stress activates Nrf2 in astrocytes, which contributes to neuroprotective ischemic preconditioning. Proceedings of the National Academy of Sciences, 108(1), E1–E2. https://doi.org/10.1073/pnas.1015229108

12. Bernard, R., Kerman, I. A., Thompson, R. C., Jones, E. G., Bunney, W. E., Barchas, J. D., Schatzberg, A. F., Myers, R. M., Akil, H., & Watson, S. J. (2011). Altered expression of glutamate signaling, growth factor, and glia genes in the locus coeruleus of patients with major depression. Molecular Psychiatry, 16(6), 634–646. https://doi.org/10.1038/mp.2010.44

13. Bernstein, H.-G., Meyer-Lotz, G., Dobrowolny, H., Bannier, J., Steiner, J., Walter, M., & Bogerts, B. (2015). Reduced density of glutamine synthetase immunoreactive astrocytes in different cortical areas in major depression but not in bipolar I disorder. Frontiers in Cellular Neuroscience, 9. https://doi.org/10.3389/fncel.2015.00273

14. Bezchlibnyk, Y. B., Sun, X., Wang, J.-F., MacQueen, G. M., McEwen, B. S., & Young, L. T. (2007). Neuron somal size is decreased in the lateral amygdalar nucleus

of subjects with bipolar disorder. Journal of Psychiatry & Neuroscience, 32(3), 203–210.Bowley, M. P., Drevets, W. C., Öngür, D., & Price, J. L. (2002). Low glial numbers in the amygdala in major depressive disorder. Biological Psychiatry, 52(5), 404–412. https://doi.org/10.1016/S0006-3223(02)01404-X

15. Bushong, E. A., Martone, M. E., & Ellisman, M. H. (2004). Maturation of astrocyte morphology and the establishment of astrocyte domains during postnatal hippocampal development. International Journal of Developmental Neuroscience, 22(2), 73–86. https://doi.org/10.1016/j.ijdevneu.2003.12.008

16. Bushong, E. A., Martone, M. E., Jones, Y. Z., & Ellisman, M. H. (2002). Protoplasmic astrocytes in ca1 stratum radiatum occupy separate anatomical domains. Journal of Neuroscience, 22(1), 183–192. https://doi.org/10.1523/JNEUROSCI.22-01-00183.2002

17. Cahoy, J. D., Emery, B., Kaushal, A., Foo, L. C., Zamanian, J. L., Christopherson, K. S., Xing, Y., Lubischer, J. L., Krieg, P. A., Krupenko, S. A., Thompson, W. J., & Barres, B. A. (2008). A transcriptome database for astrocytes, neurons, and oligodendrocytes: A new resource for understanding brain development and function. Journal of Neuroscience, 28(1), 264–278. https://doi.org/10.1523/JNEUROSCI.4178-07.2008

18. Chandley, M. J., Szebeni, K., Szebeni, A., Crawford, J., Stockmeier, C. A., Turecki, G., Miguel-Hidalgo, J. J., & Ordway, G. A. (2013). Gene expression deficits in pontine locus coeruleus astrocytes in men with major depressive disorder. Journal of Psychiatry & Neuroscience : JPN, 38(4), 276–284.

19. Choi, B. H., & Lapham, L. W. (1978). Radial glia in the human fetal cerebrum: A combined golgi, immunofluorescent and electron microscopic study. Brain Research, 148(2), 295–311. https://doi.org/10.1016/0006-8993(78)90721-7

20. Choi, B. H., & Lapham, L. W. (1980). Evolution of Bergman glia in developing human fetal cerebellum: A Golgi, electron microscopic and immunofluorescent study. Brain Research, 190(2), 369–383. https://doi.org/10.1016/0006-8993(80)90280-2

21. Chen, Y., Vartiainen, N. E., Ying, W., Chan, P. H., Koistinaho, J., & Swanson, R. A. (2001). Astrocytes protect neurons from nitric oxide toxicity by a glutathione-dependent mechanism. Journal of Neurochemistry, 77(6), 1601–1610. https://doi.org/https://doi.org/10.1046/j.1471-4159.2001.00374.x

22. Choudary, P. V., Molnar, M., Evans, S. J., Tomita, H., Li, J. Z., Vawter, M. P., Myers, R. M., Bunney, W. E., Akil, H., Watson, S. J., & Jones, E. G. (2005). Altered cortical glutamatergic and GABAergic signal transmission with glial involvement in depression. Proceedings of the National Academy of Sciences, 102(43), 15653–15658. https://doi.org/10.1073/pnas.0507901102

23. Chung, W.-S., Verghese, P. B., Chakraborty, C., Joung, J., Hyman, B. T., Ulrich, J. D., Holtzman, D. M., & Barres, B. A. (2016). Novel allele-dependent role for APOE in controlling the rate of synapse pruning by astrocytes. Proceedings of the National Academy of Sciences, 113(36), 10186–10191. https://doi.org/10.1073/pnas.1609896113

24. Chung, W.-S., Clarke, L. E., Wang, G. X., Stafford, B. K., Sher, A., Chakraborty, C., Joung, J., Foo, L. C., Thompson, A., Chen, C., Smith, S. J., & Barres, B. A. (2013). Astrocytes mediate synapse elimination through MEGF10 and MERTK pathways. Nature, 504(7480), 394–400. https://doi.org/10.1038/nature12776

25. Cobb, J. A., O'Neill, K., Milner, J., Mahajan, G. J., Lawrence, T. J., May, W. L., Miguel-Hidalgo, J., Rajkowska, G., & Stockmeier, C. A. (2016). Density of GFAP-immunoreactive astrocytes is decreased in left hippocampi in major depressive disorder. Neuroscience, 316, 209–220. https://doi.org/10.1016/j.neuroscience.2015.12.044

26. Colombo, J. A., & Reisin, H. D. (2004). Interlaminar astroglia of the cerebral cortex: A marker of the primate brain. Brain Research, 1006(1), 126–131. https://doi.org/10.1016/j.brainres.2004.02.003

27. Comparison of immunocytochemical and Holzer's methods for detection of acute and chronic gliosis in human postmortem material. (1992). The Journal of Neuropsychiatry and Clinical Neurosciences, 4(2), 168–173. https://doi.org/10.1176/jnp.4.2.168

28. Correa, F., Ljunggren, E., Mallard, C., Nilsson, M., Weber, S. G., & Sandberg, M. (2011). The Nrf2-inducible antioxidant defense in astrocytes can be both up- and down-regulated by activated microglia:Involvement of p38 MAPK. Glia, 59(5), 785–799. https://doi.org/https://doi.org/10.1002/glia.21151

29. Cotter, D., Mackay, D., Landau, S., Kerwin, R., & Everall, I. (2001). Reduced glial cell density and neuronal size in the anterior cingulate cortex in major depressive disorder. Archives of General Psychiatry, 58(6), 545–553. https://doi.org/10.1001/archpsyc.58.6.545

30. Cotter, David, Mackay, D., Chana, G., Beasley, C., Landau, S., & Everall, I. P. (2002). Reduced neuronal size and glial cell density in area 9 of the dorsolateral prefrontal cortex in subjects with major depressive disorder. Cerebral Cortex, 12(4), 386–394. https://doi.org/10.1093/cercor/12.4.386

31. Cotter, David, Mackay, D., Frangou, S., Hudson, L., & Landau, S. (2004). Cell density and cortical thickness in Heschl's gyrus in schizophrenia, major depression and bipolar disorder. The British Journal of Psychiatry, 185(3), 258–259. https://doi.org/10.1192/bjp.185.3.258

32. Cui, Y., Yang, Y., Ni, Z., Dong, Y., Cai, G., Foncelle, A., Ma, S., Sang, K., Tang, S., Li, Y., Shen, Y., Berry, H., Wu, S., & Hu, H. (2018). Astroglial Kir4.1 in the lateral habenula drives neuronal bursts in depression. Nature, 554(7692), 323–327. https://doi.org/10.1038/nature25752

33. Czéh, B., Simon, M., Schmelting, B., Hiemke, C., & Fuchs, E. (2006). Astroglial plasticity in the hippocampus is affected by chronic psychosocial stress and concomitant fluoxetine treatment. Neuropsychopharmacology, 31(8), 1616–1626. https://doi.org/10.1038/sj.npp.1300982

34. Deloulme, J. C., Raponi, E., Gentil, B. J., Bertacchi, N., Marks, A., Labourdette, G., & Baudier, J. (2004). Nuclear expression of S100B in oligodendrocyte progenitor cells correlates with differentiation toward the oligodendroglial lineage and modulates oligodendrocytes maturation. Molecular and Cellular Neuroscience, 27(4), 453–465. https://doi.org/10.1016/j.mcn.2004.07.008

35. Distler, C., Dreher, Z., & Stone, J. (1991). Contact spacing among astrocytes in the central nervous system: An hypothesis of their structural role. Glia, 4(5), 484–494. https://doi.org/10.1002/glia.440040508

36. Djukanovic, D., Hofmann, U., Sucker, A., Rittgen, W., & Schadendorf, D. (2000). Comparison of S100 protein and MIA protein as serum marker for malignant melanoma. Anticancer Research, 20(3B), 2203–2207.

37. Dossi, E., Vasile, F., Rouach, N. (2018). Human astrocytes in the diseased brain. Brain Research Bulletin, 136, 139–156. https://doi.org/10.1016/j.brainresbull.2017.02.001

38. Dudek, K. A., Dion-Albert, L., Lebel, M., LeClair, K., Labrecque, S., Tuck, E., Perez, C. F., Golden, S. A., Tamminga, C., Turecki, G., Mechawar, N., Russo, S. J., & Menard, C. (2020). Molecular adaptations of the blood–brain barrier promote stress resilience vs. Depression. Proceedings of the National Academy of Sciences, 117(6), 3326–3336. https://doi.org/10.1073/pnas.1914655117

39. Egea-Guerrero, J. J., Murillo-Cabezas, F., Gordillo-Escobar, E., Rodríguez-Rodríguez, A., Enamorado-Enamorado, J., Revuelto-Rey, J., Pacheco-Sánchez, M., León-Justel, A., Domínguez-Roldán, J. M., & Vilches-Arenas, A. (2013). S100b protein may detect brain death development after severe traumatic brain injury. Journal of Neurotrauma, 30(20), 1762–1769. https://doi.org/10.1089/neu.2012.2606

40. Ernst, C., Nagy, C., Kim, S., Yang, J. P., Deng, X., Hellstrom, I. C., Choi, K. H., Gershenfeld, H., Meaney, M. J., & Turecki, G. (2011). Dysfunction of astrocyte connexins 30 and 43 in dorsal lateral prefrontal cortex of suicide completers. Biological Psychiatry, 70(4), 312–319. https://doi.org/10.1016/j.biopsych.2011.03.038

41. Escartin, C., Galea, E., Lakatos, A., O'Callaghan, J. P., Petzold, G. C., Serrano-Pozo, A., Steinhäuser, C., Volterra, A., Carmignoto, G., Agarwal, A., Allen, N. J., Araque, A., Barbeito, L., Barzilai, A., Bergles, D. E., Bonvento, G., Butt, A. M., Chen, W.-T., Cohen-Salmon, M., … Verkhratsky, A. (2021). Reactive astrocyte nomenclature, definitions, and future directions. Nature Neuroscience. https://doi.org/10.1038/s41593-020-00783-4

42. Fabricius, K., Jacobsen, J. S., & Pakkenberg, B. (2013). Effect of age on neocortical brain cells in 90+ year old human females—A cell counting study. Neurobiology of Aging, 34(1), 91–99. https://doi.org/10.1016/j.neurobiolaging.2012.06.009

43. Falcone, C., Penna, E., Hong, T., Tarantal, A. F., Hof, P. R., Hopkins, W. D., Sherwood, C. C., Noctor, S. C., & Martínez-Cerdeño, V. (2020). Cortical interlaminar astrocytes are generated prenatally, mature postnatally, and express unique markers in human and nonhuman primates. Cerebral Cortex (New York, N.Y.: 1991). https://doi.org/10.1093/cercor/bhaa231

44. Fang, Y., Xiao, S., Zhang, S., Qiu, Q., Wang, T., & Li, X. (2016). Increased plasma s100β level in patients with major depressive disorder. CNS Neuroscience & Therapeutics, 22(3), 248–250. https://doi.org/10.1111/cns.12517

45. Fatemi, S. H., Laurence, J. A., Araghi-Niknam, M., Stary, J. M., Schulz, S. C., Lee, S., & Gottesman, I. I. (2004). Glial fibrillary acidic protein is reduced in cerebellum of subjects with major depression, but not schizophrenia. Schizophrenia Research, 69(2), 317–323. https://doi.org/10.1016/j.schres.2003.08.014

46. Forebrain engraftment by human glial progenitor cells enhances synaptic plasticity and learning in adult mice. (2013). Cell Stem Cell, 12(3), 342–353. https://doi.org/10.1016/j.stem.2012.12.015

47. Fujita, T., Chen, M. J., Li, B., Smith, N. A., Peng, W., Sun, W., Toner, M. J., Kress, B. T., Wang, L., Benraiss, A., Takano, T., Wang, S., & Nedergaard, M. (2014). Neuronal transgene expression in dominant-negative snare mice. Journal of Neuroscience, 34(50), 16594–16604. https://doi.org/10.1523/JNEUROSCI.2585-14.2014

48. Gannon, J. M., Kelly, D. L., Besch, A., Thakur, T., Khurana, N., Shurin, M. R., Shurin, G. V., Brar, J. S., Cihakova, D., Talor, M. V., & Chengappa, K. N. R. (2020). Racial differences in s100b levels in persons with schizophrenia. The Psychiatric Quarterly, 91(1), 137–145. https://doi.org/10.1007/s11126-019-09687-4

49. Gittins, R. A., & Harrison, P. J. (2011). A morphometric study of glia and neurons in the anterior cingulate cortex in mood disorder. Journal of Affective Disorders, 133(1), 328–332. https://doi.org/10.1016/j.jad.2011.03.042

50. Golgi, C. (1873). Sulla sostanza grigia del cervello. Gazetta Medica Italiana, 33, 244–246.

51. Gos, T., Schroeter, M. L., Lessel, W., Bernstein, H.-G., Dobrowolny, H., Schiltz, K., Bogerts, B., & Steiner, J. (2013). S100B-immunopositive astrocytes and oligodendrocytes in the hippocampus are differentially afflicted in unipolar and bipolar depression: A postmortem study. Journal of Psychiatric Research, 47(11), 1694–1699. https://doi.org/10.1016/j.jpsychires.2013.07.005

52. Grcevic, N., & Yates, P. O. (1957). Rosenthal fibres in tumours of the central nervous system. The Journal of Pathology and Bacteriology, 73(2), 467–472. https://doi.org/10.1002/path.1700730217

53. Gudmundsson, P., Skoog, I., Waern, M., Blennow, K., Zetterberg, H., Rosengren, L., & Gustafson, D. (2010). Is there a CSF biomarker profile related to depression in elderly women? Psychiatry Research, 176(2), 174–178. https://doi.org/10.1016/j.psychres.2008.11.012

54. Gulen, B., Serinken, M., Eken, C., Karcıoglu, Ö., Kucukdagli, O. T., Kilic, E., Akpinar, G., Nogay, S., & Kuh, M. (2016). Serum s100b as a surrogate biomarker in the diagnoses of burnout and depression in emergency medicine residents. Academic Emergency Medicine, 23(7), 786–789. https://doi.org/10.1111/acem.12973

55. Güleş, E., Iosifescu, D. V., & Tural, Ü. (2020). Plasma neuronal and glial markers and anterior cingulate metabolite levels in major depressive disorder: A pilot study. Neuropsychobiology, 79(3), 214–221. https://doi.org/10.1159/000505782

56. Hall, C. N., Reynell, C., Gesslein, B., Hamilton, N. B., Mishra, A., Sutherland, B. A., O'Farrell, F. M., Buchan, A. M., Lauritzen, M., & Attwell, D. (2014). Capillary pericytes regulate cerebral blood flow in health and disease. Nature, 508(7494), 55–60. https://doi.org/10.1038/nature13165

57. Hamidi, M., Drevets, W. C., & Price, J. L. (2004). Glial reduction in amygdala in major depressive disorder is due to oligodendrocytes. Biological Psychiatry, 55(6), 563–569. https://doi.org/10.1016/j.biopsych.2003.11.006

58. Hercher, C., Chopra, V., & Beasley, C. L. (2014). Evidence for morphological alterations in prefrontal white matter glia in schizophrenia and bipolar disorder. Journal of Psychiatry & Neuroscience : JPN, 39(6), 376–385. https://doi.org/10.1503/jpn.130277

59. Hercher, C., Parent, M., Flores, C., Canetti, L., Turecki, G., & Mechawar, N. (2009). Alcohol dependence–related increase of glial cell density in the anterior cingulate cortex of suicide completers. Journal of Psychiatry & Neuroscience : JPN, 34(4), 281–288.

60. Herculano-Houzel, S. (2009). The human brain in numbers: A linearly scaled-up primate brain. Frontiers in Human Neuroscience, 3. https://doi.org/10.3389/neuro.09.031.2009

61. Herculano-Houzel, S., & Lent, R. (2005). Isotropic fractionator: A simple, rapid method for the quantification of total cell and neuron numbers in the brain. Journal of Neuroscience, 25(10), 2518–2521. https://doi.org/10.1523/JNEUROSCI.4526-04.2005

62. Hu, H., Cui, Y., & Yang, Y. (2020). Circuits and functions of the lateral habenula in health and in disease. Nature Reviews Neuroscience, 21(5), 277–295. https://doi.org/10.1038/s41583-020-0292-4

63. Iglói, K., Doeller, C. F., Berthoz, A., Rondi-Reig, L., & Burgess, N. (2010). Lateralized human hippocampal activity predicts navigation based on sequence or place memory. Proceedings of the National Academy of Sciences, 107(32), 14466–14471. https://doi.org/10.1073/pnas.1004243107

64. Iliff, J. J., Wang, M., Liao, Y., Plogg, B. A., Peng, W., Gundersen, G. A., Benveniste, H., Vates, G. E., Deane, R., Goldman, S. A., Nagelhus, E. A., & Nedergaard, M. (2012). A paravascular pathway facilitates csf flow through the brain parenchyma and

the clearance of interstitial solutes, including amyloid β. Science Translational Medicine, 4(147), 147ra111-147ra111. https://doi.org/10.1126/scitranslmed.3003748

65. Itagaki, S., McGeer, P. L., Akiyama, H., Zhu, S., & Selkoe, D. (1989). Relationship of microglia and astrocytes to amyloid deposits of Alzheimer disease. Journal of Neuroimmunology, 24(3), 173–182. https://doi.org/10.1016/0165-5728(89)90115-X

66. Kaalund, S. S., Johansen, A., Fabricius, K., & Pakkenberg, B. (2020). Untreated patients dying with aids have loss of neocortical neurons and glia cells. Frontiers in Neuroscience, 13. https://doi.org/10.3389/fnins.2019.01398

67. Kang, S., Li, J., Bekker, A., & Ye, J.-H. (2018). Rescue of glutamate transport in the lateral habenula alleviates depression- and anxiety-like behaviors in ethanol-withdrawn rats. Neuropharmacology, 129, 47–56. https://doi.org/10.1016/j.neuropharm.2017.11.013

68. Karlsen, A. S., Korbo, S., Uylings, H. B. M., & Pakkenberg, B. (2014). A stereological study of the mediodorsal thalamic nucleus in Down syndrome. Neuroscience, 279, 253–259. https://doi.org/10.1016/j.neuroscience.2014.08.046

69. Karlsen, Anna Schou, & Pakkenberg, B. (2011). Total numbers of neurons and glial cells in cortex and basal ganglia of aged brains with down syndrome—A stereological study. Cerebral Cortex, 21(11), 2519–2524. https://doi.org/10.1093/cercor/bhr033

70. Kato, S., Hayashi, H., Nakashima, K., Nanba, E., Kato, M., Hirano, A., Nakano, I., Asayama, K., & Ohama, E. (1997). Pathological characterization of astrocytic hyaline inclusions in familial amyotrophic lateral sclerosis. The American Journal of Pathology, 151(2), 611–620.

71. Kettenmann, H., & Verkhratsky, A. (2008). Neuroglia: The 150 years after. Trends in Neurosciences, 31(12), 653–659. https://doi.org/10.1016/j.tins.2008.09.003

72. Khundakar, A., Morris, C., Oakley, A., McMeekin, W., & Thomas, A. J. (2009). Morphometric analysis of neuronal and glial cell pathology in the dorsolateral prefrontal cortex in late-life depression. The British Journal of Psychiatry, 195(2), 163–169. https://doi.org/10.1192/bjp.bp.108.052688

73. Khundakar, A., Morris, C., Oakley, A., & Thomas, A. J. (2011a). A morphometric examination of neuronal and glial cell pathology in the orbitofrontal cortex in late-life depression. International Psychogeriatrics, 23(1), 132–140. https://doi.org/10.1017/S1041610210000700

74. Khundakar, A., Morris, C., Oakley, A., & Thomas, A. J. (2011b). Morphometric analysis of neuronal and glial cell pathology in the caudate nucleus in late-life depression. The American Journal of Geriatric Psychiatry, 19(2), 132–141. https://doi.org/10.1097/JGP.0b013e3181df4642

75. Khundakar, A., & Thomas, A. J. (2009). Morphometric changes in early- and late-life major depressive disorder: Evidence from postmortem studies. International Psychogeriatrics, 21(5), 844–854. https://doi.org/10.1017/S104161020999007X

76. Khundakar, A., Morris, C., Oakley, A., & Thomas, A. J. (2011). Cellular pathology within the anterior cingulate cortex of patients with late-life depression: A morphometric study. Psychiatry Research: Neuroimaging, 194(2), 184–189. https://doi.org/10.1016/j.pscychresns.2011.04.008

77. Kim, R., Healey, K. L., Sepulveda-Orengo, M. T., & Reissner, K. J. (2018). Astroglial correlates of neuropsychiatric disease: From astrocytopathy to astrogliosis. Progress in Neuro-Psychopharmacology and Biological Psychiatry, 87, 126–146. https://doi.org/10.1016/j.pnpbp.2017.10.002

78. Korbo, L. (1999). Glial cell loss in the hippocampus of alcoholics. Alcoholism: Clinical and Experimental Research, 23(1), 164–168. https://doi.org/10.1111/j.1530-0277.1999.tb04039.x

79. Koeppen, J., Nguyen, A. Q., Nikolakopoulou, A. M., Garcia, M., Hanna, S., Woodruff, S., Figueroa, Z., Obenaus, A., & Ethell, I. M. (2018). Functional consequences of synapse remodeling following astrocyte-specific regulation of ephrin-b1 in the adult hippocampus. Journal of Neuroscience, 38(25), 5710–5726. https://doi.org/10.1523/JNEUROSCI.3618-17.2018

80. Kuga, N., Sasaki, T., Takahara, Y., Matsuki, N., & Ikegaya, Y. (2011). Large-scale calcium waves traveling through astrocytic networks in vivo. Journal of Neuroscience, 31(7), 2607–2614. https://doi.org/10.1523/JNEUROSCI.5319-10.2011

81. Lasič, E., Lisjak, M., Horvat, A., Božić, M., Šakanović, A., Anderluh, G., Verkhratsky, A., Vardjan, N., Jorgačevski, J., Stenovec, M., & Zorec, R. (2019). Astrocyte specific remodeling of plasmalemmal cholesterol composition by ketamine indicates a new mechanism of antidepressant action. Scientific Reports, 9(1), 1–12. https://doi.org/10.1038/s41598-019-47459-z

82. Lenhossék, M. v. (1895). Centrosom und Sphäre in den Spinalganglienzellen des Frosches. Archiv für mikroskopische Anatomie, 46(1), 345–369. https://doi.org/10.1007/BF02906658

83. Liddelow, S. A., Guttenplan, K. A., Clarke, L. E., Bennett, F. C., Bohlen, C. J., Schirmer, L., Bennett, M. L., Münch, A. E., Chung, W.-S., Peterson, T. C., Wilton, D. K., Frouin, A., Napier, B. A., Panicker, N., Kumar, M., Buckwalter, M. S., Rowitch, D. H., Dawson, V. L., Dawson, T. M., … Barres, B. A. (2017). Neurotoxic reactive astrocytes are induced by activated microglia. Nature, 541(7638), 481–487. https://doi.org/10.1038/nature21029

84. Liddelow, S., & Barres, B. (2017). Reactive astrocytes: Production, function, and therapeutic potential. Immunity, 46(6), 957–967. https://doi.org/10.1016/j.immuni.2017.06.006

85. López-Hidalgo, M., Hoover, W. B., & Schummers, J. (2016). Spatial organization of astrocytes in ferret visual cortex. Journal of Comparative Neurology, 524(17), 3561–3576. https://doi.org/10.1002/cne.24015

86. Luse , S. A. (1956). Electron microscopic observations of the central nervous system. The Journal of Biophysical and Biochemical Cytology, 2(5), 531–542. https://doi.org/10.1083/jcb.2.5.531

87. Marchi, N., Cavaglia, M., Fazio, V., Bhudia, S., Hallene, K., & Janigro, D. (2004). Peripheral markers of blood–brain barrier damage. Clinica Chimica Acta, 342(1), 1–12. https://doi.org/10.1016/j.cccn.2003.12.008

88. Marina, N., Christie, I. N., Korsak, A., Doronin, M., Brazhe, A., Hosford, P. S., Wells, J. A., Sheikhbahaei, S., Humoud, I., Paton, J. F. R., Lythgoe, M. F., Semyanov, A., Kasparov, S., & Gourine, A. V. (2020). Astrocytes monitor cerebral perfusion and control systemic circulation to maintain brain blood flow. Nature Communications, 11(1), 1–9. https://doi.org/10.1038/s41467-019-13956-y

89. Marín-padilla, M. (1995). Prenatal development of fibrous (White matter), protoplasmic (Gray matter), and layer I astrocytes in the human cerebral cortex: A Golgi study. Journal of Comparative Neurology, 357(4), 554–572. https://doi.org/10.1002/cne.903570407

90. Mazaré, N., Oudart, M., Moulard, J., Cheung, G., Tortuyaux, R., Mailly, P., Mazaud, D., Bemelmans, A.-P., Boulay, A.-C., Blugeon, C., Jourdren, L., Le Crom, S., Rouach, N., & Cohen-Salmon, M. (2020). Local translation in perisynaptic astrocytic processes is specific and changes after fear conditioning. Cell Reports, 32(8). https://doi.org/10.1016/j.celrep.2020.108076

91. McKeon, R. J., Schreiber, R. C., Rudge, J. S., & Silver, J. (1991). Reduction of neurite outgrowth in a model of glial scarring following CNS injury is correlated with the expression of inhibitory molecules on reactive astrocytes. Journal of Neuroscience, 11(11), 3398–3411. https://doi.org/10.1523/JNEUROSCI.11-11-03398.1991

92. McNeal, D. W., Brandner, D. D., Gong, X., Postupna, N. O., Montine, T. J., Dirk Keene, C., & Back, S. A. (2016). Unbiased stereological analysis of reactive astrogliosis to estimate age-associated cerebral white matter injury. Journal of Neuropathology & Experimental Neurology, 75(6), 539–554. https://doi.org/10.1093/jnen/nlw032

93. Medina, A., Watson, S. J., Bunney, W., Myers, R. M., Schatzberg, A., Barchas, J., Akil, H., & Thompson, R. C. (2016). Evidence for alterations of the glial syncytial function in major depressive disorder. Journal of Psychiatric Research, 72, 15–21. https://doi.org/10.1016/j.jpsychires.2015.10.010

94. Menard, C., Pfau, M. L., Hodes, G. E., Kana, V., Wang, V. X., Bouchard, S., Takahashi, A., Flanigan, M. E., Aleyasin, H., LeClair, K. B., Janssen, W. G., Labonté, B., Parise, E. M., Lorsch, Z. S., Golden, S. A., Heshmati, M., Tamminga, C., Turecki,

G., Campbell, M., … Russo, S. J. (2017). Social stress induces neurovascular pathology promoting depression. Nature Neuroscience, 20(12), 1752–1760. https://doi.org/10.1038/s41593-017-0010-3

95. Metabolic communication between astrocytes and neurons via bicarbonate-responsive soluble adenylyl cyclase. (2012). Neuron, 75(6), 1094–1104. https://doi.org/10.1016/j.neuron.2012.08.032

96. Miguel-Hidalgo, J. J., Baucom, C., Dilley, G., Overholser, J. C., Meltzer, H. Y., Stockmeier, C. A., & Rajkowska, G. (2000). Glial fibrillary acidic protein immunoreactivity in the prefrontal cortex distinguishes younger from older adults in major depressive disorder. Biological Psychiatry, 48(8), 861–873. https://doi.org/10.1016/S0006-3223(00)00999-9

97. Miguel-Hidalgo, J. J., Waltzer, R., Whittom, A. A., Austin, M. C., Rajkowska, G., & Stockmeier, C. A. (2010). Glial and glutamatergic markers in depression, alcoholism, and their comorbidity. Journal of Affective Disorders, 127(1), 230–240. https://doi.org/10.1016/j.jad.2010.06.003

98. Miguel-Hidalgo, J. J., Wilson, B. A., Hussain, S., Meshram, A., Rajkowska, G., & Stockmeier, C. A. (2014). Reduced connexin 43 immunolabeling in the orbitofrontal cortex in alcohol dependence and depression. Journal of Psychiatric Research, 55, 101–109. https://doi.org/10.1016/j.jpsychires.2014.04.007

99. Milleit, B., Smesny, S., Rothermundt, M., Preul, C., Schroeter, M. L., von Eiff, C., Ponath, G., Milleit, C., Sauer, H., & Gaser, C. (2016). Serum s100b protein is specifically related to white matter changes in schizophrenia. Frontiers in Cellular Neuroscience, 10. https://doi.org/10.3389/fncel.2016.00033

100. Mirza, B., Hadberg, H., Thomsen, P., & Moos, T. (1999). The absence of reactive astrocytosis is indicative of a unique inflammatory process in Parkinson's disease. Neuroscience, 95(2), 425–432. https://doi.org/10.1016/S0306-4522(99)00455-8

101. Moritz, S., Warnat, J., Bele, S., Graf, B. M., & Woertgen, C. (2010). The prognostic value of nse and s100b from serum and cerebrospinal fluid in patients with

spontaneous subarachnoid hemorrhage. Journal of Neurosurgical Anesthesiology, 22(1), 21–31. https://doi.org/10.1097/ANA.0b013e3181bdf50d

102. Mouton, P. R., Long, J. M., Lei, D.-L., Howard, V., Jucker, M., Calhoun, M. E., & Ingram, D. K. (2002). Age and gender effects on microglia and astrocyte numbers in brains of mice. Brain Research, 956(1), 30–35. https://doi.org/10.1016/S0006-8993(02)03475-3

103. Murphy-Royal, C., Gordon, G. R., & Bains, J. S. (2019). Stress-induced structural and functional modifications of astrocytes—Further implicating glia in the central response to stress. Glia, 67(10), 1806–1820. https://doi.org/https://doi.org/10.1002/glia.23610

104. Nagy, C., Maitra, M., Tanti, A., Suderman, M., Théroux, J.-F., Davoli, M. A., Perlman, K., Yerko, V., Wang, Y. C., Tripathy, S. J., Pavlidis, P., Mechawar, N., Ragoussis, J., & Turecki, G. (2020). Single-nucleus transcriptomics of the prefrontal cortex in major depressive disorder implicates oligodendrocyte precursor cells and excitatory neurons. Nature Neuroscience, 23(6), 771–781. https://doi.org/10.1038/s41593-020-0621-y

105. Nagy, C., Suderman, M., Yang, J., Szyf, M., Mechawar, N., Ernst, C., & Turecki, G. (2015). Astrocytic abnormalities and global DNA methylation patterns in depression and suicide. Molecular Psychiatry, 20(3), 320–328. https://doi.org/10.1038/mp.2014.21

106. Oberheim, N. A., Takano, T., Han, X., He, W., Lin, J. H. C., Wang, F., Xu, Q., Wyatt, J. D., Pilcher, W., Ojemann, J. G., Ransom, B. R., Goldman, S. A., & Nedergaard, M. (2009). Uniquely hominid features of adult human astrocytes. Journal of Neuroscience, 29(10), 3276–3287. https://doi.org/10.1523/JNEUROSCI.4707-08.2009

107. Oberheim, N. A., Tian, G.-F., Han, X., Peng, W., Takano, T., Ransom, B., & Nedergaard, M. (2008). Loss of astrocytic domain organization in the epileptic brain. Journal of Neuroscience, 28(13), 3264–3276. https://doi.org/10.1523/JNEUROSCI.4980-07.2008

108. O'Connell, K., Thakore, J., & Dev, K. K. (2013). Levels of S100B are raised in female patients with schizophrenia. BMC Psychiatry, 13(1), 146. https://doi.org/10.1186/1471-244X-13-146

109. Ogata, K., & Kosaka, T. (2002). Structural and quantitative analysis of astrocytes in the mouse hippocampus. Neuroscience, 113(1), 221–233. https://doi.org/10.1016/S0306-4522(02)00041-6

110. O'Leary, L. A., Davoli, M. A., Belliveau, C., Tanti, A., Ma, J. C., Farmer, W. T., Turecki, G., Murai, K. K., & Mechawar, N. (2020). Characterization of vimentin-immunoreactive astrocytes in the human brain. Frontiers in Neuroanatomy, 14. https://doi.org/10.3389/fnana.2020.00031

111. O'Leary, L. A., Belliveau, C., Davoli, M. A., Ma, J. C., Tanti, A., Turecki, G., & Mechawar, N. (2021). Widespread decrease of cerebral vimentin-immunoreactive astrocytes in depressed suicides. Frontiers in Psychiatry, 12. https://doi.org/10.3389/fpsyt.2021.640963

112. Öngür, D., Drevets, W. C., & Price, J. L. (1998). Glial reduction in the subgenual prefrontal cortex in mood disorders. Proceedings of the National Academy of Sciences, 95(22), 13290–13295. https://doi.org/10.1073/pnas.95.22.13290

113. Ordway, G. A., Szebeni, A., Chandley, M. J., Stockmeier, C. A., Xiang, L., Newton, S. S., Turecki, G., Duffourc, M. M., Zhu, M.-Y., Zhu, H., & Szebeni, K. (2012). Low gene expression of bone morphogenetic protein 7 in brainstem astrocytes in major depression. International Journal of Neuropsychopharmacology, 15(7), 855–868. https://doi.org/10.1017/S1461145711001350

114. Otto, M., Bahn, E., Wiltfang, J., Boekhoff, I., & Beuche, W. (1998). Decrease of S100 beta protein in serum of patients with amyotrophic lateral sclerosis. Neuroscience Letters, 240(3), 171–173. https://doi.org/10.1016/S0304-3940(97)00947-6

115. Pakkenberg, B. (1990). Pronounced reduction of total neuron number in mediodorsal thalamic nucleus and nucleus accumbens in schizophrenics. Archives of General Psychiatry, 47(11), 1023–1028. https://doi.org/10.1001/archpsyc.1990.01810230039007

116. Pannasch, U., Dossi, E., Ezan, P., & Rouach, N. (2019). Astroglial Cx30 sustains neuronal population bursts independently of gap-junction mediated biochemical coupling. Glia, 67(6), 1104–1112. https://doi.org/10.1002/glia.23591

117. Pannasch, U., Freche, D., Dallérac, G., Ghézali, G., Escartin, C., Ezan, P., Cohen-Salmon, M., Benchenane, K., Abudara, V., Dufour, A., Lübke, J. H. R., Déglon, N., Knott, G., Holcman, D., & Rouach, N. (2014). Connexin 30 sets synaptic strength by controlling astroglial synapse invasion. Nature Neuroscience, 17(4), 549–558. https://doi.org/10.1038/nn.3662

118. Pascual, O., Casper, K. B., Kubera, C., Zhang, J., Revilla-Sanchez, R., Sul, J.-Y., Takano, H., Moss, S. J., McCarthy, K., & Haydon, P. G. (2005). Astrocytic purinergic signaling coordinates synaptic networks. Science, 310(5745), 113–116. https://doi.org/10.1126/science.1116916

119. Pekny, M., Pekna, M., Messing, A., Steinhäuser, C., Lee, J.-M., Parpura, V., Hol, E. M., Sofroniew, M. V., & Verkhratsky, A. (2016). Astrocytes: A central element in neurological diseases. Acta Neuropathologica, 131(3), 323–345. https://doi.org/10.1007/s00401-015-1513-1

120. Pelinka, L. E., Kroepfl, A., Leixnering, M., Buchinger, W., Raabe, A., & Redl, H. (2004). GFAP versus S100B in serum after traumatic brain injury: Relationship to brain damage and outcome. Journal of Neurotrauma, 21(11), 1553–1561. https://doi.org/10.1089/neu.2004.21.1553

121. Pellerin, L., & Magistretti, P. J. (1994). Glutamate uptake into astrocytes stimulates aerobic glycolysis: A mechanism coupling neuronal activity to glucose utilization. Proceedings of the National Academy of Sciences, 91(22), 10625–10629. https://doi.org/10.1073/pnas.91.22.10625

122. Pelvig, D. P., Pakkenberg, H., Stark, A. K., & Pakkenberg, B. (2008). Neocortical glial cell numbers in human brains. Neurobiology of Aging, 29(11), 1754–1762. https://doi.org/10.1016/j.neurobiolaging.2007.04.013

123. Pelvig, Dorte P., Pakkenberg, H., Regeur, L., Oster, S., & Pakkenberg, B. (2003). Neocortical glial cell numbers in alzheimer's disease. Dementia and Geriatric Cognitive Disorders, 16(4), 212–219. https://doi.org/10.1159/000072805

124. Penfield, W., & Buckley, R. C. (1928). Punctures of the brain: The factors concerned in gliosis and in cicatricial contraction. Archives of Neurology & Psychiatry, 20(1), 1–13. https://doi.org/10.1001/archneurpsyc.1928.02210130004001

125. Perea, G., Navarrete, M., & Araque, A. (2009). Tripartite synapses: Astrocytes process and control synaptic information. Trends in Neurosciences, 32(8), 421–431. https://doi.org/10.1016/j.tins.2009.05.001

126. Poskanzer, K. E., & Molofsky, A. V. (2018). Dynamism of an astrocyte in vivo: Perspectives on identity and function. Annual Review of Physiology, 80(1), 143–157. https://doi.org/10.1146/annurev-physiol-021317-121125

127. Powers, B., & Sodhi, M. (2019). F88. Elevated glutamate transporter expression in females with depression. Biological Psychiatry, 85(10), S246–S247. https://doi.org/10.1016/j.biopsych.2019.03.625

128. Rainey, T., Lesko, M., Sacho, R., Lecky, F., & Childs, C. (2009). Predicting outcome after severe traumatic brain injury using the serum S100B biomarker: Results using a single (24h) time-point. Resuscitation, 80(3), 341–345. https://doi.org/10.1016/j.resuscitation.2008.11.021

129. Rajkowska, G. (2000). Postmortem studies in mood disorders indicate altered numbers of neurons and glial cells. Biological Psychiatry, 48(8), 766–777. https://doi.org/10.1016/S0006-3223(00)00950-1

130. Rajkowska, G., Hughes, J., Stockmeier, C. A., Javier Miguel-Hidalgo, J., & Maciag, D. (2013). Coverage of blood vessels by astrocytic endfeet is reduced in major depressive disorder. Biological Psychiatry, 73(7), 613–621. https://doi.org/10.1016/j.biopsych.2012.09.024

131. Rajkowska, G., Legutko, B., Moulana, M., Syed, M., Romero, D. G., Stockmeier, C. A., & Miguel-Hidalgo, J. J. (2018). Astrocyte pathology in the ventral prefrontal white

matter in depression. Journal of Psychiatric Research, 102, 150–158. https://doi.org/10.1016/j.jpsychires.2018.04.005

132. Rajkowska, G., Miguel-Hidalgo, J. J., Wei, J., Dilley, G., Pittman, S. D., Meltzer, H. Y., Overholser, J. C., Roth, B. L., & Stockmeier, C. A. (1999). Morphometric evidence for neuronal and glial prefrontal cell pathology in major depression∗∗See accompanying Editorial, in this issue. Biological Psychiatry, 45(9), 1085–1098. https://doi.org/10.1016/S0006-3223(99)00041-4

133. Rajkowska, G., & Stockmeier, C. A. (2013). Astrocyte pathology in major depressive disorder: Insights from human postmortem brain tissue. Current Drug Targets, 14(11), 1225–1236.

134. Reichenbach, A., Siegel, A., Senitz, D., & Smith, T. G. (1992). A comparative fractal analysis of various mammalian astroglial cell types. NeuroImage, 1(1), 69–77. https://doi.org/10.1016/1053-8119(92)90008-B

135. Salvesen, L., Ullerup, B. H., Sunay, F. B., Brudek, T., Løkkegaard, A., Agander, T. K., Winge, K., & Pakkenberg, B. (2015). Changes in total cell numbers of the basal ganglia in patients with multiple system atrophy—A stereological study. Neurobiology of Disease, 74, 104–113. https://doi.org/10.1016/j.nbd.2014.11.008

136. Salvesen, L., Winge, K., Brudek, T., Agander, T. K., Løkkegaard, A., & Pakkenberg, B. (2017). Neocortical neuronal loss in patients with multiple system atrophy: A stereological study. Cerebral Cortex, 27(1), 400–410. https://doi.org/10.1093/cercor/bhv228

137. Santos, S. E. D., Medeiros, M., Porfirio, J., Tavares, W., Pessôa, L., Grinberg, L., Leite, R. E. P., Ferretti-Rebustini, R. E. L., Suemoto, C. K., Filho, W. J., Noctor, S. C., Sherwood, C. C., Kaas, J. H., Manger, P. R., & Herculano-Houzel, S. (2020). Similar microglial cell densities across brain structures and mammalian species: Implications for brain tissue function. Journal of Neuroscience, 40(24), 4622–4643. https://doi.org/10.1523/JNEUROSCI.2339-19.2020

138. Schroeter, M. L., & Steiner, J. (2009). Elevated serum levels of the glial marker protein S100B are not specific for schizophrenia or mood disorders. Molecular Psychiatry, 14(3), 235–237. https://doi.org/10.1038/mp.2008.85

139. Schroeter, Matthias L., Abdul-Khaliq, H., Krebs, M., Diefenbacher, A., & Blasig, I. E. (2008). Serum markers support disease-specific glial pathology in major depression. Journal of Affective Disorders, 111(2), 271–280. https://doi.org/10.1016/j.jad.2008.03.005

140. Schroeter, Matthias L., Steiner, J., & Mueller, K. (2011). Glial pathology is modified by age in mood disorders—A systematic meta-analysis of serum S100B in vivo studies. Journal of Affective Disorders, 134(1), 32–38. https://doi.org/10.1016/j.jad.2010.11.008

141. Selinfreund, R. H., Barger, S. W., Pledger, W. J., & Eldik, L. J. V. (1991). Neurotrophic protein S100 beta stimulates glial cell proliferation. Proceedings of the National Academy of Sciences, 88(9), 3554–3558. https://doi.org/10.1073/pnas.88.9.3554

142. Serrano-Pozo, A., Gómez-Isla, T., Growdon, J. H., Frosch, M. P., & Hyman, B. T. (2013). A phenotypic change but not proliferation underlies glial responses in alzheimer disease. The American Journal of Pathology, 182(6), 2332–2344. https://doi.org/10.1016/j.ajpath.2013.02.031

143. Shabel, S. J., Proulx, C. D., Piriz, J., & Malinow, R. (2014). GABA/glutamate co-release controls habenula output and is modified by antidepressant treatment. Science, 345(6203), 1494–1498. https://doi.org/10.1126/science.1250469

144. Si, X., Miguel-Hidalgo, J. J., O'Dwyer, G., Stockmeier, C. A., & Rajkowska, G. (2004). Age-dependent reductions in the level of glial fibrillary acidic protein in the prefrontal cortex in major depression. Neuropsychopharmacology, 29(11), 2088–2096. https://doi.org/10.1038/sj.npp.1300525

145. Siegel, A., Reichenbach, A., Hanke, S., Senitz, D., Brauer, K., & Smith, T. G. (1991). Comparative morphometry of Bergmann glial (Golgi epithelial) cells. Anatomy and Embryology, 183(6), 605–612. https://doi.org/10.1007/BF00187909

146. Simard, S., Coppola, G., Rudyk, C. A., Hayley, S., McQuaid, R. J., & Salmaso, N. (2018). Profiling changes in cortical astroglial cells following chronic stress. Neuropsychopharmacology, 43(9), 1961–1971. https://doi.org/10.1038/s41386-018-0105-x

147. Smiley, J. F., Hackett, T. A., Bleiwas, C., Petkova, E., Stankov, A., Mann, J. J., Rosoklija, G., & Dwork, A. J. (2016). Reduced GABA neuron density in auditory cerebral cortex of subjects with major depressive disorder. Journal of Chemical Neuroanatomy, 76, 108–121. https://doi.org/10.1016/j.jchemneu.2015.10.008

148. Sofroniew, M. V., & Vinters, H. V. (2010). Astrocytes: Biology and pathology. Acta Neuropathologica, 119(1), 7–35. https://doi.org/10.1007/s00401-009-0619-8

149. Sosunov, A. A., Guilfoyle, E., Wu, X., McKhann, G. M., & Goldman, J. E. (2013). Phenotypic conversions of "protoplasmic" to "reactive" astrocytes in alexander disease. Journal of Neuroscience, 33(17), 7439–7450. https://doi.org/10.1523/JNEUROSCI.4506-12.2013

150. Steiner, J., Bernstein, H.-G., Bielau, H., Berndt, A., Brisch, R., Mawrin, C., Keilhoff, G., & Bogerts, B. (2007). Evidence for a wide extra-astrocytic distribution of S100B in human brain. BMC Neuroscience, 8(1), 2. https://doi.org/10.1186/1471-2202-8-2

151. Stenovec, M., Božić, M., Pirnat, S., & Zorec, R. (2020). Astroglial mechanisms of ketamine action include reduced mobility of kir4. 1-carrying vesicles. Neurochemical Research, 45(1), 109–121. https://doi.org/10.1007/s11064-019-02744-1

152. Streitbürger, D.-P., Arelin, K., Kratzsch, J., Thiery, J., Steiner, J., Villringer, A., Mueller, K., & Schroeter, M. L. (2012). Validating serum s100b and neuron-specific enolase as biomarkers for the human brain – a combined serum, gene expression and mri study. PLOS ONE, 7(8), e43284. https://doi.org/10.1371/journal.pone.0043284

153. Perry, J. C., Pakkenberg, B., Vann, S. D. (2019) Striking reduction in neurons and glial cells in anterior thalamic nuclei of older patients with Down syndrome. Neurobiology of Aging, 75, 54–61. https://doi.org/10.1016/j.neurobiolaging.2018.11.009

154. Süssmuth, S. D., Sperfeld, A. D., Hinz, A., Brettschneider, J., Endruhn, S., Ludolph, A. C., & Tumani, H. (2010). CSF glial markers correlate with survival in amyotrophic lateral sclerosis. Neurology, 74(12), 982–987. https://doi.org/10.1212/WNL.0b013e3181d5dc3b

155. Takano, T., Tian, G.-F., Peng, W., Lou, N., Libionka, W., Han, X., & Nedergaard, M. (2006). Astrocyte-mediated control of cerebral blood flow. Nature Neuroscience, 9(2), 260–267. https://doi.org/10.1038/nn1623

156. Tanaka, K., Watase, K., Manabe, T., Yamada, K., Watanabe, M., Takahashi, K., Iwama, H., Nishikawa, T., Ichihara, N., Kikuchi, T., Okuyama, S., Kawashima, N., Hori, S., Takimoto, M., & Wada, K. (1997). Epilepsy and exacerbation of brain injury in mice lacking the glutamate transporter glt-1. Science, 276(5319), 1699–1702. https://doi.org/10.1126/science.276.5319.1699

157. Tanti, A., Kim, J. J., Wakid, M., Davoli, M.-A., Turecki, G., & Mechawar, N. (2018). Child abuse associates with an imbalance of oligodendrocyte-lineage cells in ventromedial prefrontal white matter. Molecular Psychiatry, 23(10), 2018–2028. https://doi.org/10.1038/mp.2017.231

158. Tanti, Arnaud, Lutz, P.-E., Kim, J., O'Leary, L., Théroux, J.-F., Turecki, G., & Mechawar, N. (2019). Evidence of decreased gap junction coupling between astrocytes and oligodendrocytes in the anterior cingulate cortex of depressed suicides. Neuropsychopharmacology, 44(12), 2099–2111. https://doi.org/10.1038/s41386-019-0471-z

159. Torres-Platas, S. G., Nagy, C., Wakid, M., Turecki, G., & Mechawar, N. (2016). Glial fibrillary acidic protein is differentially expressed across cortical and subcortical regions in healthy brains and downregulated in the thalamus and caudate nucleus of depressed suicides. Molecular Psychiatry, 21(4), 509–515. https://doi.org/10.1038/mp.2015.65

160. Torres-Platas, Susana G., Hercher, C., Davoli, M. A., Maussion, G., Labonté, B., Turecki, G., & Mechawar, N. (2011). Astrocytic hypertrophy in anterior cingulate white matter of depressed suicides. Neuropsychopharmacology, 36(13), 2650–2658. https://doi.org/10.1038/npp.2011.154

161. Tynan, R. J., Beynon, S. B., Hinwood, M., Johnson, S. J., Nilsson, M., Woods, J. J., & Walker, F. R. (2013). Chronic stress-induced disruption of the astrocyte network is driven by structural atrophy and not loss of astrocytes. Acta Neuropathologica, 126(1), 75–91. https://doi.org/10.1007/s00401-013-1102-0

162. Van Der Voorn, P., Tekstra, J., Beelen, R. H. J., Tensen, C. P., Van Der Valk, P., & De Groot, C. J. A. (1999). Expression of mcp-1 by reactive astrocytes in demyelinating multiple sclerosis lesions. The American Journal of Pathology, 154(1), 45–51.

163. Verkhratsky, A., Rodríguez, J. J., & Parpura, V. (2013). Astroglia in neurological diseases. Future Neurology, 8(2), 149–158. https://doi.org/10.2217/fnl.12.90

164. Vonsattel, J.-P., Myers, R. H., Stevens, T. J., Ferrante, R. J., Bird, E. D., & Richardson, E. P. (1985). Neuropathological classification of huntington's disease. Journal of Neuropathology & Experimental Neurology, 44(6), 559–577. https://doi.org/10.1097/00005072-198511000-00003

165. Vos, P. E., Jacobs, B., Andriessen, T. M. J. C., Lamers, K. J. B., Borm, G. F., Beems, T., Edwards, M., Rosmalen, C. F., & Vissers, J. L. M. (2010). GFAP and S100B are biomarkers of traumatic brain injury: An observational cohort study. Neurology, 75(20), 1786–1793. https://doi.org/10.1212/WNL.0b013e3181fd62d2

166. Wallraff, A., Köhling, R., Heinemann, U., Theis, M., Willecke, K., & Steinhäuser, C. (2006). The impact of astrocytic gap junctional coupling on potassium buffering in the hippocampus. Journal of Neuroscience, 26(20), 5438–5447. https://doi.org/10.1523/JNEUROSCI.0037-06.2006

167. Webster, M. J., O'Grady, J., Kleinman, J. E., & Weickert, C. S. (2005). Glial fibrillary acidic protein mRNA levels in the cingulate cortex of individuals with depression, bipolar disorder and schizophrenia. Neuroscience, 133(2), 453–461. https://doi.org/10.1016/j.neuroscience.2005.02.037

168. Williams, M. R., Hampton, T., Pearce, R. K., Hirsch, S. R., Ansorge, O., Thom, M., & Maier, M. (2013). Astrocyte decrease in the subgenual cingulate and callosal genu

in schizophrenia. European Archives of Psychiatry and Clinical Neuroscience, 263(1), 41–52. https://doi.org/10.1007/s00406-012-0328-5

169. Wruck, W., & Adjaye, J. (2020). Meta-analysis of human prefrontal cortex reveals activation of GFAP and decline of synaptic transmission in the aging brain. Acta Neuropathologica Communications, 8(1), 26. https://doi.org/10.1186/s40478-020-00907-8

170. Xiong, Z., Zhang, K., Ren, Q., Chang, L., Chen, J., & Hashimoto, K. (2019). Increased expression of inwardly rectifying Kir4.1 channel in the parietal cortex from patients with major depressive disorder. Journal of Affective Disorders, 245, 265–269. https://doi.org/10.1016/j.jad.2018.11.016

171. Yang, Y., Cui, Y., Sang, K., Dong, Y., Ni, Z., Ma, S., & Hu, H. (2018). Ketamine blocks bursting in the lateral habenula to rapidly relieve depression. Nature, 554(7692), 317–322. https://doi.org/10.1038/nature25509

172. Zhang, Y., Sloan, S. A., Clarke, L. E., Caneda, C., Plaza, C. A., Blumenthal, P. D., Vogel, H., Steinberg, G. K., Edwards, M. S. B., Li, G., Duncan, J. A., Cheshier, S. H., Shuer, L. M., Chang, E. F., Grant, G. A., Gephart, M. G. H., & Barres, B. A. (2016). Purification and characterization of progenitor and mature human astrocytes reveals transcriptional and functional differences with mouse. Neuron, 89(1), 37–53. https://doi.org/10.1016/j.neuron.2015.11.013

173. Zhao, J., Verwer, R. W. H., van Wamelen, D. J., Qi, X.-R., Gao, S.-F., Lucassen, P. J., & Swaab, D. F. (2016). Prefrontal changes in the glutamate-glutamine cycle and neuronal/glial glutamate transporters in depression with and without suicide. Journal of Psychiatric Research, 82, 8–15. https://doi.org/10.1016/j.jpsychires.2016.06.017

Tables & Figures

Table 1 | Common astrocyte markers and their features

Name	Identity	Function	Methods	Ideal use in postmortem brain	Advantages	Disadvantages
GFAP	Type III Intermediate Filament	Reactive astrogliosis, cell structure and vesicle motility	Regional mRNA and protein expression, Stereology	White matter pathology	Best astrocyte marker for replicating postmortem studies — most commonly used marker. Strongly labels fibrous astrocytes. Selective expression in astrocytes.	Selectively labels only reactive astrocytes, does not consistently reveal fine morphology in postmortem samples, Signal is relatively weak and background is relatively higher in gray matter regions.
VIM	Type III Intermediate Filament	Reactive astrogliosis, cell structure and vesicle motility	Stereology, Morphology	Morphological comparisons	Best astrocyte marker for revealing fine astrocyte morphology in postmortem tissue. Labels blood vessels to aid astrocyte identification. Low background staining	Unsuitable for regional -omics approaches due to blood vessel and microglia expression, Reveals relatively few astrocytes.
ALDh1L1	Cytosolic enzyme	Formate removal in glutamate synthesis	Regional mRNA and protein expression, Stereology	Regional gene expression differences in astrocytes	Best astrocyte marker for revealing the entire population of astrocytes ('pan-astrocytic')	Difficult to achieve adequate immunostaining in postmortem brain tissue, Rarely reveals morphology

S100-β	Cytosolic and secreted calcium-binding protein	Neurotrophic factor for astrocyte proliferation	Stereology	Astrocyte-oligodendrocyte interactions	Best astrocyte marker for neurological conditions (as CSF levels are altered).	Requires refinement for regional -omic approaches as it is secreted and also expressed in many oligodendrocytes.
Glutamine Synthetase	Cytosolic enzyme	Glutamate catabolism for glutamate shuttling	Regional mRNA and protein expression, Stereology	Astrocyte-neuron differences	Best astrocyte marker for studying astrocyte-neuron interactions	Also expressed in many oligodendrocytes
Sox 9	Transcription Factor	Astrocyte differentiation	Regional mRNA and protein expression	Astrocyte counts and nuclear sorting	Best nuclear marker of astrocytes	Difficult to achieve adequate immunostaining in postmortem brain tissue
EAAT1/GLAST-1	Plasma membrane transporter protein	Glutamate reuptake	Regional mRNA and protein expression, % coverage	Slow glutamate reuptake	-	Not responsible for all glutamate reuptake by astrocytes
EAAT2/GLT-1	Plasma membrane transporter protein	Glutamate reuptake	Regional mRNA and protein expression, % coverage	Fast glutamate reuptake	-	Not responsible for all glutamate reuptake by astrocytes
Aquaporin-4	Endfeet water channel	Cerebral water homeostasis	Regional mRNA and protein expression, % coverage	Gliovascular interactions	Labels blood vessels	Difficult to distinguish aquaporin channels from blood vessels using IHC
Connexin-43	Gap junction	Intercellular communication	Regional mRNA and protein expression, % coverage	Astrocyte synctium (cell volume)	-	Punctate labelling, difficult to visualize
Connexin-30	Gap junction	Intercellular communication	Regional mRNA and protein expression, % coverage	Astrocyte synctium (astrocyte-neuron interaction)	-	Punctate labelling, difficult to visualize

Table 2 | Astrocyte densities

Date	Author	n (Control / Patient)	Sex m:f	Age	Markers	Region	Astrocytes/mm^3	Change in condition
1990	Pakkenberg	12 / 12	8:4 / 6:6	63±4 / 62±4	Giemsa Stain	Thalamus (mediodorsal)	18837 ± 449	Decrease in schizophrenia
						Basolateral Amygdala	14792 ± 573	No change in schizophrenia
						Nucleus Accumbens (Ventromedial)	17034 ± 681	Decrease in schizophrenia
						Nucleus Accumbens (Lateral)	12683 ± 366	Decrease in schizophrenia
						Ventral Pallidum	15847 ± 310	No change in schizophrenia
2008	Pelvig et al.	37 / 0	18 / 13	57 ± 6 / 63 ± 6	Giemsa Stain	Total Neocortex (Male)	15472±113	No change between sexes
						Total Neocortex (Female)	11545±98	No change between sexes
2011	Karlsen et al	6 / 4	0:6 / 0:4	70±3 / 66±2	Giemsa Stain	Basal Ganglia	27228 ± 1180	No change in Down Syndrome
2014	Karlsen et al	6 / 4	0:6 / 0:4	70±3 / 69±4	Giemsa Stain	Mediodorsal thalamus	29279±2902	No change in Down Syndrome
2015	Salvesen et al	11 / 11	5:6 / 5:6	68 ± ? / 66 ± 1	Giemsa Stain	Putamen	25690 ± 1239	Increase in Multiple System Atrophy
						Caudate Nucleus	31400 ± 1609	Increase in Multiple System Atrophy
						Globus Pallidus	19300 ± 1106	Increase in Multiple System Atrophy
						Subthalamic Nucleus	27600 ± 2746	No change in Multiple System Atrophy
						Red Nucleus	18200 ± 933	No change in Multiple System Atrophy
2017		11 / 11				Frontal Cortex	26200 ± 2607	Increase in Multiple System Atrophy

	Salvesen et al		5:6 / 5:6	68 ± ? / 66 ± 1	Giemsa Stain	Temporal Cortex	25500 ± 3998	Increase in Multiple System Atrophy
						Parietal Cortex	21000 ± 2406	Increase in Multiple System Atrophy
						Occipital Cortex	13900 ± 1341	No change in Multiple System Atrophy
2019	Kaalund et al.	13 / 12	13:0 / 12:0	44 ± 4 / 44 ± 4	Giemsa Stain	Frontal Cortex	11354 ± 323	No change in AIDS
						Temporal Cortex	11570 ± 338	No change in AIDS
						Parietal Cortex	12605 ± 320	No change in AIDS
						Occipital Cortex	17889 ± 757	No change in AIDS
						Neocortex	12383 ± 71	No change in AIDS
2019	Perry et al	6 / 4	0:6 / 0:4	71±4 / 69±4	Giemsa Stain	Thalamus (anterior principal nuclei)	31361 ± 889	Decrease in Down Syndrome
2000	Miguel-Hidalgo et al	15 / 14	10:5 / 7:7	47±4 / 56±5	GFAP	Dorsolateral PFC (BA9) Layers III-IV	7350 ± 1446	Positive correlation with age in MDD only
						Dorsolateral PFC (BA9) Layer V	9570 ± 1382	Positive correlation with age in MDD only
2003	Pelvig et al.	20 / 14	6:14 / 4:10	81 ± 2 / 81 ± 2	Haemotoxylin & Eosin	Total Neocortex	11779 ± 421	No change in Alzheimer's Disease
2013	Serrano-Pozo et al.	32 / 40	13:19 / 14:26	81 ± 13 / 78 ± 9	Aldh1L1	Temporopolar area (BA38)	1534±15	Increase in Alzheimer's Disease
2013	Fabricius et al.	8 / 8 / 7	0:8 / 0:8 / 0:8	72 ± 1 / 81 ± 1 / 98 ± 2	Haemotoxylin & Eosin	Total Neocortex (65–75 years)	26355 ± 560	No change across ages
						Total Neocortex (76–85 years)	26804 ± 1005	No change across ages
						Total Neocortex (94–105 years)	24686 ± 670	No change across ages
2014	Morgan et al.	10 / 8	10:0 / 8:0	24±8 / 23±8	Haemotoxylin & Eosin	Amygdala	6386 ± 1564	No change in autism
2016	Cobb et al.	17 / 17	13:4 / 12:5	52±3 / 52 ± 3	GFAP	Hippocampus (Hilus of Dentate Gyrus)	5304 ± 346	Decrease in MDD

2016	McNeal et al.	11 / 17	7:4 / 10:7	87 ± 8 / 89 ± 7	GFAP	Dorsolateral PFC and Dorsal ACC (BA 8/9/32 WM)	12044 ± 765	Increase in Vascular Brain Injury
2018	Rajkowska et al.	8 / 8	5:3 / 4:4	57±7 / 58±7	GFAP	Ventral PFC WM (BA ?)	481 ± 9	Decrease in MDD
2019	Qi et al	7 / 7	5:2 / 5:2	79±3 / 78±4	Haemotoxylin & Eosin + GFAP	Anterior Cingulate Cortex	18443 ± 1815	No change in Bipolar Disorder
2020	O'Leary et al.	8 / 0	8 : 0	60 ± 8	GFAP	Dorsolateral PFC (BA 8/9) GM	1059 ± 133	No group comparison (regional only)
						Dorsolateral PFC (BA 8/9) WM	2011 ± 222	No group comparison (regional only)
						Primary Visual Cortex (BA 17) GM	1256 ± 129	No group comparison (regional only)
						Primary Visual Cortex (BA 17) WM	1686 ± 153	No group comparison (regional only)
						Caudate Nucleus (precomissural)	2771 ± 551	No group comparison (regional only)
						Thalamus (mediodorsal)	2555 ± 448	No group comparison (regional only)
					VIM	Dorsolateral PFC (BA 8/9) GM	586 ± 132	No group comparison (regional only)
						Dorsolateral PFC (BA 8/9) WM	252 ± 85	No group comparison (regional only)
						Primary Visual Cortex (BA 17) GM	108 ± 32	No group comparison (regional only)
						Primary Visual Cortex (BA 17) WM	14 ± 4	No group comparison (regional only)
						Caudate Nucleus (precomissural)	1753 ± 339	No group comparison (regional only)

						Thalamus (mediodorsal)	1 ± 1	No group comparison (regional only)
2021	O'Leary et al.	10/10	10:0 / 10:0	41 ± 5 / 39 ± 4	GFAP	Dorsomedial PFC (BA 8/9) GM	1035 ± 232	No change in MDD
						Dorsomedial PFC (BA 8/9) WM	2668 ± 509	No change in MDD
						Caudate Nucleus (precomissural)	1142 ± 356	Decrease in MDD
						Thalamus (mediodorsal)	5902 ± 1348	Decrease in MDD
					VIM	Dorsomedial PFC (BA 8/9) GM	886 ± 316	Decrease in MDD
						Dorsomedial PFC (BA 8/9) WM	277 ± 98	Decrease in MDD
						Caudate Nucleus (precomissural)	1179 ± 355	No change in MDD
						Thalamus (mediodorsal)	2 ± 1	No change in MDD

Table 3 | Astrocyte morphometry

Date	Author	Sample Size	Tissue Preparation	Technique	Markers	Region	Soma Area (μm^2)	Process Number	Node Number	Terminal Number	Total Process Length (µm)	Mean Process Length (µm)	Process Surface Area
2009	Oberheim et al.	6	Live (Resected)	IHC + DiOlistic Labelling	GFAP + DiI/DiD	Temporal lobe GM (specific to resection)	-	38±5	-	-	-	98±5	-
2011	Torres-Platas et al.	10	Frozen	IHC	Golgi	ACC (BA 24) GM	110±12	15±1	18±2	34±3	717±59	50±4	-
						ACC (BA 24) WM	115±10	19±1	19±2	39±3	797±129	41±5	-
2018	Rajkowska et al.	8	Frozen	IHC	GFAP	Ventral PFC WM (BA11, BA12, BA47, ventral BA24)	49±7	-	-	-	-	-	-
2020	O'Leary et al.	8	Fresh	IHC	VIM	Dorsolateral PFC (BA 8/9) GM	84±9	36±2	70±7	112±8	2642±163	76±5	2238±184
						Dorsolateral PFC (BA 8/9) WM	62±7	39±2	28±3	69±4	2470±164	64±4	1918±130
						Primary Visual Cortex (BA17) GM	83±8	38±2	69±7	114±8	2820±189	79±8	2107±128
						Primary Visual Cortex (BA17) WM	53±7	28±3	24±4	65±6	2120±180	55±4	1689±129
						Caudate Nucleus (precomissural)	89±7	29±2	65±9	101±9	2396±158	89±10	2321±252

						Thalamus (mediodorsal)	63±6	34±2	22±3	57±4	1860±123	58±4	1423±137
2021	O'Leary et al.	10	Frozen	IHC	VIM	Dorsomedial PFC (BA 8/9) GM	70±5	28±2	33±2	62±4	1911±108	68±2	1377±79
						Dorsomedial PFC (BA 8/9) WM	32±2	35±1	22±2	49±2	1968±133	57±2	1625±119
						Caudate Nucleus (precomissural)	62±5	27±1	33±3	61±3	1882±126	71±4	1657±128
						Thalamus (mediodorsal)	56±4	21±1	14±2	35±2	1192±92	58±4	1019±98

Table 4 | Astrocyte morphometric subtypes

	Soma Area (μm^2)	Process Number	Node Number	Terminal Number	Total Process Length (μm)	Mean Process Length (μm)	Process Surface Area (μm^2)
Cortical protoplasmic astrocyte	79.00	34.00	57.33	96.00	2457.67	74.33	1907.33
Cortical fibrous astrocyte	49.00	34.00	24.67	63.67	2186.00	58.67	1744.00
Striatal astrocyte	75.50	25.00	39.50	68.00	1794.00	73.50	1989.00
Thalamic astrocyte	59.50	30.50	27.50	59.00	1871.00	64.50	1221.00

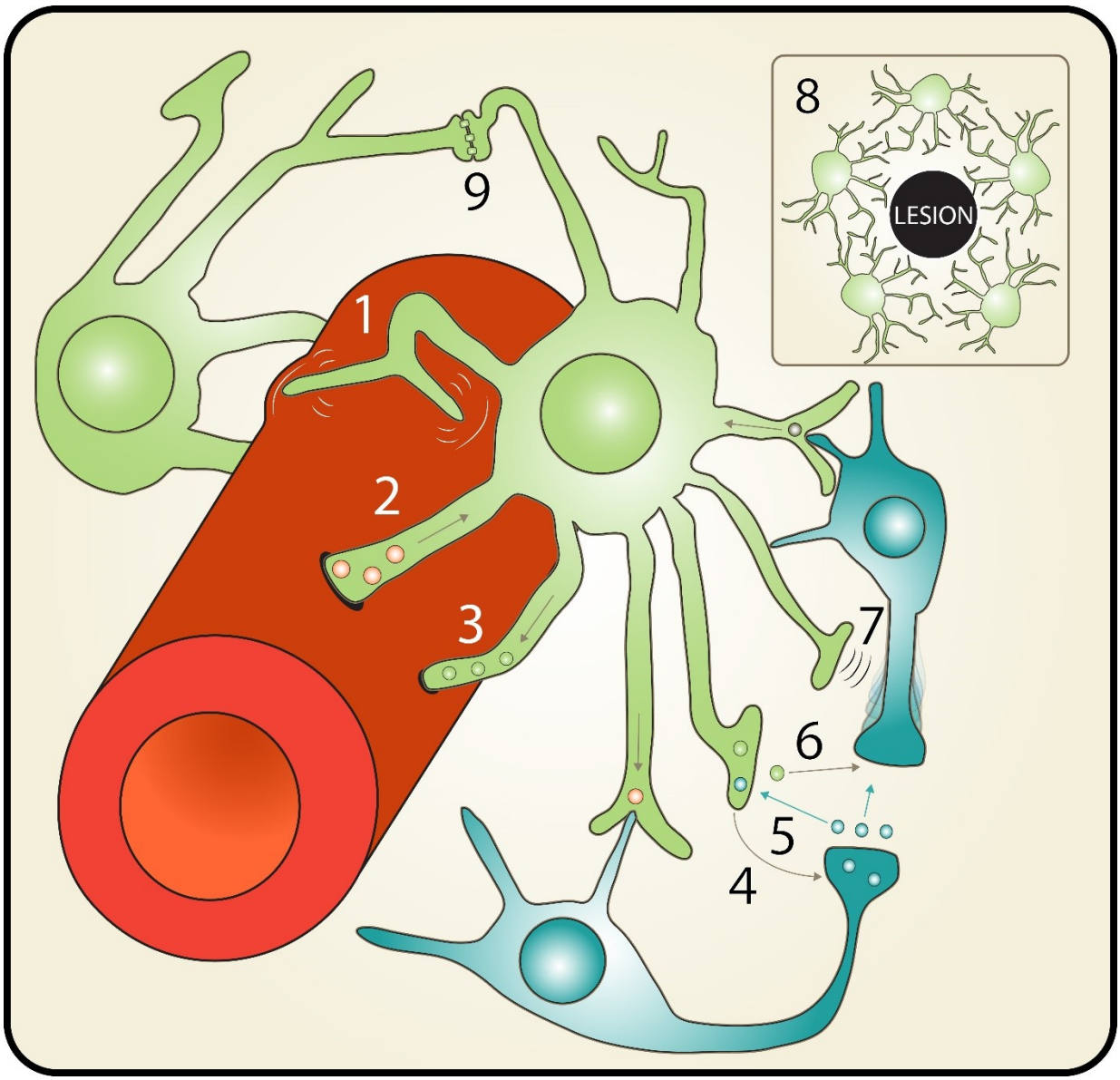

Figure 1 | General functions of astrocytes. In the brain, astrocytes control vasodilation (1), and traffic nutrients (2) and waste (3) from between the bloodstream and CSF and neurons. At the synapses, astrocytes send metabolites and neurotransmitter precursors to neurons (4), receive neuronal signals (5), and send signaling molecules called gliotransmitters (6). Astrocytes also send growth signals to neurons (7), surround neuronal lesions in a formation known as the glial scar (8), and communicate with other glial cells through gap junctions (9).

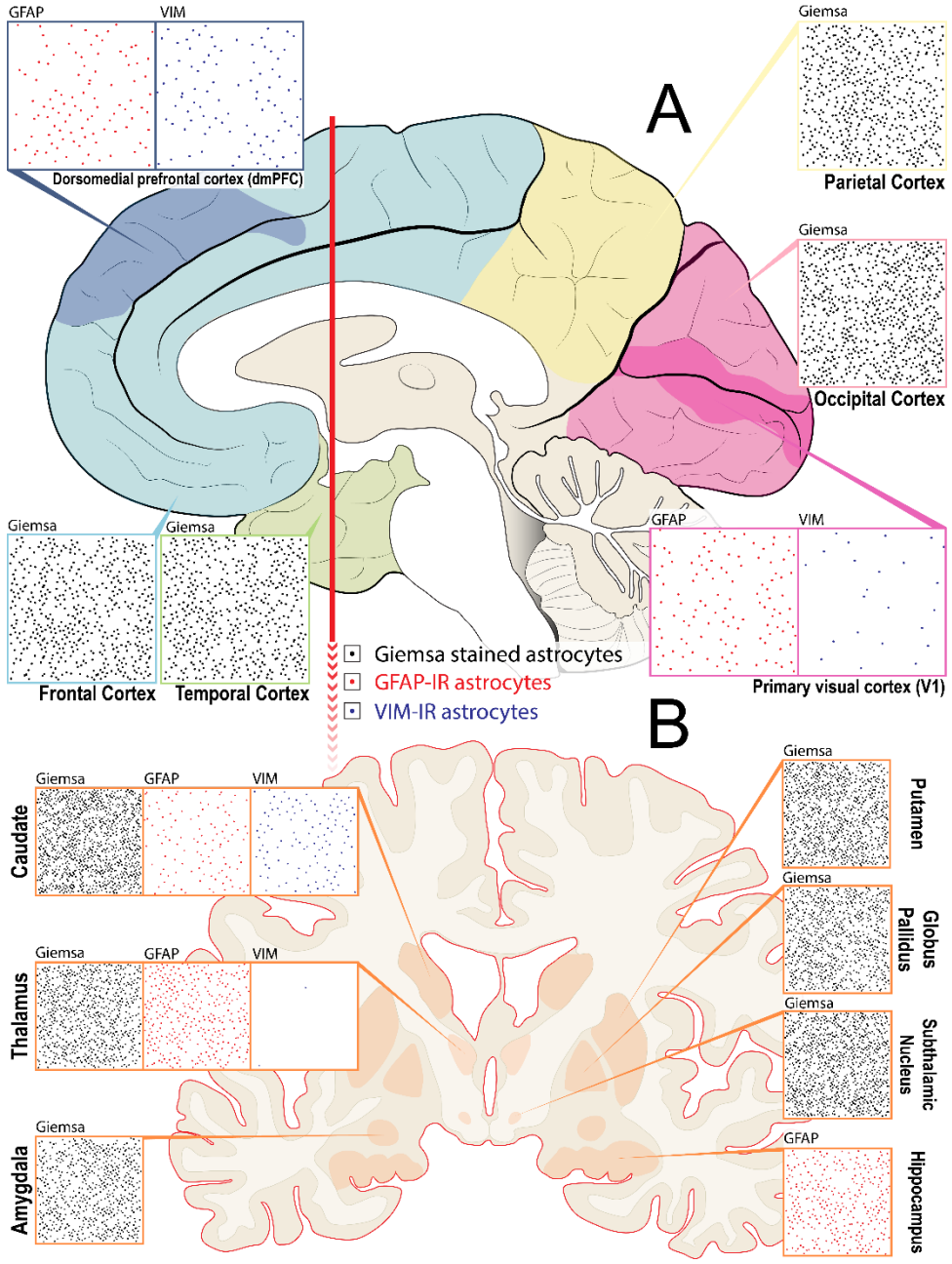

Figure 2 | Map of astrocyte densities in the human brain. Each square displays astrocyte densities converted to 1mm^2 for Giemsa staining (black), GFAP (red) and VIM (blue); somas are not to anatomical scale. (A) Astrocyte density is relatively consistent throughout cerebral lobes, and differs most between frontal and occipital lobes. Regional densities of cortical GFAP and VIM astrocytes are less than 15% of lobe densities of Giemsa-stained astrocytes. (B) Giemsa-stained subcortical astrocyte densities are larger than those in the neocortex. Variations in VIM and GFAP astrocyte densities seem proportionally greater between subcortical regions, than between cortical regions.

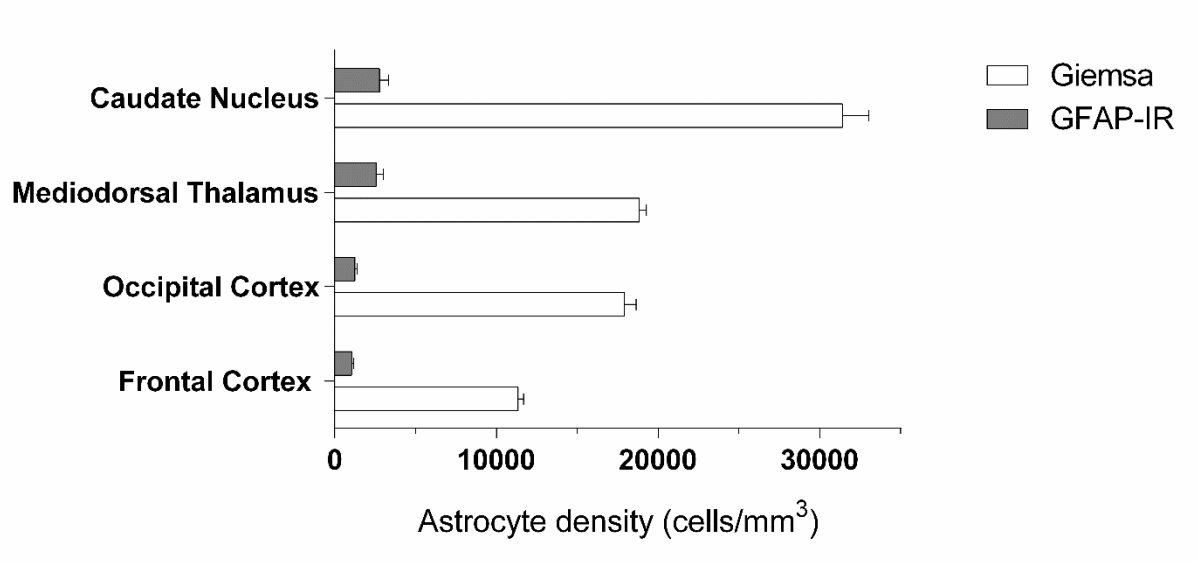

Figure 3 | Comparison of stereological densities for astrocytes labelled using GFAP DAB immunohistochemistry or Giemsa staining in postmortem brain samples from psychiatrically healthy adults. GFAP-IR astrocyte densities are more than tenfold lower than Giemsa-stained astrocyte densities in the same regions, indicating GFAP labels a minority of the total population of astrocytes in cortical and subcortical regions of the human brain. Mean and SEM values determined from previously reported results (Pakkenberg, 1990; Salvesen *et al*., 2015; Kaalund *et al*., 2020; O'Leary *et al*., 2020).

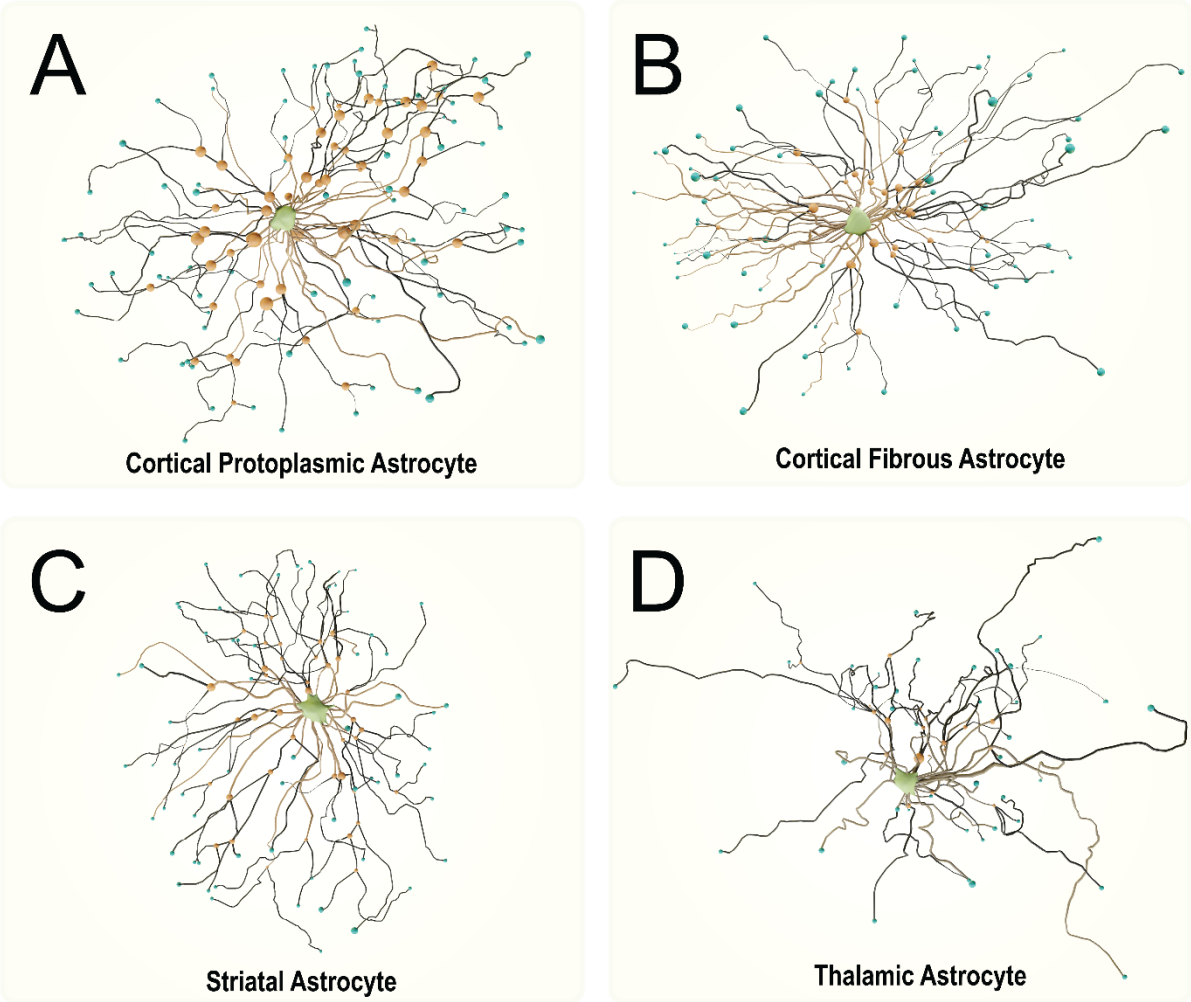

Figure 4 | Astrocyte morphometry varies regionally across human cortical and subcortical regions. Branched structure analysis features are shown; soma (green), nodes (orange), terminals (blue), primary processes (brown), non-primary processes (black). (A-B) Protoplasmic astrocytes are better distinguished from fibrous astrocytes by their greater extent and spatial distribution of branching (nodes and terminals), rather than their greater process size (length, but not number). (C-D) Striatal astrocytes and thalamic astrocytes resemble smaller morphological versions of protoplasmic and fibrous astrocytes, respectively.

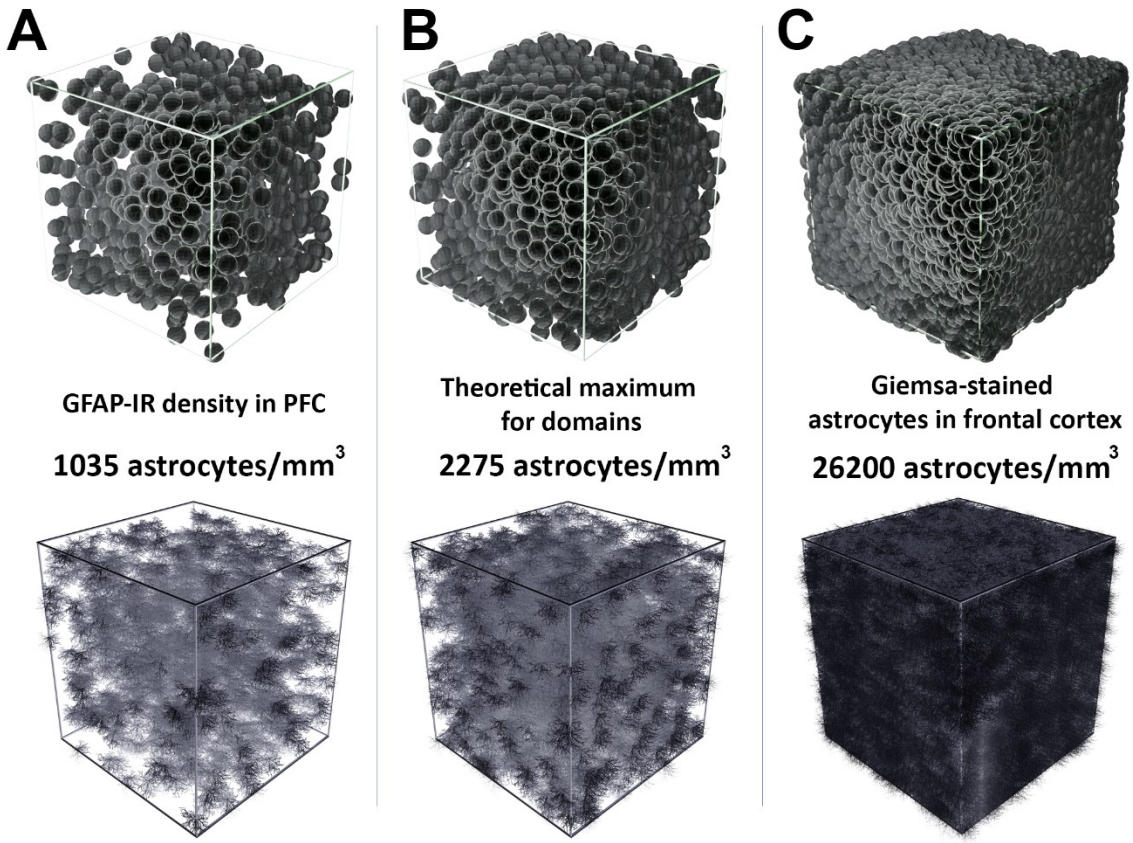

Figure 5 | Astrocyte domains are specific to GFAP-IR astrocytes. To theoretically test whether all astrocytes could exhibit a domain organization in the human cortex, we combined Giemsa-stained astrocyte densities with VIM-IR astrocyte morphometry. Using the 3D software Blender, a 1mm^3 cube was filled with a randomly distributed particle system containing either a sphere of 85µm diameter (top row), or a representative cortical astrocyte morphometric reconstruction (bottom row). While actual GFAP-IR astrocyte densities (A) are well below the maximum theoretical densities for domain organization (B), the total average density of astrocytes (C) are over 10-fold greater than the theoretical maximum allowed for a domain-like organization. This would suggest that less than 10% of astrocytes in human frontal cortex display a domain-like organization.

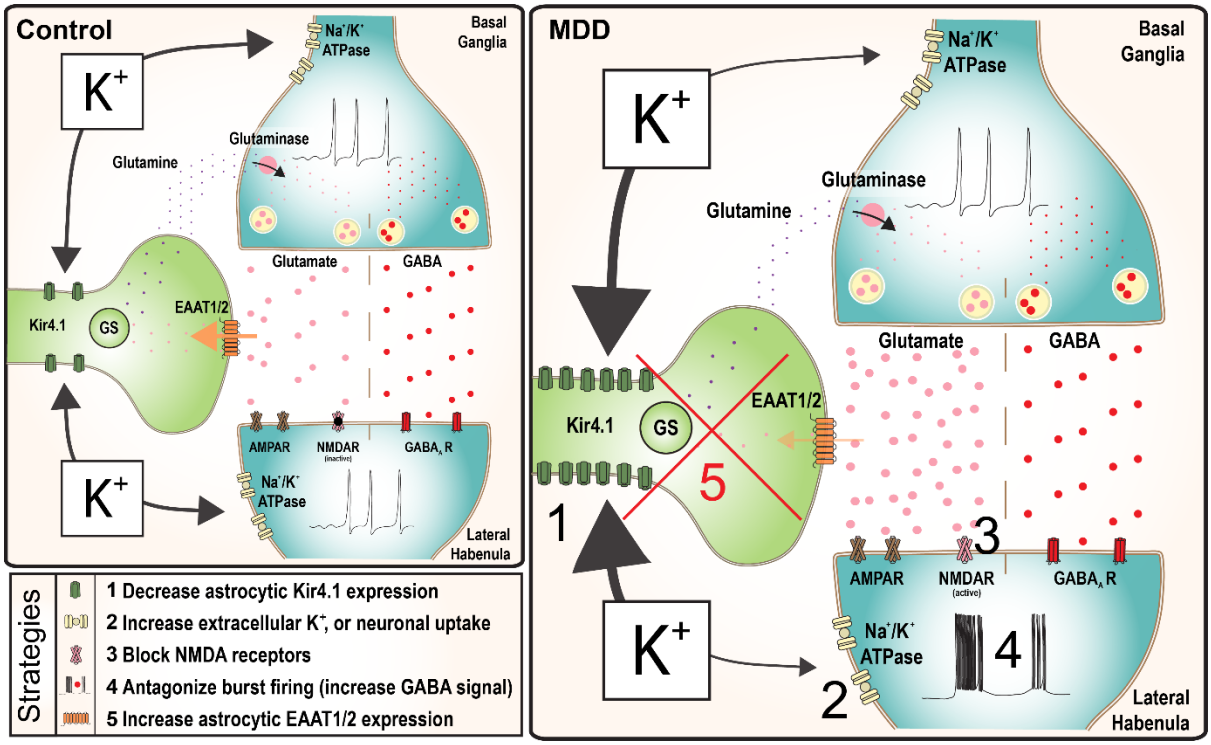

Figure 6 | A potassium imbalance theory of Major Depressive Disorder (MDD). In MDD, astrocytes pathologically overexpress $K_{ir}4.1$ (1), which depletes extracellular potassium and raises postsynaptic resting membrane potential (2), which removes the voltage block of NMDA receptors thereby activating them (3), leading to an increase in burst firing in the lateral habenula (4). Astrocyte loss in MDD may restabilize potassium balance (5), but also may impair synaptic glutamate homeostasis (reuptake and conversion). Factors counteracting these five stages could serve as new therapeutic targets for antidepressants, as highlighted under *Strategies* in the bottom left box.

CHAPTER V

Conclusions & Future Directions

1. Vimentin as a marker of astrocytes and blood vessels in the adult human brain

Chapter II attains the first aim of the PhD thesis, by providing a comprehensive and useful resource for neuroscience research by showing that vimentin reliably labels astrocytes and blood vessels (O'Leary *et al*., 2020). Reactive astrocytes are a common feature of many cerebral pathologies and yet postmortem investigations have only had GFAP as a marker to label them. By showing for the first time that vimentin labels the majority of GFAP-IR astrocytes and CD31-IR blood vessels in many postmortem adult brain regions, we show that vimentin can be reliably used to study these features in postmortem investigations.

We noted important features that make vimentin a particularly useful astrocyte marker. As vimentin is preferentially expressed by protoplasmic astrocytes than fibrous astrocytes in the cortex, it may have a particularly important function in neocortical astrocytes. This first property helped us to demonstrate, for the first time, the extent of regional heterogeneity in astrocyte densities throughout the human brain, and how this is affected by marker choice. We found astrocytes were generally more abundant in subcortical regions than in cortical regions, and that vimentin preferentially labels astrocytes with a protoplasmic or protoplasmic-like (striatal) morphology, whereas GFAP preferentially labels astrocytes with a fibrous or fibrous-like (thalamic) morphology. The relative abundance of GFAP-IR astrocytes, and the absence of vimentin-IR astrocytes, in the mediodorsal thalamus indicates there is a unique specialization of astrocytes in the human thalamus. This feature may also be evolutionary conserved given we qualitatively observed few VIM-IR in the adult mouse thalamus in our study, and previous studies which found significant heterogeneity in the density of GFAP-IR astrocytes across different thalamic nuclei (Emsley & Macklis, 2006).

A second property we noticed was that vimentin reveals a complex morphological profile suitable for fine anatomical tracing, which is not the case for any other marker of human astrocytes using DAB immunohistochemistry. This allowed us to demonstrate in the human brain, for the first time, the regional heterogeneity of astrocyte morphometry. It also allowed us to perform the first precise species comparison of astrocyte morphometry, which expanded

upon a previous observation that protoplasmic astrocytes in the frontal cortex were 2-to-3 fold larger in the human brain than in the mouse brain, by showing this was also the case in the visual cortex and striatum (Oberheim *et al*., 2009). Our precise approach additionally revealed that the two-dimensional circumference of the soma and the branching, length, surface area, termination of processes were also approximately 2-to-3 fold larger in all three studied regions, which suggests evolution has increased the scale of astrocyte morphometry between the mouse and human brain.

A third property was that vimentin labelling highlighted distinct features. Vimentin labelled a proportionally large number of twin cells, indicating it might preferentially reveal a less mature phenotype of astrocytes. We also observed long varicose bundles of VIM-IR processes with no identifiable cellular origin in the caudate nucleus, which formed networks projecting characteristically near to VIM-IR astrocytes and blood vessels. While we are unsure of the biological meaning of this second finding it may highlight a potential interplay of astrocytes with larger structural networks.

A final observation in this study was found while determining whether blood vessel density related to astrocyte density, which we sought to investigate given the capacity of vimentin to label most blood vessels in our regions of interest. We found both VIM-IR and GFAP-IR astrocyte densities inversely correlated with CD31-IR blood vessel densities. This indicates that brain regions with fewer blood vessels have more astrocytes. Our interpretation is that astrocytes could be distributed by this general principle to allow neurons far from blood vessels to receive sufficient metabolic support. This preliminary observation provides the first indication of a biological interpretation for why regionally heterogeneous densities of astrocytes exist in the human brain. Together, Chapter II demonstrates there is extensive regional heterogeneity in the density and morphometry of astrocytes in postmortem brain samples from healthy adults.

2. Widespread decrease of astrocyte density in postmortem brain regions of depressed suicides

Chapter III attains the second and third aim of this PhD thesis, by providing a stronger consensus on neuropathological changes in depressed suicides by performing multiple analyses in the same subjects in multiple regions (O'Leary *et al.,* 2020b). First, we wanted to perform

the first investigation of astrocyte densities in the thalamus or caudate nucleus of depressed suicides, as our previous study showing depressed suicides have lower GFAP mRNA and protein levels in these regions (Torres-Platas *et al*., 2016). Second, we wanted to assess whether astrocyte morphometry changes occurred in these regions given our previous report of astrocytic hypertrophy in the anterior cingulate cortex of depressed suicides, relative to controls (Torres-Platas *et al*., 2011). Third, we wanted to determine whether changes in vascular density were associated with astrocyte density changes, given the correlation observed in our study in Chapter II.

First, our major finding was that we observed that in depressed suicides, VIM-IR astrocyte densities had even more widespread and stronger decreases than GFAP-IR astrocyte densities. This indicates astrocyte density differences are widespread as they were observed in all regions. Second, we observed changes in vascular density in the prefrontal cortex white matter and mediodorsal thalamus, both of which contain astrocytes with a fibrous or fibrous-like morphology. This aligns with a previous report showing gliovascular differences in the cortical white matter but not gray matter of depressed individuals (Rajkowska *et al*., 2013). Third, we observed no changes in astrocyte morphometry between healthy controls and depressed suicides, with the exception of a significantly lower process number in the mediodorsal thalamus of depressed suicides. This indicates our previous study showing hypertrophic astrocytes in the anterior cingulate cortex may be a less widespread phenomenon than density differences, and therefore less critical to the psychopathology of depression and suicide (Torres-Platas *et al*., 2011). Together, Chapter III demonstrates that astrocyte density differences in depressed suicides are more widespread than those for blood vessels, as well as those for astrocyte morphometry. Our observations of reduced astrocyte densities in depressed suicides complements previous work showing that the ablation of astrocytes from the prefrontal cortex is sufficient to induce depressive phenotypes in rats during stress paradigms (Banasr *et al*., 2018). However, a previous study has indicated that chronic variable stress paradigms in mice decrease GFAP expression levels in the cortex, without a reduction in total astrocyte densities (transgenically labelled by Aldh1L1 expression), and an increased number of VIM-IR astrocytes (Simard *et al*., 2017). The discrepancy between cortical VIM-IR astrocyte numbers in mice undergoing chronic variable stress and depressed suicides may represent an interesting species difference in how cortical astrocytes respond to stress, and further elucidation of the mechanisms underlying changes in astrocyte densities will greatly contribute to the understanding of the cellular pathology of depression.

3. Regional heterogeneity of astrocyte density and morphology in the human brain

Chapter IV integrates the findings of Chapters II and III into the wider body of literature on astrocytes in postmortem human brain samples to inform the research field. We demonstrate the different methodologies used to visualize astrocytes and combine our morphometry data with stereological data from other groups to show that tiling is not theoretically possible for many non-GFAP-IR astrocytes in the human neocortex. We also emphasize previously unacknowledged trends that will be of use to human astrocyte researchers, such as the generally greater density of astrocytes in subcortical regions relative to cortical regions, the morphometric categorization of human cortical and subcortical astrocytes, and that GFAP and VIM DAB immunohistochemistry likely labels less than 15% of all astrocytes in a given human brain region. The review then emphasizes the wealth of data showing decreased astrocyte densities are a hallmark of depression that might help explain the biological basis for emerging biomarkers and antidepressants. These emerging biomarkers and antidepressants might be particularly effective for suicide prevention initiatives, given that S100B serum levels appears to respond to depressive episode presence and treatment, and ketamine is the only FDA-approved rapid-acting antidepressant, making it uniquely effective at treating an ongoing suicide crisis.

4. Future Directions

The results in Chapter II and III adequately address the research questions of this project.

First, in Chapter II, we quantified the regional heterogeneity of VIM-IR and GFAP-IR astrocyte densities in many brain regions. We then quantified the regional heterogeneity of VIM-IR astrocyte morphometry and found it to be greater than in homologous regions of the mouse brain. This altogether implies that astrocytes, like neurons, might have an intricate functional anatomy which prompts caution in generalizing functions and dysfunctions across regions.

Second, in Chapter III, we found VIM-IR astrocyte densities are even more affected than GFAP-IR astrocyte densities in depressed suicides, and also that CD31-IR vascular densities are less affected than astrocyte densities in depressed suicides.

Third, in Chapter III, depressed suicides had astrocyte density differences in all four regions, but morphometry differences only in one region in only one of eight measurements. This strongly supports the interpretation that astrocyte density differences are more significant and widespread than astrocyte morphometry differences in depressed suicides.

Fourth, in Chapter II and III, given the differences observed between the density of VIM-IR and GFAP-IR astrocytes in health and depression indicates that investigations using only GFAP as an astrocyte marker may not accurately reflect a representative view of astrocytes in the brain during health or illness. A general pattern emerged that GFAP preferentially labels astrocytes in regions with a fibrous or fibrous-like (thalamic) morphology, and VIM preferentially labels astrocytes in regions with a protoplasmic or protoplasmic-like (striatal) morphology. This has notable implications for investigations of astrocyte pathology in the human brain that rely on GFAP as an astrocyte marker. For instance, the present work was primarily motivated by a previous finding by the Mechawar lab that GFAP mRNA and protein levels were lower in the caudate nucleus and mediodorsal thalamus, but not in cortical regions including the prefrontal cortex, of depressed suicides relative to controls (Torres-Platas *et al*., 2016). The interpretation of this previous study was that subcortical GFAP-IR astrocytes are preferentially affected in depressed suicides, relative to cortical astrocytes. The findings in Chapter III support the first these two conclusions, as stronger decreases were seen for GFAP-IR astrocyte densities in subcortical regions of depressed suicides, however, significant differences were still observed for GFAP-IR and VIM-IR astrocytes in the prefrontal cortex grey matter. More notably, differences were seen for VIM-IR, but not GFAP-IR, astrocytes in prefrontal cortex white matter in depressed suicides. This second observation indicates that GFAP may not always reliably reflect pathological changes in astrocytes, even in postmortem samples known to have abnormal densities of multiple cell types. At a more general level, this supports the theory that astrocyte density differences are widespread throughout the brain in depressed individuals, more so than previously thought by results from studies using only GFAP as an astrocyte marker. This outcome advises future studies to use multiple immunohistochemical markers to study the anatomical properties of reactive astrocytes in postmortem human brain tissue.

In Chapter IV, we interpret these changes in VIM-IR and GFAP-IR astrocyte densities reflect a loss of astrocytes in depression and propose a ‘potassium imbalance theory’ that could explain a mechanism for this. An especially interesting avenue for future astrocyte studies in depression would be to investigate findings supporting this in humans based on previous

findings in rodent studies in humans, if only because I find they form the most coherent framework for astrocyte pathology in the mechanism of depression and ketamine as an antidepressant (Cui *et al*., 2018; Yang *et al*., 2018). This could be best performed using FISH and RNA sequencing for $K_{ir}4.1$ in astrocytes from depressed suicides, to determine whether the extent of astrocyte loss inversely correlates with the upregulation of $K_{ir}4.1$. A related avenue for future astrocyte studies in depression would be to determine the effect astrocyte loss has on the function of local neurons. Lower levels of lactate have been observed in stressed and morphine-sensitive rodents, and so if astrocyte function is effectively reduced in depression it would be interesting to observe the effect on local neuronal metabolism (Murphy-Royal *et al*., 2020; Skupio *et al*., 2020; Yin *et al*., 2020). Given the emergence of astrocyte abnormalities in cortical white matter it would be interesting to address whether this is associated with changes in myelination using SCoRE imaging in the same samples (Torres-Platas *et al*., 2011; Rajkowska *et al*., 2013; Schain *et al*., 2014).

An important question that remains to be addressed is whether the general downregulation of astrocyte markers correlates with lower astrocyte densities in the same samples. For instance, previous studies have suggested decreased gap junction coupling by astrocytes in depression, however, given the lower astrocyte densities reported in this thesis it is now unclear to what extent changes at the cellular or population level are driving differences in gap junction communication in mood-associated brain regions from depressed suicides (Ernst *et al*., 2011; Tanti *et al*., 2019). This will likely be soon revealed using a combination of single-cell sequencing approaches and immunohistochemistry in postmortem samples.

Given this thesis reports widespread changes to astrocytes throughout the brains of depressed suicides, an additional line of inquiry would be whether the cerebellum, a region with unique astrocytic subtypes, also show signs of astrocytic impairments in depressed suicides. This may require a fundamental immunohistochemistry study providing a quantitative analysis of the subtypes of cerebellar astrocytes in postmortem human brain samples, similar to that in Chapter II.

Together this thesis provides a fundamental characterization of the regional heterogeneity of astrocytes in the healthy human brain, and how this organization becomes altered in depressed suicides. By developing our understanding of the complex roles that astrocytes play in psychiatric illness, this work supports the future potential of astrocytes as novel targets of antidepressant treatments.

References

174. Alexander, W. S. (1949). Progressive fibrinoid degeneration of fibrillary astrocytes associated with mental retardation in a hydrocephalic infant1. Brain, 72(3), 373–381. https://doi.org/10.1093/brain/72.3.373

175. Allen, N. J., & Barres, B. A. (2009). Glia—More than just brain glue. Nature, 457(7230), 675–677. https://doi.org/10.1038/457675a

176. Andriezen, W. L. (1893). The neuroglia elements in the human brain. British Medical Journal, 2(1700), 227–230.

177. Attwell, D., Buchan, A. M., Charpak, S., Lauritzen, M., MacVicar, B. A., & Newman, E. A. (2010). Glial and neuronal control of brain blood flow. Nature, 468(7321), 232–243. https://doi.org/10.1038/nature09613

178. Autry, A. E., Adachi, M., Nosyreva, E., Na, E. S., Los, M. F., Cheng, P., Kavalali, E. T., & Monteggia, L. M. (2011). NMDA receptor blockade at rest triggers rapid behavioural antidepressant responses. Nature, 475(7354), 91–95. https://doi.org/10.1038/nature10130

179. Bagot, R. C., Labonté, B., Peña, C. J., & Nestler, E. J. (2014a). Epigenetic signaling in psychiatric disorders: Stress and depression. Dialogues in Clinical Neuroscience, 16(3), 281–295.

180. Bagot, R. C., Labonté, B., Peña, C. J., & Nestler, E. J. (2014b). Epigenetic signaling in psychiatric disorders: Stress and depression. Dialogues in Clinical Neuroscience, 16(3), 281–295.

181. Banasr, M., Chowdhury, G. M. I., Terwilliger, R., Newton, S. S., Duman, R. S., Behar, K. L., & Sanacora, G. (2010). Glial pathology in an animal model of depression: Reversal of stress-induced cellular, metabolic and behavioral deficits by the glutamate-modulating drug riluzole. Molecular Psychiatry, 15(5), 501–511. https://doi.org/10.1038/mp.2008.106

182. Batiuk, M. Y., Martirosyan, A., Wahis, J., de Vin, F., Marneffe, C., Kusserow, C., Koeppen, J., Viana, J. F., Oliveira, J. F., Voet, T., Ponting, C. P., Belgard, T. G., &

Holt, M. G. (2020a). Identification of region-specific astrocyte subtypes at single cell resolution. Nature Communications, 11(1), 1220. https://doi.org/10.1038/s41467-019-14198-8

183. Batiuk, M. Y., Martirosyan, A., Wahis, J., de Vin, F., Marneffe, C., Kusserow, C., Koeppen, J., Viana, J. F., Oliveira, J. F., Voet, T., Ponting, C. P., Belgard, T. G., & Holt, M. G. (2020b). Identification of region-specific astrocyte subtypes at single cell resolution. Nature Communications, 11(1), 1220. https://doi.org/10.1038/s41467-019-14198-8

184. Bayraktar, O. A., Bartels, T., Holmqvist, S., Kleshchevnikov, V., Martirosyan, A., Polioudakis, D., Ben Haim, L., Young, A. M. H., Batiuk, M. Y., Prakash, K., Brown, A., Roberts, K., Paredes, M. F., Kawaguchi, R., Stockley, J. H., Sabeur, K., Chang, S. M., Huang, E., Hutchinson, P., … Rowitch, D. H. (2020). Astrocyte layers in the mammalian cerebral cortex revealed by a single-cell in situ transcriptomic map. Nature Neuroscience, 23(4), 500–509. https://doi.org/10.1038/s41593-020-0602-1

185. Boisvert, M. M., Erikson, G. A., Shokhirev, M. N., & Allen, N. J. (2018). The aging astrocyte transcriptome from multiple regions of the mouse brain. Cell Reports, 22(1), 269–285. https://doi.org/10.1016/j.celrep.2017.12.039

186. Brancaccio, M., Edwards, M. D., Patton, A. P., Smyllie, N. J., Chesham, J. E., Maywood, E. S., & Hastings, M. H. (2019a). Cell-autonomous clock of astrocytes drives circadian behavior in mammals. Science, 363(6423), 187–192. https://doi.org/10.1126/science.aat4104

187. Brancaccio, M., Edwards, M. D., Patton, A. P., Smyllie, N. J., Chesham, J. E., Maywood, E. S., & Hastings, M. H. (2019b). Cell-autonomous clock of astrocytes drives circadian behavior in mammals. Science, 363(6423), 187–192. https://doi.org/10.1126/science.aat4104

188. Brenner, M., Johnson, A. B., Boespflug-Tanguy, O., Rodriguez, D., Goldman, J. E., & Messing, A. (2001). Mutations in GFAP , encoding glial fibrillary acidic protein, are associated with Alexander disease. Nature Genetics, 27(1), 117–120. https://doi.org/10.1038/83679

189. Bushong, E. A., Martone, M. E., Jones, Y. Z., & Ellisman, M. H. (2002). Protoplasmic astrocytes in ca1 stratum radiatum occupy separate anatomical domains. Journal of Neuroscience, 22(1), 183–192. https://doi.org/10.1523/JNEUROSCI.22-01-00183.2002

190. Cahoy, J. D., Emery, B., Kaushal, A., Foo, L. C., Zamanian, J. L., Christopherson, K. S., Xing, Y., Lubischer, J. L., Krieg, P. A., Krupenko, S. A., Thompson, W. J., & Barres, B. A. (2008). A transcriptome database for astrocytes, neurons, and oligodendrocytes: A new resource for understanding brain development and function. Journal of Neuroscience, 28(1), 264–278. https://doi.org/10.1523/JNEUROSCI.4178-07.2008

191. Cavaccini, A., Durkee, C., Kofuji, P., Tonini, R., & Araque, A. (2020). Astrocyte signaling gates long-term depression at corticostriatal synapses of the direct pathway. Journal of Neuroscience, 40(30), 5757–5768. https://doi.org/10.1523/JNEUROSCI.2369-19.2020

192. Champion, K. M., Cook, R. J., Tollaksen, S. L., & Giometti, C. S. (1994). Identification of a heritable deficiency of the folate-dependent enzyme 10-formyltetrahydrofolate dehydrogenase in mice. Proceedings of the National Academy of Sciences, 91(24), 11338–11342. https://doi.org/10.1073/pnas.91.24.11338

193. Chaudhury, D., Walsh, J. J., Friedman, A. K., Juarez, B., Ku, S. M., Koo, J. W., Ferguson, D., Tsai, H.-C., Pomeranz, L., Christoffel, D. J., Nectow, A. R., Ekstrand, M., Domingos, A., Mazei-Robison, M. S., Mouzon, E., Lobo, M. K., Neve, R. L., Friedman, J. M., Russo, S. J., … Han, M.-H. (2013). Rapid regulation of depression-related behaviours by control of midbrain dopamine neurons. Nature, 493(7433), 532–536. https://doi.org/10.1038/nature11713

194. Chen, Y.-W., & Dilsaver, S. C. (1996). Lifetime rates of suicide attempts among subjects with bipolar and unipolar disorders relative to subjects with other axis I disorders. Biological Psychiatry, 39(10), 896–899. https://doi.org/10.1016/0006-3223(95)00295-2

195. Choi, H. B., Gordon, G. R. J., Zhou, N., Tai, C., Rungta, R. L., Martinez, J., Milner, T. A., Ryu, J. K., McLarnon, J. G., Tresguerres, M., Levin, L. R., Buck, J., &

MacVicar, B. A. (2012). Metabolic communication between astrocytes and neurons via bicarbonate-responsive soluble adenylyl cyclase. Neuron, 75(6), 1094–1104. https://doi.org/10.1016/j.neuron.2012.08.032

196. Clarke, L. E., Liddelow, S. A., Chakraborty, C., Münch, A. E., Heiman, M., & Barres, B. A. (2018). Normal aging induces A1-like astrocyte reactivity. Proceedings of the National Academy of Sciences, 115(8), E1896–E1905. https://doi.org/10.1073/pnas.1800165115

197. Claus, L., Philippot, C., Griemsmann, S., Timmermann, A., Jabs, R., Henneberger, C., Kettenmann, H., & Steinhäuser, C. (2018). Barreloid borders and neuronal activity shape panglial gap junction-coupled networks in the mouse thalamus. Cerebral Cortex, 28(1), 213–222. https://doi.org/10.1093/cercor/bhw368

198. Condamine, S., Lavoie, R., Verdier, D., & Kolta, A. (2018). Functional rhythmogenic domains defined by astrocytic networks in the trigeminal main sensory nucleus. Glia, 66(2), 311–326. https://doi.org/https://doi.org/10.1002/glia.23244

199. Corkrum, M., Covelo, A., Lines, J., Bellocchio, L., Pisansky, M., Loke, K., Quintana, R., Rothwell, P. E., Lujan, R., Marsicano, G., Martin, E. D., Thomas, M. J., Kofuji, P., & Araque, A. (2020). Dopamine-evoked synaptic regulation in the nucleus accumbens requires astrocyte activity. Neuron, 105(6), 1036-1047.e5. https://doi.org/10.1016/j.neuron.2019.12.026

200. Corkrum, M., Rothwell, P. E., Thomas, M. J., Kofuji, P., & Araque, A. (2019). Opioid-mediated astrocyte–neuron signaling in the nucleus accumbens. Cells, 8(6), 586. https://doi.org/10.3390/cells8060586

201. Coull, J. A. M., Beggs, S., Boudreau, D., Boivin, D., Tsuda, M., Inoue, K., Gravel, C., Salter, M. W., & De Koninck, Y. (2005). BDNF from microglia causes the shift in neuronal anion gradient underlying neuropathic pain. Nature, 438(7070), 1017–1021. https://doi.org/10.1038/nature04223

202. Covelo, A., & Araque, A. (2018). Neuronal activity determines distinct gliotransmitter release from a single astrocyte. ELife, 7, e32237. https://doi.org/10.7554/eLife.32237

203. Cui, Y., Yang, Y., Ni, Z., Dong, Y., Cai, G., Foncelle, A., Ma, S., Sang, K., Tang, S., Li, Y., Shen, Y., Berry, H., Wu, S., & Hu, H. (2018). Astroglial Kir4.1 in the lateral habenula drives neuronal bursts in depression. Nature, 554(7692), 323–327. https://doi.org/10.1038/nature25752

204. Dahl, D. (1981). The vimentin-GFA protein transition in rat neuroglia cytoskeleton occurs at the time of myelination. Journal of Neuroscience Research, 6(6), 741–748. https://doi.org/https://doi.org/10.1002/jnr.490060608

205. Dandona, R. (2018). Gender differentials and state variations in suicide deaths in India: The Global Burden of Disease Study 1990-2016. Lancet Public Health, 3(10), e478–e489. https://doi.org/10.1016/S2468-2667(18)30138-5

206. Ding, X.-F., Liu, Y., Yan, Z.-Y., Li, X.-J., Ma, Q.-Y., Jin, Z.-Y., Liu, Y., Li, Y.-H., Liu, Y.-Y., Xue, Z., Chen, J.-X., & Lv, Z.-P. (2017, March 2). Involvement of normalized glial fibrillary acidic protein expression in the hippocampi in antidepressant-like effects of xiaoyaosan on chronically stressed mice [Research Article]. Evidence-Based Complementary and Alternative Medicine. https://doi.org/https://doi.org/10.1155/2017/1960584

207. Domingues, H. S., Portugal, C. C., Socodato, R., & Relvas, J. B. (2016). Oligodendrocyte, astrocyte, and microglia crosstalk in myelin development, damage, and repair. Frontiers in Cell and Developmental Biology, 4. https://doi.org/10.3389/fcell.2016.00071

208. dos Santos, G., Rogel, M. R., Baker, M. A., Troken, J. R., Urich, D., Morales-Nebreda, L., Sennello, J. A., Kutuzov, M. A., Sitikov, A., Davis, J. M., Lam, A. P., Cheresh, P., Kamp, D., Shumaker, D. K., Budinger, G. R. S., & Ridge, K. M. (2015). Vimentin regulates activation of the NLRP3 inflammasome. Nature Communications, 6(1), 6574. https://doi.org/10.1038/ncomms7574

209. Emsley, J. G., & Macklis, J. D. (2006). Astroglial heterogeneity closely reflects the neuronal-defined anatomy of the adult murine CNS. Neuron Glia Biology, 2(3), 175–186. https://doi.org/10.1017/S1740925X06000202

210. Ernst, C., Nagy, C., Kim, S., Yang, J. P., Deng, X., Hellstrom, I. C., Choi, K. H., Gershenfeld, H., Meaney, M. J., & Turecki, G. (2011). Dysfunction of astrocyte connexins 30 and 43 in dorsal lateral prefrontal cortex of suicide completers. Biological Psychiatry, 70(4), 312–319. https://doi.org/10.1016/j.biopsych.2011.03.038

211. Eurich, F. W. (1897). Brain: A journal of neurology. Macmillan.

212. Fabricius, K., Jacobsen, J. S., & Pakkenberg, B. (2013). Effect of age on neocortical brain cells in 90+ year old human females—A cell counting study. Neurobiology of Aging, 34(1), 91–99. https://doi.org/10.1016/j.neurobiolaging.2012.06.009

213. Farmer, W. T., Abrahamsson, T., Chierzi, S., Lui, C., Zaelzer, C., Jones, E. V., Bally, B. P., Chen, G. G., Théroux, J.-F., Peng, J., Bourque, C. W., Charron, F., Ernst, C., Sjöström, P. J., & Murai, K. K. (2016). Neurons diversify astrocytes in the adult brain through sonic hedgehog signaling. Science, 351(6275), 849–854. https://doi.org/10.1126/science.aab3103

214. Fiacco, T. A., & McCarthy, K. D. (2018). Multiple lines of evidence indicate that gliotransmission does not occur under physiological conditions. Journal of Neuroscience, 38(1), 3–13. https://doi.org/10.1523/JNEUROSCI.0016-17.2017

215. Gao, P., Postiglione, M. P., Krieger, T. G., Hernandez, L., Wang, C., Han, Z., Streicher, C., Papusheva, E., Insolera, R., Chugh, K., Kodish, O., Huang, K., Simons, B. D., Luo, L., Hippenmeyer, S., & Shi, S.-H. (2014). Deterministic progenitor behavior and unitary production of neurons in the neocortex. Cell, 159(4), 775–788. https://doi.org/10.1016/j.cell.2014.10.027

216. García-Cáceres, C., Quarta, C., Varela, L., Gao, Y., Gruber, T., Legutko, B., Jastroch, M., Johansson, P., Ninkovic, J., Yi, C.-X., Le Thuc, O., Szigeti-Buck, K., Cai, W., Meyer, C. W., Pfluger, P. T., Fernandez, A. M., Luquet, S., Woods, S. C., Torres-Alemán, I., … Tschöp, M. H. (2016). Astrocytic insulin signaling couples brain glucose uptake with nutrient availability. Cell, 166(4), 867–880. https://doi.org/10.1016/j.cell.2016.07.028

217. Gibbs, M. E., Anderson, D. G., & Hertz, L. (2006). Inhibition of glycogenolysis in astrocytes interrupts memory consolidation in young chickens. Glia, 54(3), 214–222. https://doi.org/https://doi.org/10.1002/glia.20377

218. Ginhoux, F., Greter, M., Leboeuf, M., Nandi, S., See, P., Gokhan, S., Mehler, M. F., Conway, S. J., Ng, L. G., Stanley, E. R., Samokhvalov, I. M., & Merad, M. (2010). Fate mapping analysis reveals that adult microglia derive from primitive macrophages. Science, 330(6005), 841–845. https://doi.org/10.1126/science.1194637

219. Gittins, R. A., & Harrison, P. J. (2011). A morphometric study of glia and neurons in the anterior cingulate cortex in mood disorder. Journal of Affective Disorders, 133(1), 328–332. https://doi.org/10.1016/j.jad.2011.03.042

220. Gómez-Molina, C., Sandoval, M., Henzi, R., Ramírez, J. P., Varas-Godoy, M., Luarte, A., Lafourcade, C. A., Lopez-Verrilli, A., Smalla, K.-H., Kaehne, T., & Wyneken, U. (2019). Small extracellular vesicles in rat serum contain astrocyte-derived protein biomarkers of repetitive stress. International Journal of Neuropsychopharmacology, 22(3), 232–246. https://doi.org/10.1093/ijnp/pyy098

221. Gosselin, R.-D., Gibney, S., O'Malley, D., Dinan, T. G., & Cryan, J. F. (2009). Region specific decrease in glial fibrillary acidic protein immunoreactivity in the brain of a rat model of depression. Neuroscience, 159(2), 915–925. https://doi.org/10.1016/j.neuroscience.2008.10.018

222. Grabert, K., Michoel, T., Karavolos, M. H., Clohisey, S., Baillie, J. K., Stevens, M. P., Freeman, T. C., Summers, K. M., & McColl, B. W. (2016). Microglial brain region−dependent diversity and selective regional sensitivities to aging. Nature Neuroscience, 19(3), 504–516. https://doi.org/10.1038/nn.4222

223. Guttenplan, K. A., Weigel, M. K., Adler, D. I., Couthouis, J., Liddelow, S. A., Gitler, A. D., & Barres, B. A. (2020). Knockout of reactive astrocyte activating factors slows disease progression in an ALS mouse model. Nature Communications, 11(1), 3753. https://doi.org/10.1038/s41467-020-17514-9

224. Han, X., Chen, M., Wang, F., Windrem, M., Wang, S., Shanz, S., Xu, Q., Oberheim, N. A., Bekar, L., Betstadt, S., Silva, A. J., Takano, T., Goldman, S. A., & Nedergaard,

M. (2013). Forebrain engraftment by human glial progenitor cells enhances synaptic plasticity and learning in adult mice. Cell Stem Cell, 12(3), 342–353. https://doi.org/10.1016/j.stem.2012.12.015

225. Herculano-Houzel, S. (2009). The human brain in numbers: A linearly scaled-up primate brain. Frontiers in Human Neuroscience, 3. https://doi.org/10.3389/neuro.09.031.2009

226. Herculano-Houzel, S. (2014). The glia/neuron ratio: How it varies uniformly across brain structures and species and what that means for brain physiology and evolution. Glia, 62(9), 1377–1391. https://doi.org/https://doi.org/10.1002/glia.22683

227. Herculano-Houzel, S., Collins, C. E., Wong, P., Kaas, J. H., & Lent, R. (2008). The basic nonuniformity of the cerebral cortex. Proceedings of the National Academy of Sciences, 105(34), 12593–12598. https://doi.org/10.1073/pnas.0805417105

228. Hochstim, C., Deneen, B., Lukaszewicz, A., Zhou, Q., & Anderson, D. J. (2008). The spinal cord contains positionally distinct astrocyte subtypes whose identities are specified by a homeodomain transcriptional code. Cell, 133(3), 510–522. https://doi.org/10.1016/j.cell.2008.02.046

229. Houades, V., Koulakoff, A., Ezan, P., Seif, I., & Giaume, C. (2008). Gap junction-mediated astrocytic networks in the mouse barrel cortex. Journal of Neuroscience, 28(20), 5207–5217. https://doi.org/10.1523/JNEUROSCI.5100-07.2008

230. Hultman, R., Ulrich, K., Sachs, B. D., Blount, C., Carlson, D. E., Ndubuizu, N., Bagot, R. C., Parise, E. M., Vu, M.-A. T., Gallagher, N. M., Wang, J., Silva, A. J., Deisseroth, K., Mague, S. D., Caron, M. G., Nestler, E. J., Carin, L., & Dzirasa, K. (2018). Brain-wide electrical spatiotemporal dynamics encode depression vulnerability. Cell, 173(1), 166-180.e14. https://doi.org/10.1016/j.cell.2018.02.012

231. Iliff, J. J., Lee, H., Yu, M., Feng, T., Logan, J., Nedergaard, M., & Benveniste, H. (2013). Brain-wide pathway for waste clearance captured by contrast-enhanced MRI. The Journal of Clinical Investigation, 123(3), 1299–1309. https://doi.org/10.1172/JCI67677

232. Kaalund, S. S., Johansen, A., Fabricius, K., & Pakkenberg, B. (2020). Untreated patients dying with aids have loss of neocortical neurons and glia cells. Frontiers in Neuroscience, 13. https://doi.org/10.3389/fnins.2019.01398

233. Kamphuis, W., Kooijman, L., Orre, M., Stassen, O., Pekny, M., & Hol, E. M. (2015). GFAP and vimentin deficiency alters gene expression in astrocytes and microglia in wild-type mice and changes the transcriptional response of reactive glia in mouse model for Alzheimer's disease. Glia, 63(6), 1036–1056. https://doi.org/https://doi.org/10.1002/glia.22800

234. Káradóttir, R., Cavelier, P., Bergersen, L. H., & Attwell, D. (2005). NMDA receptors are expressed in oligodendrocytes and activated in ischaemia. Nature, 438(7071), 1162–1166. https://doi.org/10.1038/nature04302

235. Káradóttir, R., Hamilton, N. B., Bakiri, Y., & Attwell, D. (2008). Spiking and nonspiking classes of oligodendrocyte precursor glia in CNS white matter. Nature Neuroscience, 11(4), 450–456. https://doi.org/10.1038/nn2060

236. Kim, R., Healey, K. L., Sepulveda-Orengo, M. T., & Reissner, K. J. (2018). Astroglial correlates of neuropsychiatric disease: From astrocytopathy to astrogliosis. Progress in Neuro-Psychopharmacology and Biological Psychiatry, 87, 126–146. https://doi.org/10.1016/j.pnpbp.2017.10.002

237. Kiyoshi, C. M., Du, Y., Zhong, S., Wang, W., Taylor, A. T., Xiong, B., Ma, B., Terman, D., & Zhou, M. (2018). Syncytial isopotentiality: A system-wide electrical feature of astrocytic networks in the brain. Glia, 66(12), 2756–2769. https://doi.org/https://doi.org/10.1002/glia.23525

238. Kol, A., Adamsky, A., Groysman, M., Kreisel, T., London, M., & Goshen, I. (2020). Astrocytes contribute to remote memory formation by modulating hippocampal–cortical communication during learning. Nature Neuroscience, 23(10), 1229–1239. https://doi.org/10.1038/s41593-020-0679-6

239. Kuchibhotla, K. V., Lattarulo, C. R., Hyman, B. T., & Bacskai, B. J. (2009). Synchronous hyperactivity and intercellular calcium waves in astrocytes in alzheimer mice. Science, 323(5918), 1211–1215. https://doi.org/10.1126/science.1169096

240. Kuffler, S. W. (1967). The Ferrier Lecture - Neuroglial cells: Physiological properties and a potassium mediated effect of neuronal activity on the glial membrane potential. Proceedings of the Royal Society of London. Series B. Biological Sciences, 168(1010), 1–21. https://doi.org/10.1098/rspb.1967.0047

241. Kuga, N., Sasaki, T., Takahara, Y., Matsuki, N., & Ikegaya, Y. (2011). Large-scale calcium waves traveling through astrocytic networks in vivo. Journal of Neuroscience, 31(7), 2607–2614. https://doi.org/10.1523/JNEUROSCI.5319-10.2011

242. Lasič, E., Bobnar, S. T., Wilhelmsson, U., Pablo, Y. de, Pekny, M., Zorec, R., & Stenovec, M. (2020). Nestin affects fusion pore dynamics in mouse astrocytes. Acta Physiologica, 228(3), e13399. https://doi.org/https://doi.org/10.1111/apha.13399

243. Leng, L., Zhuang, K., Liu, Z., Huang, C., Gao, Y., Chen, G., Lin, H., Hu, Y., Wu, D., Shi, M., Xie, W., Sun, H., Shao, Z., Li, H., Zhang, K., Mo, W., Huang, T. Y., Xue, M., Yuan, Z., … Zhang, J. (2018). Menin deficiency leads to depressive-like behaviors in mice by modulating astrocyte-mediated neuroinflammation. Neuron, 100(3), 551-563.e7. https://doi.org/10.1016/j.neuron.2018.08.031

244. Lenhossék, M. (1895). Der feinere Bau des Nervensystems im Lichte neuester Forschungen: Eine allgemeine Betrachtung der Strukturprinzipien des Nervensystems, nebst einer Darstellung des feineren Baues des Rückenmarkes. Fischer.

245. Lester, D. (1986). Genetics, twin studies, and suicide. Suicide & Life-Threatening Behavior, 16(2), 274–285. https://doi.org/10.1111/j.1943-278x.1986.tb00355.x

246. Leventopoulos, M., Rüedi-Bettschen, D., Knuesel, I., Feldon, J., Pryce, C. R., & Opacka-Juffry, J. (2007). Long-term effects of early life deprivation on brain glia in Fischer rats. Brain Research, 1142, 119–126. https://doi.org/10.1016/j.brainres.2007.01.039

247. Li, B., Piriz, J., Mirrione, M., Chung, C., Proulx, C. D., Schulz, D., Henn, F., & Malinow, R. (2011). Synaptic potentiation onto habenula neurons in the learned helplessness model of depression. Nature, 470(7335), 535–539. https://doi.org/10.1038/nature09742

248. Li, K., Zhou, T., Liao, L., Yang, Z., Wong, C., Henn, F., Malinow, R., Yates, J. R., & Hu, H. (2013). Bcamkii in lateral habenula mediates core symptoms of depression. Science, 341(6149), 1016–1020. https://doi.org/10.1126/science.1240729

249. Liddelow, S. A., Guttenplan, K. A., Clarke, L. E., Bennett, F. C., Bohlen, C. J., Schirmer, L., Bennett, M. L., Münch, A. E., Chung, W.-S., Peterson, T. C., Wilton, D. K., Frouin, A., Napier, B. A., Panicker, N., Kumar, M., Buckwalter, M. S., Rowitch, D. H., Dawson, V. L., Dawson, T. M., … Barres, B. A. (2017). Neurotoxic reactive astrocytes are induced by activated microglia. Nature, 541(7638), 481–487. https://doi.org/10.1038/nature21029

250. Lima, A., Sardinha, V. M., Oliveira, A. F., Reis, M., Mota, C., Silva, M. A., Marques, F., Cerqueira, J. J., Pinto, L., Sousa, N., & Oliveira, J. F. (2014). Astrocyte pathology in the prefrontal cortex impairs the cognitive function of rats. Molecular Psychiatry, 19(7), 834–841. https://doi.org/10.1038/mp.2013.182

251. Liu, F., Wu, J., Gong, Y., Wang, P., Zhu, L., Tong, L., Chen, X., Ling, Y., & Huang, C. (2017). Harmine produces antidepressant-like effects via restoration of astrocytic functions. Progress in Neuro-Psychopharmacology and Biological Psychiatry, 79, 258–267. https://doi.org/10.1016/j.pnpbp.2017.06.012

252. Liu, Qingqing, He, H., Yang, J., Feng, X., Zhao, F., & Lyu, J. (2020). Changes in the global burden of depression from 1990 to 2017: Findings from the Global Burden of Disease study. Journal of Psychiatric Research, 126, 134–140. https://doi.org/10.1016/j.jpsychires.2019.08.002

253. Liu, Qiong, Li, B., Zhu, H.-Y., Wang, Y.-Q., Yu, J., & Wu, G.-C. (2011). Glia atrophy in the hippocampus of chronic unpredictable stress-induced depression model rats is reversed by electroacupuncture treatment. Journal of Affective Disorders, 128(3), 309–313. https://doi.org/10.1016/j.jad.2010.07.007

254. Lorsch, Z. S., Hamilton, P. J., Ramakrishnan, A., Parise, E. M., Salery, M., Wright, W. J., Lepack, A. E., Mews, P., Issler, O., McKenzie, A., Zhou, X., Parise, L. F., Pirpinias, S. T., Ortiz Torres, I., Kronman, H. G., Montgomery, S. E., Loh, Y.-H. E., Labonté, B., Conkey, A., … Nestler, E. J. (2019). Stress resilience is promoted by a

Zfp189 -driven transcriptional network in prefrontal cortex. Nature Neuroscience, 22(9), 1413–1423. https://doi.org/10.1038/s41593-019-0462-8

255. Luse, S. A. (1956). Electron microscopic observations of the central nervous system. The Journal of Biophysical and Biochemical Cytology, 2(5), 531–542. https://doi.org/10.1083/jcb.2.5.531

256. Ma, B., Buckalew, R., Du, Y., Kiyoshi, C. M., Alford, C. C., Wang, W., McTigue, D. M., Enyeart, J. J., Terman, D., & Zhou, M. (2016). Gap junction coupling confers isopotentiality on astrocyte syncytium. Glia, 64(2), 214–226. https://doi.org/https://doi.org/10.1002/glia.22924

257. Mächler, P., Wyss, M. T., Elsayed, M., Stobart, J., Gutierrez, R., von Faber-Castell, A., Kaelin, V., Zuend, M., San Martín, A., Romero-Gómez, I., Baeza-Lehnert, F., Lengacher, S., Schneider, B. L., Aebischer, P., Magistretti, P. J., Barros, L. F., & Weber, B. (2016). In vivo evidence for a lactate gradient from astrocytes to neurons. Cell Metabolism, 23(1), 94–102. https://doi.org/10.1016/j.cmet.2015.10.010

258. Magavi, S., Friedmann, D., Banks, G., Stolfi, A., & Lois, C. (2012). Coincident generation of pyramidal neurons and protoplasmic astrocytes in neocortical columns. Journal of Neuroscience, 32(14), 4762–4772. https://doi.org/10.1523/JNEUROSCI.3560-11.2012

259. Marques, S., Zeisel, A., Codeluppi, S., Bruggen, D. van, Falcão, A. M., Xiao, L., Li, H., Häring, M., Hochgerner, H., Romanov, R. A., Gyllborg, D., Muñoz-Manchado, A. B., Manno, G. L., Lönnerberg, P., Floriddia, E. M., Rezayee, F., Ernfors, P., Arenas, E., Hjerling-Leffler, J., … Castelo-Branco, G. (2016). Oligodendrocyte heterogeneity in the mouse juvenile and adult central nervous system. Science, 352(6291), 1326–1329. https://doi.org/10.1126/science.aaf6463

260. Martín, R., Bajo-Grañeras, R., Moratalla, R., Perea, G., & Araque, A. (2015a). Circuit-specific signaling in astrocyte-neuron networks in basal ganglia pathways. Science, 349(6249), 730–734. https://doi.org/10.1126/science.aaa7945

261. Martín, R., Bajo-Grañeras, R., Moratalla, R., Perea, G., & Araque, A. (2015b). Circuit-specific signaling in astrocyte-neuron networks in basal ganglia pathways. Science, 349(6249), 730–734. https://doi.org/10.1126/science.aaa7945

262. Martin-Fernandez, M., Jamison, S., Robin, L. M., Zhao, Z., Martin, E. D., Aguilar, J., Benneyworth, M. A., Marsicano, G., & Araque, A. (2017). Synapse-specific astrocyte gating of amygdala-related behavior. Nature Neuroscience, 20(11), 1540–1548. https://doi.org/10.1038/nn.4649

263. Masuda, T., Sankowski, R., Staszewski, O., Böttcher, C., Amann, L., Sagar, Scheiwe, C., Nessler, S., Kunz, P., van Loo, G., Coenen, V. A., Reinacher, P. C., Michel, A., Sure, U., Gold, R., Grün, D., Priller, J., Stadelmann, C., & Prinz, M. (2019). Spatial and temporal heterogeneity of mouse and human microglia at single-cell resolution. Nature, 566(7744), 388–392. https://doi.org/10.1038/s41586-019-0924-x

264. Mathiisen, T. M., Lehre, K. P., Danbolt, N. C., & Ottersen, O. P. (2010). The perivascular astroglial sheath provides a complete covering of the brain microvessels: An electron microscopic 3D reconstruction. Glia, 58(9), 1094–1103. https://doi.org/https://doi.org/10.1002/glia.20990

265. Maxwell, D. S., & Kruger, L. (1965). The fine structure of astrocytes in the cerebral cortex and their response to focal injury produced by heavy ionizing particles. Journal of Cell Biology, 25(2), 141–157. https://doi.org/10.1083/jcb.25.2.141

266. Mazaré, N., Oudart, M., Moulard, J., Cheung, G., Tortuyaux, R., Mailly, P., Mazaud, D., Bemelmans, A.-P., Boulay, A.-C., Blugeon, C., Jourdren, L., Le Crom, S., Rouach, N., & Cohen-Salmon, M. (2020). Local translation in perisynaptic astrocytic processes is specific and changes after fear conditioning. Cell Reports, 32(8). https://doi.org/10.1016/j.celrep.2020.108076

267. McGuffin, P., Katz, R., Watkins, S., & Rutherford, J. (1996). A hospital-based twin register of the heritability of dsm-iv unipolar depression. Archives of General Psychiatry, 53(2), 129–136. https://doi.org/10.1001/archpsyc.1996.01830020047006

268. McKeon, R. J., Schreiber, R. C., Rudge, J. S., & Silver, J. (1991). Reduction of neurite outgrowth in a model of glial scarring following CNS injury is correlated with the

expression of inhibitory molecules on reactive astrocytes. Journal of Neuroscience, 11(11), 3398–3411. https://doi.org/10.1523/JNEUROSCI.11-11-03398.1991

269. Ménard, C., Hodes, G. E., & Russo, S. J. (2016). Pathogenesis of depression: Insights from human and rodent studies. Neuroscience, 321, 138–162. https://doi.org/10.1016/j.neuroscience.2015.05.053

270. Menet, V., Prieto, M., Privat, A., & Ribotta, M. G. y. (2003). Axonal plasticity and functional recovery after spinal cord injury in mice deficient in both glial fibrillary acidic protein and vimentin genes. Proceedings of the National Academy of Sciences, 100(15), 8999–9004. https://doi.org/10.1073/pnas.1533187100

271. Molofsky, A. V., Kelley, K. W., Tsai, H.-H., Redmond, S. A., Chang, S. M., Madireddy, L., Chan, J. R., Baranzini, S. E., Ullian, E. M., & Rowitch, D. H. (2014). Astrocyte-encoded positional cues maintain sensorimotor circuit integrity. Nature, 509(7499), 189–194. https://doi.org/10.1038/nature13161

272. Morel, L., Chiang, M. S. R., Higashimori, H., Shoneye, T., Iyer, L. K., Yelick, J., Tai, A., & Yang, Y. (2017). Molecular and functional properties of regional astrocytes in the adult brain. Journal of Neuroscience, 37(36), 8706–8717. https://doi.org/10.1523/JNEUROSCI.3956-16.2017

273. Morquette, P., Verdier, D., Kadala, A., Féthière, J., Philippe, A. G., Robitaille, R., & Kolta, A. (2015). An astrocyte-dependent mechanism for neuronal rhythmogenesis. Nature Neuroscience, 18(6), 844–854. https://doi.org/10.1038/nn.4013

274. Muroyama, Y., Fujiwara, Y., Orkin, S. H., & Rowitch, D. H. (2005). Specification of astrocytes by bHLH protein SCL in a restricted region of the neural tube. Nature, 438(7066), 360–363. https://doi.org/10.1038/nature04139

275. Murphy-Royal, C., Johnston, A. D., Boyce, A. K. J., Diaz-Castro, B., Institoris, A., Peringod, G., Zhang, O., Stout, R. F., Spray, D. C., Thompson, R. J., Khakh, B. S., Bains, J. S., & Gordon, G. R. (2020). Stress gates an astrocytic energy reservoir to impair synaptic plasticity. Nature Communications, 11(1), 2014. https://doi.org/10.1038/s41467-020-15778-9

276. Nagai, J., Rajbhandari, A. K., Gangwani, M. R., Hachisuka, A., Coppola, G., Masmanidis, S. C., Fanselow, M. S., & Khakh, B. S. (2019). Hyperactivity with disrupted attention by activation of an astrocyte synaptogenic cue. Cell, 177(5), 1280-1292.e20. https://doi.org/10.1016/j.cell.2019.03.019

277. Naghavi, M. (2019). Global, regional, and national burden of suicide mortality 1990 to 2016: Systematic analysis for the Global Burden of Disease Study 2016. BMJ, 364, l94. https://doi.org/10.1136/bmj.l94

278. Nagy, C., Maitra, M., Tanti, A., Suderman, M., Théroux, J.-F., Davoli, M. A., Perlman, K., Yerko, V., Wang, Y. C., Tripathy, S. J., Pavlidis, P., Mechawar, N., Ragoussis, J., & Turecki, G. (2020). Single-nucleus transcriptomics of the prefrontal cortex in major depressive disorder implicates oligodendrocyte precursor cells and excitatory neurons. Nature Neuroscience, 23(6), 771–781. https://doi.org/10.1038/s41593-020-0621-y

279. Nasca, C., Bigio, B., Zelli, D., de Angelis, P., Lau, T., Okamoto, M., Soya, H., Ni, J., Brichta, L., Greengard, P., Neve, R. L., Lee, F. S., & McEwen, B. S. (2017). Role of the astroglial glutamate exchanger xct in ventral hippocampus in resilience to stress. Neuron, 96(2), 402-413.e5. https://doi.org/10.1016/j.neuron.2017.09.020

280. Nestler, E. J., & Hyman, S. E. (2010). Animal models of neuropsychiatric disorders. Nature Neuroscience, 13(10), 1161–1169. https://doi.org/10.1038/nn.2647

281. Newman, L. A., Korol, D. L., & Gold, P. E. (2011). Lactate produced by glycogenolysis in astrocytes regulates memory processing. PLOS ONE, 6(12), e28427. https://doi.org/10.1371/journal.pone.0028427

282. Noctor, S. C., Flint, A. C., Weissman, T. A., Dammerman, R. S., & Kriegstein, A. R. (2001). Neurons derived from radial glial cells establish radial units in neocortex. Nature, 409(6821), 714–720. https://doi.org/10.1038/35055553

283. Noctor, S. C., Martínez-Cerdeño, V., Ivic, L., & Kriegstein, A. R. (2004). Cortical neurons arise in symmetric and asymmetric division zones and migrate through specific phases. Nature Neuroscience, 7(2), 136–144. https://doi.org/10.1038/nn1172

284. Oberheim, N. A., Takano, T., Han, X., He, W., Lin, J. H. C., Wang, F., Xu, Q., Wyatt, J. D., Pilcher, W., Ojemann, J. G., Ransom, B. R., Goldman, S. A., & Nedergaard, M. (2009). Uniquely hominid features of adult human astrocytes. Journal of Neuroscience, 29(10), 3276–3287. https://doi.org/10.1523/JNEUROSCI.4707-08.2009

285. Oberheim, N. A., Wang, X., Goldman, S., & Nedergaard, M. (2006). Astrocytic complexity distinguishes the human brain. Trends in Neurosciences, 29(10), 547–553. https://doi.org/10.1016/j.tins.2006.08.004

286. O'Leary, L. A., Belliveau, C., Davoli, M. A., Ma, J. C., Tanti, A., Turecki, G., & Mechawar, N. (2020). Widespread decrease of cerebral vimentin-immunoreactive astrocytes in depressed suicides. BioRxiv, 2020.12.12.422510. https://doi.org/10.1101/2020.12.12.422510

287. O'Leary, L. A., Davoli, M. A., Belliveau, C., Tanti, A., Ma, J. C., Farmer, W. T., Turecki, G., Murai, K. K., & Mechawar, N. (2020). Characterization of vimentin-immunoreactive astrocytes in the human brain. Frontiers in Neuroanatomy, 14. https://doi.org/10.3389/fnana.2020.00031

288. Østergaard, S. D. (2018). Increasing male preponderance in suicide coinciding with a reduction by half in total suicides in the danish population should raise awareness of male depression. The American Journal of Psychiatry, 175(4), 381–382. https://doi.org/10.1176/appi.ajp.2018.17121357

289. Parmigiani, E., Leto, K., Rolando, C., Figueres-Oñate, M., López-Mascaraque, L., Buffo, A., & Rossi, F. (2015). Heterogeneity and bipotency of astroglial-like cerebellar progenitors along the interneuron and glial lineages. Journal of Neuroscience, 35(19), 7388–7402. https://doi.org/10.1523/JNEUROSCI.5255-14.2015

290. Parpura, V., Basarsky, T. A., Liu, F., Jeftinija, K., Jeftinija, S., & Haydon, P. G. (1994). Glutamate-mediated astrocyte–neuron signalling. Nature, 369(6483), 744–747. https://doi.org/10.1038/369744a0

291. Pekny, M., Levéen, P., Pekna, M., Eliasson, C., Berthold, C. h., Westermark, B., & Betsholtz, C. (1995). Mice lacking glial fibrillary acidic protein display astrocytes devoid of intermediate filaments but develop and reproduce normally. The EMBO Journal, 14(8), 1590–1598. https://doi.org/10.1002/j.1460-2075.1995.tb07147.x

292. Pekny, Milos, Johansson, C. B., Eliasson, C., Stakeberg, J., Wallén, Åsa, Perlmann, T., Lendahl, U., Betsholtz, C., Berthold, C.-H., & Frisén, J. (1999). Abnormal reaction to central nervous system injury in mice lacking glial fibrillary acidic protein and vimentin. Journal of Cell Biology, 145(3), 503–514. https://doi.org/10.1083/jcb.145.3.503

293. Pekny, Milos, Pekna, M., Messing, A., Steinhäuser, C., Lee, J.-M., Parpura, V., Hol, E. M., Sofroniew, M. V., & Verkhratsky, A. (2016). Astrocytes: A central element in neurological diseases. Acta Neuropathologica, 131(3), 323–345. https://doi.org/10.1007/s00401-015-1513-1

294. Pellerin, L., & Magistretti, P. J. (1994). Glutamate uptake into astrocytes stimulates aerobic glycolysis: A mechanism coupling neuronal activity to glucose utilization. Proceedings of the National Academy of Sciences, 91(22), 10625–10629. https://doi.org/10.1073/pnas.91.22.10625

295. Pelvig, D. P., Pakkenberg, H., Stark, A. K., & Pakkenberg, B. (2008a). Neocortical glial cell numbers in human brains. Neurobiology of Aging, 29(11), 1754–1762. https://doi.org/10.1016/j.neurobiolaging.2007.04.013

296. Pelvig, D. P., Pakkenberg, H., Stark, A. K., & Pakkenberg, B. (2008b). Neocortical glial cell numbers in human brains. Neurobiology of Aging, 29(11), 1754–1762. https://doi.org/10.1016/j.neurobiolaging.2007.04.013

297. Perea, G., Yang, A., Boyden, E. S., & Sur, M. (2014). Optogenetic astrocyte activation modulates response selectivity of visual cortex neurons in vivo. Nature Communications, 5(1), 3262. https://doi.org/10.1038/ncomms4262

298. Potokar, M., Stenovec, M., Gabrijel, M., Li, L., Kreft, M., Grilc, S., Pekny, M., & Zorec, R. (2010). Intermediate filaments attenuate stimulation-dependent mobility of

endosomes/lysosomes in astrocytes. Glia, 58(10), 1208–1219. https://doi.org/https://doi.org/10.1002/glia.21000

299. Powers, B., Kleinman, J. E., Hyde, T. M., Ajilore, O., Leow, A., & Sodhi, M. S. (2019). Differential expression of glutamate transporters and monoaminergic genes in major depression and suicide. BioRxiv, 596403. https://doi.org/10.1101/596403

300. Pringle, N. P., Yu, W.-P., Howell, M., Colvin, J. S., Ornitz, D. M., & Richardson, W. D. (2003). Fgfr3 expression by astrocytes and their precursors: Evidence that astrocytes and oligodendrocytes originate in distinct neuroepithelial domains. Development, 130(1), 93–102. https://doi.org/10.1242/dev.00184

301. Rajkowska, G., & A. Stockmeier, C. (2013). Astrocyte pathology in major depressive disorder: Insights from human postmortem brain tissue. Current Drug Targets, 14(11), 1225–1236.

302. Rajkowska, G., Hughes, J., Stockmeier, C. A., Javier Miguel-Hidalgo, J., & Maciag, D. (2013). Coverage of blood vessels by astrocytic endfeet is reduced in major depressive disorder. Biological Psychiatry, 73(7), 613–621. https://doi.org/10.1016/j.biopsych.2012.09.024

303. Rajkowska, G., Legutko, B., Moulana, M., Syed, M., Romero, D. G., Stockmeier, C. A., & Miguel-Hidalgo, J. J. (2018). Astrocyte pathology in the ventral prefrontal white matter in depression. Journal of Psychiatric Research, 102, 150–158. https://doi.org/10.1016/j.jpsychires.2018.04.005

304. Ramirez, F., Moscarello, J. M., LeDoux, J. E., & Sears, R. M. (2015). Active avoidance requires a serial basal amygdala to nucleus accumbens shell circuit. Journal of Neuroscience, 35(8), 3470–3477. https://doi.org/10.1523/JNEUROSCI.1331-14.2015

305. Roux, L., Benchenane, K., Rothstein, J. D., Bonvento, G., & Giaume, C. (2011). Plasticity of astroglial networks in olfactory glomeruli. Proceedings of the National Academy of Sciences, 108(45), 18442–18446. https://doi.org/10.1073/pnas.1107386108

306. Sántha, P., Veszelka, S., Hoyk, Z., Mészáros, M., Walter, F. R., Tóth, A. E., Kiss, L., Kincses, A., Oláh, Z., Seprényi, G., Rákhely, G., Dér, A., Pákáski, M., Kálmán, J., Kittel, Á., & Deli, M. A. (2016). Restraint stress-induced morphological changes at the blood-brain barrier in adult rats. Frontiers in Molecular Neuroscience, 8. https://doi.org/10.3389/fnmol.2015.00088

307. Sasaki, T., Kuga, N., Namiki, S., Matsuki, N., & Ikegaya, Y. (2011). Locally synchronized astrocytes. Cerebral Cortex, 21(8), 1889–1900. https://doi.org/10.1093/cercor/bhq256

308. Savtchouk, I., & Volterra, A. (2018). Gliotransmission: Beyond black-and-white. Journal of Neuroscience, 38(1), 14–25. https://doi.org/10.1523/JNEUROSCI.0017-17.2017

309. Skupio, U., Tertil, M., Bilecki, W., Barut, J., Korostynski, M., Golda, S., Kudla, L., Wiktorowska, L., Sowa, J. E., Siwiec, M., Bobula, B., Pels, K., Tokarski, K., Hess, G., Ruszczycki, B., Wilczynski, G., & Przewlocki, R. (2020). Astrocytes determine conditioned response to morphine via glucocorticoid receptor-dependent regulation of lactate release. Neuropsychopharmacology, 45(2), 404–415. https://doi.org/10.1038/s41386-019-0450-4

310. Snyder, J. S., Soumier, A., Brewer, M., Pickel, J., & Cameron, H. A. (2011). Adult hippocampal neurogenesis buffers stress responses and depressive behaviour. Nature, 476(7361), 458–461. https://doi.org/10.1038/nature10287

311. Sofroniew, M. V., & Vinters, H. V. (2010). Astrocytes: Biology and pathology. Acta Neuropathologica, 119(1), 7–35. https://doi.org/10.1007/s00401-009-0619-8

312. Sosunov, A. A., Wu, X., Tsankova, N. M., Guilfoyle, E., McKhann, G. M., & Goldman, J. E. (2014). Phenotypic heterogeneity and plasticity of isocortical and hippocampal astrocytes in the human brain. Journal of Neuroscience, 34(6), 2285–2298. https://doi.org/10.1523/JNEUROSCI.4037-13.2014

313. Stamatakis, A. M., & Stuber, G. D. (2012). Activation of lateral habenula inputs to the ventral midbrain promotes behavioral avoidance. Nature Neuroscience, 15(8), 1105–1107. https://doi.org/10.1038/nn.3145

314. Sultan, S., Li, L., Moss, J., Petrelli, F., Cassé, F., Gebara, E., Lopatar, J., Pfrieger, F. W., Bezzi, P., Bischofberger, J., & Toni, N. (2015). Synaptic integration of adult-born hippocampal neurons is locally controlled by astrocytes. Neuron, 88(5), 957–972. https://doi.org/10.1016/j.neuron.2015.10.037

315. Suzuki, A., Stern, S. A., Bozdagi, O., Huntley, G. W., Walker, R. H., Magistretti, P. J., & Alberini, C. M. (2011a). Astrocyte-neuron lactate transport is required for long-term memory formation. Cell, 144(5), 810–823. https://doi.org/10.1016/j.cell.2011.02.018

316. Suzuki, A., Stern, S. A., Bozdagi, O., Huntley, G. W., Walker, R. H., Magistretti, P. J., & Alberini, C. M. (2011b). Astrocyte-neuron lactate transport is required for long-term memory formation. Cell, 144(5), 810–823. https://doi.org/10.1016/j.cell.2011.02.018

317. Takano, T., Tian, G.-F., Peng, W., Lou, N., Libionka, W., Han, X., & Nedergaard, M. (2006). Astrocyte-mediated control of cerebral blood flow. Nature Neuroscience, 9(2), 260–267. https://doi.org/10.1038/nn1623

318. Tan, Z., Liu, Y., Xi, W., Lou, H., Zhu, L., Guo, Z., Mei, L., & Duan, S. (2017). Glia-derived ATP inversely regulates excitability of pyramidal and CCK-positive neurons. Nature Communications, 8(1), 13772. https://doi.org/10.1038/ncomms13772

319. Tanti, A., Lutz, P.-E., Kim, J., O'Leary, L., Théroux, J.-F., Turecki, G., & Mechawar, N. (2019). Evidence of decreased gap junction coupling between astrocytes and oligodendrocytes in the anterior cingulate cortex of depressed suicides. Neuropsychopharmacology, 44(12), 2099–2111. https://doi.org/10.1038/s41386-019-0471-z

320. Tolentino, J. C., & Schmidt, S. L. (2018). Dsm-5 criteria and depression severity: Implications for clinical practice. Frontiers in Psychiatry, 9. https://doi.org/10.3389/fpsyt.2018.00450

321. Torres-Platas, S. G., Nagy, C., Wakid, M., Turecki, G., & Mechawar, N. (2016a). Glial fibrillary acidic protein is differentially expressed across cortical and subcortical regions in healthy brains and downregulated in the thalamus and caudate nucleus of

depressed suicides. Molecular Psychiatry, 21(4), 509–515. https://doi.org/10.1038/mp.2015.65

322. Torres-Platas, S. G., Nagy, C., Wakid, M., Turecki, G., & Mechawar, N. (2016b). Glial fibrillary acidic protein is differentially expressed across cortical and subcortical regions in healthy brains and downregulated in the thalamus and caudate nucleus of depressed suicides. Molecular Psychiatry, 21(4), 509–515. https://doi.org/10.1038/mp.2015.65

323. Torres-Platas, Susana G., Hercher, C., Davoli, M. A., Maussion, G., Labonté, B., Turecki, G., & Mechawar, N. (2011a). Astrocytic hypertrophy in anterior cingulate white matter of depressed suicides. Neuropsychopharmacology, 36(13), 2650–2658. https://doi.org/10.1038/npp.2011.154

324. Torres-Platas, Susana G., Hercher, C., Davoli, M. A., Maussion, G., Labonté, B., Turecki, G., & Mechawar, N. (2011b). Astrocytic hypertrophy in anterior cingulate white matter of depressed suicides. Neuropsychopharmacology, 36(13), 2650–2658. https://doi.org/10.1038/npp.2011.154

325. Tsai, H.-H., Li, H., Fuentealba, L. C., Molofsky, A. V., Taveira-Marques, R., Zhuang, H., Tenney, A., Murnen, A. T., Fancy, S. P. J., Merkle, F., Kessaris, N., Alvarez-Buylla, A., Richardson, W. D., & Rowitch, D. H. (2012). Regional astrocyte allocation regulates cns synaptogenesis and repair. Science, 337(6092), 358–362. https://doi.org/10.1126/science.1222381

326. Tye, K. M., Mirzabekov, J. J., Warden, M. R., Ferenczi, E. A., Tsai, H.-C., Finkelstein, J., Kim, S.-Y., Adhikari, A., Thompson, K. R., Andalman, A. S., Gunaydin, L. A., Witten, I. B., & Deisseroth, K. (2013). Dopamine neurons modulate neural encoding and expression of depression-related behaviour. Nature, 493(7433), 537–541. https://doi.org/10.1038/nature11740

327. Tynan, R. J., Beynon, S. B., Hinwood, M., Johnson, S. J., Nilsson, M., Woods, J. J., & Walker, F. R. (2013). Chronic stress-induced disruption of the astrocyte network is driven by structural atrophy and not loss of astrocytes. Acta Neuropathologica, 126(1), 75–91. https://doi.org/10.1007/s00401-013-1102-0

328. van Hall, G., Stømstad, M., Rasmussen, P., Jans, Ø., Zaar, M., Gam, C., Quistorff, B., Secher, N. H., & Nielsen, H. B. (2009). Blood lactate is an important energy source for the human brain. Journal of Cerebral Blood Flow & Metabolism, 29(6), 1121–1129. https://doi.org/10.1038/jcbfm.2009.35

329. Vardjan, N., Gabrijel, M., Potokar, M., Švajger, U., Kreft, M., Jeras, M., de Pablo, Y., Faiz, M., Pekny, M., & Zorec, R. (2012). IFN-γ-induced increase in the mobility of MHC class II compartments in astrocytes depends on intermediate filaments. Journal of Neuroinflammation, 9(1), 144. https://doi.org/10.1186/1742-2094-9-144

330. Vaughn, J. E., & Grieshaber, J. A. (1972). An electron microscopic investigation of glycogen and mitochondria in developing and adult rat spinal motor neuropil. Journal of Neurocytology, 1(4), 397–412. https://doi.org/10.1007/BF01102942

331. Wang, X., Lou, N., Xu, Q., Tian, G.-F., Peng, W. G., Han, X., Kang, J., Takano, T., & Nedergaard, M. (2006). Astrocytic Ca 2+ signaling evoked by sensory stimulation in vivo. Nature Neuroscience, 9(6), 816–823. https://doi.org/10.1038/nn1703

332. World Health Organization (WHO) (2014) Preventing suicide: A global imperative. Retrieved December 24, 2020, from http://www.who.int/mental_health/suicide-prevention/world_report_2014/en/

333. Wilhelmsson, U., Li, L., Pekna, M., Berthold, C.-H., Blom, S., Eliasson, C., Renner, O., Bushong, E., Ellisman, M., Morgan, T. E., & Pekny, M. (2004). Absence of glial fibrillary acidic protein and vimentin prevents hypertrophy of astrocytic processes and improves post-traumatic regeneration. Journal of Neuroscience, 24(21), 5016–5021. https://doi.org/10.1523/JNEUROSCI.0820-04.2004

334. Wilhelmsson, U., Stillemark-Billton, P., Borén, J., & Pekny, M. (2019). Vimentin is required for normal accumulation of body fat. Biological Chemistry, 400(9), 1157–1162. https://doi.org/10.1515/hsz-2019-0170

335. Wilkinson, S. T., Ballard, E. D., Bloch, M. H., Mathew, S. J., Murrough, J. W., Feder, A., Sos, P., Wang, G., Zarate, C. A., & Sanacora, G. (2017). The effect of a single dose of intravenous ketamine on suicidal ideation: A systematic review and individual

participant data meta-analysis. American Journal of Psychiatry, 175(2), 150–158. https://doi.org/10.1176/appi.ajp.2017.17040472

336. Xie, L., Kang, H., Xu, Q., Chen, M. J., Liao, Y., Thiyagarajan, M., O'Donnell, J., Christensen, D. J., Nicholson, C., Iliff, J. J., Takano, T., Deane, R., & Nedergaard, M. (2013). Sleep drives metabolite clearance from the adult brain. Science, 342(6156), 373–377. https://doi.org/10.1126/science.1241224

337. Xiong, W., Cao, X., Zeng, Y., Qin, X., Zhu, M., Ren, J., Wu, Z., Huang, Q., Zhang, Y., Wang, M., Chen, L., Turecki, G., Mechawar, N., Chen, W., Yi, G., & Zhu, X. (2019). Astrocytic epoxyeicosatrienoic acid signaling in the medial prefrontal cortex modulates depressive-like behaviors. Journal of Neuroscience, 39(23), 4606–4623. https://doi.org/10.1523/JNEUROSCI.3069-18.2019

338. Yang, Y., Cui, Y., Sang, K., Dong, Y., Ni, Z., Ma, S., & Hu, H. (2018). Ketamine blocks bursting in the lateral habenula to rapidly relieve depression. Nature, 554(7692), 317–322. https://doi.org/10.1038/nature25509

339. Yu, X., Taylor, A. M. W., Nagai, J., Golshani, P., Evans, C. J., Coppola, G., & Khakh, B. S. (2018). Reducing astrocyte calcium signaling in vivo alters striatal microcircuits and causes repetitive behavior. Neuron, 99(6), 1170-1187.e9. https://doi.org/10.1016/j.neuron.2018.08.015

340. Yun, S. P., Kam, T.-I., Panicker, N., Kim, S., Oh, Y., Park, J.-S., Kwon, S.-H., Park, Y. J., Karuppagounder, S. S., Park, H., Kim, S., Oh, N., Kim, N. A., Lee, S., Brahmachari, S., Mao, X., Lee, J. H., Kumar, M., An, D., … Ko, H. S. (2018). Block of A1 astrocyte conversion by microglia is neuroprotective in models of Parkinson's disease. Nature Medicine, 24(7), 931–938. https://doi.org/10.1038/s41591-018-0051-5

341. Zamanian, J. L., Xu, L., Foo, L. C., Nouri, N., Zhou, L., Giffard, R. G., & Barres, B. A. (2012). Genomic analysis of reactive astrogliosis. Journal of Neuroscience, 32(18), 6391–6410. https://doi.org/10.1523/JNEUROSCI.6221-11.2012

342. Zanos, P., Moaddel, R., Morris, P. J., Georgiou, P., Fischell, J., Elmer, G. I., Alkondon, M., Yuan, P., Pribut, H. J., Singh, N. S., Dossou, K. S. S., Fang, Y., Huang,

X.-P., Mayo, C. L., Wainer, I. W., Albuquerque, E. X., Thompson, S. M., Thomas, C. J., Zarate Jr, C. A., & Gould, T. D. (2016). NMDAR inhibition-independent antidepressant actions of ketamine metabolites. Nature, 533(7604), 481–486. https://doi.org/10.1038/nature17998

343. Zhang, Ye, Sloan, S. A., Clarke, L. E., Caneda, C., Plaza, C. A., Blumenthal, P. D., Vogel, H., Steinberg, G. K., Edwards, M. S. B., Li, G., Duncan, J. A., Cheshier, S. H., Shuer, L. M., Chang, E. F., Grant, G. A., Hayden Gephart, M. G., & Barres, B. A. (2016). Purification and characterization of progenitor and mature human astrocytes reveals transcriptional and functional differences with mouse. Neuron, 89(1), 37–53. https://doi.org/10.1016/j.neuron.2015.11.013

344. Zhang, Yuan, Du, L., Bai, Y., Han, B., He, C., Gong, L., Huang, R., Shen, L., Chao, J., Liu, P., Zhang, H., Zhang, H., Gu, L., Li, J., Hu, G., Xie, C., Zhang, Z., & Yao, H. (2020). CircDYM ameliorates depressive-like behavior by targeting miR-9 to regulate microglial activation via HSP90 ubiquitination. Molecular Psychiatry, 25(6), 1175–1190. https://doi.org/10.1038/s41380-018-0285-0

345. Zhang, Yuan, Du, L., Bai, Y., Han, B., He, C., Gong, L., Huang, R., Shen, L., Chao, J., Liu, P., Zhang, H., Zhang, H., Gu, L., Li, J., Hu, G., Xie, C., Zhang, Z., & Yao, H. (2020). CircDYM ameliorates depressive-like behavior by targeting miR-9 to regulate microglial activation via HSP90 ubiquitination. Molecular Psychiatry, 25(6), 1175–1190. https://doi.org/10.1038/s41380-018-0285-0